SDR Engineering Consultants, Inc.

RETAINER CONTRACT FOR BRIDGE PRESERVATION STATEWIDE

STATE PROJECT NO. H.009859.5

RC BOX CULVERTS TESTING AND RATING STATEWIDE

FINAL REPORT

For Reference Only!
Please contact DOTD Bridge Rating for questions and comments.

Louisiana Department of Transportation and Development

Submitted by: ______________________ Date: 07/15/2020
Zhiong Liang, PhD, PE, Project Manager
SDR Engineering Consultants, Inc.

Approved by: ______________________ Date: 07/15/2020
Mohsen Shahawy, PhD, PE, Quality Assurance Manager,
SDR Engineering Consultants, Inc.

TABLE OF CONTENTS

EXECUTIVE SUMMARY

Significant number of cast-in-place (CIP) reinforced concrete box culverts were constructed using the old standard details developed in the 40's and revised later in the 70's by Louisiana Department of Highways. The reinforcement details given on those standard plans do not provide moment continuity between the slab/raft and exterior walls connections (negative moment zones). In addition, exterior walls are reinforced at the inner face only without any reinforcement at the outer face. Accordingly, culverts constructed using those old detailing standards were found to typically produce low load rating factors when current AASHTO procedures are followed. Nevertheless, these culverts have been in service for an extended period of time and their actual performance has been satisfactory with minimum signs of distress.

Culverts behave differently from structures resting on ground, primarily due to the development of a composite-system action between the culvert structural elements and the interacting soil envelope, both of which contribute to the structural behavior of the overall system. Satisfactory performance of culverts can be attributed to several factors including actual strength of the concrete material which is typically greater than as built concrete strength, culvert-soil interaction, construction quality and the level of conservatism of the AASHTO procedures used to distribute live load through fills.

Numerical modeling technique used for structural analysis of culvert and soil-structure interaction have significant impact on the load rating results. Simple structural analytical models, e.g. 2D frame-element analysis, are typically used due to simplicity and time saving, however, the load rating results are generally more conservative (under estimated) when compared to results obtained from more complex numerical modeling techniques using 3D plate element models.

The scope of this project is to assess the load rating of representative CIP-RC box culverts from the Louisiana DOTD inventory and develop a load rating procedure that is representative of the actual field performance of these old culverts. The project was carried out in two phases. Phase I comprised literature review of the published standards and reports; performing preliminary analytical study using 2D frame element models to investigate the influential parameters and examination of LADOTD culvert inventory.

Phase II comprised non Destructive Testing (NDT) of Twelve CIP RC box culverts with different configurations representative of the LADOT inventory and conducting an extended parametric study that included development of 120 three-dimensional (3D) finite element models for culverts with different configurations (fill heights, span lengths and culvert lengths) and the corresponding two dimensional (2D) frame element models. The purpose of the parametric study was to develop correction factors that can be used to correlate moments values obtained from 3D analysis with those obtained from 2D analysis.

Field live load testing of the culverts was conducted after instrumenting each culvert with a structural health monitoring (SHM) system consisting of sensors including displacement and strain sensors.

Three-dimensional (3D) finite element models were built for each tested culvert. AASHTO's Manual for Bridge Evaluation (MBE) rating methodology was followed in this research to distribute the live loads through the soil fill, and standard plans were used to obtain the reinforcing details of the culverts.

Two approaches; namely pinned connections and moment connections were used in the modeling and analysis of the RC culverts. The results from both approaches were compared and evaluated. Based on the evaluation, it is determined that using the moment connections approach combined with the at-rest horizontal earth pressure linear distribution coefficient, K_o of 0.50 and the 3D-2D correction factors results in more realistic load rating values that are representative of observed field conditions. Results from the parametric study and the field tests were used to develop guidelines for load rating of RC box culverts.

1. BACKGROUND

Buried structures including reinforced concrete box culverts behave differently from structures resting on ground. This is primarily due to the development of a composite-system action between the culvert structural elements and the interacting soil envelope, both of which contribute to the structural behavior of the overall system. In addition, the distribution of applied surface loads is mainly affected by the soil mass surrounding the culverts and the presence of pavement.

1.1 PROBLEM DEFINITION

Significant number of RC box culverts were constructed using standard plans and details developed in the 60's and 70's by Louisiana Department of Highways. The reinforcement details given on those standard plans do not provide moment continuity between the slab/raft and exterior walls connections (negative moment zones) as shown in Error! Reference source not found.. In addition, exterior walls are reinforced at the inner face only without any reinforcement at the outer face. Accordingly, culverts constructed using those old detailing standards were found to typically produce low load rating factors when current AASHTO procedures are followed. Nevertheless, these culverts have been in service for an extended period and their actual performance has been satisfactory with no signs of distress.

(a) Single cell

(b) Double cell

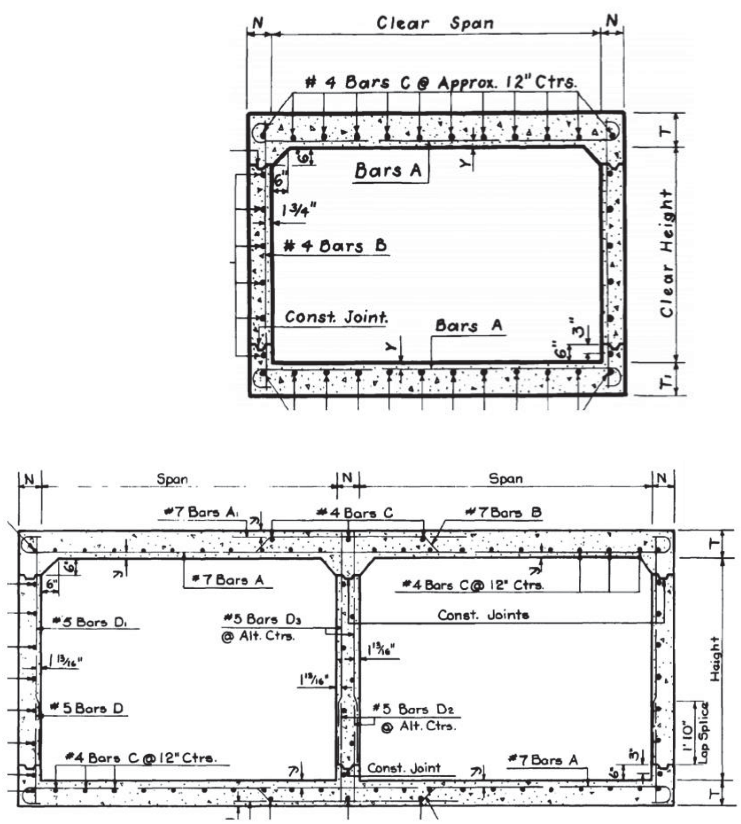

Figure 1: LADOTD standard reinforcement details of single- & double-cell RC box culvert

Simple structural analytical models, e.g. 2D frame-element analysis, are typically used due to simplicity and time saving, however, the load rating results are generally more conservative (under estimated) when compared to results obtained from more complex numerical modeling techniques using 3D models.

Due to lack of national standards, the vast majority of State Departments of Transportation (DOTs) do not have official guidelines and/or policies for load rating of culverts. The 2013 Interim Revisions to the Second Edition of AASHTO Manual for Bridge Evaluation (MBE) introduced for the first-time article 6A.5.12 for rating of reinforced concrete box culverts using the Load and Resistance Factor Rating (LRFR) method only.

Currently, Louisiana Department of Transportation and Development (LADOTD) does not have official guidelines and/or policies for loading rating of RC box culverts. Due to the lack of standards, LADOTD currently suspended the load rating of concrete culverts since the rating results based on AASHTO LRFD specifications do not properly reflect the actual performance of these culverts.

2. SCOPE AND WORK PLAN

This project consists of two phases as shown in Figure 2.

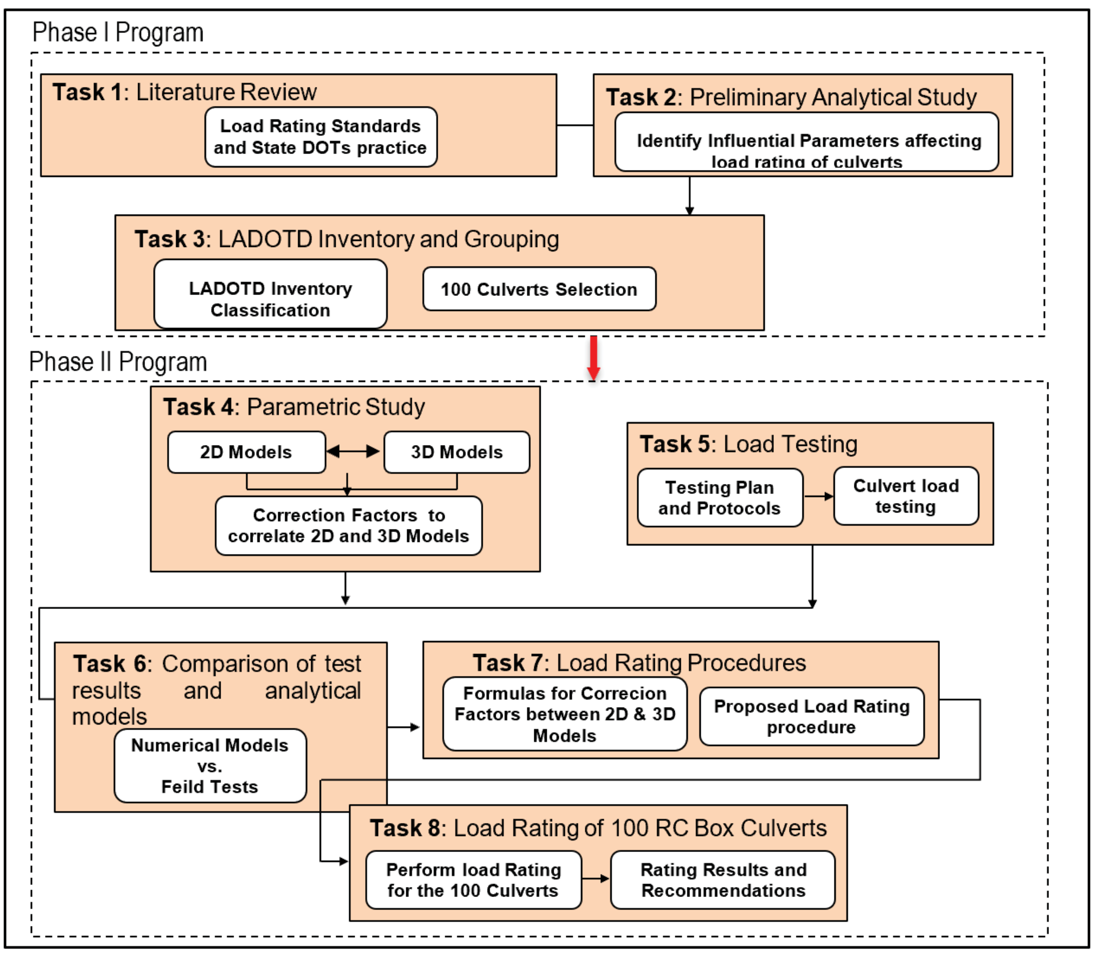

Figure 2: Organizational chart presenting the workplan of the project

2.1 Phase I Program

Task 1: Literature Review

This task comprised critical review of available literature including LADOTD standard plans, relevant specifications, published national and international research projects, and official policies or guidelines adopted by state DOTs. In addition, different modelling techniques used for calculating the load effects were investigated as well as the soil structure interaction effect. More emphasis was given to parameters that affects the load rating of the RC box culverts.

Task 2: Preliminary Analytical Study

A preliminary analytical investigation was conducted to identify the influential parameters that influence load rating of the RC box culverts. Those parameters were considered in the selection of the 100 culverts to be load rated in Phase II.

Task 3: LADOTD Culvert Inventory and Selection of 100 Representative Culverts

This task comprised review of the available LADOTD inventory of RC box culverts and selection of 100 culverts, representative of the inventory, for evaluation and load rating using the guidelines to be developed in Phase II. The selected culverts were grouped based on common details, configuration, site conditions and other parameters that affect the load rating results, such as depth of fill and size of culvert. In addition, twelve culverts (selected out of the 100) were selected for testing in phase II for the purpose of validating the analytical modeling.

2.2 Phase II Program

A description of the tasks completed in Phase II is presented in the following sections:

Task 4: Parametric Study

This task included analytical modeling of RC box culverts using 2D and 3D FE models to incorporate the effects of different parameters. The objective of the parametric study is to develop correction factors that correlate the moments form the 2D and the 3D finite element models.

Task 5: Field Testing

This task comprised load testing of twelve RC box culverts selected from LADOTD culvert inventory. Standard diagnostic field load testing was conducted on 12 culverts that were selected from the 100 culverts outlined in Task 3. The experimental field-testing results were used to: (1) validate the correction factors developed in Task 4 and (2) verify the performance of the unreinforced exterior wall/slab junctions.

Task 6: Comparison of FE Models and Test Results

This task comprised development of 3D FE models for the tested culverts and comparing the results from the models to the results obtained from the field tests.

Task 7: Development of Correction Factors Formulas and Load Rating Procedure

This task comprised development of formulas to determine the correction factors used to correlate the results from 2D and 3D modeling. In addition, development of a load rating procedure for LADOTD culverts based on the correlation of the 3D and 2D analytical modeling along with other considerations

Task 8: Rating of 100 Representative RC Box Culverts

The proposed procedure for load rating the RC box culverts shall be used to rate the 100 box culverts selected in Task 3.

2.3 ANTICIPATED DELIVERABLES

The deliverable from this project can be summarized as follows:

- Identification of the impact of the different modeling techniques and development of 2D/3D correction factors to account for the analysis reliability using different techniques.
- Proposal of new and/or adjusted load rating procedure to account for the 2D/3D correction factors developed under this project.
- Load rating of 100 selected culverts from LADOTD culvert inventory using the proposed rating procedure.

3. PHASE I PROGRAM

Phase I of the project was completed in August 2019 and a report summarizing the findings along with the proposed work plan for Phase II was submitted to DOTD. The following sections represent key findings from the three tasks completed in Phase I program.

3.1 TASK 1: LITERATURE REVIEW

3.1.1 National Standards

There are three primary publications that are used for load rating: AASHTO Manual for Bridge Evaluation (AASHTO-MBE, 2003), AASHTO Standard Specifications for Highway Bridges (AASHTO-SSHB, 2002) and AASHTO LRFD bridge design specification (AASHTO-LRFD, 2017). Typically, States' DOTs provide their own guide that comply with the federal standard regulations and address their own special needs or details.

The 2013 Interim Revisions to the Second Edition of AASHTO-MBE (2003) introduced for the first time Article 6A.5.12 for the rating of reinforced concrete box culverts using the Load and Resistance Factor Rating (LRFR) method only. However, the 2013 revisions state that for the load rating of top slabs of concrete box culverts, the lane load shall not be applied without providing any justification to support this major change in design philosophy. The exclusion of the lane load as being part of the design vehicular live load is not consistent with the AASHTO-SSHB (2002) and AASHTO-LRFD (2017). The 2014 interim revision includes additional guidance on live load for LRFR rating of culverts. The 2016 interim revision states on MBE section 6B (ASR, LFR) that simplified modeling approach may be over conservative. Appendix A of the AASHTO-MBE (2003) presents an example for load rating a single-cell CIP RC box culvert. The example shows modelling procedures, load and capacity calculations. AASHTO-SSHB (2002) provides guidance for simplified direct stiffness (simplified frame element) analysis, dead and live load distribution, strength reduction factors, and capacity calculation. AASHTO-LRFD (2017) includes additional guidance for values of basic rating parameters that are needed for soil-structure interaction approach.

AASHTO realized that current specifications for culvert load rating may be overly conservative or inadequate, since the calibration for LRFR was based primarily on the bridge response to gross truck weight while the culvert response should be calibrated based on a single axle or single wheel. Therefore, a new NCHRP project is initiated and currently underway (NCHRP 15-54) to propose modifications to AASHTO-MBE (2003) provisions and AASHTO-LRFD (2017) accordingly. The project final report should be available late this year (2019).

3.1.2 Current DOTs Practices and Published NCHRP Reports

An examination of the entire 50 States Departments of Transportation (DOTs) websites revealed that vast majority of the state DOTs do not have any published specifications, guidelines, or policies for load rating of culverts. In addition, some states only direct the engineer to the AASHTO MBE (until 2013 did not have any articles related to culverts), while other states give some additional information to be coupled with the AASHTO MBE. Few states add to the MBE by specifying the use of either BRASS-CULVERT or Bridge Rating software. Few states give tables or predefined rating factors based on the year built and materials used.

TxDOT has published a load rating guide for RC box Culvert with limited information for other types of culverts (Lawson et al. 2017). The guide includes step-by-step procedures for RC box culverts without restriction on the design era, number of spans, culvert geometry, or fill height. The guide employed AASHTO-SSHB (2002) provisions along with AASHTO-MBE (2003). In addition, the guide presents four analytical models of increasing complexity and sophistication. The first three models are simple and are recommended for conventional load rating, while the fourth model is for specialized application and research purposes. The guide includes a recommended software for each level with step-by-step procedures.

WSDOT (2018) refer to the latest AASHTO-MBE (2003) for culvert load rating and refer to AASHTO-LRFD (2017) for live load distribution. In addition, WSDOT does not rate culverts with span lengths up to 24 ft. and fill depth more than 8 ft.

LADOTD does not have official guidelines and/or policies for loading rating of RC box culverts. Due to the lack of standards, LADOTD currently suspended the load rating of concrete culverts since the rating results based on AASHTO LRFD specifications do not properly reflect the actual load-carrying capacity of these culverts.

A survey was conducted by (Lawson et al. 2010) to identify (1) the load rating procedures, if any, and (2) most problematic load rating areas facing DOTs in load rating their culverts. Survey results from Delaware, Illinois, Minnesota, and Texas indicated that the current culvert load rating procedures, most often, suggest posting or deficiency of the culvert while the actual performance showed no distress or malfunctional. In addition, it was found that the current practice for DOTs is to replace culverts based on hydraulic mal-functionality and not on the structural requirements. Louisiana state response to this survey was that load rating of concrete culverts is currently suspended since the rating results based on AASHTO LRFD specifications do not properly reflect the actual load-carrying capacity of these culverts.

A recent NCHRP project (NCHRP 15-54) was conducted to investigate the accuracy of culvert load rating procedures provided in MBE and specifications in AASHTO-LRFD (2017). The project includes diagnosed field testing of seven existing culverts of various types and extensive numerical 2D and 3D FEM simulations to propose modifications to the existing load rating procedures. A general response to a survey conducted nationwide showed that RC concrete box culverts do not rate well while no physical sign of distress exists. Several recommendations and changes were proposed for load rating procedures. The recommendations include changes in the live load distribution through the fill depth. Also, especially for the RC box culvert the shear calculation and haunch effect in the culvert analysis. Moreover, a new approach for the effect of the surcharge load was proposed to reflect the actual measured effect.

3.1.3 Review of State Departments of Transportation Standard Plans

Louisiana DOTD (LADOTD)

Reinforced Concrete (RC) box culverts constitute a large portion of Louisiana's bridge inventory and were mainly constructed using standard plans and details developed in the 60's and 70's by Louisiana Department of Highways. The reinforcement details given on those standard plans do not provide moment continuity between the slab/raft and exterior walls connections (negative moment zones) as shown in Figure 3. In addition, exterior walls are reinforced at the inner face only without any reinforcement at the outer face. Accordingly, culverts constructed using those old detailing standards typically produce low load rating factors when AASHTO procedures are followed.

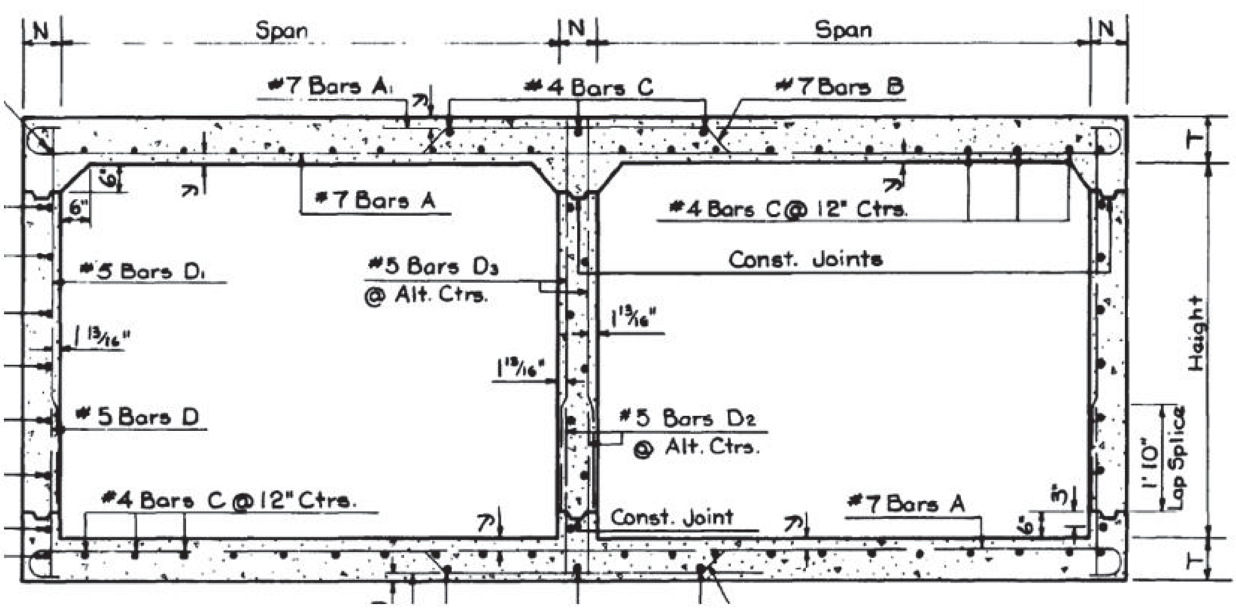

Figure 3: LADOTD standard reinforcement details of double-cell RC box culvert in Louisiana DOTD

Texas DOT (TXDOT)

Texas DOT has a large inventory of culverts that consists of 13,192 constructed between 1905 and 2008. Texas DOT archive files have standard details that go back to 1920s and multi-cell culverts prevailed the population of culvert designs. The reinforcement details provide continuity between the exterior walls and the top/bottom slabs of the culvert. Figure 4 shows standard reinforcement details for multi-cell box culvert from Texas DOT.

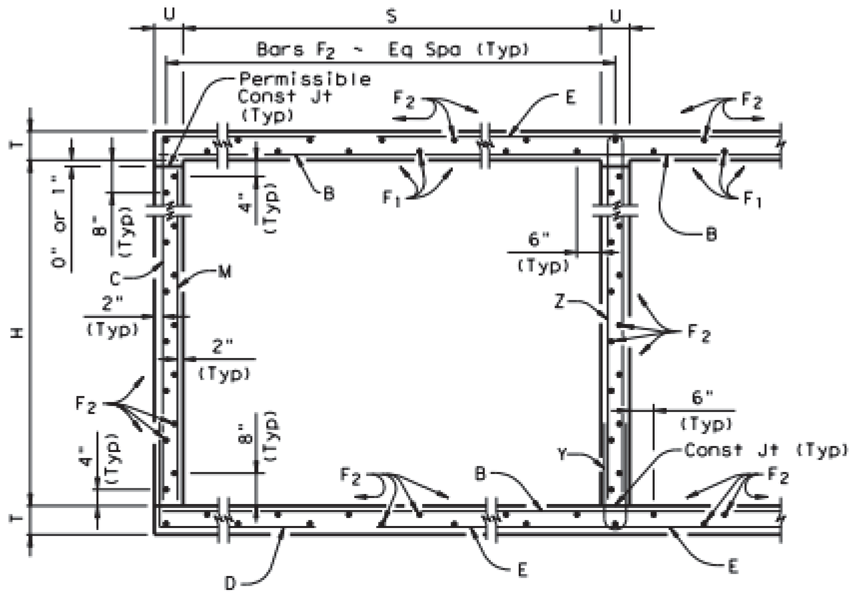

Figure 4: Texas standard reinforcement details of multi-cell RC box culvert in Texas DOT

Colorado DOT (CDOT)

The standard reinforcement details for multicell culverts utilized by Colorado DOT, are shown in Figure 5. The reinforcement details provide continuity between the external walls and the top slab of the culvert.

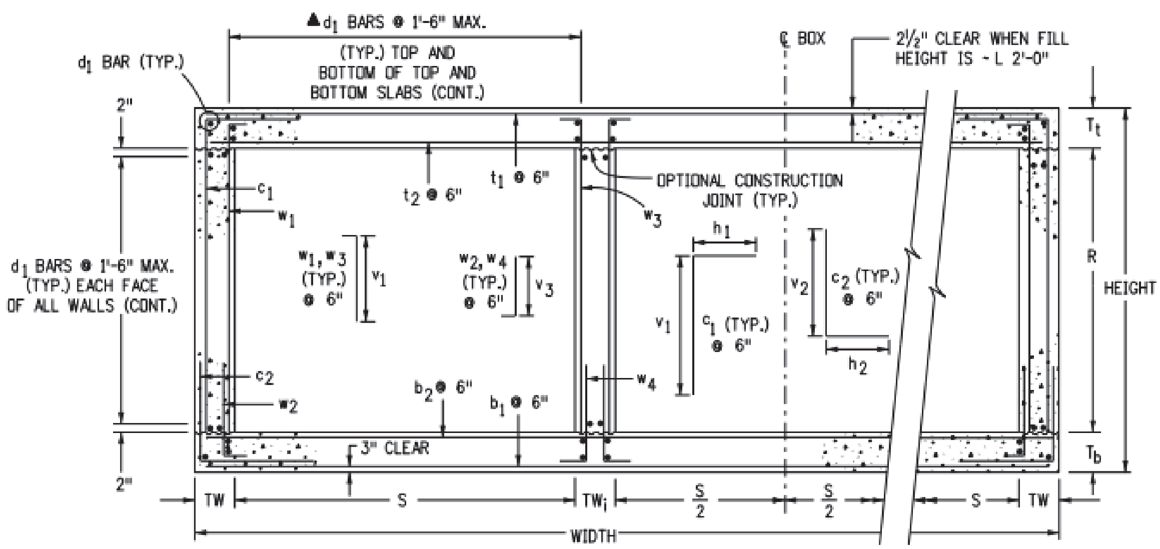

Figure 5: Colorado standard reinforcement details of Multi-cell RC box culvert in Colorado DOT

3.1.4 Parameters Affecting Load Rating of RC Culverts

Culverts are buried structures which are subjected to earth pressures in addition to traffic live load. This section presents a literature review of the previous studies conducted to investigate the effect of different parameters on structural behavior and the load rating analysis of CIP RC box culverts.

3.1.4.1 Earth Loads (EV, EH, and ES)

The effect of fill height (H) can be divided into three types of load: (1) vertical earth pressure (EV), (2) lateral earth pressure (EH), and (3) uniform surcharge (ES). As built plans and/or in-situ measurements can be used to determine the depth of the fill. Vertical earth pressure (EV) represents the weight of the soil above the culvert. AASHTO-LRFD (2017) takes into account soil structure interaction when calculating the vertical earth pressure and relates it to the installation procedure. Lateral earth pressure (EH) represents lateral soil pressure exerted on the culvert exterior walls and varies linearly with fill height. Uniform surcharge (ES) is the additional lateral earth pressure from the continuous roadway fill and distributed uniformly along the culvert height. For live load rating calculation, the lateral pressure should be decreased by 50% with load factor equals to 1.0.

It should be noted that, for the lateral soil pressure exerted on the culvert exterior walls, AASHTO LRFD assumes the at-rest linear distribution for the soil pressure using a lateral soil coefficient, K_o ,that is determined based on the angle of internal friction for granular fills.

Other studies imply that the distribution of the lateral soil pressure on the culvert exterior walls can be influenced with the soil arching effect and the deformations of the exterior walls. A research project conducted by Texas Transportation Institute for the Texas State Department of Highways and Public Transportation presented a procedure to determine the lateral soil pressure distribution on the exterior walls of reinforced concrete box culverts. The study is supported by field measured data for the lateral pressure on the walls as well as the response of the culvert.

An 8 ft. by 44 ft. reinforced concrete box culvert was constructed and instrumented with twenty pressure cells on the top and side slabs, and with six resistance strain gauges on the tension reinforcing steel in the top slab. Earth pressures, reinforcing steel strains and top slab deflections were measured for various combinations of dead load and live load. Dead loads were due to backfill and earth covers up to 8 ft over the top slab. Live loads were applied by parking a test vehicle having a 48 kip tandem rear axle at various distances from the centerline of the culvert along a perpendicular roadway constructed on the embankment above the culvert.

A set of empirical equations was developed to fit the measured earth pressures. The results indicated that the lateral soil pressure exerted on the exterior walls of the culvert exhibited a nonlinear distribution due to soil arching effects. Figure 6 shows a comparison of the lateral soil pressure determined based on AASHTO and the findings of this study.

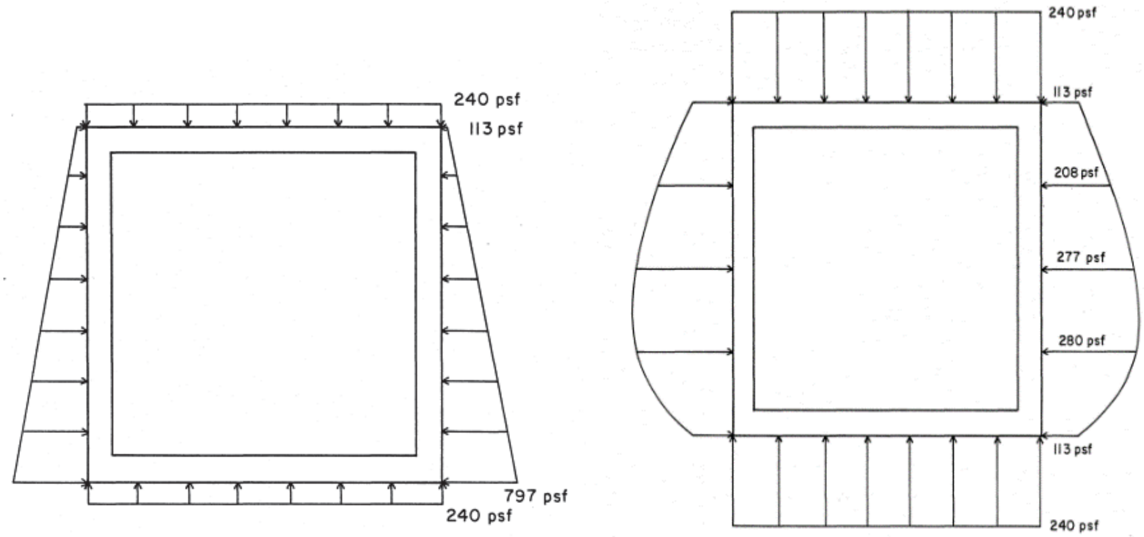

Figure 6: (a) at rest linear distribution for the lateral soil pressure (AASHTO) on culvert exterior wall and (b) measured nonlinear distribution for the lateral soil pressure due to soil arching effects.

The lateral earth pressure including the soil arching effect can be determined at several elevations along the height of the exterior wall using the following equations:

$$\boldsymbol{P_{ho} = k_o \sigma_v} \qquad \text{Eq. 1}$$

$$\boldsymbol{\sigma_v = \frac{\gamma}{c-1}\, z \left[1 - \left(\frac{z}{z_t}\right)^{c-1}\right] + q_v \left(\frac{z}{z_t}\right)^{c}} \qquad \text{Eq. 2}$$

$$\boldsymbol{c = \frac{2k_o \tan\emptyset}{\tan\left(45 - {}^{\emptyset}/_{2}\right)}} \qquad \text{Eq. 3}$$

Where:

σ_v: vertical pressure

k_o: lateral earth pressure coefficient

γ: unit weight of soil

$\emptyset$: angle of internal friction of soil

q_v: vertical surcharge pressure

z: height above reference plane

z_t: depth of reference plane from the top of the culvert

For instance, AASHTO at-rest lateral soil pressure exerted on the exterior walls of a 3 cell 8x8 culvert with a height of fill equal to 8.0 ft. and an angle of internal friction equal Ø to 31 degrees is shown in Figure 7.

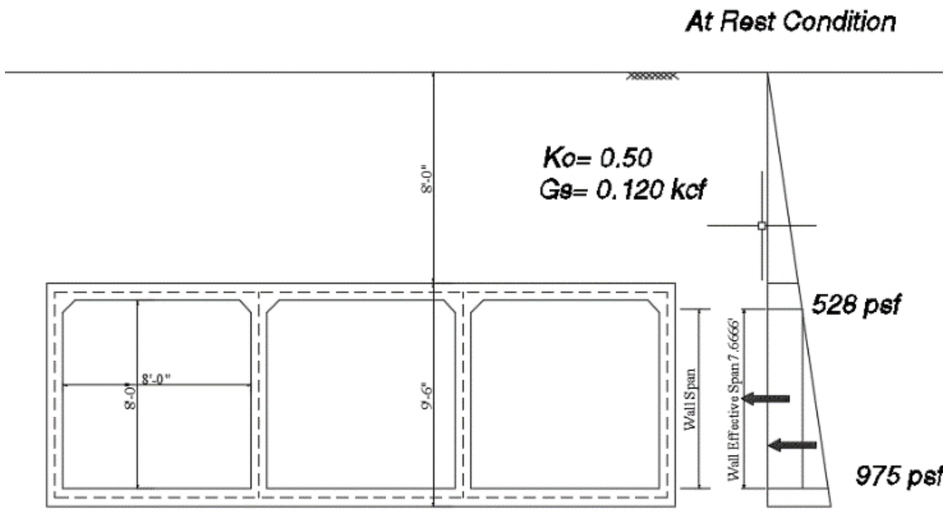

Figure 7: At rest lateral soil pressure linear distribution on the exterior wall of a culvert with 8.0 ft fill height

The lateral soil pressure including the soil arching effect was determined using equations Eq. 1 to Eq. 3 for the 3-cell 8x8 culvert as shown in Figure 8.

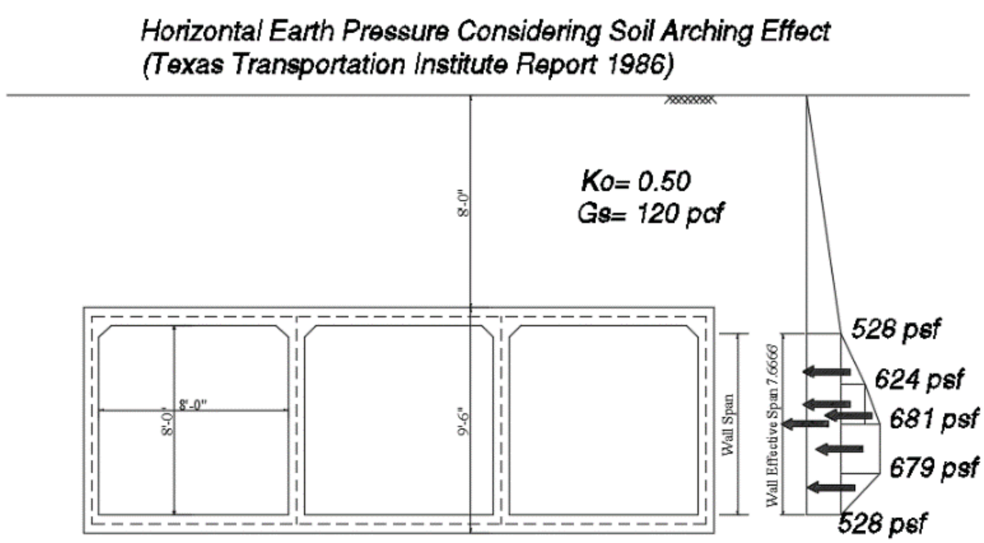

Figure 8: lateral soil pressure including soil arching effects on the exterior wall of a culvert with 8.0 ft fill height

It should be noted that the moment at mid height of the exterior wall was determined under the lateral soil pressure for the two cases shown in Figure 7 and Figure 8. The results indicated that the moment computed from the case of the at rest linear distribution as specified by AASHTO (Figure 7) was 13% greater than the moment computed from the case of the nonlinear soil lateral pressure distribution considering soil arching effect (Figure 8).

3.1.4.2 Distribution of Wheel load through earth fills (LL)

Live load distribution is one of the key parameters that influence design and rating of culverts. The wheel load passes to pavement layer and spreads slightly through the layer. The load is then attenuated through the soil layer till it reaches the top surface of the culvert top slab. Upon reaching the surface of the top slab, the load is distributed in the culvert span direction (in plane direction) and culvert length direction (out-of-plane direction). The culvert walls carry the load down to the bottom slab which spreads into the surrounding foundation soil. This process is illustrated in schematic representation on Figure 9.

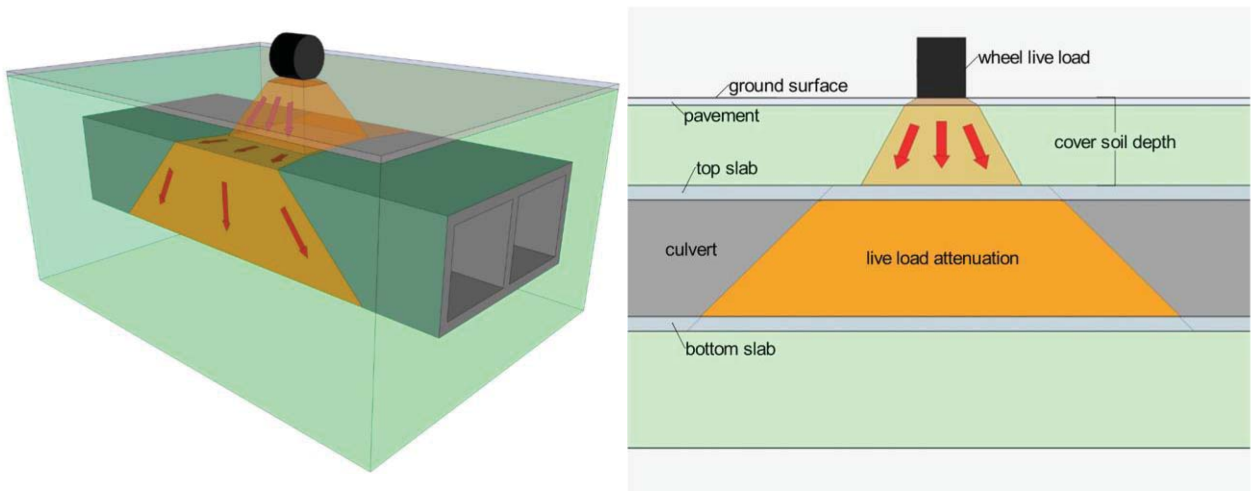

Figure 9: Illustration of live load distribution for RC box culverts (Wood et al., 2016)

The live load distribution is typically assumed to be distributed as a surface load over a predetermined area whose dimensions are varied linearly with the depth. The wheel contact area with the wearing surface is typically 10 in. x 20 in. and spread to larger area through the fill height. Figure 10 shows the area at which the live load is distributed from the contact with the road surface through the fill height for three different cases. A different approach was adopted by AASHTO-LRFD (2017) that lead to increase of the live load pressure.

NCHRP Project 15-29 (Peterson et al, 2010) investigated how surface live loads are distributed through the surrounding soil mass to the buried culvert. The project comprised of an extensive (830) three-dimensional (3-D) numerical modeling using soil-structure models for different types of culverts and different parameters. Modeling results showed that surface live load distribution is mainly dependent on depth of backfill, soil characteristics, and culvert properties. The project proposed Simplified Design Equations (SDEs) for spread of surface live load through soil mass. Further, the project proposed revisions to the AASHTO LRFD BDS, which was introduced in the 2013 Interim Revisions and adopted in AASHTO LRFD BDS 7th Edition.

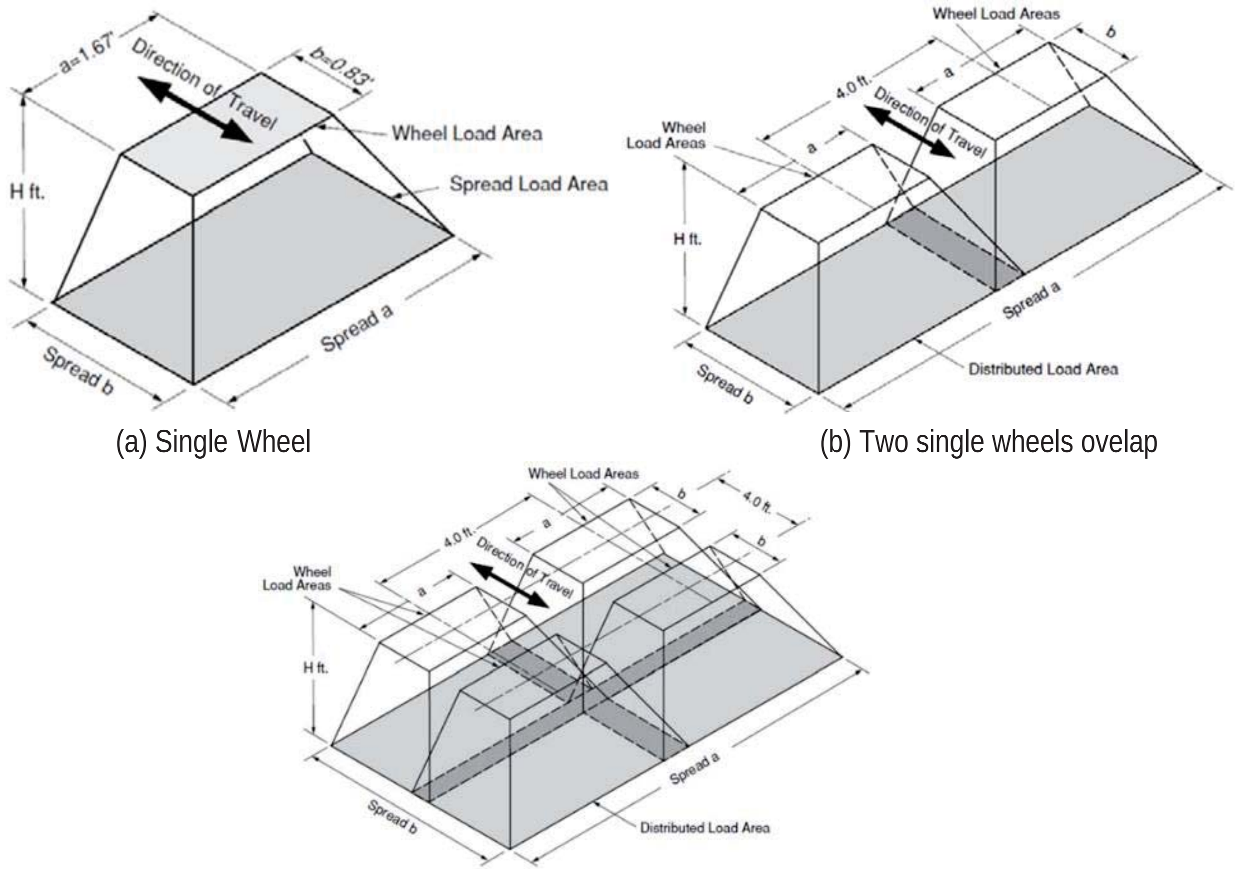

(a) Single Wheel

(b) Two single wheels ovelap

(c) two axles of two single wheels overlap

Figure 10: Area of live load distribution for different wheel configuration (Okeil et al., 2018)

According to AASHTO-LRFD BDS 8th Edition (2017), for single cell-span culverts, the effect of live load can be neglected if the fill depth is more than 8 ft. or exceeds the span length. For multi-cell culvert, the live load effect can be neglected in case of fill depth greater than the distance between the inside faces of end walls. The live load distribution for transverse and perpendicular directions are calculated as follow:

For fill depth (H) less than 2 ft., as specified in AASHTO-LRFD (2017), the following equations shall be used as specified in Article 4.6.2.10.2-1:

$$\boldsymbol{E = 96 + 1.44S} \quad \text{Eq. 4}$$

$$\boldsymbol{E_{span} = l_t + LLDF \times H} \quad \text{Eq. 5}$$

where: E is the equivalent distribution width perpendicular to span (in.), S is the clear span (ft.), E_{span} is the equivalent distribution length parallel to span (in.), l_t is the length of tire contact area parallel to span, as specified in Article 3.6.1.2.5 (in.), $LLDF$ factor for distribution of live load with depth of fill, 1.15 or 1.00, and H is depth of fill from top of culvert to top of pavement (in.)

For fill depth (H) more than 2 ft., the load shall be distributed over a rectangle area (A_{ll}) calculated using the following equation, as specified in AASHTO-LRFD (2017), Article 3.6.1.2.6:

$$A_{ll} = l_w w_w \qquad \text{Eq. 6}$$

where: l_w is the live load distribution length at depth of fill H (ft.) and w_w is the live load distribution width at depth of fill H (ft.).

The distribution of live load of the adjacent wheels of the same axle may or may not overlap, depending on several factors. Therefore, an interaction depth, H_{int_t}, shall be determined first and compared with the depth of fill (H) to determine whether the loaded areas of the two wheels will overlap or not. Then the width of the loaded area(s) on the top slab of the culvert in the transverse direction, w_w, can be determined using Eq. 8 for the case of no overlap of loaded areas or Eq. 9 for the case of overlap of the loaded areas

$$H_{int\_t} = \frac{s_w - \frac{w_t}{12} - \frac{0.06D_i}{12}}{LLDF} \qquad \text{Eq. 7}$$

$$w_w = \frac{w_t}{12} + LLDF(H) + 0.06\frac{D_i}{12} \qquad H < H_{int-t} \qquad \text{Eq. 8}$$

$$w_w = \frac{w_t}{12} + s_w + LLDF(H) + 0.06\frac{D_i}{12} \qquad H \geq H_{int-t} \qquad \text{Eq. 9}$$

where: H_{int-t} is the wheel interaction depth transverse to culvert span (ft), $s_w$is the wheel spacing, 6.0 ft., w_t is the tire patch width, 20 (in.), D_i is the inside diameter or clear span of the culvert (in.), $LLDF$ is the live load distribution factor as specified in Table 3.6.1.2.6a-1 (AASHTO-LRFD, 2017), H is the depth of fill over culvert from the surface of the culvert to top of the pavement (ft)

The procedure for load distribution of adjacent axles in the longitudinal direction (traffic direction) is similar to the transverse direction. The length of the loaded area on the top slab of the culvert for the adjacent axles can be determined from either Eq. 11 or Eq. 12 as follows:

$$H_{int-p} = \frac{s_s - \frac{l_t}{12}}{LLDF} \qquad \text{Eq. 10}$$

$$l_w = \frac{l_t}{12} + LLDF(H) \qquad H < H_{int-p} \qquad \text{Eq. 11}$$

$$\boldsymbol{l_w = \frac{l_t}{12} + s_a + LLDF(H)} \qquad \boldsymbol{H \geq H_{int-p}} \qquad \text{Eq. 12}$$

where: H_{int-p} is the axle interaction depth parallel to culvert span (ft.), s_a is the axle spacing (ft.) and l_t is the tire patch length, 10 (in.)

Furthermore, AASHTO-LRFD (2017) specifies a dynamic load allowance (IM) for culverts which varies with the depth of the backfill. The dynamic load allowance ranges from 33% for direct contact culverts (no backfill) to 0 % at 8 ft. and higher depth of backfill. It can be determined using the following equation:

$$\boldsymbol{IM = 33\ (1.0 - 0.125 D_E) \geq 0\%} \qquad \text{Eq. 13}$$

where: D_E is the minimum depth of earth cover above the structure.

3.1.4.3 Live Load Surcharge (LS)

AASHTO-LRFD specification and MBE-Manual assume uniform lateral surcharge load to represent the pressure exerted on the exterior walls of the culvert when a truck wheel approaches the culvert. The lateral surcharge load should be applied to the exterior walls as follows:

$$\Delta_{\boldsymbol{p}} = \boldsymbol{k_o \gamma_s h_{eq}} \qquad \text{Eq. 14}$$

where: Δ_p is the constant horizontal earth pressure due to live load surcharge (ksf), γ_s is the total unit weight of soil (kcf), k_o is the coefficient of lateral earth pressure, h_{eq} is the equivalent height of soil for vehicular load (ft).

Based on *NCHRP 15-54* study, the previous equation is used for the calculation of uniform surcharge load for both retaining walls and RC box culverts despite their different behavior. The approaching wheel increases the overturning moment while produces a small lateral pressure on the culvert. Besides, the live load surcharge is assumed uniform, while field tests have showed that it decreases rapidly with the increase of the backfill depth. Moreover, the maximum lateral pressure occurs at the top slab of the culvert and therefore is transmitted directly through the top slab and does not create bending moments in the wall sections.

The ASTM standards (ASTM C1577), which is similar to AASHTO M273, proposes a different equation to calculate the lateral pressure on precast reinforced concrete box sections for depths of fill less than two feet as follows:

p-lat(H) = 700/H < 800 psf Eq. 15

where: p-lat(H) is the lateral soil pressure induced from an approaching wheel load and exerted on the wall of the culvert at depth H (psf), and H is the height from the surface of the fill to the depth where pressure is calculated (ft).

Figure 11 (adopted from *NCHRP 15-54* report) shows a comparison between the live load surcharge based on 2.0 ft. backfill depth from (1) the AASHTO-LRFD equation, (2) ASTM standards equation, and (3) three cases of axle loads with different spacing to the center line of wall from FEM models. The FEM models show that the surcharge pressure is maximum at the culvert surface and diminishes rapidly with the depth. Also, majority of the surcharge load is transmitted as thrust force through the top slab.

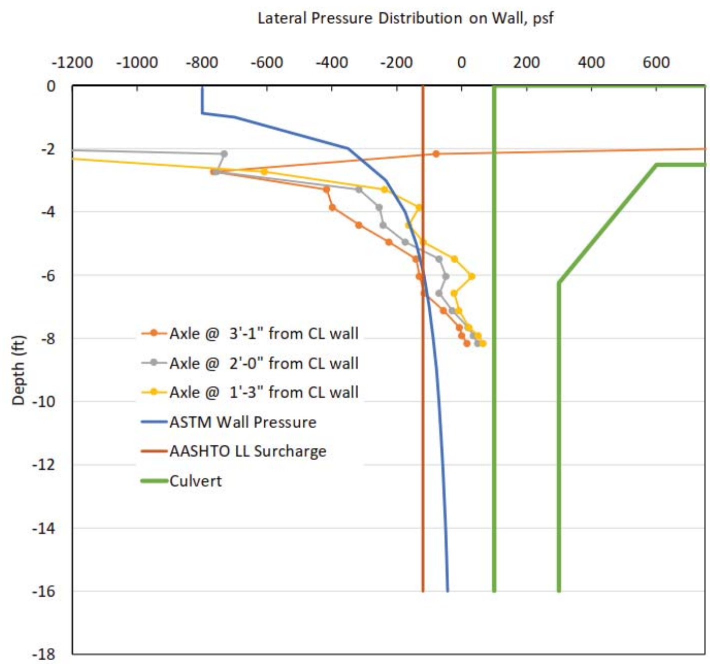

Figure 11: Live load surcharge pressure on culvert wall against backfill depth (adopted from NCHRP 15-54)

NCHRP 15-54 study recommended to use the equation form ASTM standards for culverts with depth of fill above the top slab that is less than 2.0 ft., and that no lateral surcharge shall be applied for culverts with fill heights above the top slab greater than 2 ft.

Findings pertaining to live load surcharge from NCHRP 15-54 study were summarized in Ballot LRFD 4 form that is submitted to AASHTO committee for possible inclusion in the provisions of MBE and AASHTO LRFD (2017).

3.1.4.4 Pavement type

The effect of pavement layer type on the live load distribution is usually ignored while conducting the load rating of culverts. However, the pavement help spreading the live load faster than the soil, as the pavement has much higher flexural stiffness than the soil (Abdel-Karim et al., 1990).

Kansas Department of Transportation (KDOT) conducted a study to investigate the effects of pavement type on the live load distribution on the top slab of the culvert. In this study, two field tests were carried out on the concrete box culverts under rigid and flexible pavements, respectively. Besides, finite difference numerical models of the tested culverts were created in the Fast Lagrangian Analysis of Continua in three dimensions (FLAC3D) software and were verified against the field test results. The verified models were then used to perform a parametric study to better understand the effects of the pavement type (flexible and rigid pavement) and thickness on the pressure distribution. The results showed that, for the same pavement thickness, the vertical pressure on the top slab was lower under rigid pavement than flexible pavement. Also, increasing the pavement thickness help reduce the maximum vertical pressure.

Lawson et al. (2016) conducted a parametric study with different types of pavement. Depending on the type of pavement, the load rating improved with increased pavement stiffness for low and medium fill depth. When high fill height is used, pavement stiffness does not affect the live load distribution and subsequently load rating.

Seo et al. (2017) proposed a system-level pavement stiffness model while calculating load demands. The model accounts for the additional stiffness of the pavement for live load attenuation. A cross beam was modeled across the top row of finite element nodes. They conducted a parametric study for different types of pavements and found that the load rating increases in case of Asphalt with intermediate thickness and concrete pavements. Also, they conducted a comparison between the proposed model and two other models: AASHTO-recommended structural-frame model and production-oriented soil-structure interaction without pavement stiffness. The results showed an increase in the load factor for the proposed model compared to the other two models. The increase in the load factor was 10%, 46% and 147% for seal coat, intermediate asphalt, and concrete pavement, respectively.

3.1.4.5 Modulus of Subgrade Reaction

Lawson et al. (2010) showed that the modulus of subgrade reaction has a very minimal effect on the load rating of the RC box culvert. The analysis was conducted three times on each culvert with three different subgrade reactions: 75 pci, 150 pci and 250 pci. Also, It was found that soil modulus of elasticity could affect the load rating of the culvert and especially for higher fill depths (more than 6 ft.).

3.1.4.6 Height of Fill

The height of the backfill is defined as the vertical distance from the surface of the top slab to the surface of the pavement. The relation between the fill height and the load rating of RC culvert is highly nonlinear (Wood et al. 2015), as shown in Figure 12. This is due to the simultaneous linear increase in dead load and nonlinear decrease in live load attenuation with the increase in the backfill depth. At the maximum designed backfill depth, the live load dissipates, and the culvert is designed for the dead load. Several researchers studied the effect of the backfill for CIP RC culvert. Acharya (2012) shows that vertical pressure decreases with the increase of fill height (ranges from 1.6 ft. to 8.2 ft.). McGrath et al. (2005) showed that the live load distribution in the culvert direction (out of plan direction) is significant for fill depth less than or equals to 2ft., while the out of plan distribution is slightly presented in deeply buried culverts. In a recent study by Sharifi (2018), it was found that the live load effect decreases in bi-linear relationship with the backfill height (ranges from 1 ft. to 12 ft.), as shown in Figure 13. Also, for 10 ft. fill height, the maximum live load force was less than 10% of the maximum dead load force.

Lawson et al. (2010) investigated the effect of the fill height on seven culverts with different backfill heights. The analysis of each case was conducted five times with different analysis technique and/or different soil modulus. The results show that increasing the fill height increases the sensitivity of the soil modulus. Also, the load rating reaches the maximum value when the fill height reaches the maximum designed backfill height.

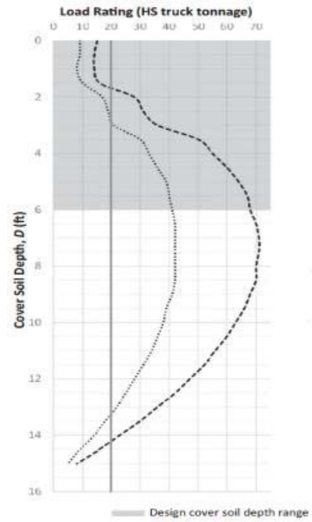

Figure 12: Effect of fill height on the load rating (adopted from Wood et al., 2015)

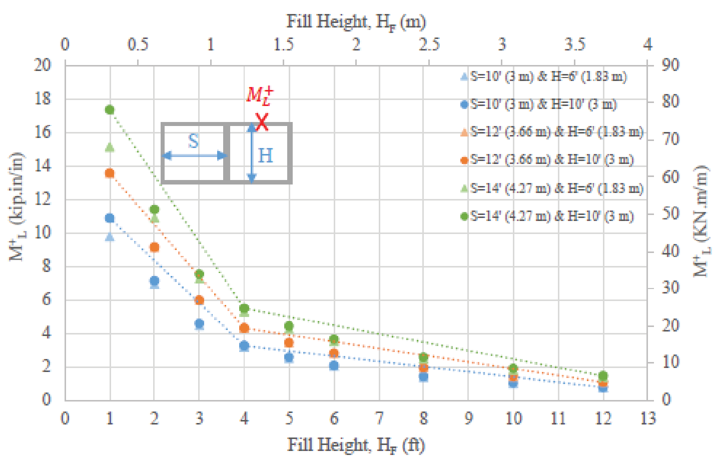

Figure 13: Effect of fill height on the positive bending moment due to live load (adopted from Acharya (2012))

3.1.5 Analysis Techniques for RC Culverts

Numerical models of buried structures can vary from a simple two-dimensional linear-elastic frame-element model to a complicated three-dimensional non-linear shell- or solid-element model. The complexity of the model and the sophistication of the constitutive relationships used for modeling culverts greatly affect the overall reliability and load rating results. As the sophistication of the models increases, some of the excess conservatism can be removed to produce higher and more accurate load ratings that closely reflect actual field conditions. Therefore, the choice of the modeling approach and standardizing modeling assumptions are essential for achieving higher load rating results where traditional simple analysis methods showed significant deficiencies.

In general, numerical modeling techniques can be categorized into two main categories, Structure Models and Soil-Structure Models. Structure models do not explicitly consider soil-structure interaction; however, structure models can be enhanced by considering some of the soil effects. Soil-structure models include modeling of the soil mass surrounding the buried structure and its interface with the structure. While soil-structure models encompass higher level of complexity in comparison to structure models, the latter is more commonly used by structural engineers for design and load rating of culverts. It should be noted however, that structure models are not always suitable for the all types of culverts, e.g. pipes, where soil-structure models are deemed more appropriate.

3.1.5.1 Two-dimensional (2-D) Frame Element Model

In two-dimensional (2-D) frame-element models a strip of the cross-section of the culvert (normal to flow) having a constant unit width (e.g. 1.0 ft. or 1.0 m), as shown in Figure 14 (a) is analyzed. The different elements of the culvert (top slab, walls, and bottom slab) are represented by linear-elastic, frame-type elements connected at nodes as shown in Figure 14 (b) utilizing frame analysis matrix methods. Generally, 2-D frame-element models are simple to construct and require less computational time.

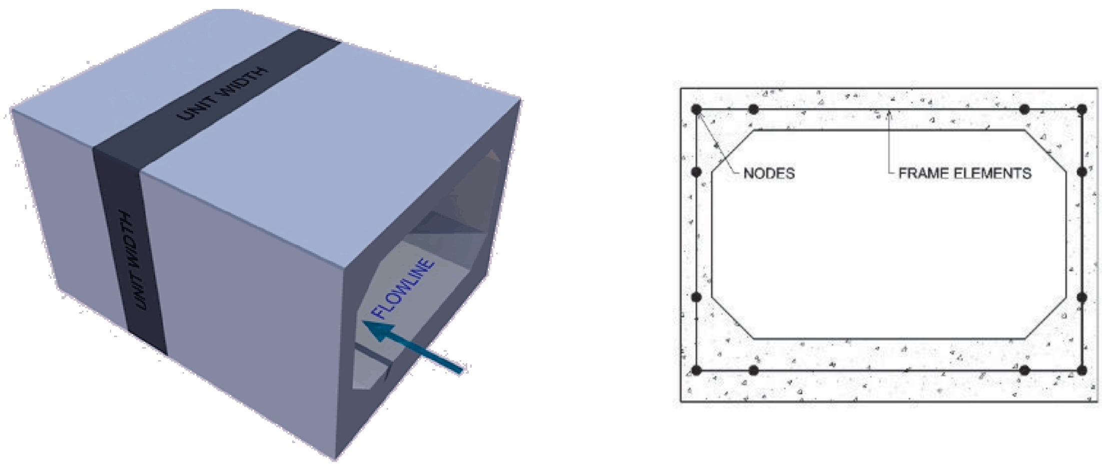

(a) idealization of 2-D frame models

(b) 2-D frame-element model

Figure 14: Idealization of two-dimensional (2-D) frame-element structural model

Typically, 2-D frame-element structural models neglect the effect of soil-structure interaction and rely on static loading to balance the load between and top and bottom slabs. Accordingly, the frame is assumed to have a knife-edge, pinned support at one end and roller support at the other end with loads applied to the top and bottom slabs, as shown in Figure 15 (a). For design purposes, the use of 2-D frame-element models without any soil consideration yields conservative designs and therefore, is acceptable. However, for load rating purposes, such over-conservatism is less desirable, especially if special heavy loads are to be considered. This modeling technique does not account for “actual” behavior and the influence of culvert geometry in resisting applied loads. While the use of this model is referenced in both the LRFD specifications and MBE, it is the least sophisticated for use in load rating and most often lead to unrealistic low load rating values (Okeil et al., 2018).

These models can be slightly enhanced by considering soil effect primarily by introducing vertical compression springs to support the bottom slab, as shown in Figure 15 (b). The use of vertical springs to mimic the supporting soil foundation rather than the use of knife-edge supports yields a better representation of the culvert boundary conditions. In this case, loads need not be applied to the bottom slab, since they will be implicitly introduced to the bottom slab as the reactions of the springs. While the model does not account for soil-structure interactions, it does account for the effect of differential settlement in the foundation and allows for more natural distributions of the applied loads across the bottom slab. This behavior is mainly dependent on the properties of the compression spring (linear or non-linear) and the relative stiffness between the soil and the bottom slab. Accordingly, this modeling technique might be suitable for some load rating cases depending on the load intensity, soil type and depth of backfill.

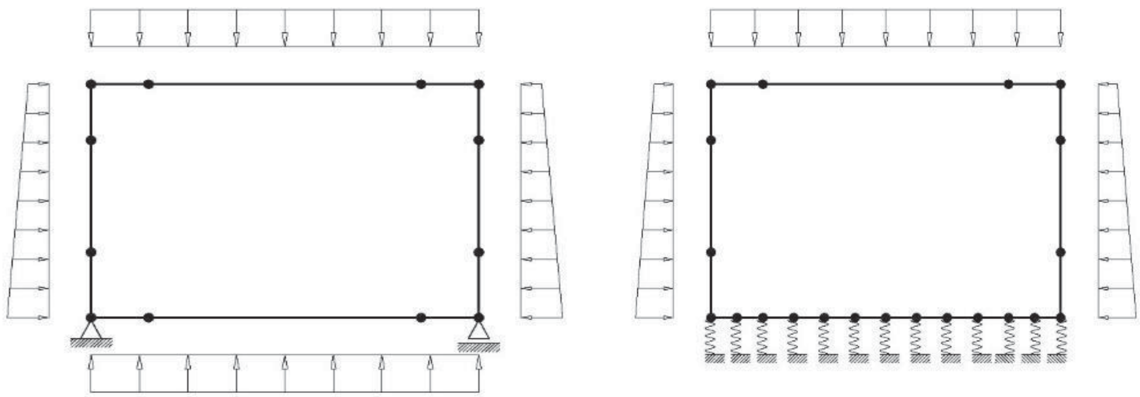

(a) Not considering soil effect

(a) Considering soil effect

Figure 15: Consideration of soil effect in two-dimensional frame-element structural models

Okeil et al. (2018) conducted a study to quantify the effect of including the soil effect as springs under the culvert bottom slab. The study showed the results from three models, two models with different spring properties and one without springs. The maximum variation of the governing forces was found to be 4.0%. Also, the maximum deflection variation between the three cases was 4.3%. In addition, the study showed that if backfill springs are added to the side walls, the spring reaction will be activated when the wall passes the original location not from the deflected position (under dead load), which doesn't represent the actual behavior of the culvert. The compression springs prevented the wall from free rotation and removing the springs yields similar rotations to those measured in field. Another study by Wood et al. (2010 showed that including the springs in the model has a negligible effect on the rating factor. Similar conclusion was drawn by M&M (2019).

3.1.5.2 Three-dimensional (3-D) Shell Element Model

Shell elements are used to model the different structural elements of the culvert including walls, top slab, bottom slab as shown in Figure 16. The entire length of the culvert is included in the model, thus accounting for the effect of continuity and enabling load distribution in two directions i.e. two-way bending action of the top slab of the culvert. Similar to 2-D frame-element model with soil effect, 3-D shell-element models utilize vertical compression springs to represent the soil foundation supporting the bottom slab. The combination of modeling the entire length of the culvert and the use of springs to represent the supporting soil renders this modeling technique as a robust tool for design and an appropriate method for load rating analysis. It is worth noting that this modeling approach is more time consuming in terms of model assembly, computation, and post-processing in comparison to 2-D frame models. However, the gain in terms of simulating the actual behavior and achieving reliable and repeatable results justifies the additional time. It should be also noted that this model does not fully account for soil-structure interaction, while differential settlement of the foundation and distributions of the live load are considered. For soil-structure interaction to be fully considered, the soil mass surrounding the culvert need to be modeled with the respective soil constitutive relationships. These types of models are identified herein as “Soil-Structural Models”.

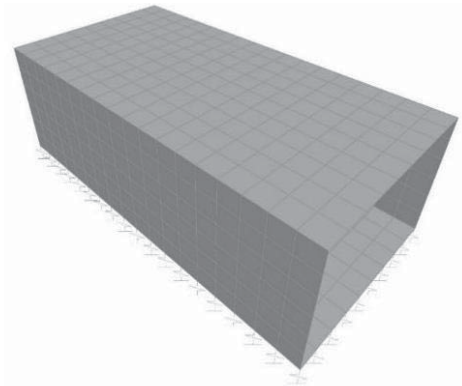

Figure 16: Three-dimensional shell-element models

The effect of the rigidity of the connection between the walls and the top slab of the culvert was investigated by Okeil et al. (2018) by introducing rigid shell elements at the corners (Figure 17). In addition, rotational springs were introduced at the connection between the walls and slabs. The stiffness of rotational springs was calibrated against the load testing results. The crack was assumed to occur at the slab which results in partial moment release at the cracked location. The rotational springs inside the wall thickness were assumed fixed while the ones inside the slab section were varied depending on the reinforcement details and experimental results.

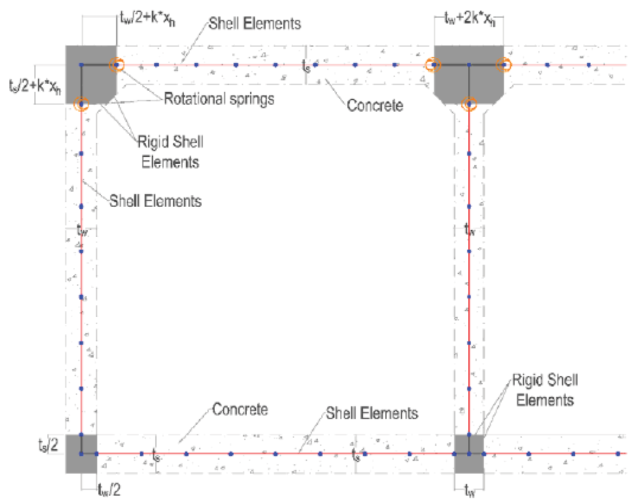

Figure 17: 3D-Modeling of culverts using shell elements with rotational springs at wall/slab connections (Okeil et al., 2018)

3.1.5.3 Two-Dimensional Soil-Structure Model

The 2-D soil-structure models represent the soil mass surrounding the culvert using finite elements and the structural members of the culvert are modeled utilizing frame elements. Several soil constitutive relationships have been developed and are available for finite element analysis of soils ranging from linear elastic to nonlinear hardening models, Lade (2005). However, Peterson el al. (2010) indicates that linear-elastic soil material behavior is inadequate to model buried structures. Surface live loads are applied to the soil mass, which in turn are transmitted to the culvert. This modeling technique allows the culvert and soil self-weights to be automatically distributed through body forces and the live load to be distributed automatically in one plane. Lawson et al. (2010), based on results from 100 TXDOT culverts inventory, showed that the load rating increases using this type of modeling compared to the spring model.

3.1.5.4 Three-Dimensional Soil-Structure Model

The 3-D soil-structure finite element model is the most sophisticated numerical analysis approach. Similar to 2-D soil-structure models, the 3-D models can utilize the wide range of constitutive soil relationships. While 3-D soil-structure model yields the most reliable results, it is computationally intensive and time consuming. Therefore, it is imperative to choose the computationally convenient soil model that can reasonably simulate the soil-structure interaction. Typically, the 2-D soil-structure model is used to select the soil constitutive model before extending these models to 3-D for full investigation of actual behavior of buried structures. Figure 18 shows a 3-D finite element mesh of the soil mass surrounding a box culvert.

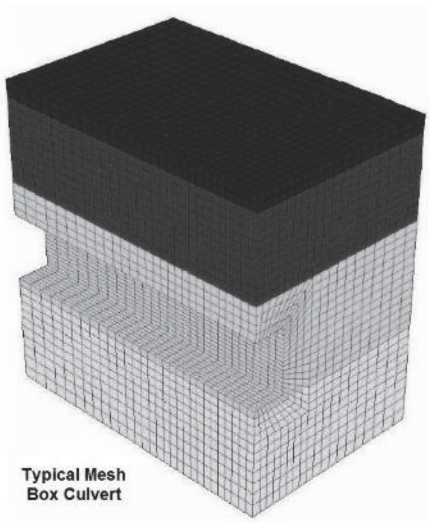

Figure 18: Three-dimensional finite element mesh of soil-structure model of box culvert

Okeil et al. (2018) performed eight load tests of CIP RC box culverts from LADOTD inventory to investigate their behavior and performance for load rating. The measured strain levels showed that the load levels were below the cracking load levels. In addition, the controlling load rating was the midspan moment in the exterior cell slabs. The test results were used to calibrate 3D-finite element models which can be used for load rating of culverts if the conventional methods resulted in low rating values. Other load tests were conducted by the Lawson et al. (2010) on three in-service RC box culverts from TxDOT inventory. The experimental test results were compared with the values from different modeling techniques. It was concluded that load tests give a very high load rating at the critical sections compared to modelling techniques which indicates that all the proposed modelling techniques can be conservatively used for load rating.

3.2 TASK 2: PRELIMINARY ANALYTICAL STUDY

Preliminary analysis was carried out using finite element modeling approach utilizing the available commercial software Midas Civil (2019). Different modelling techniques were implemented. A parametric study was performed to investigate the effect of several parameters on load rating of Multi-cell RC box culverts. The investigated parameters include number of cells, span length of cell, height of cell, depth of backfill, modulus of subgrade reaction, length of the culvert and the skew angle of culvert.

AASHTO HL-93 loading (Truck and tandem) was considered for this preliminary study. For all models, the Truck or Tandem were positioned to produce maximum internal forces in the critical sections of the top slab of the culvert.

The preliminary study results indicated several parameters could influence the load rating of the culverts. The influential parameters were found to be the span length of the cell, depth of fill, the culvert length and the length/total width ratio of the culvert. In the light of the results, a FE models' matrix was developed for the parametric study in Phase II. The models included in the matrix were configured to cover possible configurations for the culverts and, in the meantime, consider the findings from LADOTD culvert inventory classification presented in Task 3 in the following section.

Details of the preliminary analytical study along with the results can be found in Phase I report.

3.3 TASK 3: LADOTD RC CULVERT INVENTORY AND SELECTION OF 100 REPRESENTATIVE CULVERTS

A detailed study of LADOTD culvert inventory was performed and the inventory was classified based on different parameters including; number of cells, span length of cell, total width of culvert, depth of backfill, length of culvert and skew angle of the culvert. The results of the study are presented in the following sections:

3.3.1 Inventory Classification

The total number of the studied CIP RC box culverts in LADOTD inventory is *1509* culverts, as shown in Figure 19. This study focuses only on multi-cell culverts with total span length more than or equals to 20 feet. Previous studies have indicated that multicell culverts with number of cells exceeding *4* can be conservatively modeled and analyzed as *4* cell culverts.

Therefore, a total of *416* culverts of the inventory were excluded from further investigation. The excluded culverts consist of the following: single cell culverts *(77)*; multi-cell culverts that do not have a project number or plans *(202)*; and finally culverts with number of cells more than 5 cells *(137)*.

Therefore, the total number of culverts considered for the investigation is *1093* culverts. The following section presents the inspection of LADOTD culvert inventory and identifying the counts of the culverts based on different parameters that affects the load rating of the RC box culverts.

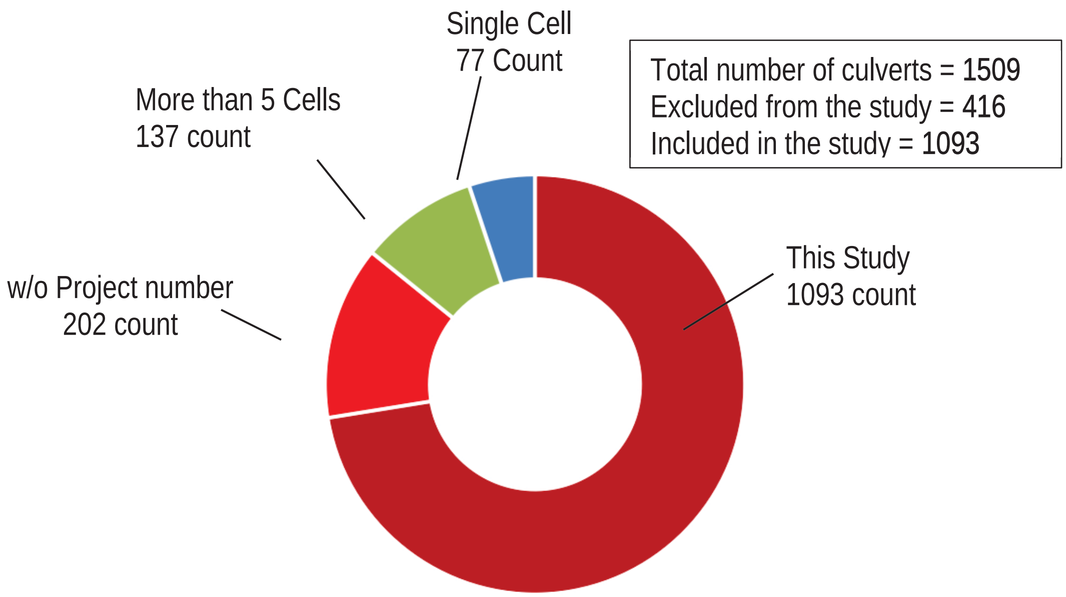

Figure 19: Classification of LADOTD inventory for CIP RC box culverts

This section presents the classification of the 1018 culverts of LADOTD culvert inventory based on different parameters considered in this study. The inventory classification is presented using pie charts showing counts and percentages for each parameter. Based on the literature, six parameters believed to affect the load rating were selected for investigation. The selected parameters include number of cells; span length of the cell; total span length of culvert, depth of backfill, length of culvert and skew angle.

Results of the inventory inspection were used to conduct a preliminary analytical study and to select the 100 representative culverts from the inventory.

3.3.1.1 Number of Cells

Figure 20 shows the classification of the inventory based on the number of cells of the culvert. It can be seen from the figure that culverts with 3 and 4 cells constitute more than 70 percent of the inventory. This entails more emphasis for the 3 and 4 multicell culverts in the analytical program and field testing to be conducted in phase II of this project.

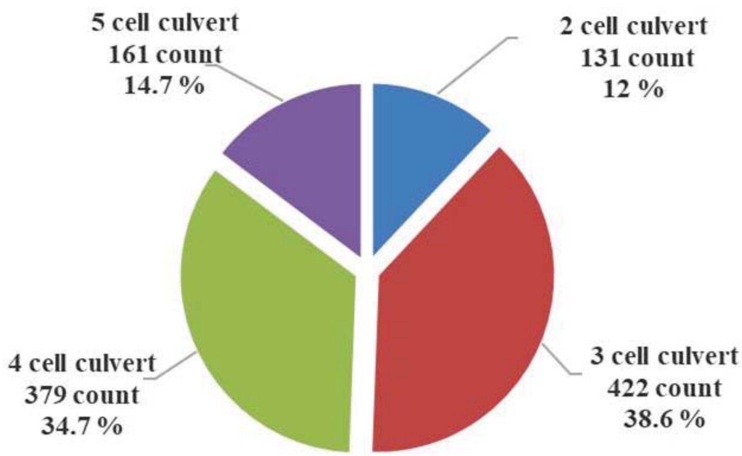

Figure 20: Classification based on the number of cells

3.3.1.2 Span Length of Cell

Figure 21 shows the classification of the inventory based on maximum span length of the cell opening. The figure shows clearly that 8 ft to 10 ft. span lengths constitute together more than 45 percent of the inventory. Also, span length ranges between 5 ft. to 7 ft. represents more than 40 percent of the inventory. Therefore, span lengths form 5 ft. to 10 ft. constitute more than 85% of the inventory. The 5 ft. to 10 ft. span length range was selected for preliminary analysis.

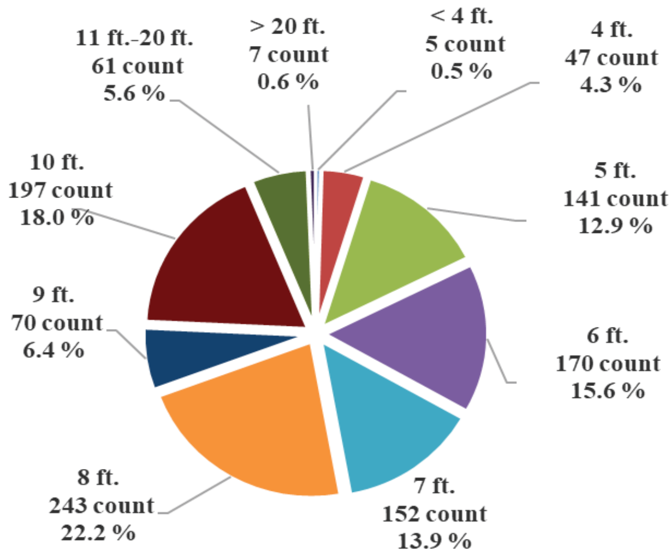

Figure 21: Classification based on span length of the cell

3.3.1.3 Total Width of the Culvert

The total width of the culvert is defined as the distance between the inside faces of the external walls of the culvert. Figure 22 shows the classification of the inventory based on the total width of the culvert. It can be seen from the figure that culverts with total width between 20 ft. and 25ft. constitute more than 30 percent of the inventory. In general, culverts with total width ranging from 20 ft to 35 ft. represents more than 80 percent of the inventory.

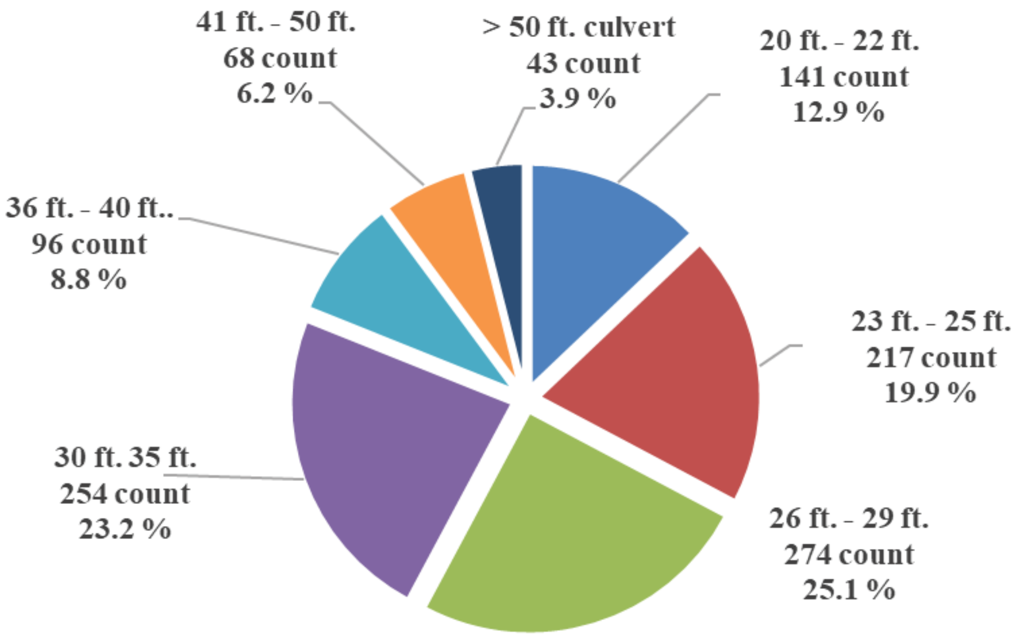

Figure 22: Classification based on the total width of the culvert

3.3.1.4 Height of Fill

Figure 23 shows the classification of LADOTD culvert inventory based on the height of the backfill above the top slab of the culvert. It can be seen from the figure that culverts with shallow fill heights less than 2 ft. represents approximately, 24 percent of the inventory. Also, culverts with medium fill heights (between 2ft. and 4 ft.) represent approximately, 46 percent of the inventory, while culverts with deeper backfills (4 ft. < H_f < 8 ft.) are 24 % percent and finally culverts with fill heights larger than 8 ft. are only 6 percent of the inventory. Therefore, shallow and medium fill height culverts constitute majority of the inventory.

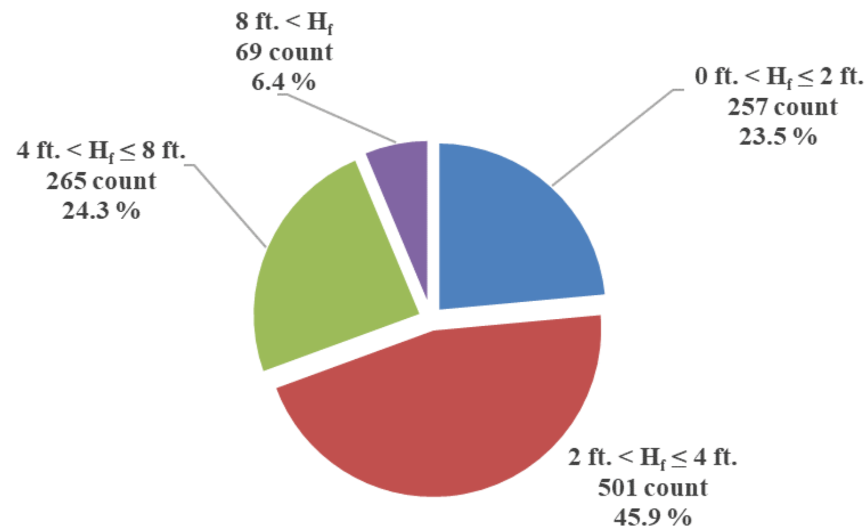

Figure 23: Classification of the inventory based on height of backfill

3.3.1.5 Length of Culvert

Figure 24 shows classification of the culvert inventory based on the length of the culvert. It can be seen from the figure that the length data for 363 culverts (33 percent of culverts) was missing. Culverts with lengths ranging between 20 ft. and 36 ft., which is representative of a two (2) lane roadway, constitutes almost 9 percent of the inventory. Culverts with total length ranging from 36 ft to 48 ft., which is representative of a three (3) lane roadway, constitutes almost 20 percent of the inventory. Finally, culverts with total lengths greater than 48 ft. represent 38 percent of the inventory.

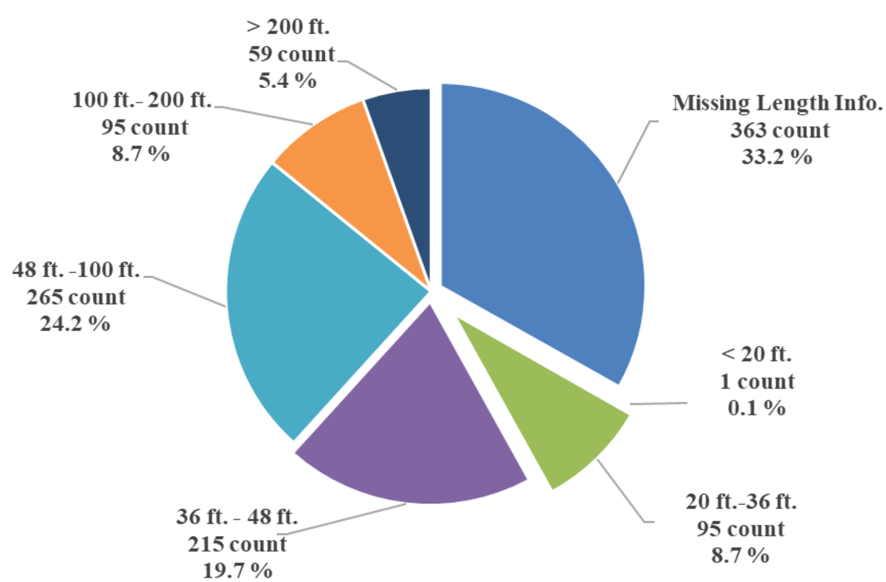

Figure 24: Classification of the inventory based on length of culvert

3.3.1.6 Length to Total Width Ratio

The length to total width ratio of the culvert was found to be a significant parameter that affects the load distribution within the top slab of the culvert. Therefore, this ratio was determined for all culverts in the inventory and the inventory was classified based on that ratio as shown in Figure 25. As can be seen from the figure that the data for the length/width ratio was missing for 363 culverts (33 percent of culverts). Culverts with ratios between 0 and 2 constituted almost 35 percent of the inventory. Culverts with ratios between 2 and 6 constituted almost 26 percent of the inventory. Culverts with ratios higher than 6 constituted almost 6.5 percent of the inventory.

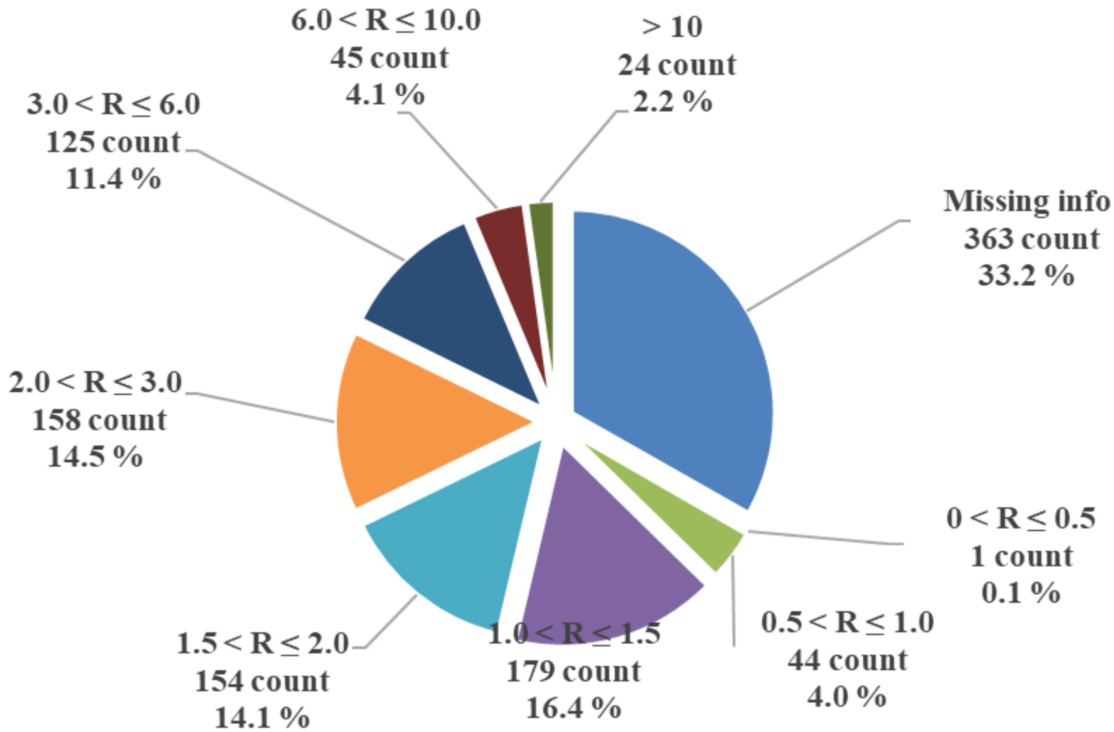

Figure 25: Classification of the inventory based on culvert length/width ratio

3.3.1.7 Skew Angle of Culvert

Figure 26 shows the classification of the culvert based on skew angle of the culvert. It can be seen from the figure that majority of the culverts have a skew angle equals to 0° with a percentage more than 70 percent.

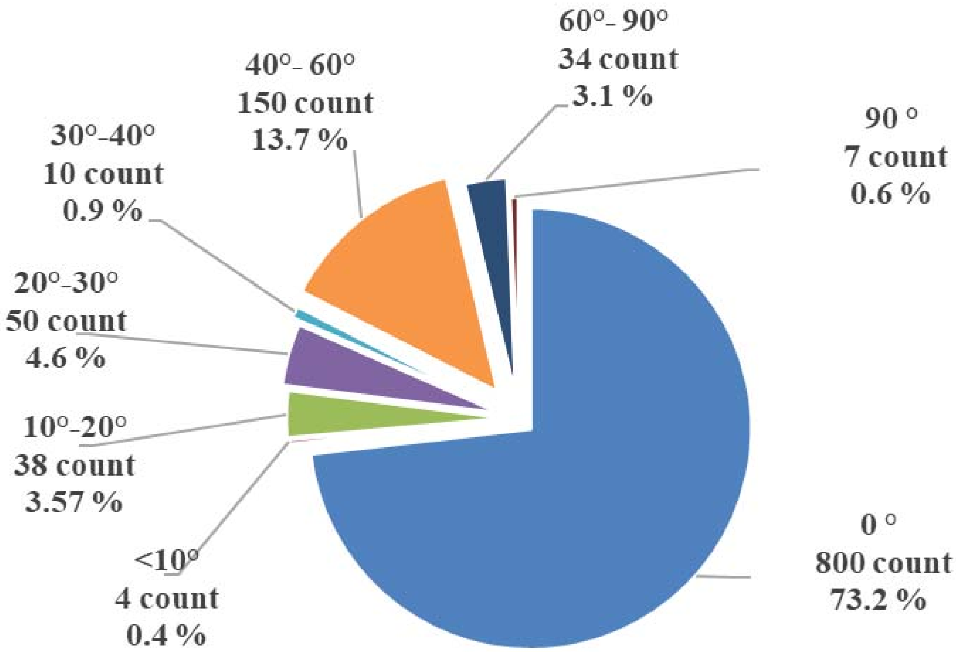

Figure 26: Classification of the inventory based on skew angle

3.3.2 Selection of 100 Representative Culverts from LADOTD Inventory

3.3.2.1 Selection Criteria and Grouping

100 representative culverts of Louisiana inventory were selected for evaluation and load rating based on the guidelines to be developed in Phase II of the project. Based on the inventory inspection results and the preliminary analytical results presented in the previous sections; 100 representative culverts were selected from the inventory for further evaluation and load rating. The 100 culverts were grouped into four (4) categories based on the key parameters. The parameters included depth of fill, span length, length of culvert and skew angle.

4. PHASE II PROGRAM

4.1 TASK 4: PARAMETRIC STUDY

The main objective of conducting the parametric study is to develop correction factors that can correlate moments values obtained from the sophisticated 3D FE models with those obtained from conventional 2D models.

4.1.1 FE Models Matrix

The Results of LADOTD inventory classification along with the preliminary analytical study were used to develop an analytical model matrix to capture the effects of cell size, backfill height and culvert length. Those parameters were found to be the most influential parameters in the preliminary study conducted in Phase-I. The geometrics and soil parameters for the culverts in the matrix were designed to represent culvert configurations that constitute majority of the LADOTD's inventory. Table 1 shows the matrix developed for the parametric study. A total of *(120)* 3D models and *(30)* 2D models were built to develop the correction factors.

As can be seen from the matrix in Table 1, five culvert sizes were considered in the study including 5 ft. x 5 ft., 7 ft. x 7 ft., 8 ft. x 8 ft., 10 ft. x 10 ft. and 12 ft. x 12 ft. culverts. The corresponding slab and wall thicknesses were obtained based on LADOTD standard plans. Six backfill heights were considered in the study including 1.0 ft, 2.0 ft., 3.0 ft, 4.0 ft., 6.0 ft., and 9.0 ft. The selected fill heights represent shallow, medium, and deep fills. The backfill heights include the wearing surface thickness. It is worth noting that inspection of the culvert inventory revealed that no culverts had backfill heights exceeding 8.8 ft. and therefore a maximum fill height of 9 ft. was considered in the study.

The culvert total length in the direction perpendicular to the culvert span was varied such that the culvert length to width ratio (L/W) varied from 1.0 to 3.0. The following L/W ratios were considered in the analysis: 1.0, 1.5, 2.0, and 3.0. The culvert inventory classification indicated very few culverts with length/width ratio below 1.0 and therefore the study focused on the range 1 to 3 which represents majority of the inventory.

Five (5) culvert sizes, six (6) fill heights and four (4) length/width ratios constituted the 120 3D FE models.

It should be noted that five (5) models were added later to the matrix to consider fill heights equal to 1.99 ft. which is slightly below 2 ft. This is because AASHTO implements formulas for live load distribution on the top slab of the culvert for fill heights less than 2 ft. and other formulas for fill heights greater than 2 ft. Therefore, the 2 ft. fill height represents a borderline between the two load distribution methodologies.

The material properties and boundary conditions were kept constant for all models. The unit concrete weight was taken equals to $0.15\ kcf$ with a compressive strength equals to $3.0\ ksi$. A 6-inch wearing surface was assumed with unit weight equals to $0.140\ kcf$. A modulus of subgrade reaction of $0.15 \frac{kip}{in^2}/in$ was used for determining the stiffness of the linear soil springs used in the 2D and 3D models. The soil unit weight was taken equal to $0.120\ kcf$. The culverts were assumed to have uniform fill depth along the culvert length. The at-rest lateral earth pressure coefficient, K_O, was taken equal to 0.50.

Table 1: FE Models Matrix

Model No.	Number of Cells	Span length S (ft)	Height- H (ft)	Total Width W (ft)	Total length L (ft)	Length/Width Ratio L/W	Fill Depth H_f (ft.)
C1	3	5	5	17	17	1.0	1.0
C2	3	5	5	17	17	1.0	2.0
C3	3	5	5	17	17	1.0	3.0
C4	3	5	5	17	17	1.0	4.0
C5	3	5	5	17	17	1.0	6.0
C6	3	5	5	17	17	1.0	9.0
C7	3	7	7	23	23	1.0	1.0
C8	3	7	7	23	23	1.0	2.0
C9	3	7	7	23	23	1.0	3.0
C10	3	7	7	23	23	1.0	4.0
C11	3	7	7	23	23	1.0	6.0
C12	3	7	7	23	23	1.0	9.0
C13	3	8	8	26	26	1.0	1.0
C14	3	8	8	26	26	1.0	2.0
C15	3	8	8	26	26	1.0	3.0
C16	3	8	8	26	26	1.0	4.0
C17	3	8	8	26	26	1.0	6.0
C18	3	8	8	26	26	1.0	9.0
C19	3	10	10	32	32	1.0	1.0
C20	3	10	10	32	32	1.0	2.0
C21	3	10	10	32	32	1.0	3.0
C22	3	10	10	32	32	1.0	4.0
C23	3	10	10	32	32	1.0	6.0
C24	3	10	10	32	32	1.0	9.0
C25	3	12	12	39	39	1.0	1.0
C26	3	12	12	39	39	1.0	2.0
C27	3	12	12	39	39	1.0	3.0
C28	3	12	12	39	39	1.0	4.0
C29	3	12	12	39	39	1.0	6.0
C30	3	12	12	39	39	1.0	9.0

Table 1 (Cont'd): FE Models Matrix

Model No.	Number of Cells	Span length S (ft)	Height- H (ft)	Total Width W (ft)	Total length L (ft)	Length/Width Ratio L/W	Fill Depth H_f (ft.)
C31	3	5	5	17	25	1.5	1.0
C32	3	5	5	17	25	1.5	2.0
C33	3	5	5	17	25	1.5	3.0
C34	3	5	5	17	25	1.5	4.0
C35	3	5	5	17	25	1.5	6.0
C36	3	5	5	17	25	1.5	9.0
C37	3	7	7	23	34	1.5	1.0
C38	3	7	7	23	34	1.5	2.0
C39	3	7	7	23	34	1.5	3.0
C40	3	7	7	23	34	1.5	4.0
C41	3	7	7	23	34	1.5	6.0
C42	3	7	7	23	34	1.5	9.0
C43	3	8	8	26	38	1.5	1.0
C44	3	8	8	26	38	1.5	2.0
C45	3	8	8	26	38	1.5	3.0
C46	3	8	8	26	38	1.5	4.0
C47	3	8	8	26	38	1.5	6.0
C48	3	8	8	26	38	1.5	9.0
C49	3	10	10	32	47	1.5	1.0
C50	3	10	10	32	47	1.5	2.0
C51	3	10	10	32	47	1.5	3.0
C52	3	10	10	32	47	1.5	4.0
C53	3	10	10	32	47	1.5	6.0
C54	3	10	10	32	47	1.5	9.0
C55	3	12	12	39	57	1.5	1.0
C56	3	12	12	39	57	1.5	2.0
C57	3	12	12	39	57	1.5	3.0
C58	3	12	12	39	57	1.5	4.0
C59	3	12	12	39	57	1.5	6.0
C60	3	12	12	39	57	1.5	9.0

Table 1 (Cont'd): FE Models Matrix

Model No.	Number of Cells	Span length S (ft)	Height H (ft)	Total Width W (ft)	Total length L (ft)	Length/Width Ratio L/W	Fill Depth H_f (ft.)
C61	3	5	5	17	33	2.0	1.0
C62	3	5	5	17	33	2.0	1.99
C62	3	5	5	17	33	2.0	2.0
C63	3	5	5	17	33	2.0	3.0
C64	3	5	5	17	33	2.0	4.0
C65	3	5	5	17	33	2.0	6.0
C66	3	5	5	17	33	2.0	9.0
C67	3	7	7	23	45	2.0	1.0
C68*	3	7	7	23	45	2.0	1.99
C68	3	7	7	23	45	2.0	2.0
C69	3	7	7	23	45	2.0	3.0
C70	3	7	7	23	45	2.0	4.0
C71	3	7	7	23	45	2.0	6.0
C72	3	7	7	23	45	2.0	9.0
C73	3	8	8	26	50	2.0	1.0
C74*	3	8	8	26	50	2.0	1.99
C74	3	8	8	26	50	2.0	2.0
C75	3	8	8	26	50	2.0	3.0
C76	3	8	8	26	50	2.0	4.0
C77	3	8	8	26	50	2.0	6.0
C78	3	8	8	26	50	2.0	9.0
C79	3	10	10	32	64	2.0	1.0
C80*	3	10	10	32	64	2.0	1.99
C80	3	10	10	32	64	2.0	2.0
C81	3	10	10	32	64	2.0	3.0
C82	3	10	10	32	64	2.0	4.0
C83	3	10	10	32	64	2.0	6.0
C84	3	10	10	32	64	2.0	9.0
C85	3	12	12	39	77	2.0	1.0
C86*	3	12	12	39	77	2.0	1.99
C86	3	12	12	39	77	2.0	2.0
C87	3	12	12	39	77	2.0	3.0
C88	3	12	12	39	77	2.0	4.0
C89	3	12	12	39	77	2.0	6.0
C90	3	12	12	39	77	2.0	9.0

Table 1 (Cont'd): FE Models Matrix

Model No.	Number of Cells	Span length S (ft)	Height H (ft)	Total Width W (ft)	Total length L (ft)	Length/Width Ratio L/W	Fill Depth H_f (ft.)
C91	3	5	5	17	50	3.0	1.0
C92	3	5	5	17	50	3.0	2.0
C93	3	5	5	17	50	3.0	3.0
C94	3	5	5	17	50	3.0	4.0
C95	3	5	5	17	50	3.0	6.0
C96	3	5	5	17	50	3.0	9.0
C97	3	7	7	23	68	3.0	1.0
C98	3	7	7	23	68	3.0	2.0
C99	3	7	7	23	68	3.0	3.0
C100	3	7	7	23	68	3.0	4.0
C101	3	7	7	23	68	3.0	6.0
C102	3	7	7	23	68	3.0	9.0
C103	3	8	8	26	77	3.0	1.0
C104	3	8	8	26	77	3.0	2.0
C105	3	8	8	26	77	3.0	3.0
C106	3	8	8	26	77	3.0	4.0
C107	3	8	8	26	77	3.0	6.0
C108	3	8	8	26	77	3.0	9.0
C109	3	10	10	32	94	3.0	1.0
C110	3	10	10	32	94	3.0	2.0
C111	3	10	10	32	94	3.0	3.0
C112	3	10	10	32	94	3.0	4.0
C113	3	10	10	32	94	3.0	6.0
C114	3	10	10	32	94	3.0	9.0
C115	3	12	12	39	117	3.0	1.0
C116	3	12	12	39	117	3.0	2.0
C117	3	12	12	39	117	3.0	3.0
C118	3	12	12	39	117	3.0	4.0
C119	3	12	12	39	117	3.0	6.0
C120	3	12	12	39	117	3.0	9.0

4.1.2 Finite Element Model Development

4.1.2.1 Two-Dimensional FE Model

Parallel analysis utilizing Two-dimensional (2-D) was also performed. The beam element is defined by two nodes with six degrees of freedom (DOF) at each node (three rotational DOF and three translational DOF). Beam elements were utilized to model the top/bottom slab sections and the wall sections. The beam element formulation is based on the "Timoshenko Beam Theory", which considers the stiffness effects of tension/compression, shear, bending, and torsional deformations. All wall/slab connections were assumed to be rigid connections (allow moment transfer). Linear compression springs were assigned at the bottom slab with one node connected to the slab, and the other node is fixed. Figure 27 shows a typical 2-D frame element model used for modeling the culverts.

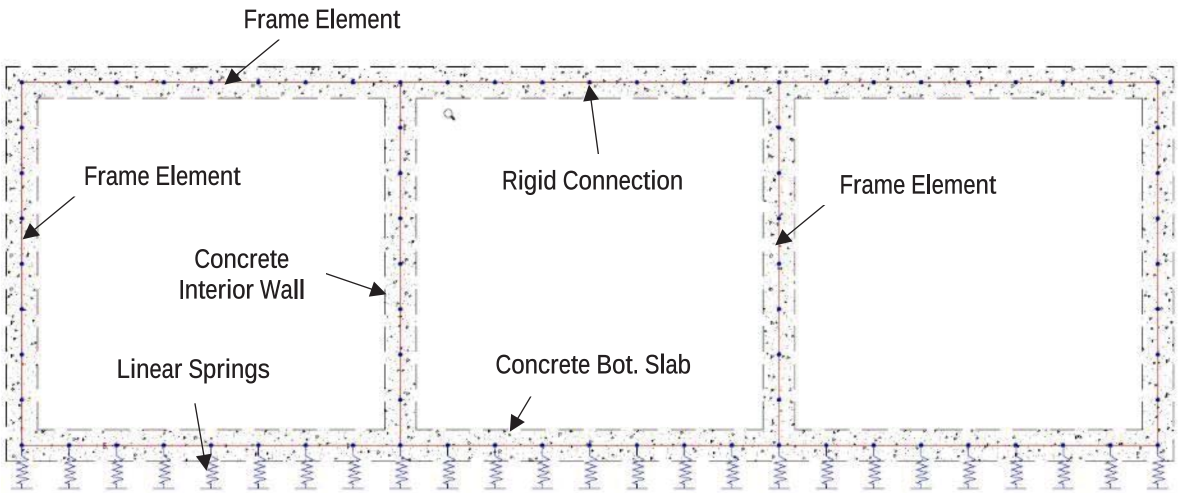

Figure 27: Schematic representation of the 2-D frame element model

4.1.2.2 Three-Dimensional FE Model

Three-dimensional (3-D) FE models were generated. Plate elements were utilized to model the top/bottom slabs and the walls of the culverts. The plate element accounts for in-plane tension/compression, in-plane/out-of-plane shear, and out-of-plane bending behaviors. Each node of the plate elements has five degrees of freedom (three translational and two rotational) those degrees of freedom are multiplied by the corresponding stiffness to generate the nodal forces, as shown in Figure 28. The plate element can be defined using three or four nodes located on the same plane. The out-of-plane stiffness can be based on either thin plate theory (Kirchhoff element) or thick plate theory (Kirchhoff-Mindlin element). Similar to the 2D model, all wall/slab connections were assumed to be rigid connections. Linear compression springs were applied at the bottom slab. Figure 29 shows a typical 3-D model used for culvert modeling.

As shown in Figure 29, the edge beams located at the begin and end of the culverts were included in the model. It is believed that those edge beams provide additional stiffness at the end of the slab that can influence the load distribution in the two directions of the slab. Those edge beams are also shown in the standard plans.

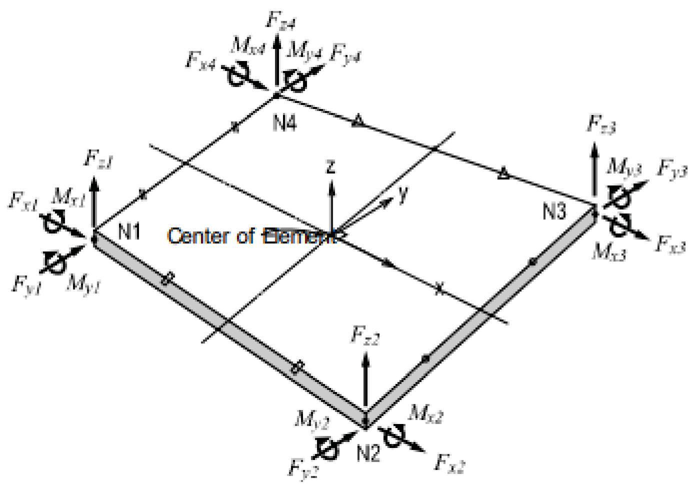

Figure 28: Nodal forces for the plate element

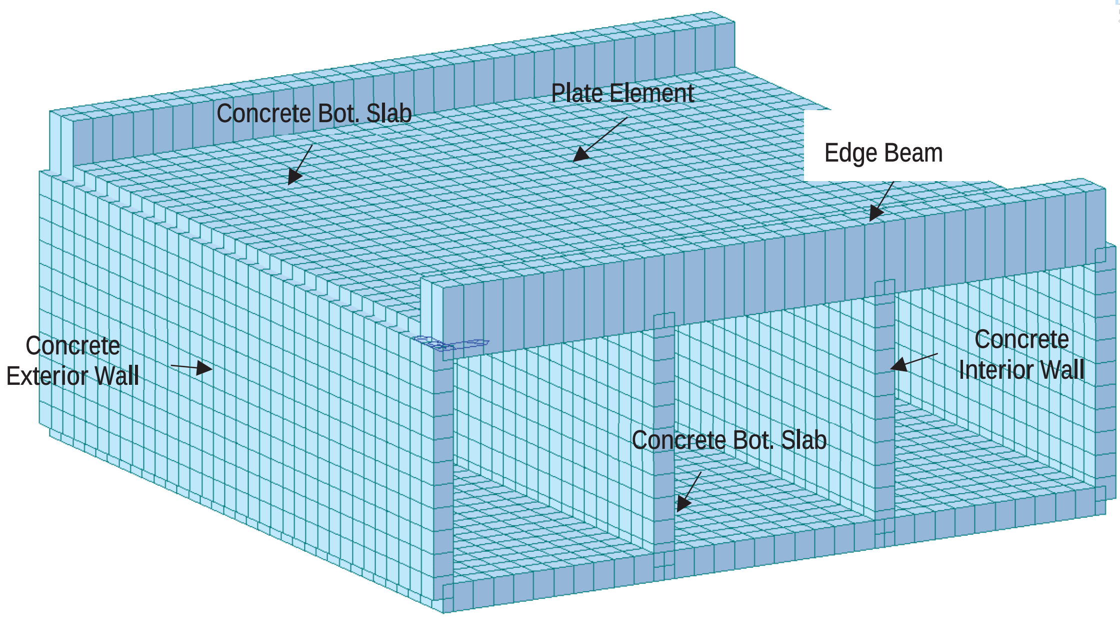

Figure 29: Typical 3-D shell element model

4.1.2.3 Load Cases and positioning

The main objective of the parametric study is to develop correction factors that can be used to correlate the moments obtained from 3D models and 2D models. Given the fact that dead loading generates the same internal forces for both modeling techniques, therefore the correction factors were developed for live load only.

Besides, the results from the preliminary analytical study conducted in Phase I indicated that most of the culverts were controlled by the HL-93 tandem loading owing to the close spacing between the axles of the tandem. The research team agreed with LADOTD to conduct the parametric study using the HL-93 tandem loading only. The tandem loading was positioned on the top slab such that maximum internal forces can be generated at the key sections under investigation. Positioning of the tandem loading was based on influence line diagrams generated at those sections. Figure 30 shows the location of positive and negative moment sections under investigation, along with the tandem loading positioning. Two positive sections were selected in the middle of exterior and interior spans, as shown in Figure 30 (a) and (b). Two sections were chosen to investigate the negative moment at both the exterior wall and the interior wall, as shown in Figure 30 c-d.

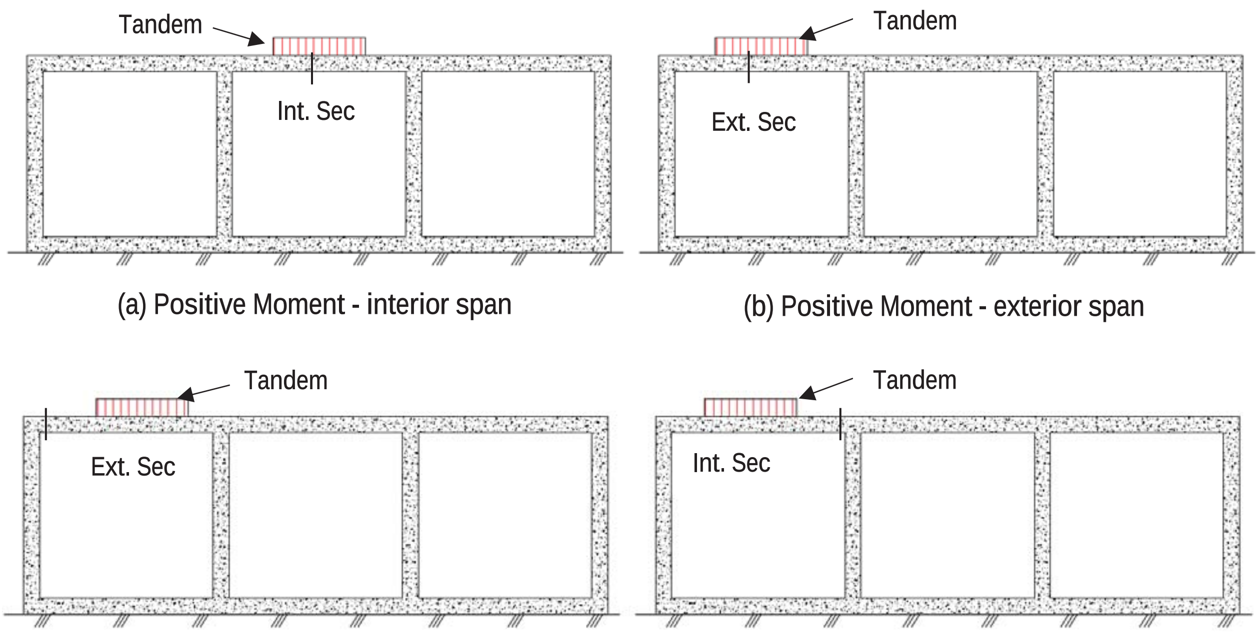

(a) Positive Moment - interior span

(b) Positive Moment - exterior span

(a) Negative Moment - exterior wall

(b) Negative Moment - interior wall

Figure 30: Positioning of Tandem loading to produce maximum positive and negative moments at midspan and wall sections of the exterior and interior cells

AASHTO Live load distribution procedures indicate that the load intensity and configuration on the surface of the top slab varies with the backfill height. The intensity of the live loading on the top slab of the culvert was determined for each fill height in accordance with AASHTO-LRFD (2017) and all cases are summarized in Table 2. It can be seen that the load intensity decreases with the increase of the backfill height. Also, the configuration of the live load at the surface of the top slab varies depending on the fill height. (See Figure 32)

For fill heights less than 2.0 ft., each axel of the tandem is distributed on one loaded area perpendicular to the culvert span, as shown in

Figure 31a. For fill heights equal or greater than 2.0 ft., the live load can be distributed on either four separate areas with each area centered with each of the tandem wheels (

Figure 31b), or two loaded areas parallel to the culvert span (

Figure 31c), or finally one area centered with the four tandem wheels (

Figure 31d).

The roadway configuration and location with respect to the culvert length was configured such that, after the load is distributed through fill, the entire loaded area remains within the culvert length limits. Figure 32 shows an example of the live load distribution on the top slab for 5 x 5 culverts for different fill heights. Figure 33 shows the live load distribution in the direction perpendicular to the culvert span.

Table 2: Live load intensity on the top slab of the culvert

Model No.	Size (ft. X ft.)	Total Width W (ft)	Fill Depth H_f (ft.)	Distribution Length W_w (ft.)	Distribution Width L_w (ft.)	Area (ft.^{2})	Live load Intensity (kip/ft.^{2})
C1	5x5	16.5	1.0	9.0	2.0	18.0	2.15
C2	5x5	16.5	2.0	4.5	3.0	13.5	1.39
C3	5x5	16.5	3.0	5.5	8.0	44.0	0.82
C4	5x5	16.5	4.0	12.5	9.0	112.5	0.62
C5	5x5	16.5	6.0	15.0	11.5	172.5	0.38
C6	5x5	16.5	9.0	18.0	15.0	270.0	0.22
C7	7x7	22.5	1.0	9.0	2.0	18.2	2.12
C8	7x7	22.5	2.0	4.5	3.0	13.7	1.37
C9	7x7	22.5	3.0	5.5	8.1	44.5	0.81
C10	7x7	22.5	4.0	12.5	9.1	113.8	0.61
C11	7x7	22.5	6.0	15.0	11.6	174.4	0.37
C12	7x7	22.5	9.0	18.0	15.2	273.0	0.22
C13	8x8	25.5	1.0	9.0	2.0	18.4	2.11
C14	8x8	25.5	2.0	4.5	3.1	13.8	1.36
C15	8x8	25.5	3.0	5.5	8.2	44.9	0.81
C16	8x8	25.5	4.0	12.5	9.2	114.7	0.61
C17	8x8	25.5	6.0	15.0	11.7	175.9	0.37
C18	8x8	25.5	9.0	18.0	14.8	266.1	0.23
C19	10x10	31.5	1.0	9.5	2.0	18.7	2.07
C20	10x10	31.5	2.0	5.0	3.0	14.8	1.27
C21	10x10	31.5	3.0	5.5	7.9	43.3	0.84
C22	10x10	31.5	4.0	12.5	8.9	110.8	0.63
C23	10x10	31.5	6.0	15.0	11.3	169.9	0.38
C24	10x10	31.5	9.0	18.5	14.8	273.3	0.22
C25	12x12	39.0	1.0	9.5	2.0	19.0	2.03
C26	12x12	39.0	2.0	5.0	3.0	15.0	1.25
C27	12x12	39.0	3.0	5.5	8.0	44.0	0.82
C28	12x12	39.0	4.0	12.5	9.0	112.5	0.62
C29	12x12	39.0	6.0	15.0	11.5	172.5	0.38
C30	12x12	39.0	9.0	18.5	15.0	277.5	0.22

The live load distribution in the directions parallel and perpendicular to the culvert spans are provided for all culvert sizes in Appendix A.

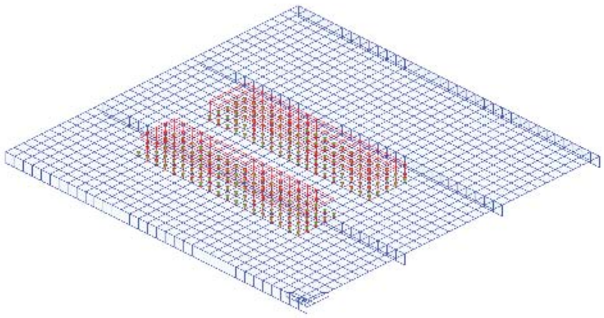

(a) Two Perpendicular batches (1 ft. fill height)

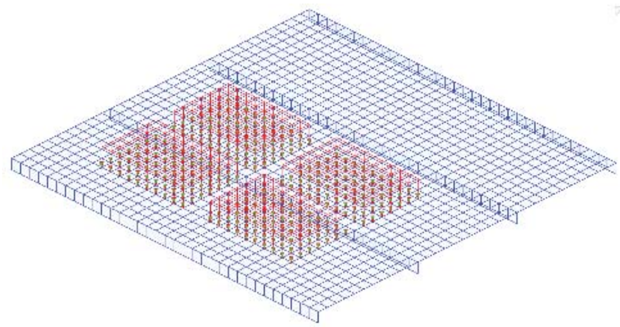

(b) Four separate batches (2 ft. fill height)

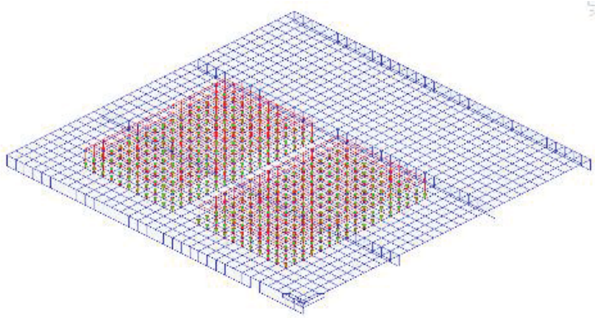

(c) Two parallel batches (3 ft. fill height)

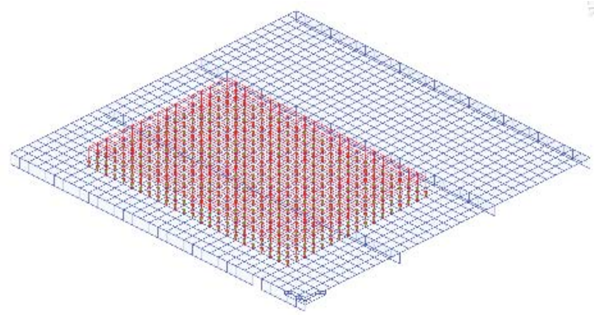

(d) One batch (4 ft. to 9 ft. fill height)

Figure 31: Live load configurations at the surface of the top slab

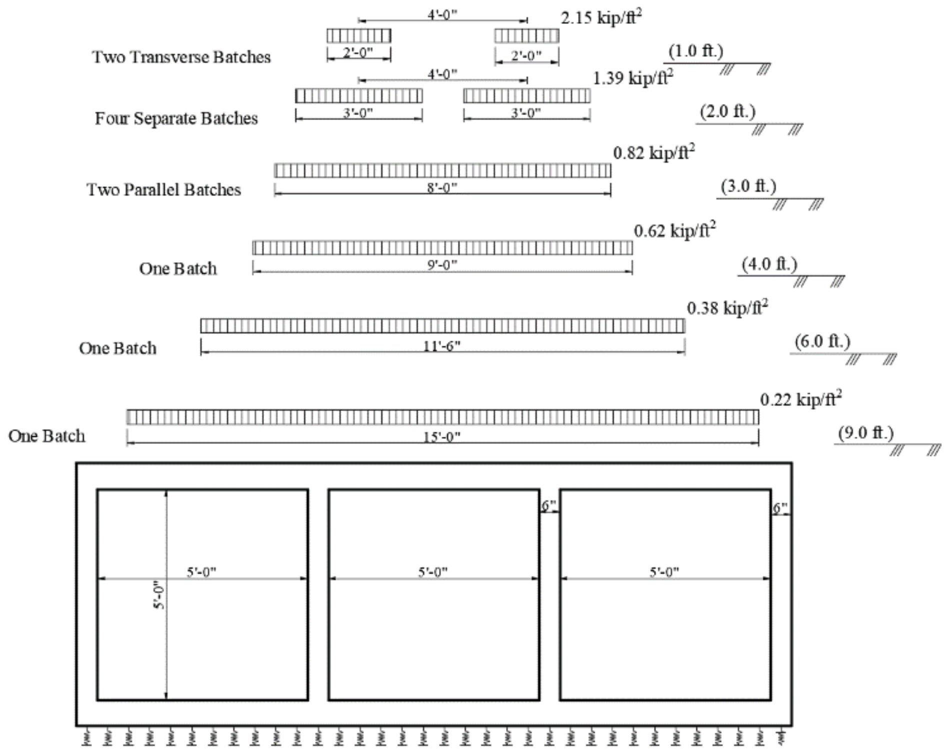

Figure 32: Live load distribution at the surface of the top slab in the direction parallel to culvert span for different fill heights

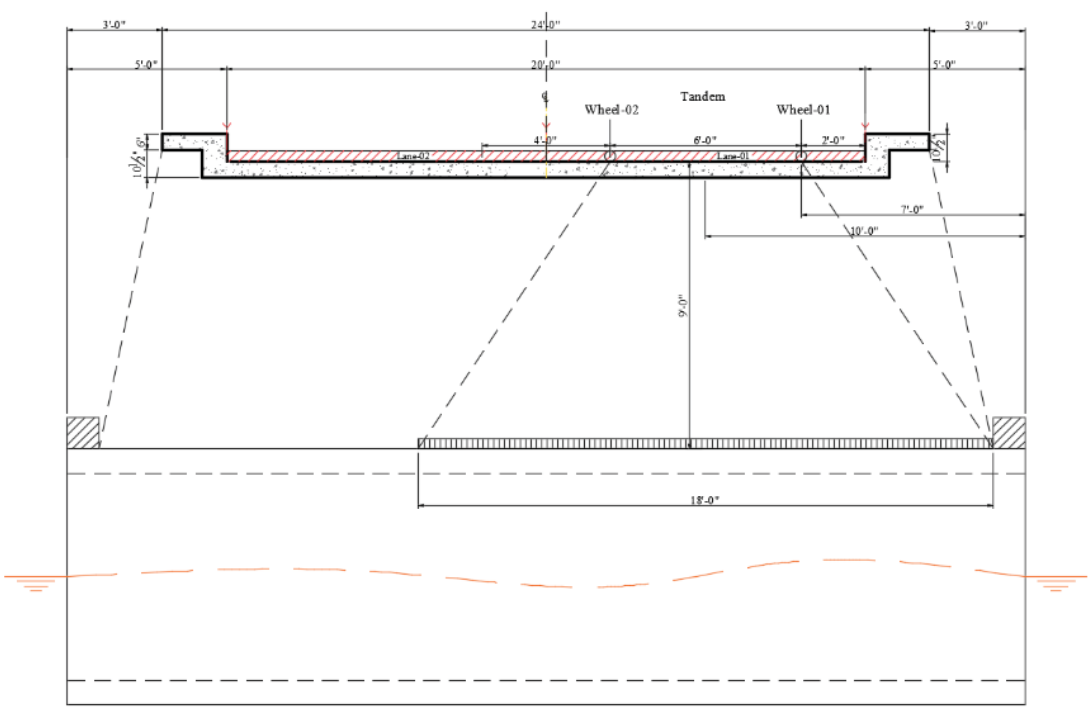

Figure 33: Truck positioning in the direction perpendicular to culvert span

4.1.3 Parametric Study Results

The analysis was performed, and the results were extracted at the identified critical sections of the top slab. Sample results for the 12 x12 culverts are presented in **Figure 34**. Same findings are valid to other culvert sizes (5 x5, 7x7, 8x8 and 10x10).

The charts in **Figure 34** shows the variation of the live load moment with the culvert Length/Width (L/W) ratio for the six fill heights (1.0, 2.0, 3.0, 4.0, 6.0 and 9.0 ft.). The live load moments were extracted at the critical sections from the 3D models. As can be seen form the results, the live load moments exhibited no variation for the this investigated domain of L/W ratios (1.0 to 3.0). Based on this finding, it was decided to develop the moment correction factors for different culvert sizes based on the results extracted for the culvert Length/Width ratio of 2.0 which is considered representative of the other L/W ratios (1.0, 1.5 and 3.0).

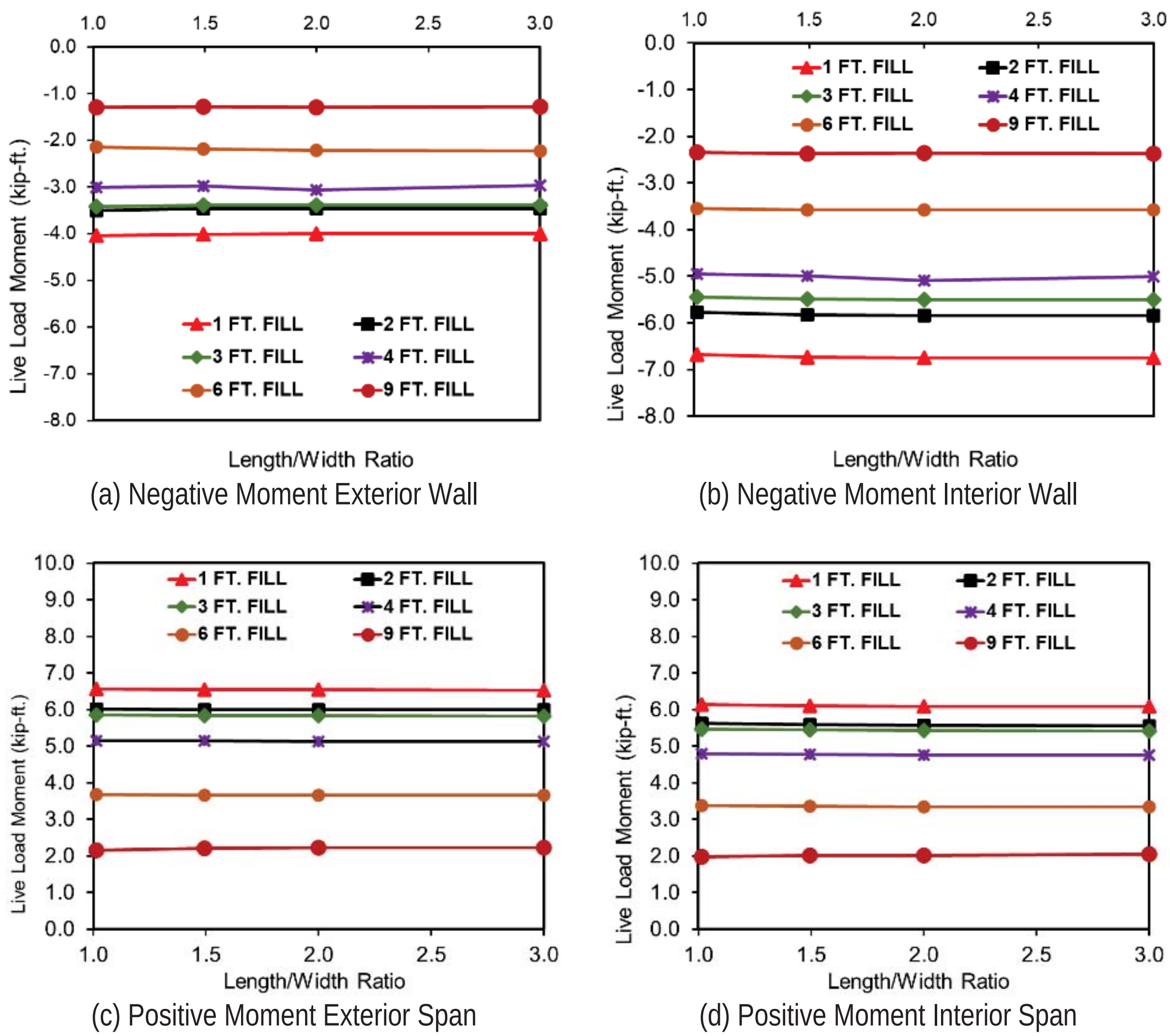

(a) Negative Moment Exterior Wall

(b) Negative Moment Interior Wall

(c) Positive Moment Exterior Span

(d) Positive Moment Interior Span

Figure 34: Live load moment from 3D models for 12X12 culverts

Figure 35 through Figure 39 and

Table 3 through Table 7 present the 2D and 3D live load moments extracted at the four critical sections of the top slab for the five culvert sizes (5x5, 7x7, 8x8, 10x10 and 12x12).

The charts given in Figure 35 through Figure 39 represent a comparison between the live load moments extracted from the 2D frame element model and the corresponding 3D plate element model at the four critical sections of the top slab. As can be seen from the results, for any given critical section, the 2D live load moments were usually greater than the 3D moments for the entire investigated domain of fill heights (1.0 ft to 9 ft.). This can be attributed to the two-way bending action of the top slab of the culvert than can only be captured using the 3D models versus the one-way action assumed in the 2D model. The two-way action in the slab considers bending of the slab in the two directions and therefore the live load is distributed in the two directions, which results in lesser bending moments in the span direction as compared to the 2D frame element model. The culvert length effect can only be incorporated in the analysis when using 3D FE models.

As expected and can be seen in Figure 35 through Figure 39, the live load moments from the 2D and 3D analysis decrease with the increase of the fill height. This is attributed to the fact that the live load is distributed on a larger area with the increase of fill height. It is also evident that the difference between the 3D moments and the 2D moments decreases as the fill height increases. This is expected because for larger fill heights, the load is distributed over a larger area on the top slab of the culvert and thus lesser two-way load distribution is expected for those cases. (similar to dead load behavior)

The results also showed lesser difference between the 2D and 3D moments for the negative moment sections as compared to positive moment sections and that the difference between 2D and 3D moments was more pronounced in the larger size culverts (12x12) as compared to the smaller culverts (5x5).

All charts show a discontinuity at the fill height equal to 2.0 ft., which occurred as a result of using different equations for the live load distribution for the fill heights less than 2.0 ft. and the fill heights equal to or greater than 2.0 ft. per AASHTO-LRFD (2017). It is worth noting that the two methods of load distribution yield the same load intensity at fill heights of 1.99 ft. and 2 ft. However, the load configuration for the two cases are different. For the 1.99 ft. fill, the two tandem axles are distributed on two loaded areas similar to the configuration shown in

Figure 31 (a), however for the 2 ft fill, the four wheels of the tandem are distributed on four discrete areas similar to the configuration shown in

Figure 31 (b).As shown in the charts, the live load moment from the 3D analysis at 1.99 ft. fill was usually higher than the moment at 2.0 ft. fill.

Comparing the results of live load moments presented in Figure 35 to Figure 39, it can be concluded that 3D plate models offers a better and more accurate capacity of the existing inventory.. These results were used to develop 2D/3D correction factors used to correlate between the conventional 2D frame element models and the sophisticated 3D plate element models. Thus, engineers can use those correction factors to modify the conservative values for the live load moment obtained from 2D analysis, and hence account for the culvert length effects into the simplified 2-D frame analysis.

Table 3: Live load moment from 2D and 3D models for 5X5 culverts

GEOMETRY				3D MODELS				2D MODELS			
				Negative		Positive		Negative		Positive	
MODEL	SIZE	L/W	hf (ft.)	EXT.	INT.	EXT.	INT.	EXT.	INT.	EXT.	INT.
C1	5X5	1.0	1	-1.02	-1.78	2.84	2.45				
C2	5X5	1.0	2	-0.82	-1.75	1.87	1.65				
C3	5X5	1.0	3	-0.77	-1.68	1.82	1.62				
C4	5X5	1.0	4	-0.61	-1.46	1.40	1.19				
C5	5X5	1.0	6	-0.45	-1.14	0.89	0.64				
C6	5X5	1.0	9	-0.17	-0.68	0.52	0.37				
C31	5X5	1.5	1	-0.98	-1.88	2.96	2.51				
C32	5X5	1.5	2	-0.72	-1.62	1.74	1.55				
C33	5X5	1.5	3	-0.67	-1.57	1.69	1.51				
C34	5X5	1.5	4	-0.58	-1.41	1.44	1.19				
C35	5X5	1.5	6	-0.41	-1.11	0.90	0.62				
C36	5X5	1.5	9	-0.18	-0.65	0.53	0.37				
C61	5X5	2.0	1	-0.98	-1.89	2.97	2.50	-1.40	-2.20	3.31	2.88
C61*	5X5	2.0	1.99	-0.89	-1.80	2.40	2.09	-1.22	-2.06	2.73	2.43
C62	5X5	2.0	2	-0.72	-1.60	1.74	1.54	-1.22	-2.06	2.73	2.43
C63	5X5	2.0	3	-0.67	-1.58	1.69	1.50	-0.99	-1.76	2.01	1.91
C64	5X5	2.0	4	-0.58	-1.42	1.44	1.18	-0.78	-1.46	1.52	1.36
C65	5X5	2.0	6	-0.41	-1.11	0.90	0.61	-0.48	-1.14	0.93	0.68
C66	5X5	2.0	9	-0.18	-0.64	0.53	0.37	-0.19	-0.67	0.54	0.40
C91	5X5	3.0	1	-0.98	-1.89	2.96	2.49				
C92	5X5	3.0	2	-0.72	-1.63	1.74	1.52				
C93	5X5	3.0	3	-0.67	-1.57	1.69	1.50				
C94	5X5	3.0	4	-0.58	-1.42	1.44	1.18				
C95	5X5	3.0	6	-0.41	-1.09	0.90	0.61				
C96	5X5	3.0	9	-0.18	-0.63	0.53	0.37				

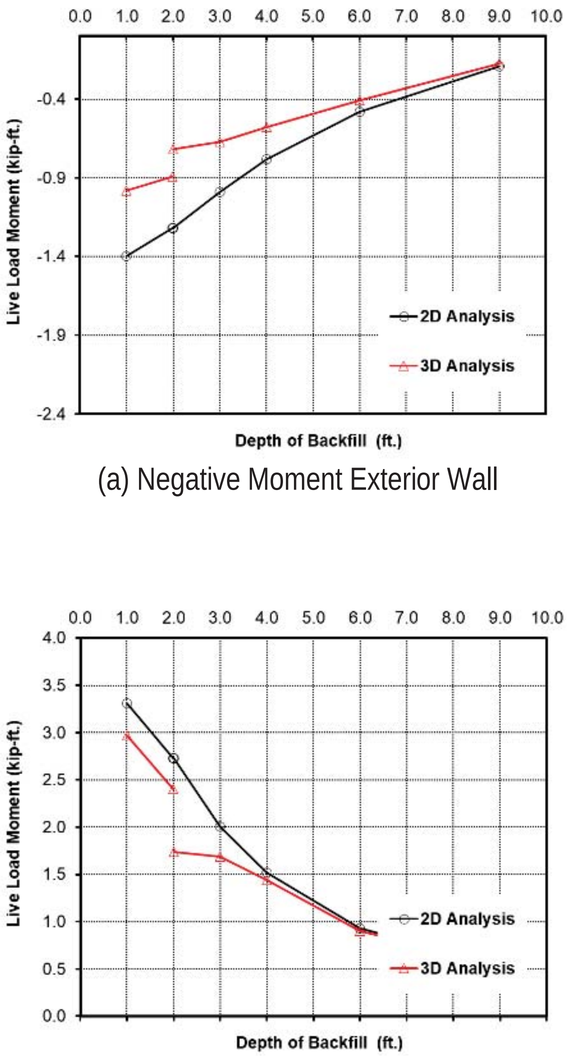

(a) Negative Moment Exterior Wall

(b) Negative Moment Interior Wall

(c) Positive Moment Exterior Span

(d) Positive Moment Interior Span

Figure 35: Live load moment from 2D and 3D models for 5X5 culverts

Table 4: Live load moment from 2D and 3D models for 7X7 culverts

GEOMETRY				3D MODELS				2D MODELS			
				Negative		Positive		Negative		Positive	
MODEL	SIZE	L/W	hf (ft.)	EXT.	INT.	EXT.	INT.	EXT.	INT.	EXT.	INT.
C7	7x7	1.0	1	-2.09	-3.79	4.17	3.86				
C8	7x7	1.0	2	-1.39	-2.69	3.00	2.73				
C9	7x7	1.0	3	-1.28	-2.56	2.95	2.69				
C10	7x7	1.0	4	-1.06	-2.20	2.48	2.24				
C11	7x7	1.0	6	-0.66	-1.69	1.57	1.33				
C12	7x7	1.0	9	-0.41	-1.21	0.96	0.69				
C37	7x7	1.5	1	-2.04	-3.83	4.17	3.83				
C38	7x7	1.5	2	-1.34	-2.73	3.00	2.70				
C39	7x7	1.5	3	-1.23	-2.60	2.95	2.66				
C40	7x7	1.5	4	-1.02	-2.20	2.48	2.22				
C41	7x7	1.5	6	-0.65	-1.74	1.57	1.31				
C42	7x7	1.5	9	-0.38	-1.23	0.96	0.67				
C67	7x7	2.0	1	-2.04	-3.84	4.17	3.82	-2.28	-4.03	5.21	4.79
C67*	7x7	2.0	1.99	-1.82	-3.72	3.70	3.43	-2.12	-3.83	4.75	4.36
C68	7x7	2.0	2	-1.34	-2.74	3.00	2.69	-2.12	-3.83	4.75	4.36
C69	7x7	2.0	3	-1.23	-2.60	2.95	2.65	-1.57	-2.82	3.71	3.42
C70	7x7	2.0	4	-1.01	-2.19	2.47	2.21	-1.19	-2.29	2.80	2.57
C71	7x7	2.0	6	-0.66	-1.69	1.57	1.30	-0.75	-1.75	1.70	1.46
C72	7x7	2.0	9	-0.39	-1.24	0.96	0.67	-0.45	-1.27	1.01	0.72
C97	7x7	3.0	1	-2.04	-3.84	4.17	3.81				
C98	7x7	3.0	2	-1.34	-2.74	3.00	2.68				
C99	7x7	3.0	3	-1.23	-2.60	2.95	2.64				
C100	7x7	3.0	4	-1.02	-2.22	2.47	2.20				
C101	7x7	3.0	6	-0.65	-1.72	1.57	1.30				
C102	7x7	3.0	9	-0.39	-1.23	0.96	0.67				

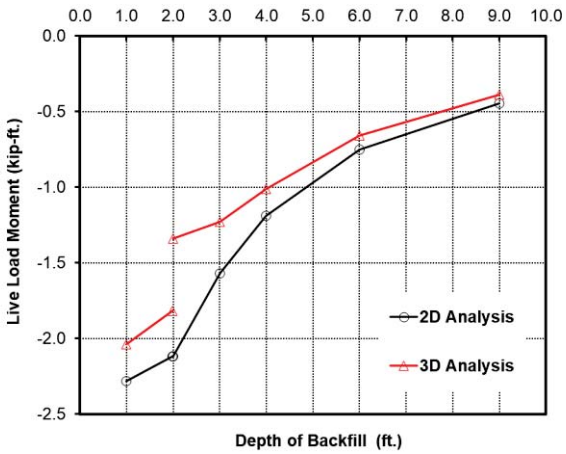

(a) Negative Moment Exterior Wall

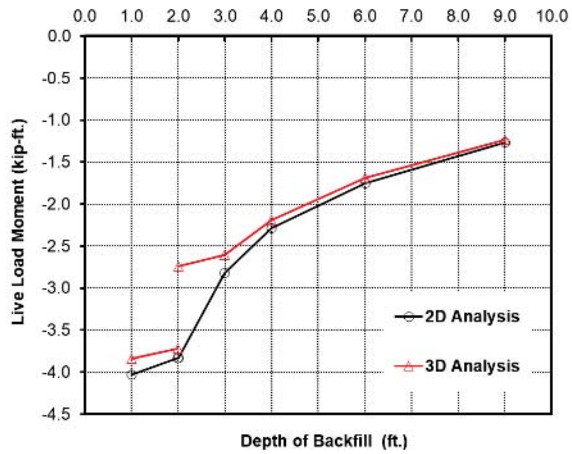

(b) Negative Moment Interior Wall

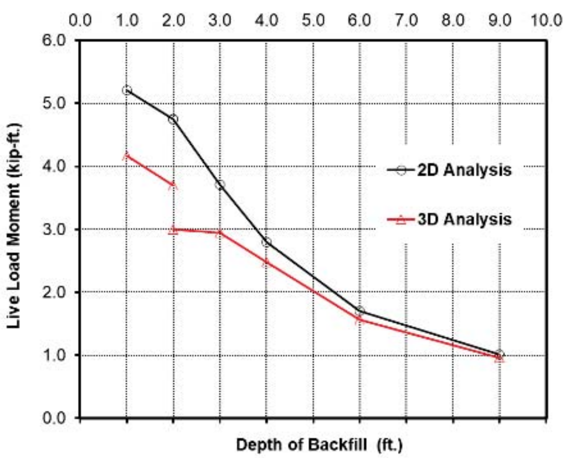

(b) Positive Moment Exterior Span

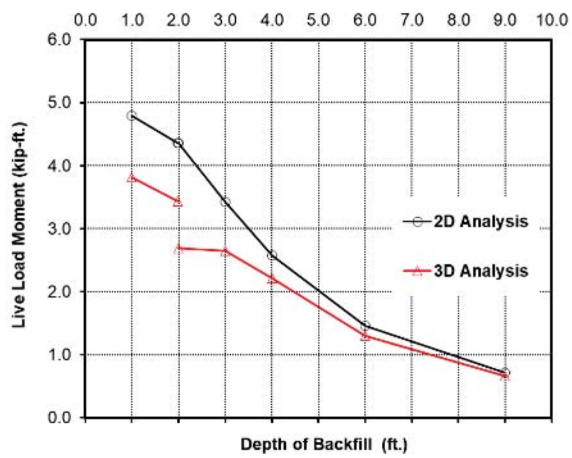

(d) Positive Moment Interior Span

Figure 36: Live load moment from 2D and 3D models for 7X7 culverts

Table 5: Live load moment from 2D and 3D models for 8X8 culverts

GEOMETRY				3D MODELS				2D MODELS			
				Negative		Positive		Negative		Positive	
MODEL	SIZE	L/W	hf (ft.)	EXT.	INT.	EXT.	INT.	EXT.	INT.	EXT.	INT.
C13	8X8	1.0	1	-2.79	-4.81	4.79	4.46				
C14	8X8	1.0	2	-2.04	-3.49	3.63	3.31				
C15	8X8	1.0	3	-1.88	-3.34	3.36	3.24				
C16	8X8	1.0	4	-1.56	-2.80	3.00	2.74				
C17	8X8	1.0	6	-0.97	-1.89	1.92	1.70				
C18	8X8	1.0	9	-0.60	-1.56	1.24	1.02				
C43	8X8	1.5	1	-2.75	-4.86	4.79	4.44				
C44	8X8	1.5	2	-1.99	-3.54	3.62	3.29				
C45	8X8	1.5	3	-1.84	-3.39	3.36	3.22				
C46	8X8	1.5	4	-1.52	-2.84	2.99	2.72				
C47	8X8	1.5	6	-0.96	-1.92	1.92	1.68				
C48	8X8	1.5	9	-0.57	-1.58	1.24	0.99				
C73	8X8	2.0	1	-2.74	-4.86	4.78	4.43	-3.24	-5.28	6.31	5.98
C73*	8X8	2.0	1.99	-2.59	-4.56	4.39	4.00	-3.04	-4.95	5.88	5.48
C74	8X8	2.0	2	-1.99	-3.55	3.62	3.28	-3.04	-4.95	5.88	5.48
C75	8X8	2.0	3	-1.83	-3.39	3.35	3.21	-2.33	-3.77	4.63	4.32
C76	8X8	2.0	4	-1.49	-2.71	2.99	2.71	-1.79	-2.84	3.52	3.30
C77	8X8	2.0	6	-0.99	-1.88	1.91	1.67	-1.13	-1.93	2.14	1.97
C78	8X8	2.0	9	-0.59	-1.57	1.23	0.99	-0.67	-1.60	1.33	1.11
C103	8X8	3.0	1	-2.743	-4.862	4.78	4.419				
C104	8X8	3.0	2	-1.988	-3.547	3.609	3.268				
C105	8X8	3.0	3	-1.83	-3.393	3.351	3.2				
C106	8X8	3.0	4	-1.517	-2.849	2.989	2.697				
C107	8X8	3.0	6	-0.958	-1.925	1.912	1.665				
C108	8X8	3.0	9	-0.566	-1.577	1.233	0.969				

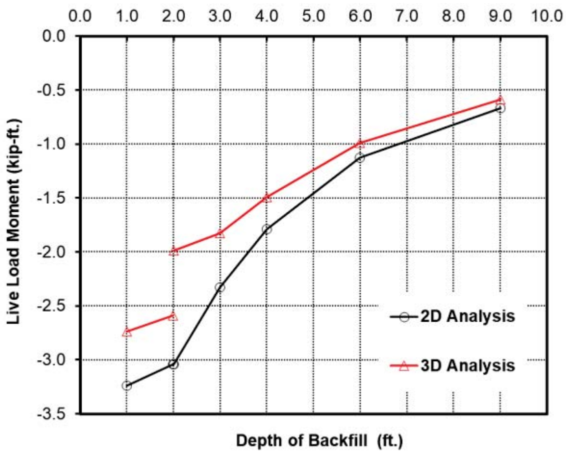

(a) Negative Moment Exterior Wall

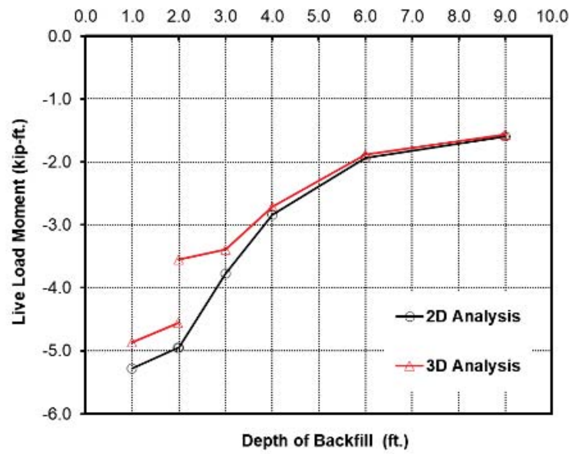

(b) Negative Moment Interior Wall

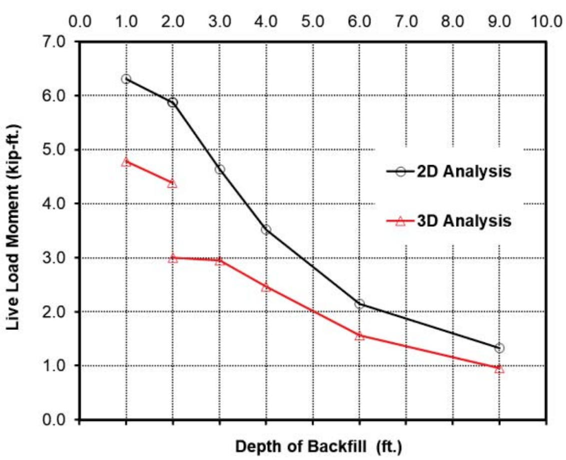

(b) Positive Moment Exterior Span

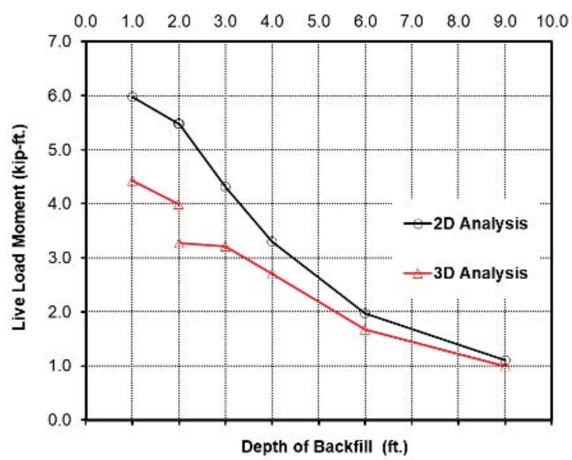

(c) Positive Moment Interior Span

Figure 37: Live load moment from 2D and 3D models for 8X8 culverts

Table 6: Live load moment from 2D and 3D models for 10X10 culverts

GEOMETRY				3D MODELS				2D MODELS			
				Negative		Positive		Negative		Positive	
MODEL	SIZE	L/W	hf (ft.)	EXT.	INT.	EXT.	INT.	EXT.	INT.	EXT.	INT.
C19	10X10	1.0	1	-4.28	-6.13	5.34	4.90				
C20	10X10	1.0	2	-3.22	-5.04	4.78	4.44				
C21	10X10	1.0	3	-3.25	-4.81	4.71	4.42				
C22	10X10	1.0	4	-2.88	-4.25	4.07	3.79				
C23	10X10	1.0	6	-1.82	-2.71	2.71	2.50				
C24	10X10	1.0	9	-1.01	-1.82	1.66	1.48				
C49	10X10	1.5	1	-4.25	-6.18	5.34	4.88				
C50	10X10	1.5	2	-3.17	-5.09	4.77	4.42				
C51	10X10	1.5	3	-3.22	-4.86	4.70	4.40				
C52	10X10	1.5	4	-2.85	-4.28	4.06	3.77				
C53	10X10	1.5	6	-1.79	-2.70	2.70	2.48				
C54	10X10	1.5	9	-0.99	-1.80	1.66	1.47				
C79	10X10	2.0	1	-4.24	-6.19	5.33	4.87	-5.12	-7.20	7.90	7.28
C80*	10X10	2.0	1.99	-3.63	-5.92	5.29	4.82	-4.89	-6.87	7.81	7.29
C80	10X10	2.0	2	-3.19	-5.10	4.76	4.41	-4.63	-6.51	7.49	6.91
C81	10X10	2.0	3	-3.21	-4.87	4.69	4.39	-4.02	-5.61	6.61	6.14
C82	10X10	2.0	4	-2.84	-4.29	4.06	3.76	-3.20	-4.55	5.12	4.76
C83	10X10	2.0	6	-1.78	-2.68	2.70	2.47	-2.04	-2.78	3.20	2.96
C84	10X10	2.0	9	-0.99	-1.78	1.66	1.46	-1.15	-1.87	1.85	1.67
C109	10X10	3.0	1	-4.25	-6.19	5.33	4.86				
C110	10X10	3.0	2	-3.15	-5.10	4.76	4.40				
C111	10X10	3.0	3	-3.21	-4.87	4.70	4.38				
C112	10X10	3.0	4	-2.84	-4.30	4.06	3.75				
C113	10X10	3.0	6	-1.78	-2.75	2.70	2.47				
C114	10X10	3.0	9	-0.99	-1.75	1.65	1.46				

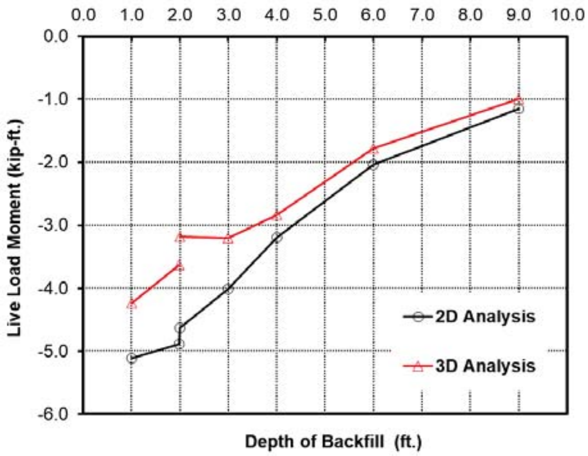

(a) Negative Moment Exterior Wall

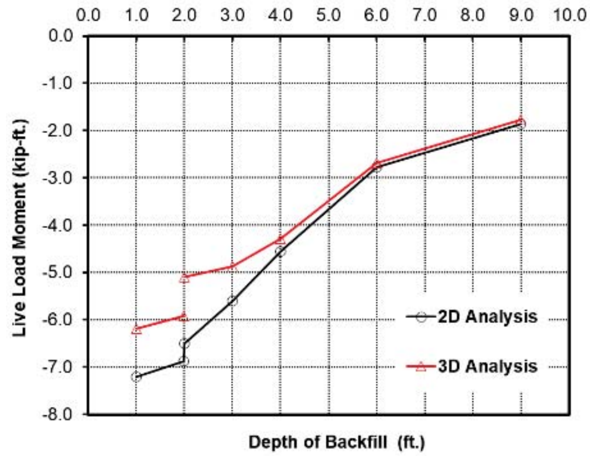

(b) Negative Moment Interior Wall

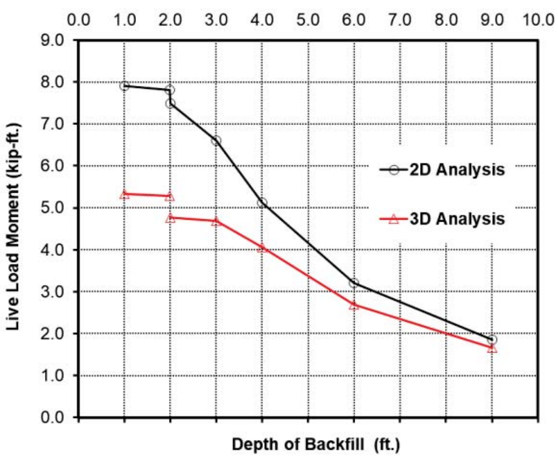

(c) Positive Moment Exterior Span

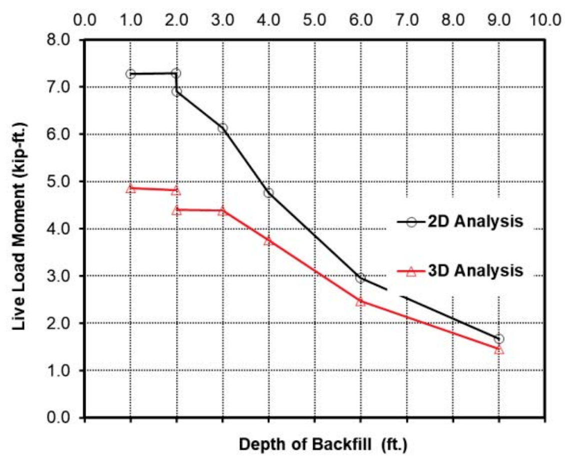

(d) Positive Moment Interior Span

Figure 38: Live load moment from 2D and 3D models for 10X10 culverts

Table 7: Live load moment from 2D and 3D models for 12X12 culverts

GEOMETRY				3D MODELS				2D MODELS			
				Negative		Positive		Negative		Positive	
MODEL	SIZE	L/W	hf (ft.)	EXT.	INT.	EXT.	INT.	EXT.	INT.	EXT.	INT.
C25	12X12	1.0	1	-4.05	-6.68	6.56	6.14				
C26	12X12	1.0	2	-3.50	-5.78	6.02	5.62				
C27	12X12	1.0	3	-3.42	-5.45	5.85	5.47				
C28	12X12	1.0	4	-3.01	-4.95	5.15	4.80				
C29	12X12	1.0	6	-2.15	-3.54	3.67	3.38				
C30	12X12	1.0	9	-1.30	-2.34	2.15	1.98				
C55	12X12	1.5	1	-4.01	-6.73	6.55	6.11				
C56	12X12	1.5	2	-3.47	-5.83	6.00	5.59				
C57	12X12	1.5	3	-3.39	-5.50	5.84	5.44				
C58	12X12	1.5	4	-2.98	-4.99	5.14	4.78				
C59	12X12	1.5	6	-2.19	-3.57	3.66	3.36				
C60	12X12	1.5	9	-1.28	-2.37	2.21	2.01				
C85	12X12	2.0	1	-4.00	-6.75	6.54	6.09	-5.84	-8.78	11.07	10.04
C85*	12X12	2.0	1.99	-3.84	-6.47	6.47	6.04	-5.59	-8.32	10.72	9.71
C86	12X12	2.0	2	-3.46	-5.84	6.00	5.58	-5.33	-7.94	10.27	9.27
C87	12X12	2.0	3	-3.39	-5.51	5.83	5.43	-4.59	-6.40	9.04	8.29
C88	12X12	2.0	4	-3.06	-5.09	5.14	4.76	-3.75	-5.64	7.20	6.60
C89	12X12	2.0	6	-2.22	-3.58	3.66	3.35	-2.50	-3.84	4.70	4.30
C90	12X12	2.0	9	-1.29	-2.36	2.22	2.01	-1.48	-2.44	2.78	2.52
C115	12X12	3.0	1	-4.00	-6.75	6.54	6.08				
C116	12X12	3.0	2	-3.46	-5.85	5.99	5.56				
C117	12X12	3.0	3	-3.39	-5.51	5.83	5.42				
C118	12X12	3.0	4	-2.97	-5.01	5.13	4.75				
C119	12X12	3.0	6	-2.23	-3.58	3.65	3.34				
C120	12X12	3.0	9	-1.28	-2.38	2.23	2.05				

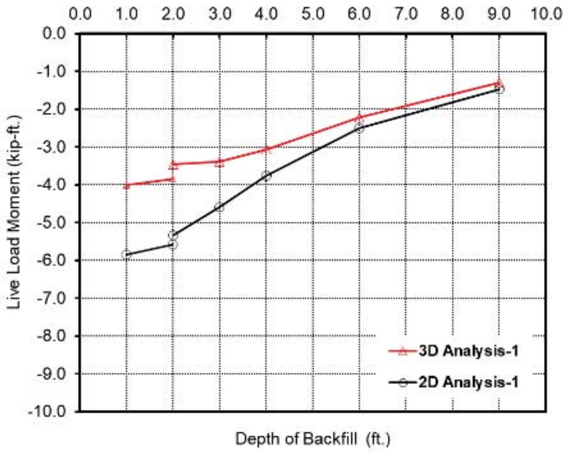

(a) Negative Moment Exterior Wall

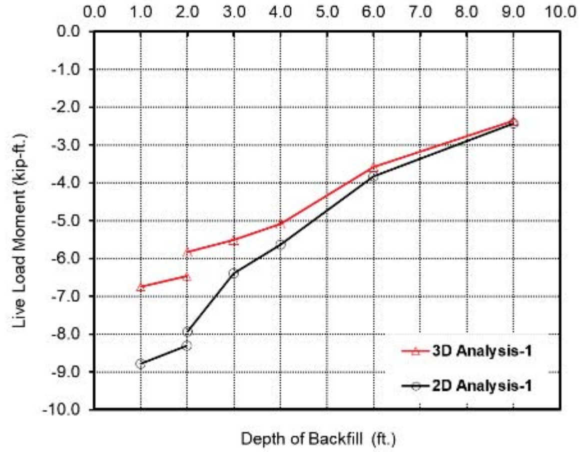

(b) Negative Moment Interior Wall

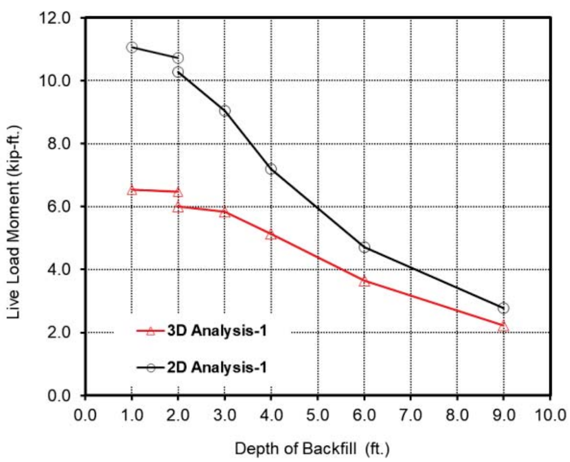

(c) Positive Moment Exterior Span

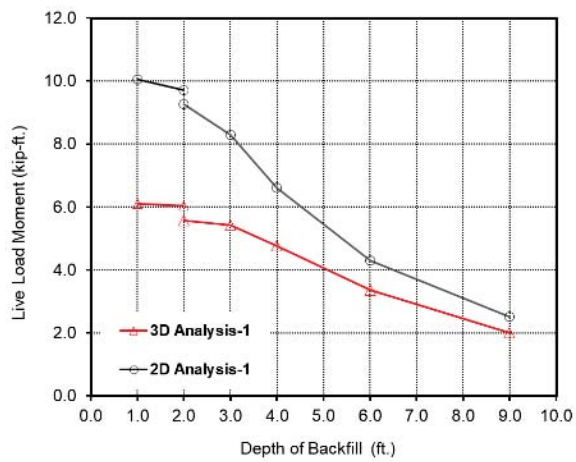

(d) Positive Moment Interior Span

Figure 39: Live load moment from 2D and 3D models for 12X12 culverts

4.1.4 2D/3D Correction Factors

The correction factor for any given section was determined as the ratio between the live load moment obtained from the 3D model to moment obtained from 2D model. Correction factors were plotted against the height of fill for each critical section for the five culvert sizes as shown in Figure 40.

As can be seen in Figure 40, the correction factors differ between positive and negative moment sections. Also, it was found that the culvert size and the height of fill influence the correction factors.

For simplicity and as shown from the results, the correction factors can be assumed to be constant for the shallow fill heights less than 2.0 ft. for all culvert sizes.

For fill heights 2 ft. to 4 ft., it was found that the correction factor increases linearly with the fill height and same trend is observed for fill heights 4 ft. to 9 ft.. These observations are idealized as two linear segments from 2.0 ft to 4.0 ft., and from 4.0 ft. to 9.0 ft. The results also revealed that the correction factors vary with the culvert size.

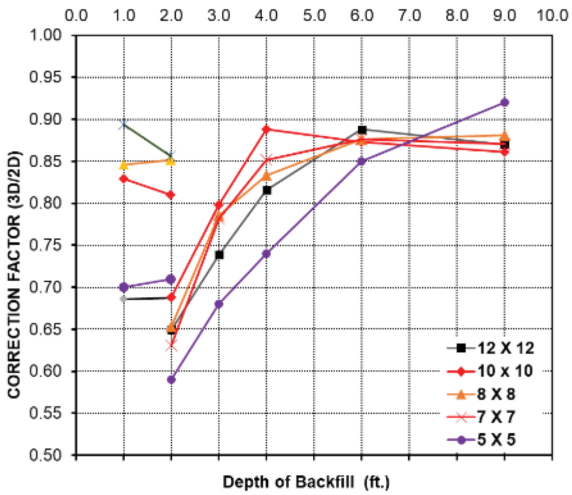

(a) Negative Moment Exterior Wall

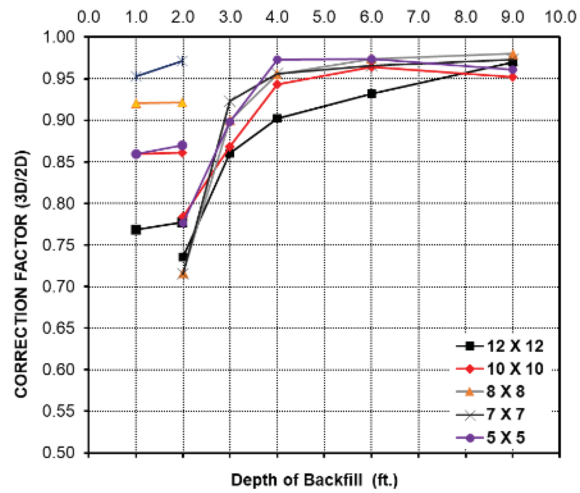

(b) Negative Moment Interior Wall

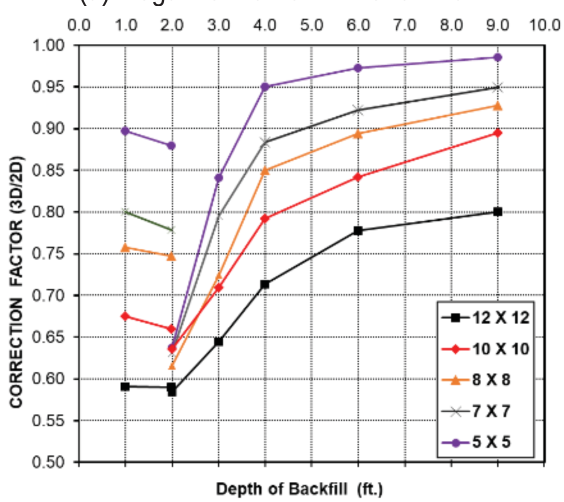

(c) Positive Moment Exterior Span

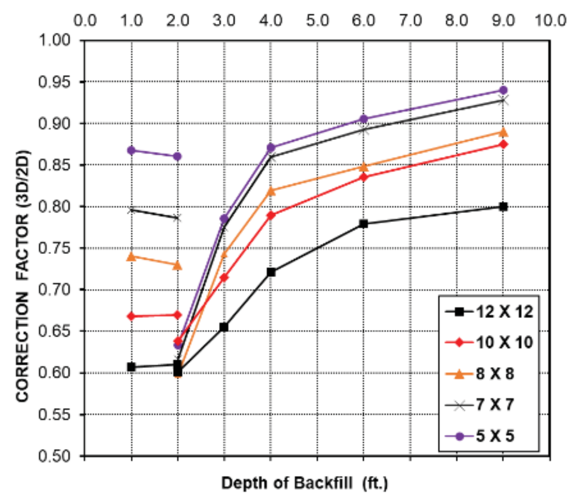

(d) Positive Moment Interior Span

Figure 40: Correction factors between 2D and 3D models for culvert with different sizes

4.1.5 Formulas for 2D/3D Correction Factors

Charts shown in **Figure 40** have shown that the correction factor/fill height relations can be idealized as three segments by breaking the fill heights into three domains as follows: 1.0 - 2.0 ft, 2.0 - 4.0 ft and 4.0 - 9.0 ft. The formulas were developed for the correction factors for the three domains a function of the height of fill and the cell span length.

Figure 41 shows an example of the correction factor graphs and dividing the fill height into three domains: 1.0 - 2.0 ft, 2.0 - 4.0 ft and 4.0 - 9.0 ft. The first domain from 1.0 - 2.0 ft., correction factor is a constant value that varies with the culvert span length. For the 2.0 - 4.0 ft domain and the 4.0 - 9.0 ft. domain, correction factors were developed using linear equations that are function fill height and culvert span length. Same was repeated for all four culvert top slab sections presented in **Figure 40**.

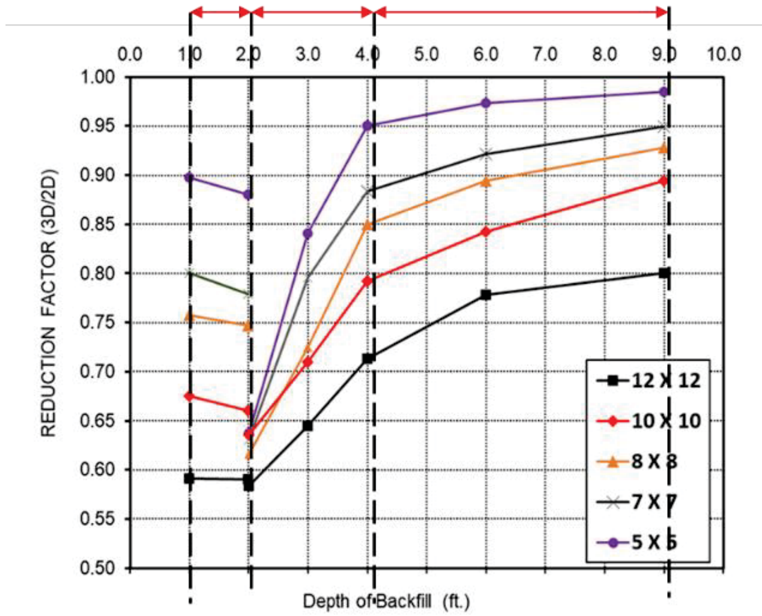

Figure 41: Development of formulas for the correction factors

A series of equations was developed for each of the four critical sections in the top slab of the culvert and the equations are presented in Table 8. The correction factor for the positive moment can be calculated from the equations given in the table at the mid-span of the exterior span and interior span. Similarly, the correction factor for the negative moment can be calculated at the face of the exterior wall and the face of the interior wall. The equations are expressed in two variables backfill depth H_f and Span length L_s. It should be noted that the equations given in Table 8 can be used only for fill heights between 1ft. and 9 ft. and for culvert with cell span lengths between 5ft. and 12 ft.

Table 8: Formulas for 2D/3D correction factors

Section	Backfill Height	Exterior Cell	Interior Cell
Positive	$1.0 \leq H_f < 2.0$	$0.9 + 0.044\,(5 - L_s)$	$0.87 + 0.037\,(5 - L_s)$
	$2.0 \leq H_f < 4.0$	$0.156H_f + 0.34 + 0.018(5 - L_s)$	$0.119H_f + 0.408 + 0.012(5 - L_s)$
	$4.0 \leq H_f < 9.0$	$0.007H_f + 0.926 + 0.029(5 - L_s)$	$0.0137H_f + 0.819 + 0.02(5 - L_s)$
Negative	$1.0 \leq H_f < 2.0$	$0.89 - 0.03\,(12 - L_s)$	$0.95 - 0.026\,(12 - L_s)$
	$2.0 \leq H_f < 4.0$	$0.1H_f + 0.493 - 0.017(12 - L_s)$	$0.094H_f + 0.61 - 0.01(12 - L_s)$
	$4.0 \leq H_f < 9.0$	$0.007H_f + 0.856 - 0.012(12 - L_s)$	$0.002H_f + 0.966 - 0.007(12 - L_s)$

The 2D/3D correction factors were determined at the four slab sections for culverts with different sizes using the equations summarized in Table 8 and the results are presented in the charts shown in Figure 42.

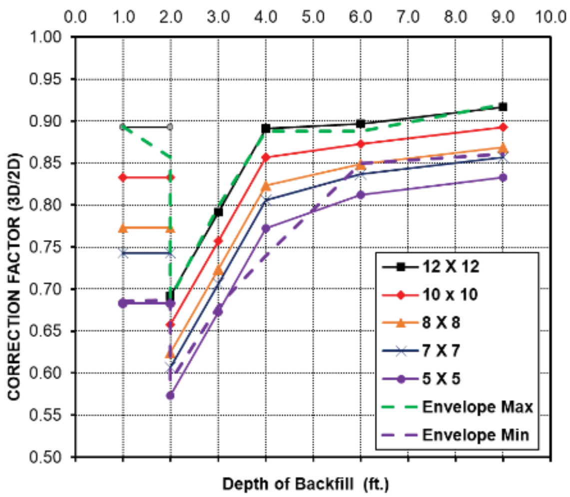

(a) Negative Moment Exterior Wall

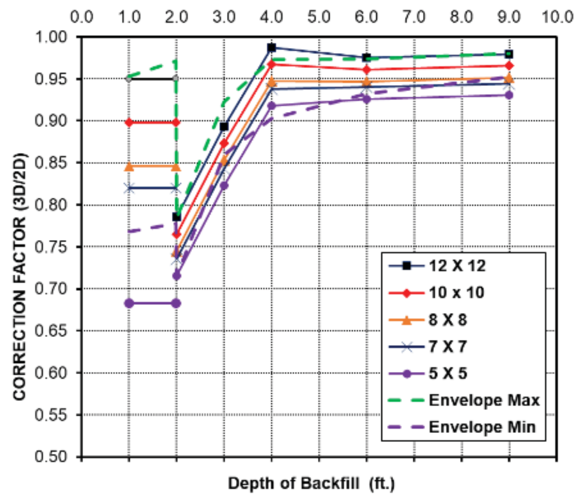

(b) Negative Moment Interior Wall

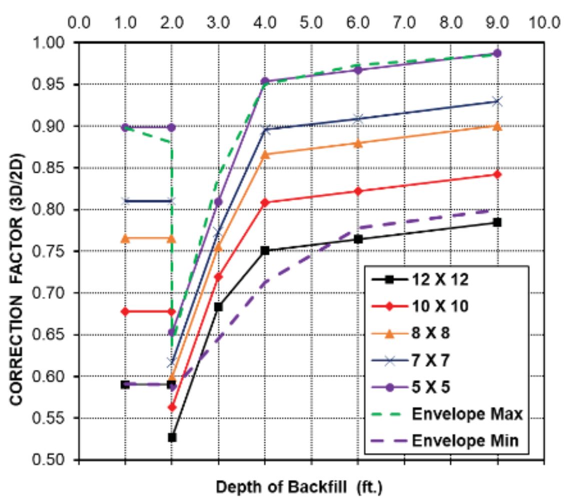

(c) Positive Moment Exterior Span

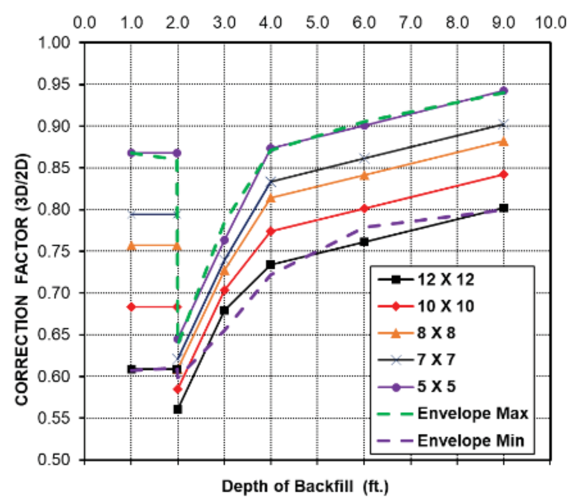

(d) Positive Moment Interior Span

Figure 42: Correction factors between 3D and 2D models for culvert with different sizes

4.2 TASK 5: DIAGNOSTIC LOAD TESTING OF 12 CULVERTS FROM THE LADOTD INVENTORY

4.2.1 Selection Criteria for Test Culverts

Twelve culverts were selected from Louisiana culvert inventory for diagnostic field testing. The culverts were selected such that different parameters affecting the load rating of the RC box culvert can be encompassed during testing. The configurations of those culverts were determined after discussion between the research team and LA DOTD team. The selections included different backfill heights, culvert sizes, and number of cells. Also, the location of those culverts covered different soil zones in Louisiana. All the selected culverts are CIP reinforced concrete box culverts that were built in the years from 1939 to 1971 using Louisiana standard plans for CIP Box culverts. It should be noted that culverts constructed during that period utilized different revisions of the standard plans and that several revisions were made to the reinforcement orders along with the slabs and the walls thicknesses during the period from the 50's to the 70's. Therefore, the twelve culverts were chosen to consider those facts to be representative of the culvert inventory.

The roadway for all culverts consisted of asphalt wearing surface. Figure 43 shows the geographical distribution of the tested culverts in the state of Louisiana. Tabulated information of the tested culverts along with more details on the location, ADT, and foundation zone is given in Table 9.

As can be seen in Table 9, the culverts were divided into three groups based on the fill height over the top slab of the culvert. The groups included culverts with Shallow fills (1ft to 2ft), culverts with medium fills (2ft to 6ft), and culverts with deep fills (6ft to 8ft).

Table 9: Culverts selected for diagnostic load testing

Culvert	Asset Name	Year Built	Fill Height Group	Parish	Latitude	Longitude	Foundation Zone
1	004770	1949	Shallow Fill (1-2)	Acadia	30.41519	-92.2302	2
2	004780	1939		Acadia	30.42065	-92.239	2
3	005450	1960	Medium Fill (2-6)	Acadia	30.09405	-92.3638	2
4	004360	1957		Acadia	30.16097	-92.3206	2
5	005488	1971		Acadia	30.33403	-92.4836	2
6	008910	1965		St. Martin	30.24832	-91.8201	1
7	008490	1966		St. Landry	30.61255	-91.9631	1
8	004510	1961		Acadia	30.33436	-92.3267	2
9	056860	1966		Livingston	30.56951	-90.6313	2
10	048410	1950	Deep Fill (6-8)	Franklin	32.13961	-91.7357	4
11	048450	1955		Franklin	32.11741	-91.6054	4
12	063720	1969		Washington	30.79647	-90.20074	2

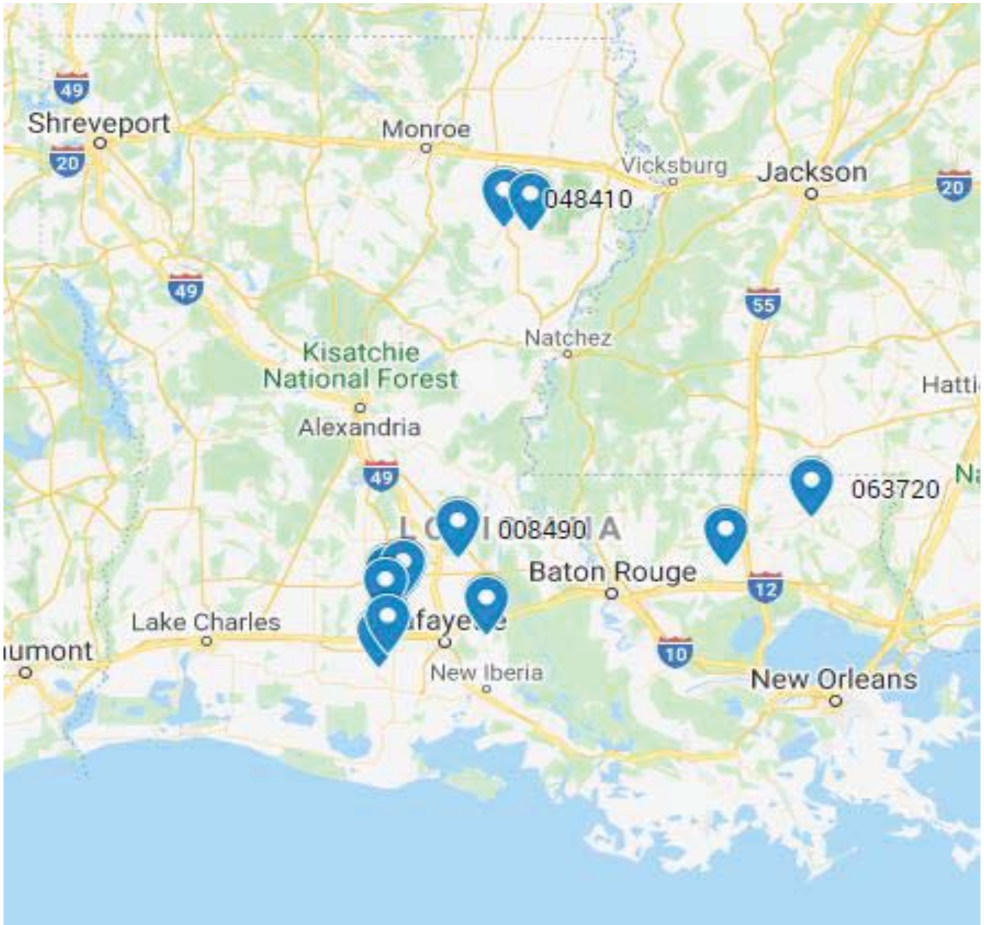

Figure 43: Locations of the twelve tested RC box culverts

Table 10 summarizes the geometric characteristics of the tested RC box culverts. The backfill height was taken from LADOTD inventory information and was verified by the research team on-site. All culverts are square CIP box RC culverts with clear cell span length that ranges from 5 ft. to 10 ft. The number of cells varies from 2 to 4. The fill heights ranged from 1.00 ft to 8.00 ft. For all culverts, the roadway crossing over the culvert consisted of two lanes with asphalt pavement. All culverts were not skewed i.e. culvert is perpendicular to the road.

The latest inspection report and standard plans for each culvert were provided to the project team before the field tests to extract dimensions and other details necessary for planning each test and setting an appropriate instrumentation plan. The wall and slab thicknesses were extracted from the provided plans and confirmed from site inspection.

Table 10: Geometric characteristics of the tested RC box culverts

Culvert	Asset Name	Year Built	Group	Fill Height (ft.)	Number of Cells	Maximum Span (ft.)	Culvert Length (ft.)	Slab / Wall Thickness (in.)
1	004770	1949	Shallow Fill (1-2)	1.00	4	6	35	8 / 6
2	004780	1939		1.25	4	6	35	8 / 6
3	005450	1960	Medium Fill (2-6)	2.92	4	8	39	9 / 8
4	004360	1957		2.33	3	10	37	10 / 10
5	005488	1971		2.25	3	7	41	8.5 / 7
6	008910	1965		2.67	3	7*	42	8.5 / 7
7	008490	1966		3.33	2	10	45	10 / 10
8	004510	1961		4.58	3	7	43	8.5 / 7
9	056860	1966		2.50	4	6	38	8 / 6
10	048410	1950	Deep Fill (6-8)	6.58	3	9	61	9.5 / 9
11	048450	1955		6.00	4	5	63	7.5 / 5
12	063720	1969		8.00	4	8	96	9 / 8

4.2.2 SHM System and Instrumentation

The project data was used to design an instrumentation plan that is capable of capturing the behavior of the tested culverts in an exterior cell and one adjacent interior cell. The culverts were instrumented with of 21 sensors used to measure strain and deformations during the test. The 21 sensors include 19 strain gauges and 2 Linear Variable Differential Transducers (LVDTs). Each culvert carries a two-lane roadway. Two sections along the longitudinal direction of the culvert were instrumented such that the each of the two instrumented sections are located at the middle of a traffic lane of the road. Figure 45 shows the instrumentation plans for the two instrumented sections.

All the strain gauges were mounted parallel to the traffic direction, which is perpendicular to the culvert walls. The gauges mounted on the slab near the exterior and interior walls were installed at the end of the haunch. However, those located on the wall were installed 2.0 in. from the end of the haunch. The positions of the sensors inside the two instrumented cells (one exterior and one adjacent interior) can be seen in the cross-sectional detail view shown in Figure 44.

Two LVDTs were installed at midspan of the exterior cell and the interior cell to capture the deformation of the box under all four load paths.

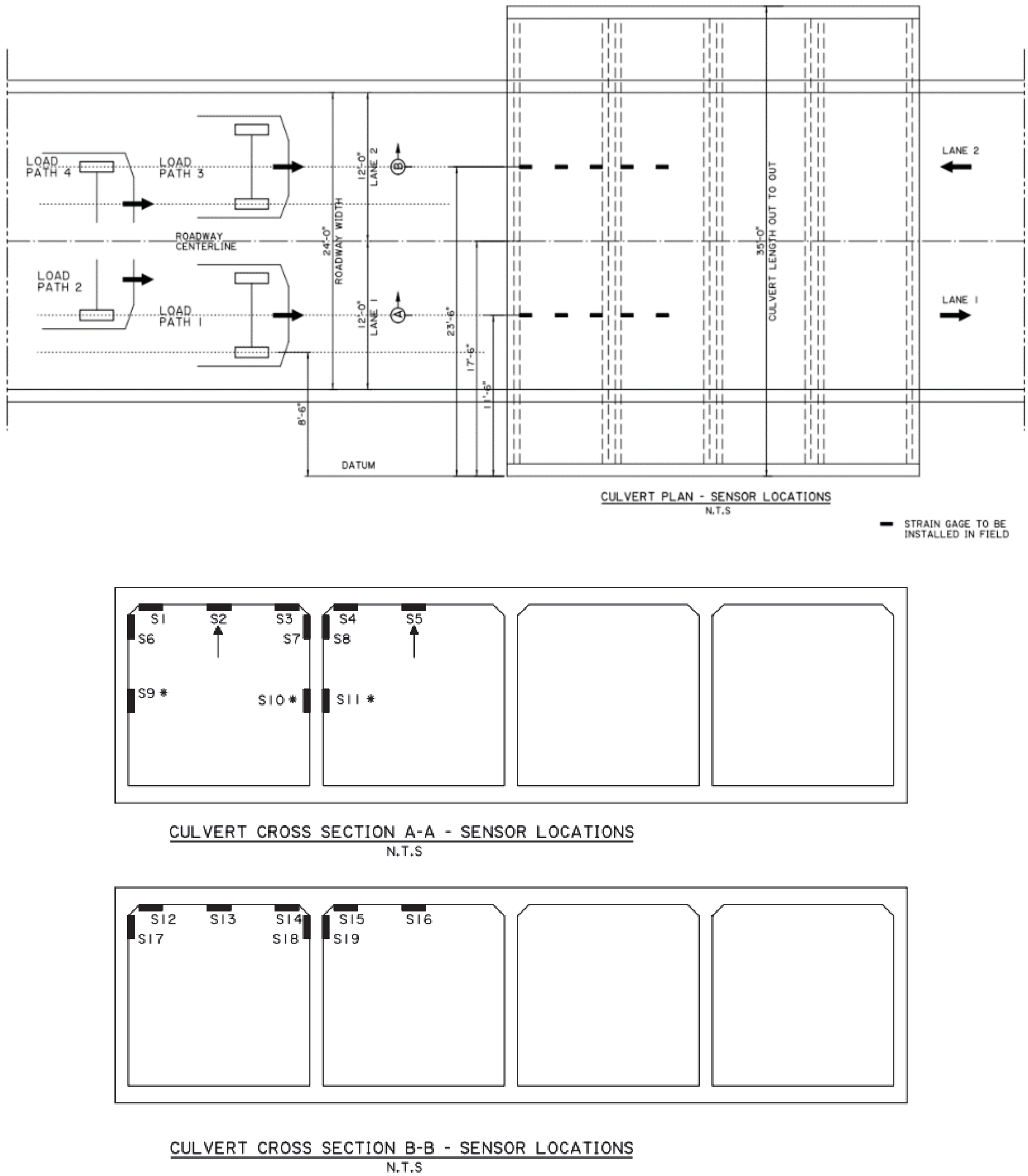

Figure 44: Typical instrumentation plan for the culvert

Figure 45: Photo showing the sensors installed in the exterior cell of the culvert

4.2.3 Loading Truck

Three-axle trucks were used to load all the culverts. Figure 46 shows the truck configuration. The truck had a gross vehicle weight (GVW) of approximately 66 kips, which is approximately equal to the AASHTO design truck (HL-93). The front axle of the truck was weighed to be 18 kips.

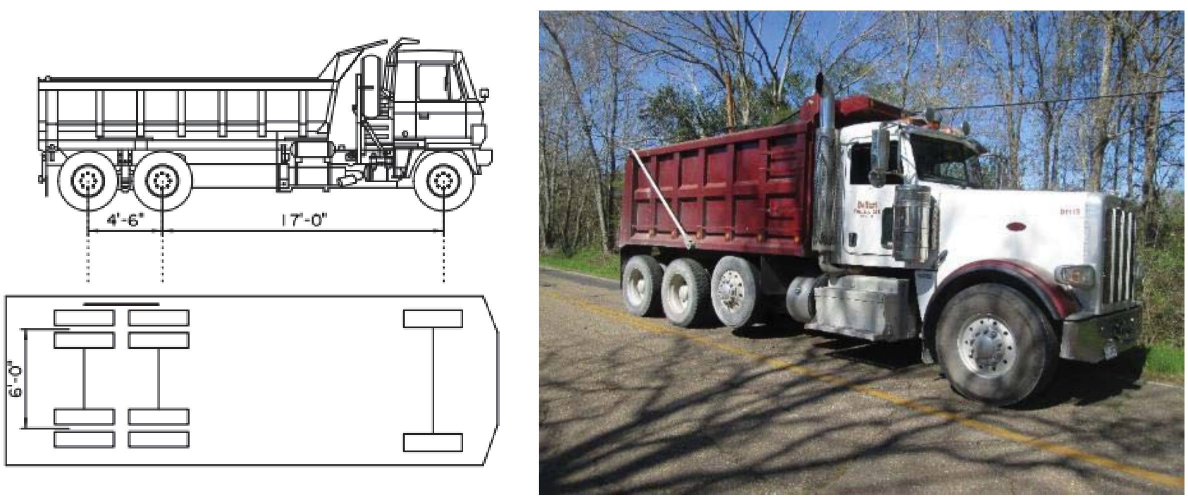

Figure 46: Three axle dump truck used in the testing

4.2.4 Load Cases

Four load paths for the test truck were identified and the truck was stopped at four positions for each path and data was recorded. Load path 1 and load path 2 where the truck was running on lane 1 of the road and load path 3 and load path 4 where the truck was running on lane 2. The load paths are designed to produce maximum straining actions in the sections of the top slab of the culvert. Load paths 1 and 3 were configured such that the instrumented section of the culvert is centered with the truck axels, while load paths 2 and 4 designed to have the instrumented section of the culvert under the wheels. Figure 44 shows the four load paths for a typical culvert. The four truck positions for each load path is shown in Figure 47. The truck positions were designed to produce maximum straining actions at midspan of the exterior and interior cells of the culvert.

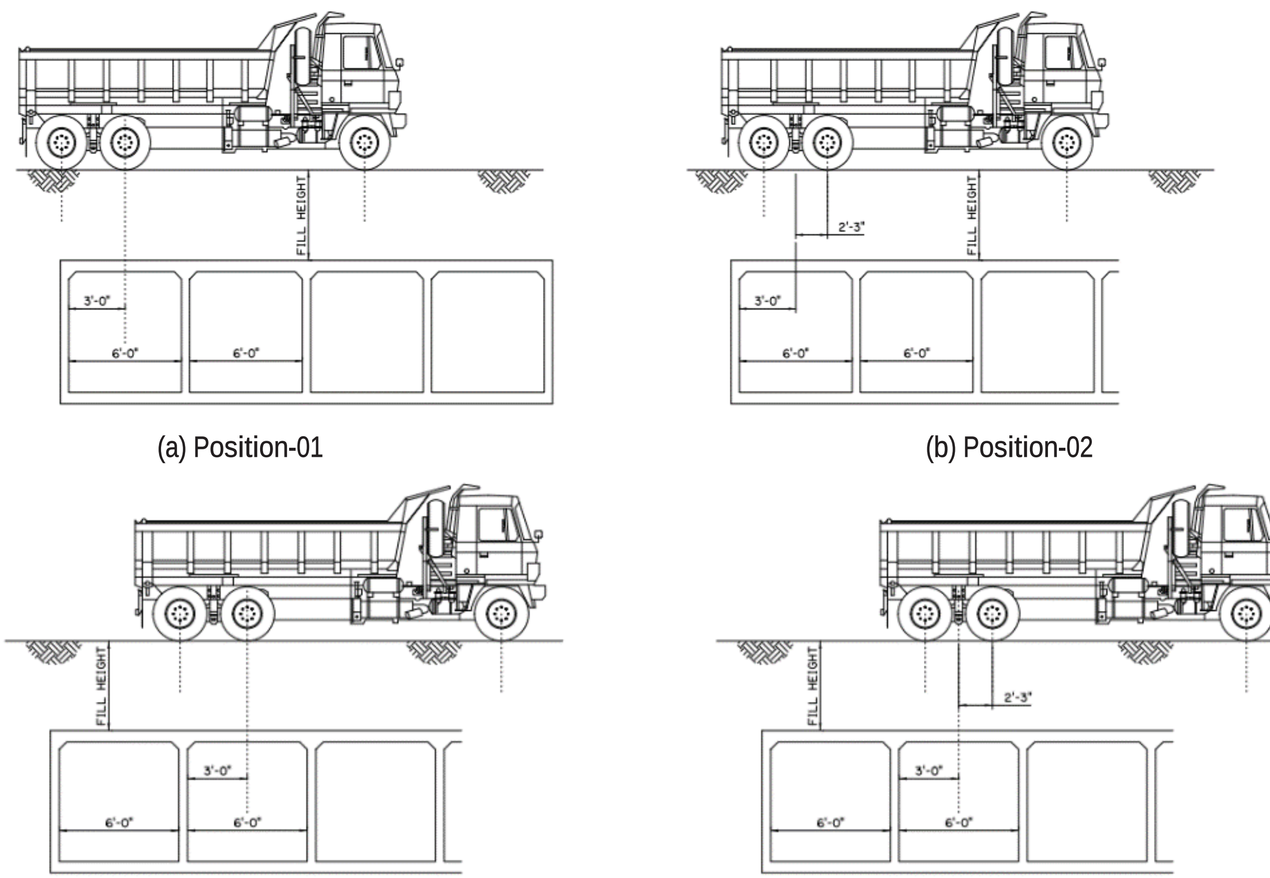

(a) Position-01 (b) Position-02

(c) Position-03 (d) Position-04

Figure 47: Loading positions for each loading path

Dynamic tests were conducted on all culverts on the two load paths 1 and 3 shown in Figure 44. The test was conducted by having the test truck drive at 5.0 mph towards the culvert. The sensors' reading was recorded continuously during the test.

4.2.5 FE Models for Tested Culverts

FE models were developed for each of the tested culverts using Midas civil. A view for the typical FE model of the tested culverts is shown in Figure 48. The finite element analysis was carried out twice for each culvert to model two conditions between the exterior walls and the top slab. First model considers a rigid connection between the exterior walls and the top slab. The rigid connection provides full framing action that fully transfers the moment between the exterior wall and slab. The second model assumes no moment transfer between the exterior wall and the top slab assuming a pinned connection between the wall and the slab. The two models were developed to assess the behavior of the top slab for the two conditions and compare the analytical results to the measured data from the field test.

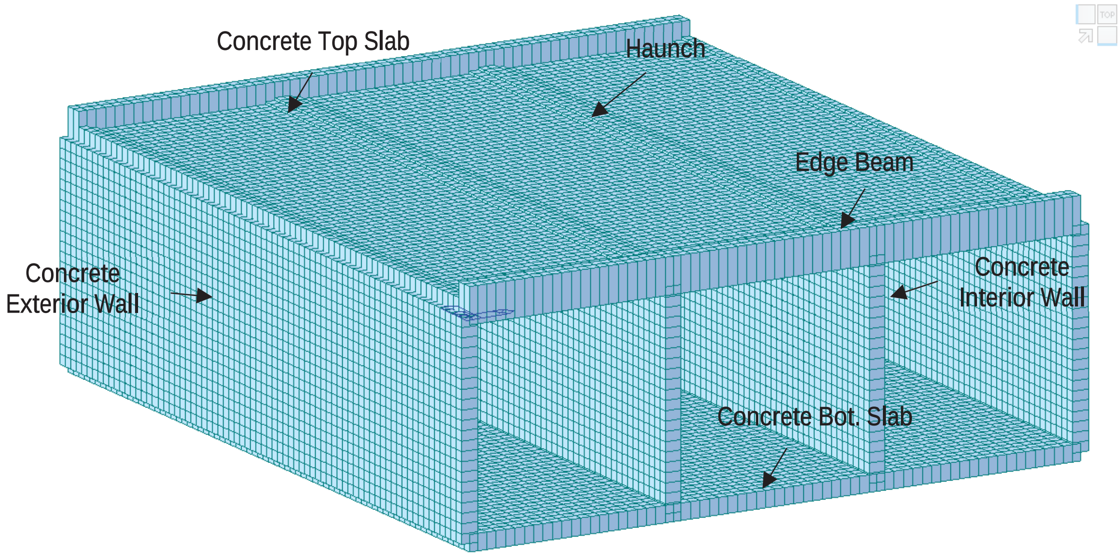

Figure 48: Typical 3D model for the tested culverts

The loading positions of the test truck in the field were simulated accurately in the FE models such that the strain values along the top slab can be extracted from the models and compared to the measured data.

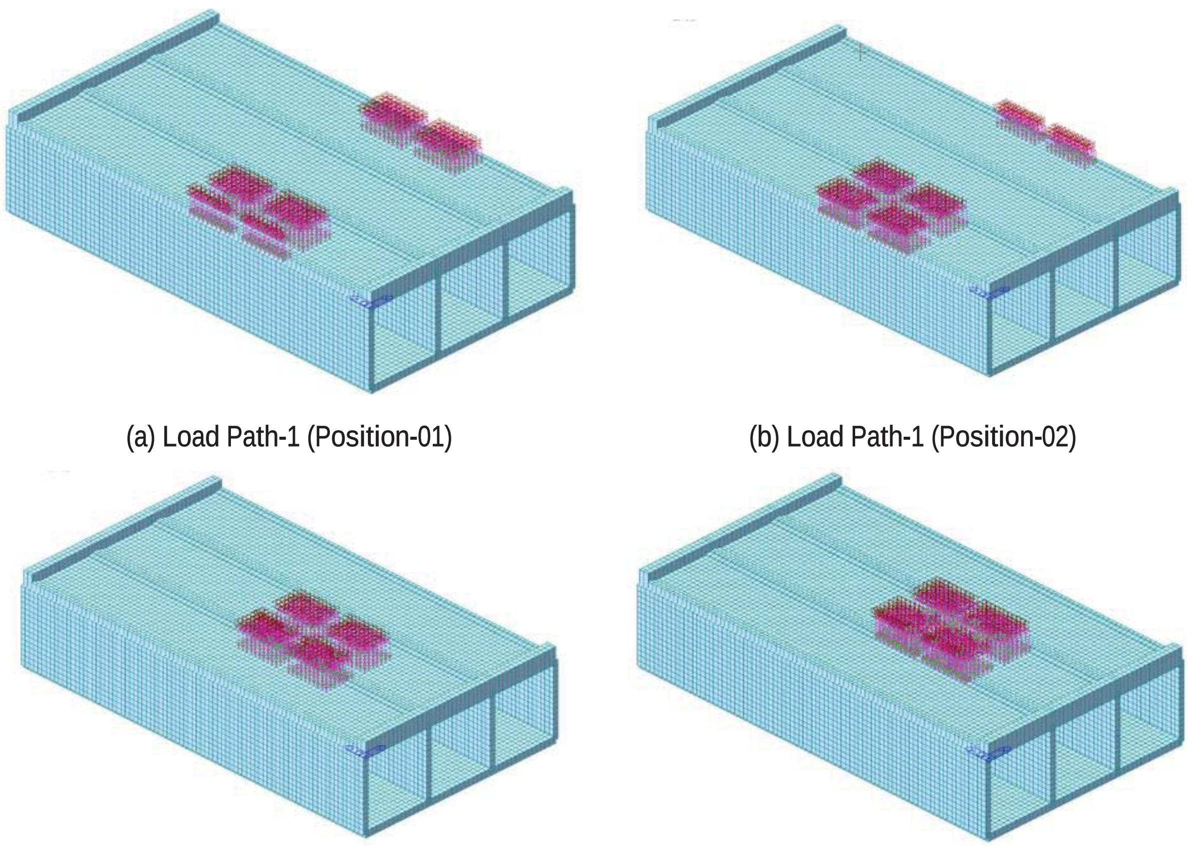

(a) Load Path-1 (Position-01) (b) Load Path-1 (Position-02)

(c) Load Path-1 (Position-03) (d) Load Path-1 (Position-04)

Figure 49: Truck load positions for load path 1

4.2.6 Results and Discussion

Results from the field testing and the corresponding FE model are presented briefly for culvert RC# 004360. The detailed test results of all other tested culverts along with the FE results are presented in Appendix B.

The measured and predicted strain profiles along the top slab of culvert #004360 as obtained from the field test and the FE models are compared in Figure 50. The measured strain is plotted on the vertical axis against the location of the gauge measured from the centerline of the exterior wall. The corresponding strain values obtained from both FE models assuming the rigid connection and the pinned connection are also presented in the same graph. It is worth noting that the as built concrete strength for class A concrete (3.5 ksi) was used in the FE models and the strains were determined based on this strength.

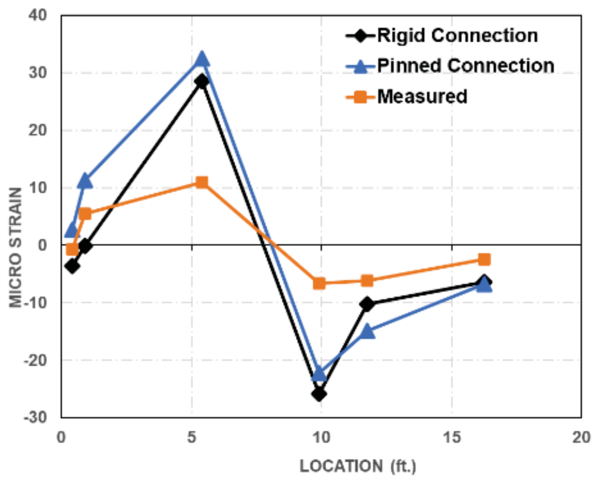

(a) Load Path-1 (Position-01)

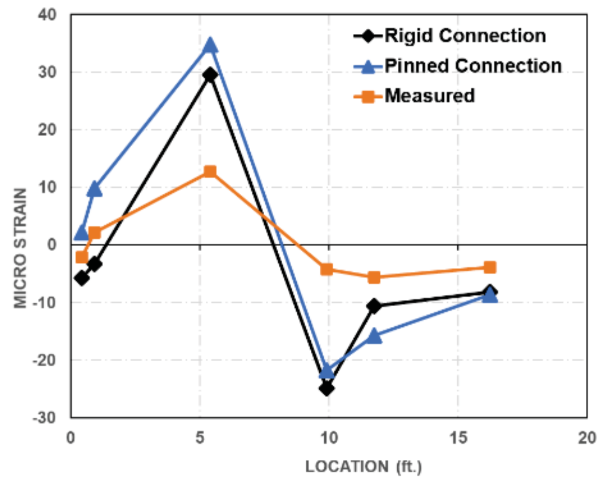

(b) Load Path-1 (Position-02)

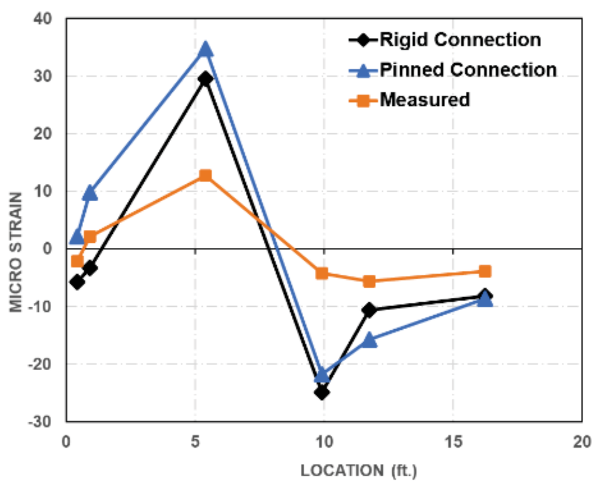

(c) Load Path-1 (Position-03)

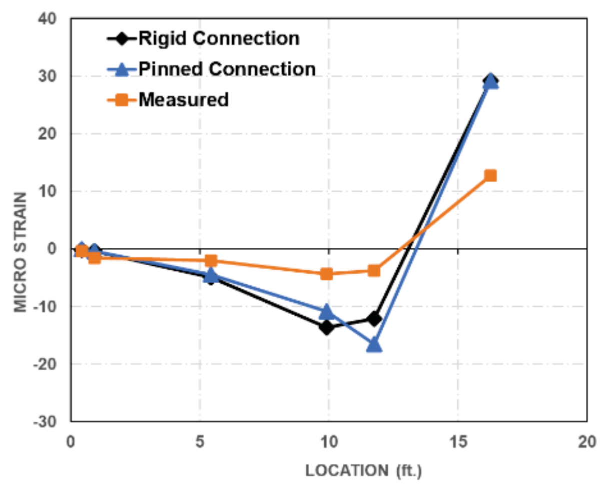

(d) Load Path-1 (Position-04)

Figure 50: Strain profiles along the top slab of culvert #004360 from the field test and FE models

It is readily seen from Figure 60 that the measured strains along the top slab were significantly lower than those estimated using the finite element analysis for the two conditions of the connection. The comparison indicated that strain values predicted from the finite element models were 2 to 3 times greater than the measured values. Same result was obtained for all other test culverts. This finding can be attributed to several strength enhancement factors that are reflected in the actual behavior of the culvert. Among those factors could be the actual strength of the concrete in the culvert which is typically greater than the as-built concrete strength (3.5 ksi) that is used in the FE models.

Other factor could be the level of conservatism built in the AASHTO formulas that are used for the live load distribution through fill. The actual distribution of the load can result in less effects in the culvert. Moreover, the soil structure interaction effect can also influence the behavior of the culverts.

It can be concluded that the actual response of the culvert was found to be less than the response predicted using the 3D finite element models that assume the as-built concrete strength and utilizing AASHTO procedures for the live load distribution through fills.

Results from the dynamic test were used to assess the live load surcharge effect due to a truck approaching the culvert. Figure 51 and Figure 52 shows the deformation and strains recorded during the dynamic test for RC# 004360.

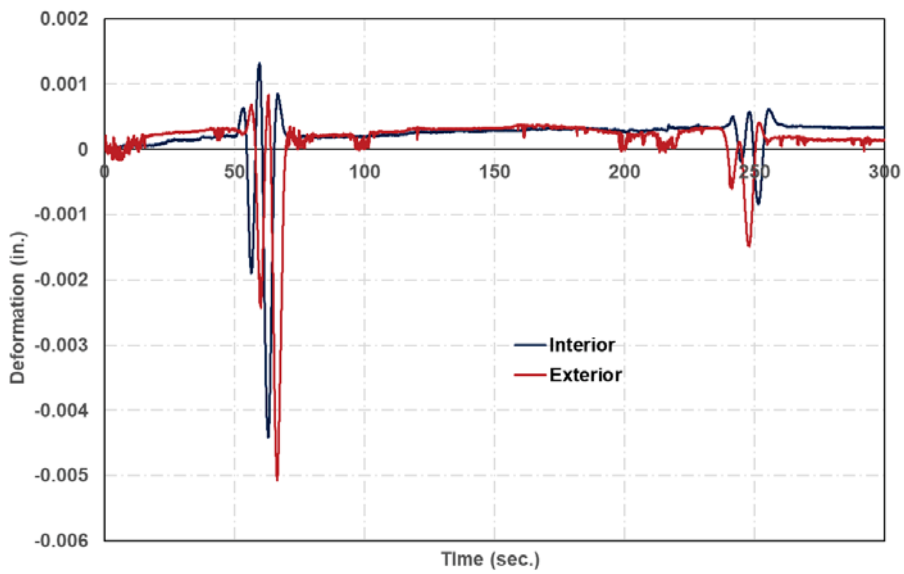

Figure 51: Deformations at midspan of exterior and interior cells during dynamic test, RC# 004360

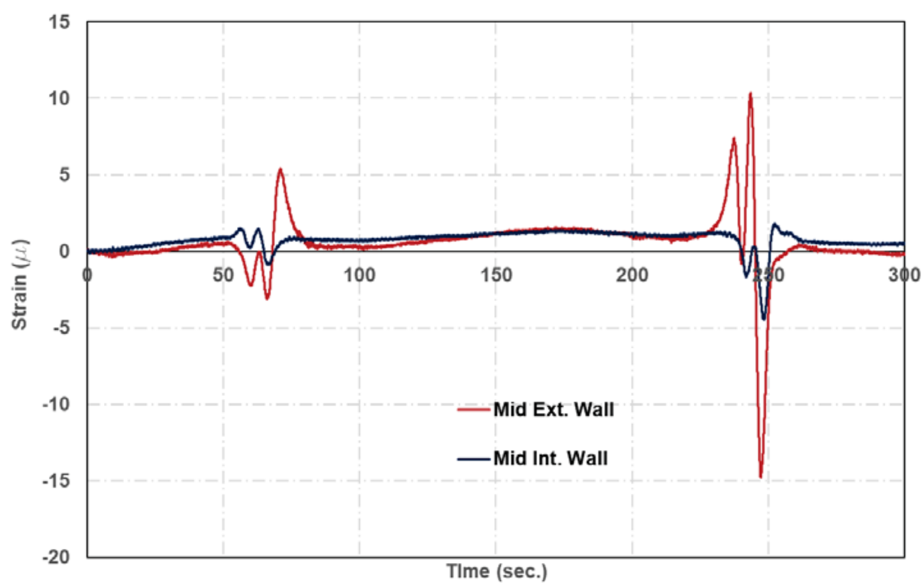

Figure 52: Strain at the mid height of the exterior and interior walls during dynamic test, RC# 004360

4.3 TASK 6: DEVELOPMENT OF LOAD RATING GUIDELINES

4.3.1 Culverts Selected for Load Rating

A sample consisting of 12 culverts was selected for load rating based on the new procedure. Ten of the 12 culverts were included in the test program of this study. The culverts were selected to include different parameters affecting the load rating of the RC box culvert. The culvert configurations include different fill heights, culvert sizes, and number of cells. Characteristics for the rated culverts are summarized in **Table 11**. In addition, the selected sample of culvert represents culverts with years of construction from 1939 to 1971 where various revisions of standard plans were used in the construction of the culverts. **Table 11** shows the standard plan revisions used in the construction for each culvert. It should be noted that the last two culverts in **Table 11** are not actual structures. Those two culverts represent a repetition for RC# 063720 under fill heights equal to 7 ft. and 6 ft. in order to have a complete representative sample that covers different fill heights.

Table 11: Culverts selected for load rating

Culvert #	Asset Name	Year Built	Std. Plan	Group	Fill Height (ft.)	Number of Cells	Maximum Span (ft.)	Culvert Length (ft.)	Slab / Wall Thickness (in.)
1	004770	1949	CC 13-15	Shallow Fill (1-2)	1.00	4	6	35	7 / 7
2	004780	1939	CC 13-15		1.25	4	6	35	7 / 7
3	005450	1960	CC 80-15	Medium Fill (2-6)	2.92	4	8	39	9 / 8
4	004360	1957	CC 80-15		2.33	3	10	37	11 / 10
5	005488	1971	CC.S.M.7-10 S 90		2.00	3	7	41	8.5 / 7
6	008910	1965			2.67	3	7	42	8.5 / 7
7	008490	1966			3.33	2	10	45	10 / 10
8	004510	1961	CC 80-15		4.58	3	7	43	8.5 / 7
9	056860	1966	CC.S.M.4-6 S 90		2.5	4	6	38	8 / 6
10	063720	1969	CC.S.M.7-10 S 90	Deep Fill (6-8)	8.00	4	8	96	9 / 8
11*	063720*	--			7.00	4	8	96	9 / 8
12**	063720*	--			6.00	4	8	96	9 / 8

4.3.2 Addressing 2D Frame Model Challenges

Bridge rating software utilizes the simplified two-dimensional (2-D) frame-element model for the load rating of the culverts. The frame element model represents a strip of the cross-section of the culvert (normal to flow) having a constant unit width (1.0 ft.). The different elements of the culvert (top slab, walls, and bottom slab) are represented by linear-elastic, frame-type elements connected at nodes as shown in Figure 53 utilizing frame analysis matrix methods. 2-D frame-element models are simple to construct and require less computational time. 2-D frame-element models can be slightly enhanced by considering soil effect to some extent in the model. This is achieved primarily by introducing vertical compression springs to support the bottom slab, as shown in Figure 53. The use of vertical springs to mimic the supporting soil foundation rather than the use of knife-edge supports yields a better representation of the culvert boundary conditions. In this case, loads need not be applied to the bottom slab since they will be implicitly introduced to the bottom slab as the reactions of the springs. The modulus of subgrade reaction used in the analysis of the culverts was taken equal to 150 pci which represents soils with medium profile soils consisting of sands and/or sand gravel mixtures with moderate amounts of silts and clay. It is worth noting that the effect of the modulus of subgrade reaction on the rating results of the culverts was investigated in Phase I of the project. The results indicated that, in general, varying the modulus of subgrade showed minimal effect on the live load moments in the top slab and bottom slab sections with difference less than 7%.

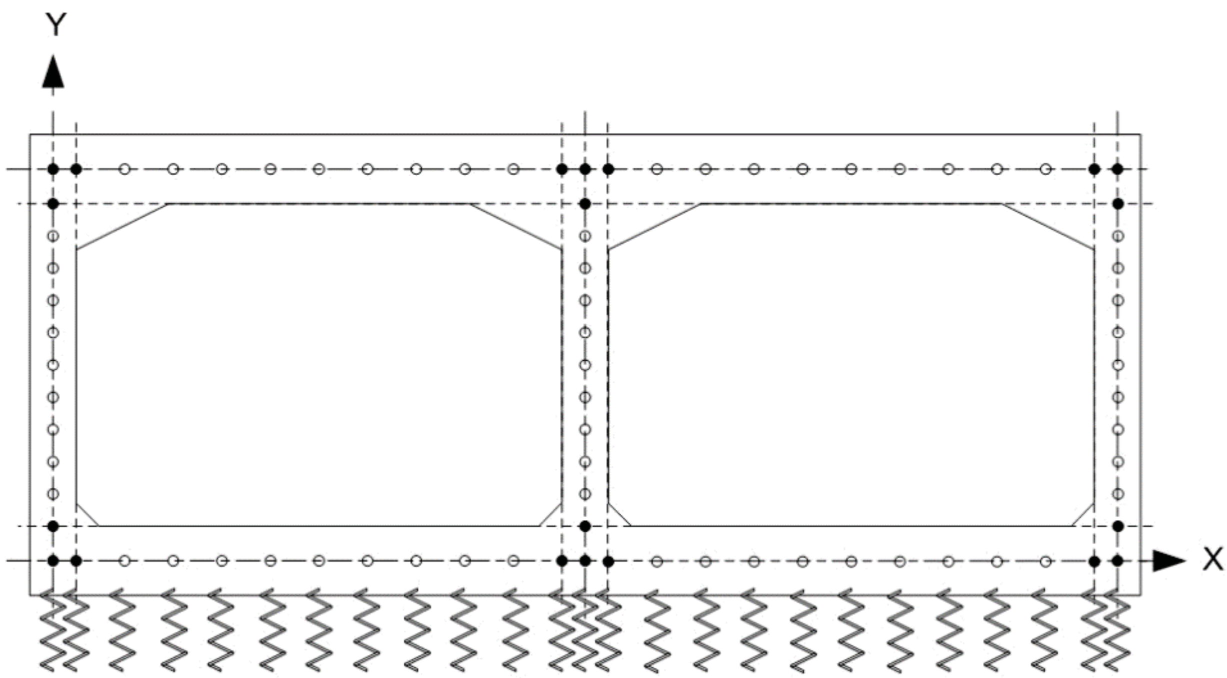

Figure 53: 2D Frame element model in Bridge Rating

4.3.2.1 Applying 2D/3D Correction Factors

As discussed in Task 4 parametric study, the culvert length was found to be a key parameter affecting load distribution within the top slab of the culvert. This can be attributed to the two-way bending action of the top slab of the culvert. The length effects can only be studied using 3-D models. Therefore, the parametric study was performed with a main objective of developing correction factors that can correlate the internal forces from 3-D shell models and the conventional 2-D frame element models.

The live load moments obtained from 3-D models were compared to their counterparts from 2-D frame element models and a set of charts was developed to compare the moments from 2-D and 3-D analysis. Then a set of formulas was developed; where the engineer can obtain a correction factor to correct the live load moment obtained from 2-D analysis, and hence account for the culvert length effects into the simplified 2-D frame analysis.

The formulas summarized in Table 8 were used to determine the correction factors for the 12 culverts. The correction factors were determined for the positive and negative moment sections for the exterior and the interior cell of the culvert. The average of the four correction factors was used as a representative value that encompasses the variation of the correction factors between the sections of the culvert. The average correction factors were used for the culverts and are summarized in Table 12.

Table 12: 2D/3D Corrections Factors for the 12 Culverts

Culvert	Size	Fill	Fill Height (ft)	Correction for Exterior Cell		Correction for Interior Cell		Average Correction Factor
				Positive Moment	Negative Moment	Positive Moment	Negative Moment	
004770	(4) 6x6	Shallow (0-2)	1.00	0.86	0.71	0.83	0.79	0.80
004780	(4) 6x6		1.25	0.86	0.71	0.83	0.79	0.80
004360	(3) 10x10	Medium (2-6)	2.33	0.61	0.69	0.63	0.81	0.68
004510	(3) 7x7		4.50	0.90	0.83	0.84	0.94	0.88
005450	(4) 8x8		2.92	0.74	0.72	0.72	0.84	0.76
005488	(3) 7x7		2.00	0.62	0.61	0.62	0.75	0.65
056860	(4) 6x6		2.50	0.71	0.64	0.69	0.79	0.71
008910	(3) 7x7		2.67	0.72	0.68	0.70	0.81	0.73
008490	(2) 10x10		3.33	0.77	0.79	0.74	0.90	0.80
063720	(4) 8x8	Deep (6-8)	8.00	0.90	0.86	0.87	0.95	0.90
063720	(4) 8x8		7.00	0.89	0.86	0.85	0.95	0.89
063720	(4) 8x8		6.00	0.88	0.85	0.84	0.95	0.88

Incorporating the correction factors in the 2D models can be contingent on the flexibility of the software used for the rating of the culverts. For instance, not all software commonly used for rating are flexible enough to allow overwriting the live load moments from 2D analysis with those produced from 3D analysis. For bridge rating software, it is recommended to apply the correction factors as scale factors for the live load design and legal vehicles as shown in Figure 54.

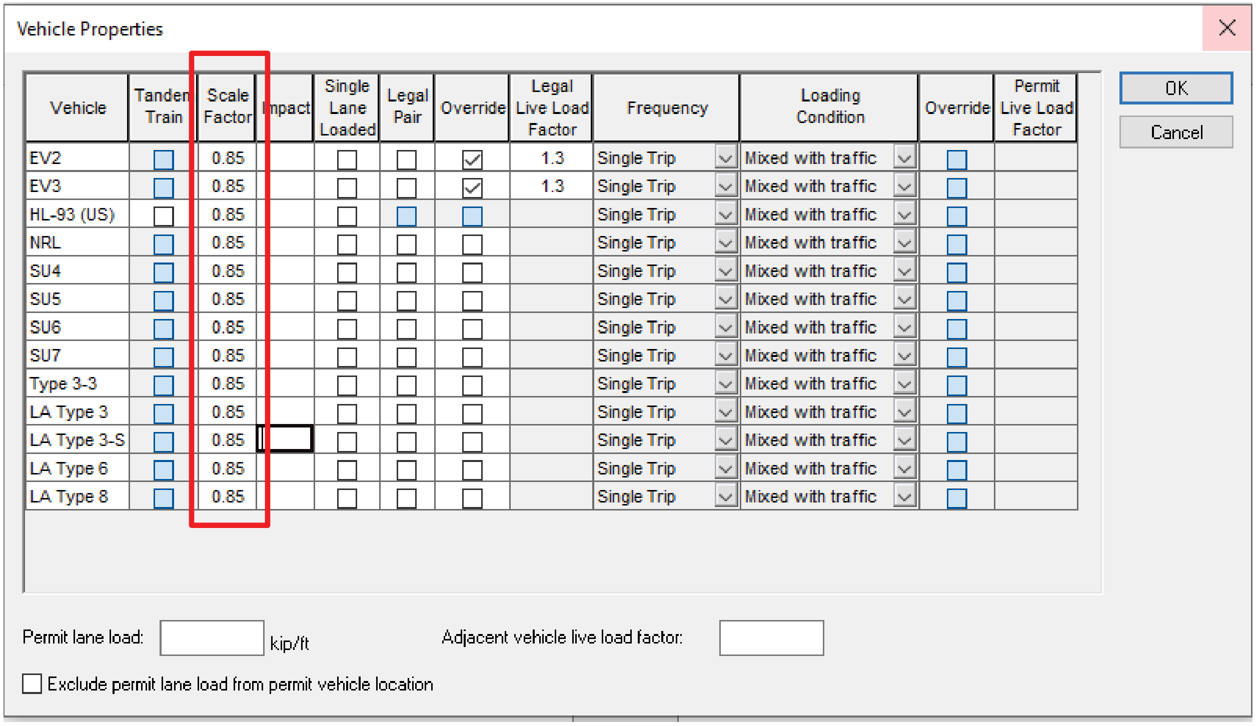
Vehicle Properties

Vehicle	Tandem Train	Scale Factor	Impact	Single Lane Loaded	Legal Pair	Override	Legal Live Load Factor	Frequency	Loading Condition	Override	Permit Live Load Factor
EV2		0.85				✓	1.3	Single Trip	Mixed with traffic		
EV3		0.85				✓	1.3	Single Trip	Mixed with traffic		
HL-93 (US)		0.85						Single Trip	Mixed with traffic		
NRL		0.85						Single Trip	Mixed with traffic		
SU4		0.85						Single Trip	Mixed with traffic		
SU5		0.85						Single Trip	Mixed with traffic		
SU6		0.85						Single Trip	Mixed with traffic		
SU7		0.85						Single Trip	Mixed with traffic		
Type 3-3		0.85						Single Trip	Mixed with traffic		
LA Type 3		0.85						Single Trip	Mixed with traffic		
LA Type 3-S		0.85						Single Trip	Mixed with traffic		
LA Type 6		0.85						Single Trip	Mixed with traffic		
LA Type 8		0.85						Single Trip	Mixed with traffic		

OK
Cancel
Permit lane load: kip/ft
Adjacent vehicle live load factor:
Exclude permit lane load from permit vehicle location

Figure 54: Correction factors applied as scale factors for design and legal vehicles in BRr.

4.3.2.2 Rigid Elements in the Walls

In traditional 2D frame element analysis, frame elements are used to model the top/bottom slabs and the walls. Frame elements are modelled at the center lines of the members and the joints are located at the junctions of the frame elements. Hence, the height of the exterior wall considered in the analysis is measured from centerline of the top slab to centerline of the bottom slab.

It is believed that the portions of the wall lying within the top and bottom slab thicknesses should not be considered part of the wall height spanning between the slabs. See **Figure 55** for illustration.

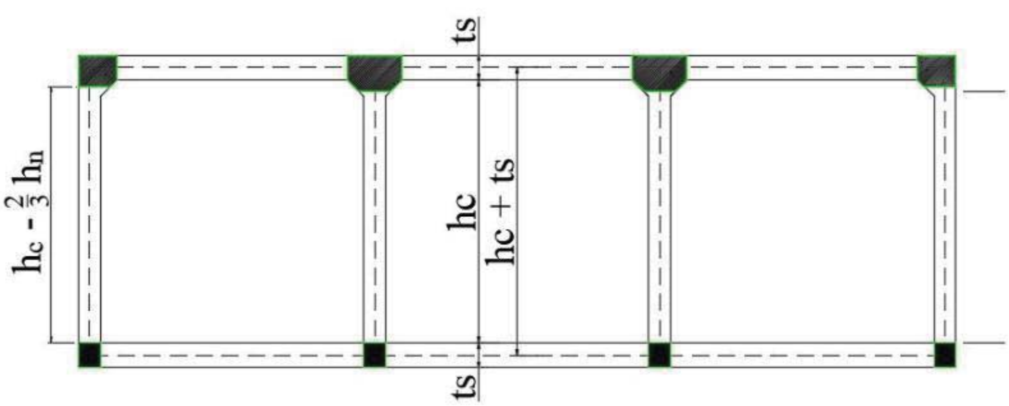

Figure 55: Rigid parts that need be extracted from culvert height

Therefore, it is recommended that the height of the modeled walls should not include the rigid portions of the wall i.e. the portions of the walls lying within the top and bottom slab thicknesses and the top haunch in the slab. Therefore, a simple adjustment to the input clear height of the culvert is recommended to extract the rigid portions of the wall members from the frame analysis. The clear height of the wall can be determined using the following equation:

$$\boldsymbol{h'_c = h_c - t_s - \frac{2}{3}h_n} \qquad \text{Eq. 16}$$

Where:

h'_c: clear height of the walls after extracting the rigid parts

h_c: clear height of the walls as given in the as built plans

t_s: thickness of the top or bottom slab

h_n: thickness of the haunch as given in the as built plans

It should be noted that review of the standard plans and field observations of the culverts indicated that haunches are utilized only in the top slab of the culvert while the bottom slab maintains a constant thickness along the entire length. The proposed adjustment of the clear wall height of the culvert can be easily implemented in Bridge Rating through the clear height input as shown in Figure 56.

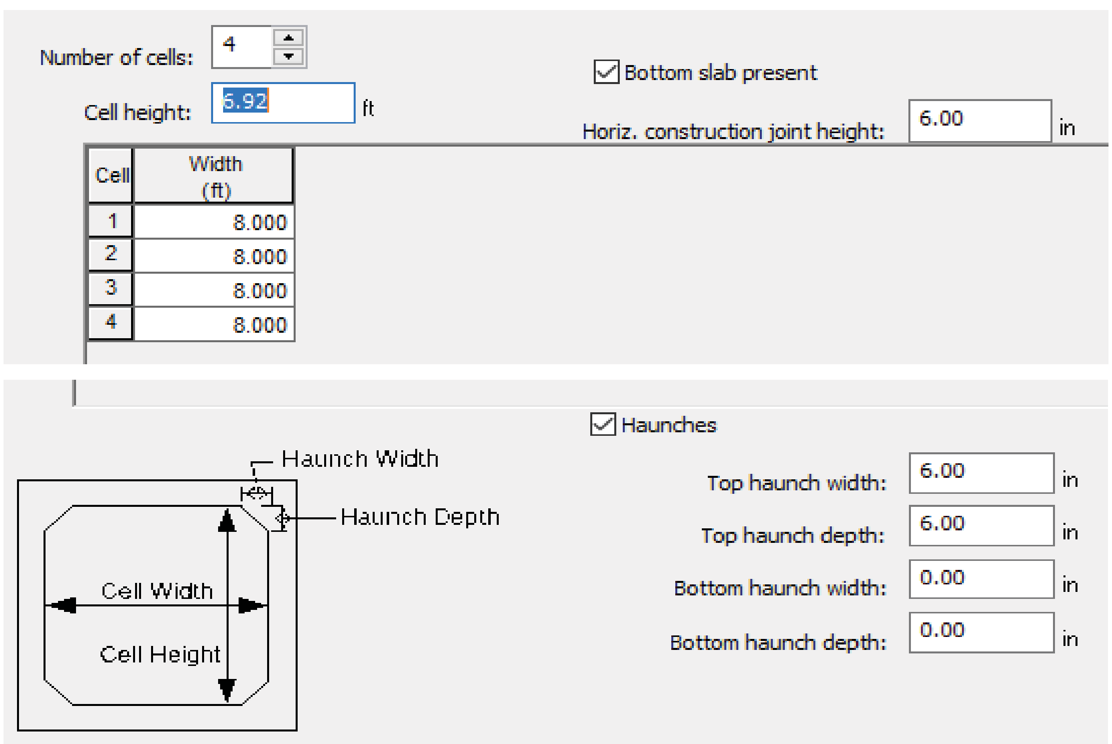

Figure 56: Adjustment of the clear height of the culvert in Bridge Rating Software

4.3.2.3 Rigid Elements in Top and Bottom Slabs

Same rationale can be applied for the portions of the top or the bottom slab lying within walls thicknesses. Those rigid parts should not be considered part of the span length in the 2D frame analysis model. See Figure 57 for illustration.

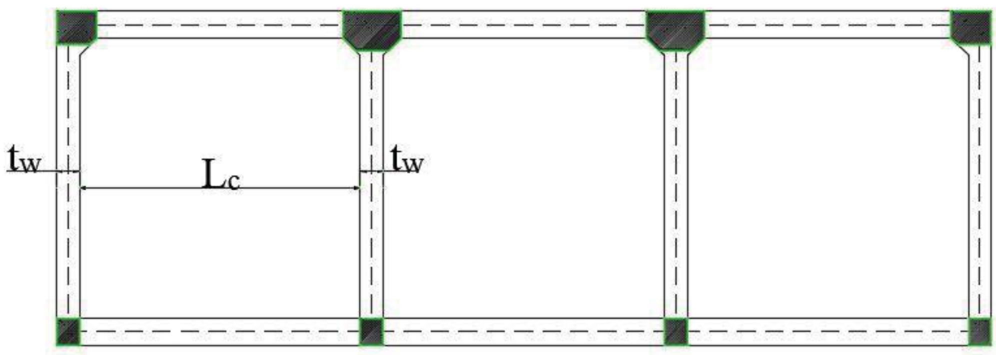

Figure 57: Rigid parts that need be extracted from culvert span length

It should be noted that inspection of the standard plans of the culverts indicated that haunches are used only at the wall/top slab junctions of the culvert while the bottom slab maintains a constant thickness along the entire length. It is recommended that the rigid portions of the slab, i.e. the portions of the slab lying within the wall thicknesses, should be ignored when determining the span length of the top/bottom slabs.

Therefore, a simple adjustment to the input clear span length of the culvert is recommended to extract the rigid portions of the slab from the frame analysis. The clear span length of the slab can be determined using the following equation:

$$\boldsymbol{L_c' = L_c - t_w} \qquad \text{Eq. 17}$$

Where:

L_c': clear span length of the culvert after extracting the rigid parts

L_c: clear span length of the culvert as given in the as built plans

t_w: smaller thickness of the thicknesses of the interior or exterior wall

The proposed adjustment of the clear span length of the culvert can be easily implemented in Bridge Rating through the clear height input as shown in Figure 58.

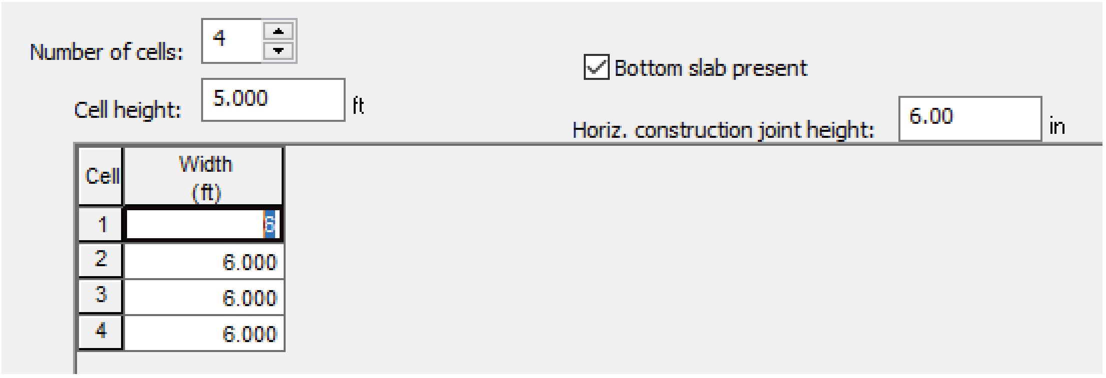

Figure 58: Adjustment of the clear span length of the culvert in Bridge Rating Software

4.3.3 Load Rating Analysis

Two approaches; namely pinned connections approach and moment connections approach; were used for load rating of the culverts. The model assumptions and rating results are described for each approach in the following sections:

4.3.3.1 Approach 1: Pinned Connections between Walls and Top/Bottom Slabs

4.3.3.1.1 Model Assumptions

As discussed before, concrete box culverts are constructed using standard plans and details developed in the 60's and 70's by Louisiana Department of Highways. Exterior walls of the culvert are reinforced at the inner face only without any reinforcement at the outer face. Such reinforcement details, shown in Figure 1, do not provide moment continuity between the top/bottom slabs and the exterior walls beyond the cracking moment level of the section. Thus, the level of moment continuity developed at the connection between the exterior walls and top slab remain questionable and contingent on relation between the applied moment on the section and the cracking moment of the section. Therefore, this issue remains undetermined and affects the analytical models used in load rating of these culverts. One conservative and simple approach is to ignore the cracking moment capacity of the section and assume pinned connections between the exterior walls/top slab and the exterior wall/bottom slab of the culvert.

Another issue is the capability of the rating software to model the pinned connections between the exterior walls and the top or bottom slabs. For bridge rating, it is possible to apply pinned connections between the walls and the slabs, however, the pinned connections will be applied at both exterior and interior walls as shown in Figure 59 and therefore a side sway support need to be provided to the model to ensure stability of the frame model.

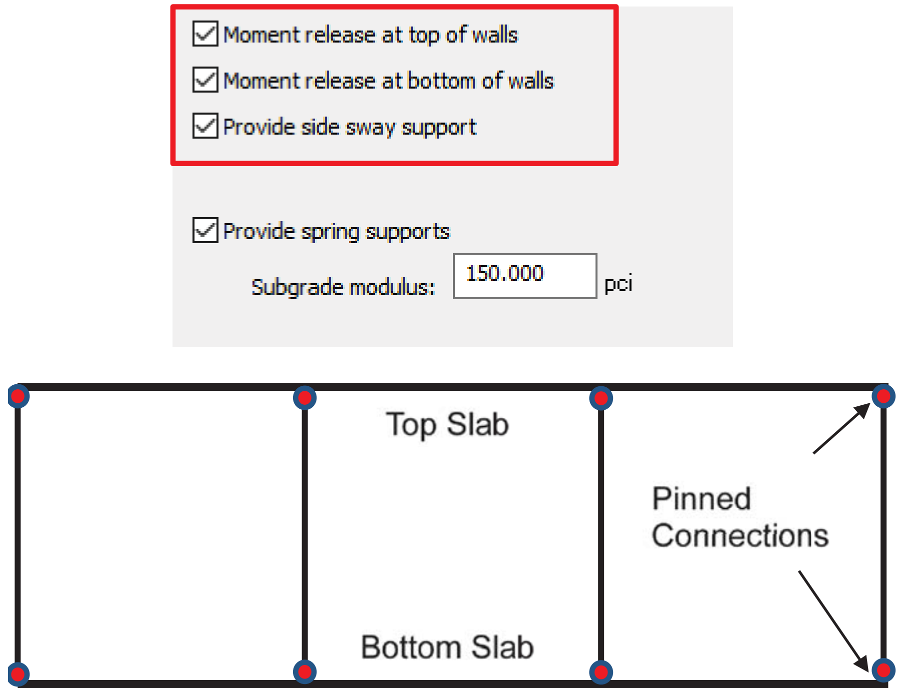

Figure 59: Applying the pinned connections to the 2D frame model in Bridge Rating software

4.3.3.1.2 Rating Results and Discussion

Table 13 presents the rating results for the culverts using the pinned connections approach and assuming at rest linear horizontal earth pressure distribution as specified in AASHTO LRFD Specifications. The 3D/2D correction factors were determined using the expressions presented in 4.1.5 and applied as reduction factor for the live load design and legal vehicles as described under section 4.3.2.1.

As can be seen from the results, the rating for the culverts with shallow fills (0 ft-2 ft) was controlled by the positive moment in the top slab of the exterior cells of the culvert with rating factors equal to 0.515 and 0.572. This is attributed to the fact that those culverts were constructed in the years 1939 and 1949 when old revision of the standard plans CC-13-15 was used. The plans show little amounts of reinforcement used in the top and bottom slabs (#4 @ 7 in) and for the walls of the culvert (#4 @12) per the design specifications during these years. It should be noted that the pinned connection approach assumes pin connections between the walls and the top/bottom slabs, such assumption increases the positive moment in the exterior cell top slab and the provided reinforcement in the section is not sufficient to provide adequate capacity.

For culverts with medium fills (2 ft -6 ft), with the exception of one culvert, the rating for all culverts was controlled by the positive moment in the mid height section of the exterior wall of the culvert. It should be noted that the pinned connection approach assumes pin connections between the walls and the top/bottom slabs, therefore the walls behave as simply supported members under the horizonal earth pressure load (EH), earth surcharge load (ES) and the live load surcharge (LS), such assumption increases the positive moment at mid height of the exterior walls and the provided reinforcement in the section is not sufficient to provide the required capacity.

For culverts with deep fills (6 ft -8 ft), the rating factors for all the culverts were zero and the controlling member is the mid height section of the exterior wall of the culvert. This is attributed to the fact that the combined dead load moment from the horizonal earth pressure load (EH) and the earth surcharge load (ES) exceed the nominal capacity of the section and therefore the analysis yielded zero for the rating factors.

It can be concluded that using the pinned connections approach combined with the at-rest horizontal earth pressure linear distribution with at rest coefficient K_0 of 0.50 yielded rating factors below 1.0 for 10 out of the 12 culverts. Therefore, further steps need be taken to improve the ratings especially for the culverts with the deep fills (6-8ft).

Table 13: Load Rating Results of the culverts using pinned connection approach and using the at-rest linear distribution for the horizontal earth pressure (AASHTO LRFD Specifications)

Culvert	Size	Fill	Fill Height (ft)	3D/2D correction factor	At rest coefficient K_o	% of LS Load Applied	Controlling Section (Legal Load)	RF
004770	(4) 6x6	Shallow (0-2)	1.00	0.80	0.50	100%	Top Slab	0.515
004780	(4) 6x6		1.25	0.80	0.50	100%	Top Slab	0.572
004360	(3) 10x10	Medium (2-6)	2.33	0.68	0.50	100%	Top Slab	0.756
004510	(3) 7x7		4.50	0.88	0.50	100%	Ext wall mid height	1.610
005450	(4) 8x8		2.92	0.76	0.50	100%	Ext wall mid height	1.534
005488	(3) 7x7		2.00	0.65	0.50	100%	Ext wall mid height	0.982
056860	(4) 6x6		2.50	0.71	0.50	100%	Ext wall mid height	0.692
008910	(3) 7x7		2.67	0.73	0.50	100%	Ext wall mid height	0.878
008490	(2) 10x10		3.33	0.80	0.50	100%	Ext wall mid height	0.579
063720	(4) 8x8	Deep (6-8)	8.00	0.90	0.50	100%	Ext wall mid height	0.000
063720	(4) 8x8		7.00	0.89	0.50	100%	Ext wall mid height	0.000
063720	(4) 8x8		6.00	0.88	0.50	100%	Ext wall mid height	0.000

In an attempt to enhance the load ratings results, the culverts were analyzed under horizontal earth pressure that consider the soil arching effect per the approach presented in the Texas Transportation Institute Research Report (1986) and section 3.1.4.1 in this report.

Table 14 summarizes the rating results for the 12 culverts.

It should be noted that the horizontal earth pressure considering the soil arching effect assumes a nonlinear pressure distribution on the exterior wall. Since Bridge rating uses the at-rest linear distribution for the horizontal earth pressure as specified by AASHTO, therefore an adjustment was made to the lateral soil coefficient K_0 such that the moment at mid height of the wall resulting from the at rest linear distribution is equal to the moment obtained using the nonlinear distribution considering the soil arching effect. The value for lateral soil coefficient K_0 that satisfies this condition was found to be 0.42.

Such adjustment of the soil lateral coefficient K_0 can be implemented easily in Bridge rating software as shown in Figure 60.

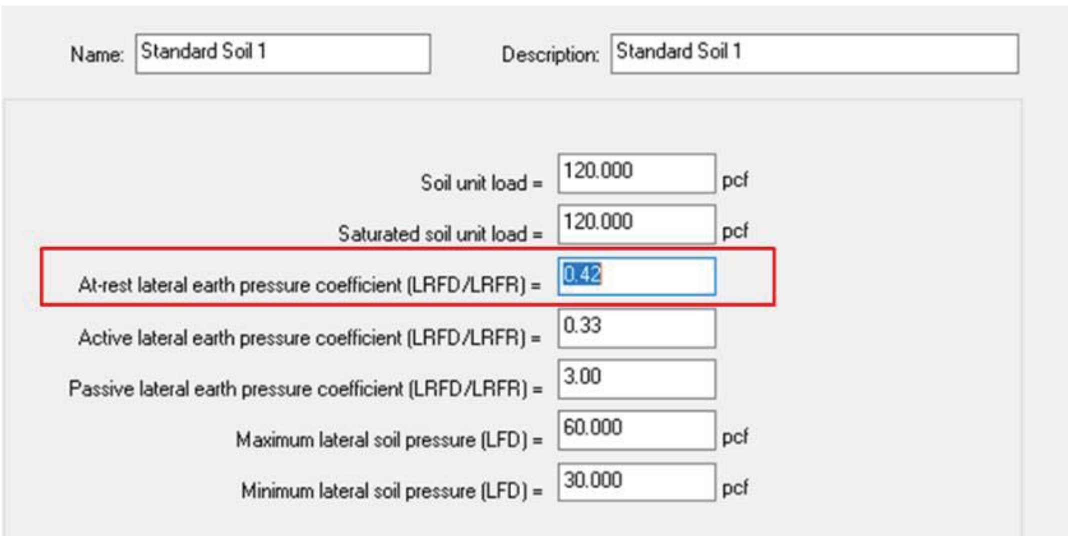

Figure 60: Adjustment of soil lateral coefficient in Bridge rating

As can be seen from the results shown in Table 14, ratings for the culverts with shallow fills (0 ft-2 ft) remain controlled by the positive moment in the top slab of the exterior cells of the culvert. Except for one culvert, the ratings factors for all culverts with medium fills (2 ft -6 ft) was greater than 1.0. The rating factors under legal vehicles for six culverts ranged from 1.063 to 2.018. However, for the culvers with deep fills, the rating factors for all culverts were < 1.0.

It can be concluded that using the pinned connections approach applied in conjunction with the soil arching horizontal earth pressure non-linear distribution with at rest coefficient K_0 of 0.42 resulted in enhancement in the load rating, however, culverts with deep fills (6-8ft) remained deficient.

Table 14: Load Rating Results of the culverts using pinned connection approach and using the horizontal earth pressure considering the soil arching effect (Texas Transportation Institute Research Report 1986)

Culvert	Size	Fill	Fill Height (ft)	3D/2D correction factor	At rest coefficient K_o	% of LS Load Applied	Controlling member (Legal Load)	RF
004770	(4) 6x6	Shallow (0-2)	1.00	0.80	0.42	100%	Top Slab	0.515
004780	(4) 6x6		1.25	0.80	0.42	100%	Top Slab	0.572
004360	(3) 10x10	Medium (2-6)	2.33	0.68	0.42	100%	Top Slab	0.756
004510	(3) 7x7		4.50	0.88	0.42	100%	Top Slab	2.018
005450	(4) 8x8		2.92	0.76	0.42	100%	Top Slab	1.688
005488	(3) 7x7		2.00	0.65	0.42	100%	Top Slab	1.253
056860	(4) 6x6		2.50	0.71	0.42	100%	Ext wall mid height	1.063
008910	(3) 7x7		2.67	0.73	0.42	100%	Ext wall mid height	1.324
008490	(2) 10x10		3.33	0.80	0.42	100%	Ext wall mid height	1.120
063720	(4) 8x8	Deep (6-8)	8.00	0.90	0.42	100%	Ext wall mid height	0.093
063720*	(4) 8x8		7.00	0.89	0.42	100%	Ext wall mid height	0.311
063720*	(4) 8x8		6.00	0.88	0.42	100%	Ext wall mid height	0.509

In general, using the pinned connections approach, is not recommended since this approach assumes pin connections at the wall/slab junctions and such assumption increases the positive moment in the exterior cell top slab where the provided reinforcement is usually not sufficient to provide adequate capacity. Especially for culverts with shallow fills (0-2ft.) that were constructed using the old revisions of the standard plans (CC-13-15).

In addition, the pinned connection approach applies simple span moment on the exterior walls of the culvert and therefore the ratings are usually controlled by the exterior walls especially for the culverts with deep fills (6ft. – 8ft.)

4.3.3.2 Approach 2: Moment Connections between Walls and Top/Bottom Slabs

4.3.3.2.1 Model Assumptions

This model assumes moment connections between the walls and the slabs of the culvert. Though it seems not reasonable to assume moment connections between the exterior walls and the top/bottom slabs because of the lack of the corner reinforcement that is necessary to develop the framing action between the exterior walls and the slabs. The hypothesis for this approach stands to the fact that the sum of the unfactored forces at the unreinforced sections of the exterior wall and the slabs is less than the cracking moment of the sections.

The cracking moment, M_{cr}, for the top slab and the wall sections was determined using the as-built concrete strength of 3.5 ksi. In addition, the summation of the unfactored section forces at the key sections of the top slab and the exterior walls of the culverts was determined using the 3D FE models developed for those culverts in Task 5. The moment values are summarized in **Table 15**. It was found that the summation of the unfactored section forces at each critical bending moment section poses less demand than the uncracked section capacities. This implies that the considered culverts are still behaving as uncracked RC sections under service loads.

Table 15: Summation of unfactored forces and cracking moment of key sections of top slabs and walls

Culvert	Size	Fill	Top Slab Sections			Wall Sections		
			M_{DL+LL}	M_{cr}	Ratio %	M_{DL+LL}	M_{cr}	Ratio %
004770	6x6	Shallow (0-2)	0.60	4.38	14	0.64	2.46	26
004780	6x6		0.65	4.38	15	0.65	2.46	26
004360	10x10	Medium (2-6)	3.00	6.85	44	4.12	6.85	60
004510	7x7		1.27	4.95	26	1.61	3.35	48
005450	8x8		2.08	5.55	37	2.22	4.38	51
005488	7x7		1.02	4.95	21	1.15	3.35	34
056860	6x6		0.68	4.38	16	1.26	2.46	51
008910	7x7		1.01	5.55	18	1.20	4.38	27
008490	10x10		4.39	6.85	64	5.39	6.85	79
063720	8x8	Deep (6-8)	2.46	5.55	44	3.37	4.38	77

This hypothesis implies that the capacity of the unreinforced section can be limited to the cracking moment of the section. It should be noted that, for Bridge rating software, the nominal capacity of the concrete sections is only determined for sections that have reinforcing steel. Therefore, it is recommended to apply virtual reinforcements at the four corners of the culvert such that the nominal capacity of the section is limited to 70 percent of the cracking moment of the section. Figure 61 shows the applied virtual reinforcement at the corners of the culvert in Bridge Rating Software.

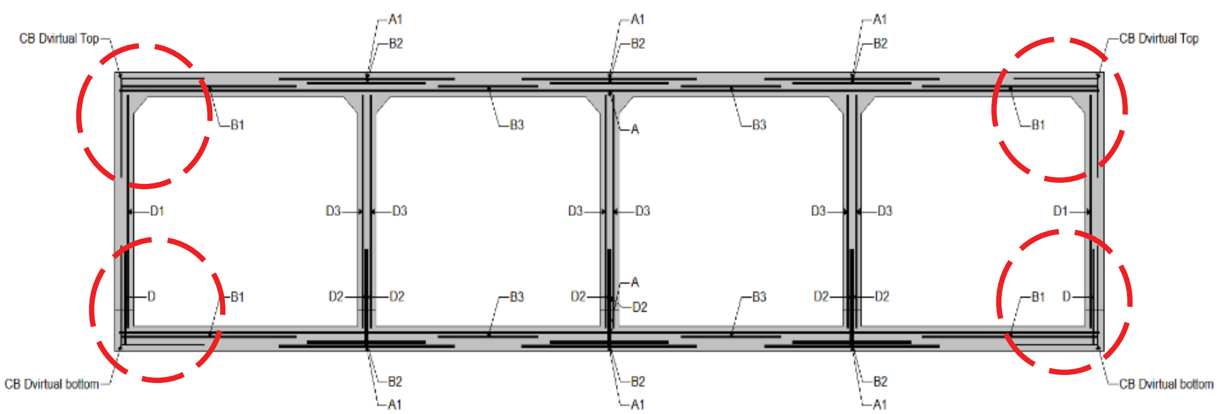

Figure 61: Virtual reinforcements applied at the culvert four corners

The following equations can be used to determine the virtual reinforcement at the corners of the culverts.

$$f_r = 7.5\sqrt{f_c} \quad \text{Eq. 18}$$

$$M_{cr} = \frac{f_r I_s}{y_s} \quad \text{Eq. 19}$$

$$A_{sv} = \frac{\beta\, M_{cr}}{0.90\, d_s\, f_y} \qquad \text{Eq. 20}$$

$$\beta = 0.70 \qquad \text{Eq. 21}$$

It should be noted that previous studies have shown that, typically the measured concrete strengths based on concrete cores extracted from the culverts is usually greater than the as built concrete strength which is assumed to be between 3000 to 4000 psi. The average measured concrete strength for 8 culverts that were load tested recently in the LTRC project No. 16-3ST was found to be 8300 psi. However, as a conservative practice, the cracking moment is determined using the concrete strength indicated in the as built plans.

The rationale behind using 70% of the cracking moment is attributed to the brittle nature of unreinforced concrete sections.

It is worth noting that the standard plans show that the haunches are applied at the top slab corners only and the bottom slab maintain a constant thickness along the entire length. It is typical that the wall sections have smaller thickness than the slab sections because of the beneficial influence from the compression axial force. In addition, the cracking moment for wall section is usually greater than the slab section due to the axial force effect. Calculations have shown that the axial force effect can increase the cracking moment of the wall section by about 5 to 10%.

Therefore, it is recommended for each corner of the culvert, to determine the virtual reinforcement using the cracking moment of the slab section and the cracking moment of wall section and use the least of the two values.

The virual reinforcement was determined using the procedure described above for the 12 culverts and the results are summarized in Table 16.

Table 16: Virtual reinforcement to be applied at the corners of the culverts

Culvert	Size	Fill	Fill Height (ft)	Virtual Reinforcements			
				Top Corners		Bottom Corners	
004770	(4) 6x6	Shallow (0-2)	1.00	0.182	#4@14	0.182	#4@12
004780	(4) 6x6		1.25	0.182	#4@14	0.182	#4@12
004360	(3) 10x10	Medium (2-6)	2.33	0.239	#4@12	0.245	#4@10
004510	(3) 7x7		4.50	0.207	#4@12	0.211	#4@12
005450	(4) 8x8		2.92	0.196	#4@12	0.196	#4@12
005488	(3) 7x7		2.00	0.196	#4@12	0.196	#4@12
056860	(4) 6x6		2.50	0.178	#4@14	0.196	#4@12
008910	(3) 7x7		2.67	0.196	#4@12	0.196	#4@12
008490	(2) 10x10		3.33	0.223	#4@12	0.245	#4@10
063720	(4) 8x8	Deep (6-8)	8.00	0.207	#4@12	0.211	#4@12
063720*	(4) 8x8		7.00	0.207	#4@12	0.211	#4@12
063720**	(4) 8x8		6.00	0.207	#4@12	0.211	#4@12

4.3.3.2.2 Rating Results and Discussion

Table 17 presents the rating results for the culverts using the moment connections approach and assuming at rest linear horizontal earth pressure distribution as specified in AASHTO LRFD Specifications. The 3D/2D correction factors were determined using the expressions presented in section 4.1.5 and applied as reduction factor for the live load design and legal vehicles as described in section 4.3.2.1.

As can be seen from the results, with the exception of one culvert, the rating for all culverts (with shallow fills (0 ft-2 ft), medium fills (2 ft -6 ft) and deep fills) was controlled by the bottom section of the exterior wall with rating factors ranging from 1.060 to 1.729. It should be noted that no haunch is applied at the exterior wall/bottom slab junction and since the wall section thickness is less than the bottom slab thickness therefore the bottom wall section controls the rating.

The moment connections approach assumes full framing action between the walls and the top/bottom slabs, which entails better moment distribution between the negative moment and positive moment sections in the slab and the walls and therefore results in greater ratings.

It should be noted that the assumption of the full framing action between the exterior wall and the top/bottom slab despite of the lack of the corner reinforcement remains reasonable given the fact that the sum of the unfactored forces at the unreinforced sections of the exterior wall and the slabs is less than the cracking moment of the sections and hence the capacity of these sections can be limited to the cracking moment of the section.

It can be concluded that using the moment connections approach combined with the at-rest horizontal earth pressure linear distribution with at rest coefficient K_0 of 0.50 yielded rating factors above 1.0 for culverts with different fill heights.

Table 17: Load Rating Results of the culverts using moment connections approach and using the at-rest linear distribution for the horizontal earth pressure (AASHTO LRFD Specifications)

Culvert	Size	Fill	Fill Height (ft)	3D/2D correction	At rest coefficient K_o	% of LS Load Applied	Controlling member (Legal Load)	RF
004770	(4) 6x6	Shallow (0-2)	1.00	0.80	0.50	100%	Ext wall Bot section	1.119
004780	(4) 6x6		1.25	0.80	0.50	100%	Ext wall Bot section	1.147
004360	(3) 10x10	Medium (2-6)	2.33	0.68	0.50	100%	Ext wall Bot section	1.110
004510	(3) 7x7		4.50	0.88	0.50	100%	Bottom Slab	1.749
005450	(4) 8x8		2.92	0.76	0.50	100%	Ext wall Bot section	1.353
005488	(3) 7x7		2.00	0.65	0.50	100%	Ext wall Bot section	1.252
056860	(4) 6x6		2.50	0.71	0.50	100%	Ext wall Bot section	1.568
008910	(3) 7x7		2.67	0.73	0.50	100%	Ext wall Bot section	1.436
008490	(2) 10x10		3.33	0.80	0.50	100%	Ext wall Bot section	1.279
063720	(4) 8x8	Deep (6-8)	8.00	0.90	0.50	100%	Ext wall Bot section	1.009
063720*	(4) 8x8		7.00	0.89	0.50	100%	Ext wall Bot section	1.131
063720**	(4) 8x8		6.00	0.88	0.50	100%	Ext wall Bot section	1.249

Since the ratings for the culverts were controlled by the bottom section in the exterior wall, it is suggested that further improvement of the rating factors for the culverts can be achieved as shown in Table 18 when analyzing the culverts under horizontal earth pressure that consider the soil arching effect per the approach presented in Texas Transportation Institute Research Report (1986).

Table 18: Load Rating Results of the culverts using moment connections approach and using the horizontal earth pressure considering the soil arching effect (Texas Transportation Institute Research Report 1986)

Culvert	Size	Fill	Fill Height (ft)	3D/2D correction	At rest coefficient K_o	% of LS Load Applied	Controlling member (Legal Load)	RF
004770	(4) 6x6	Shallow (0-2)	1.00	0.80	0.42	100%	Ext wall Bot section	1.152
004780	(4) 6x6		1.25	0.80	0.42	100%	Ext wall Bot section	1.183
004360	(3) 10x10	Medium (2-6)	2.33	0.68	0.42	100%	Ext wall Bot section	1.255
004510	(3) 7x7		4.50	0.88	0.42	100%	Bottom Slab	2.096
005450	(4) 8x8		2.92	0.76	0.42	100%	Ext wall Bot section	1.504
005488	(3) 7x7		2.00	0.65	0.42	100%	Ext wall Bot section	1.360
056860	(4) 6x6		2.50	0.71	0.42	100%	Ext wall Bot section	1.706
008910	(3) 7x7		2.67	0.73	0.42	100%	Ext wall Bot section	1.585
008490	(2) 10x10		3.33	0.80	0.42	100%	Ext wall Bot section	1.432
063720	(4) 8x8	Deep (6-8)	8.00	0.90	0.42	100%	Ext wall Bot section	1.407
063720*	(4) 8x8		7.00	0.89	0.42	100%	Ext wall Bot section	1.471
063720**	(4) 8x8		6.00	0.88	0.42	100%	Ext wall Bot section	1.537

4.3.4 Live load distribution factor for culverts with fill heights less than 2.0 ft.

AASHTO's tire pressure load distribution is based on the assumption of the distributing the wheel load to an area of tire contact area (about 20" by 10" for 32-kip tandem axle) plus 15% of fill thickness. Thus, the LRFR live load distribution factor of 1.15 should be used. This is an extremely conservative assumption, ASCE 15-98 "Standard Practice for Direct Design of Buried Precast Concrete Pipe using Standard Installations (SIDD)" allows the use of 1.75. Florida DOT sponsored a theoretical study by University of Florida entitled "Design Live Loads on Box Culverts" (2002), using conservative assumptions of overlapping stresses from two 6-foot spaced 25-kip axles and equivalent load effects from the assumed loads, the distribution factor was found to be about 2.0. Note that the above studies do not include the layered effect from the pavement structures which could result in further distribution enhancement.

Based on the above, it is recommended that the live load distribution factor be taken equal to 1.15 for culverts with fill heights greater than 2 ft., however, for culverts with fill heights less than 2 ft., live load distribution factor can be taken equal to 1.75. The input for BRr LRFR live load distribution factor can be adjusted as shown in **Figure 62**.

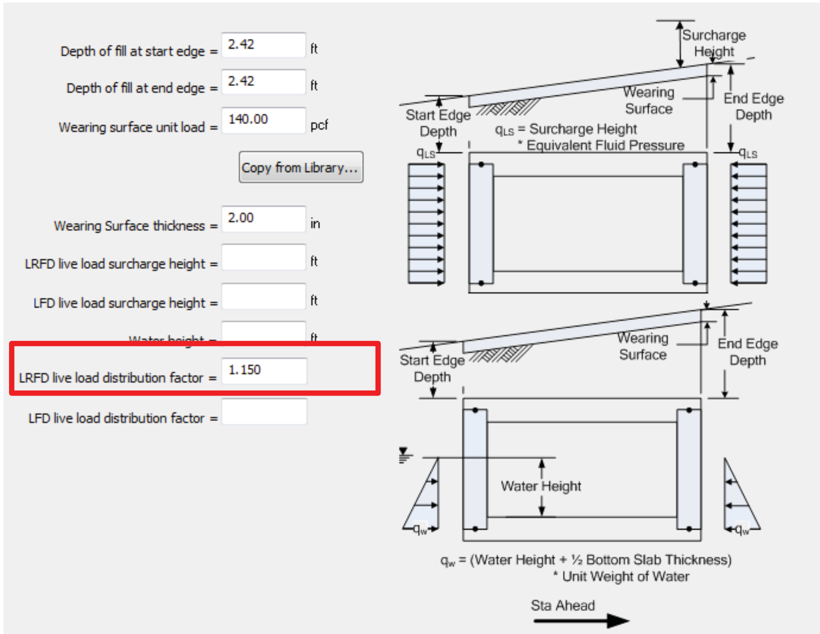

Figure 62: Adjustment of the live load distribution factor in BRr software

4.3.5 Live load surcharge (LS)

As presented in section 3.1.4.3, AASHTO-LRFD specification suggests a uniform lateral surcharge load that is applied on the entire height of the exterior wall of the culvert as a representation of the pressure exerted on the wall when a truck wheel approaches the culvert. The NCHRP 15-54 study have shown that such assumption can be considered extremely conservation given the fact that the surcharge pressure decreases rapidly with the increase of the fill depth. Moreover, field tests from previous research have shown that the maximum lateral pressure occurs at the top slab of the culvert and therefore is transmitted directly through the top slab and does not create bending moments in the wall sections.

NCHRP 15-54 study recommends to use the ASTM equation (Eq. 12 in the report) to determine the live load surcharge for culverts with fill height above the top slab that is less than 2 ft., and that no lateral live load surcharge shall be applied for culverts with fill heights above the top slab greater than 2 ft.

Though NCHRP recommends not to apply surcharge load on culverts with fill heights greater than 2 ft., it is quite interesting to investigate the differences between the ASTM equation and the AASHTO provisions for the live load surcharge especially for the culverts with deep fills. Therefore, the two methods were used to determine the surcharge to be applied to the exterior wall of a culvert that has a fill height equal to 8 ft. above the top slab. It should be noted that the rating analysis for the 12 culverts presented in **Tables 13, 14, 17 and 18** was carried out using AASHTO LRFD provisions for live load surcharge.

The live load surcharge on the exterior wall of a 3-cell culvert with a fill height equal to 8 ft. above the top slab was determined using the ASTM equation and the AASHTO LRFD approach for sake of comparison. The live load surcharge distributions from the two methods are compared in **Figure 63**.

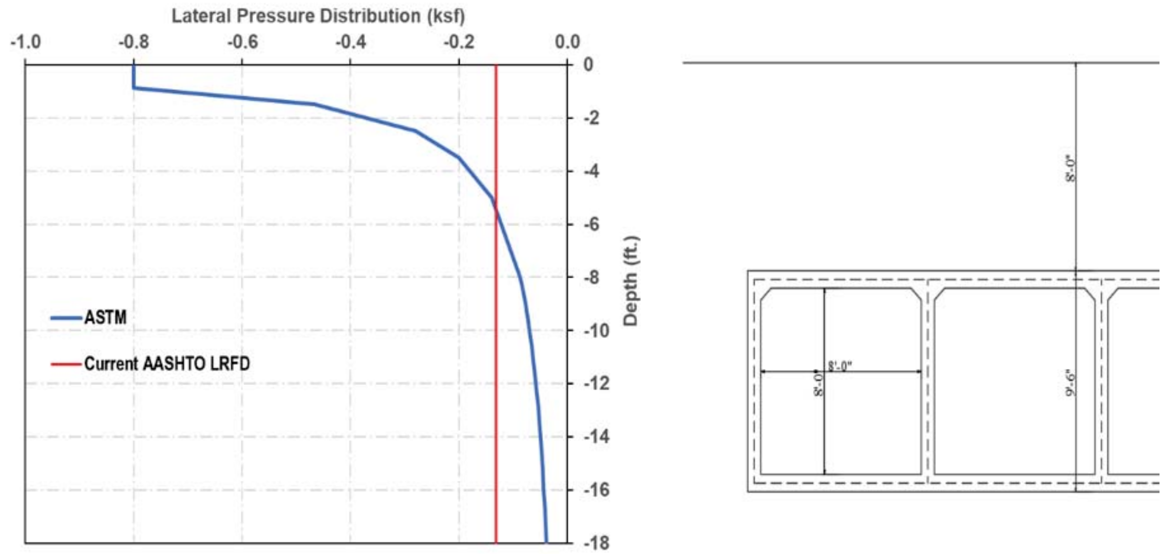

Figure 63: Live load surcharge from ASTM standards versus AASHTO LRFD

As can be seen from Figure 63, ASTM standards equation provides more realistic distribution for the surcharge load that decreases with the fill depth, however, the AASHTO provisions which assumes a constant pressure with the depth of fill. The ASTM equation yields a distribution that remains in line with the field test findings. Such observations between the two methods implies that the ASTM equation results in a lesser applied load than AASHTO and therefore lesser moments on the exterior walls of the culvert and thus higher ratings.

Therefore, it is recommended to consider the NCHRP recommendations pertaining to live load surcharge when performing the rating analysis for reinforced concrete box culverts.

It should be noted that the exterior wall bottom section controlled the ratings for most of the culverts (Table 17) and therefore such recommendation can help improve the ratings of the exterior wall sections.

4.3.6 Recommended Load Rating Procedure

The following steps summarizes the recommended procedure for load rating of reinforced concrete box culverts based on the findings presented in the previous sections of this project. Based on the rating results obtained from the pinned connections approach and the moment connections approach presented in sections 4.3.3.1 and 4.3.3.2. It is recommended to use the moment connections approach for the rating analysis of the reinforced concrete box culverts as illustrated in the following steps:

Step 1: Determine the 3D/2D correction factors using the expressions in 4.1.5 and apply the live load scale factors in Bridge rating as outlined in section 4.3.2.1

Step 2: Determine the clear height of the culvert after extracting the rigid parts. Define the clear height of the culvert in Bridge rating as outlined in section 4.3.2.2

Step 3: Determine the clear span length of the culvert after extracting the rigid parts. Define the clear span length of the culvert in Bridge rating as outlined in section 4.3.2.3

Step 4: The lateral soil coefficient K_0 shall be taken equal to 0.50 and the at-rest lateral soil pressure linear distribution per AASHTO LRFD shall be adopted for the analysis.

Step 5: The live load surcharge (LS) shall be determined per article 3.11.6.4 of AASHTO LRFD.

Step 6: Assume full moment connections at the junctions of the exterior walls and the top/bottom slabs. Determine the virtual reinforcement to be applied at the corners of the culvert as outlined in section 4.3.3.2.1.

Step 7: Run the analysis to determine the rating factors.

Step 8 to *step 10* can be applied individually or combined, as needed, to improve the ratings for the culverts.

Step 8: The lateral soil pressure on the exterior walls of the culvert can be modified to consider the soil arching effect as outlined in Texas Transportation Institute report (1986) (also see section 3.1.4.1 of this report). The lateral soil coefficient K_0 input in Bridge rating shall be adjusted such that the moment at mid height of the wall resulting from the at rest linear distribution is equal to the moment from the nonlinear distribution considering the soil arching effect. See Figure 60 for illustration.

Step 9: NCHRP 15-54 recommendations for the live load surcharge (section 4.3.5) can be applied for the rating analysis of the culverts.

Step 10: For culverts with fill heights above the top slab less than 2 ft., live load distribution factor can be taken equal to 1.75. See Figure 62 for illustration.

5. APPENDIX A: LIVE LOAD DISTRIBUTION ON THE TOP SLAB OF THE CULVERT FOR FE MODELS

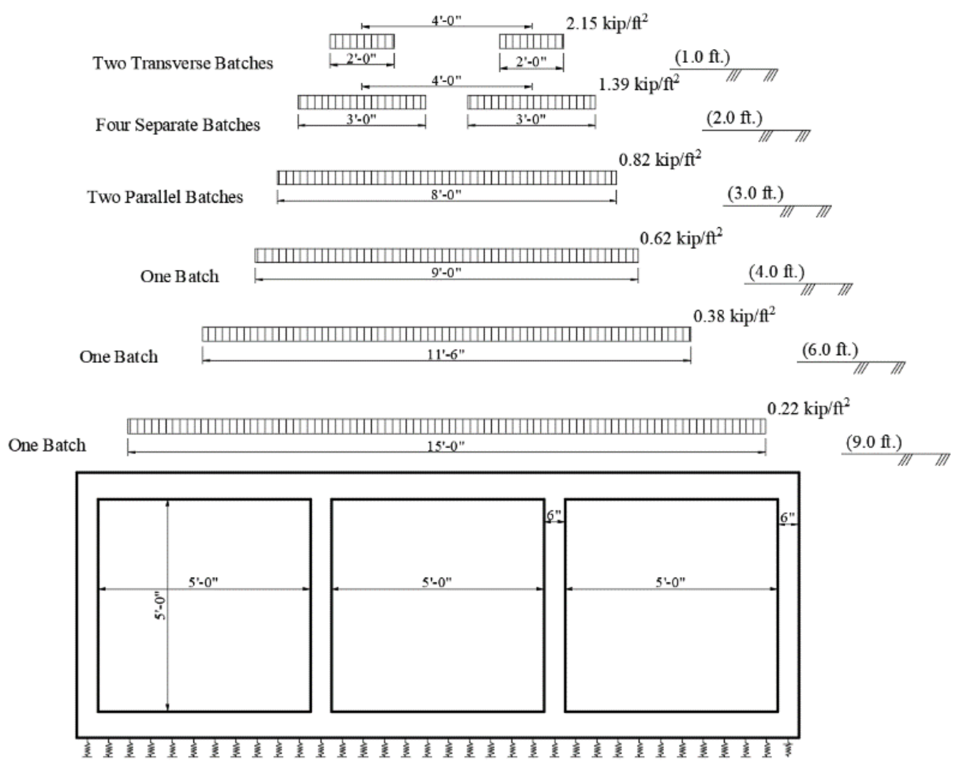

Live load distribution at the surface of the top slab in the direction parallel to span for 5 x 5 culverts

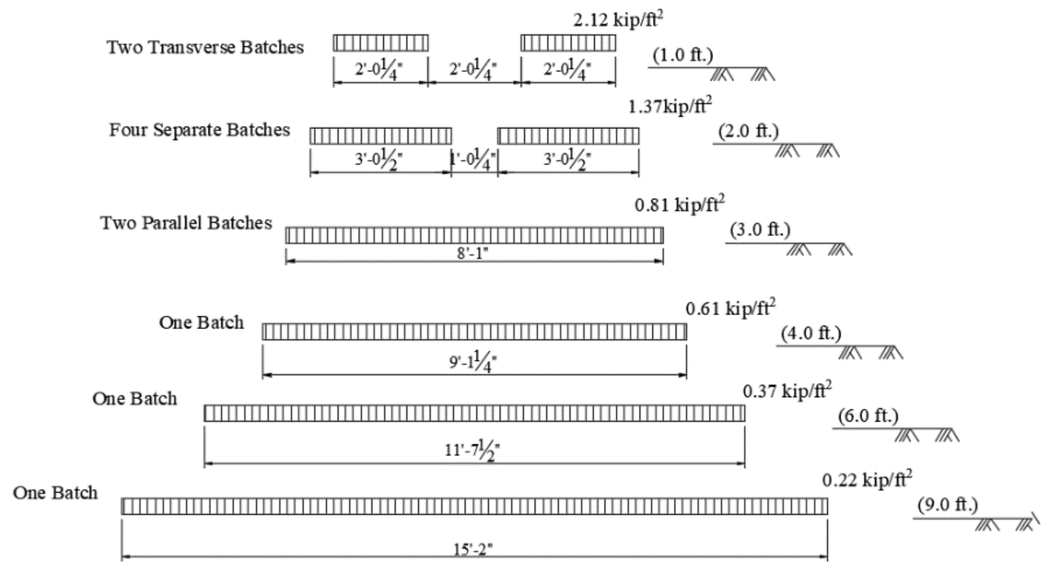

Live load distribution at the surface of the top slab in the direction parallel to span for 7 x 7 culverts

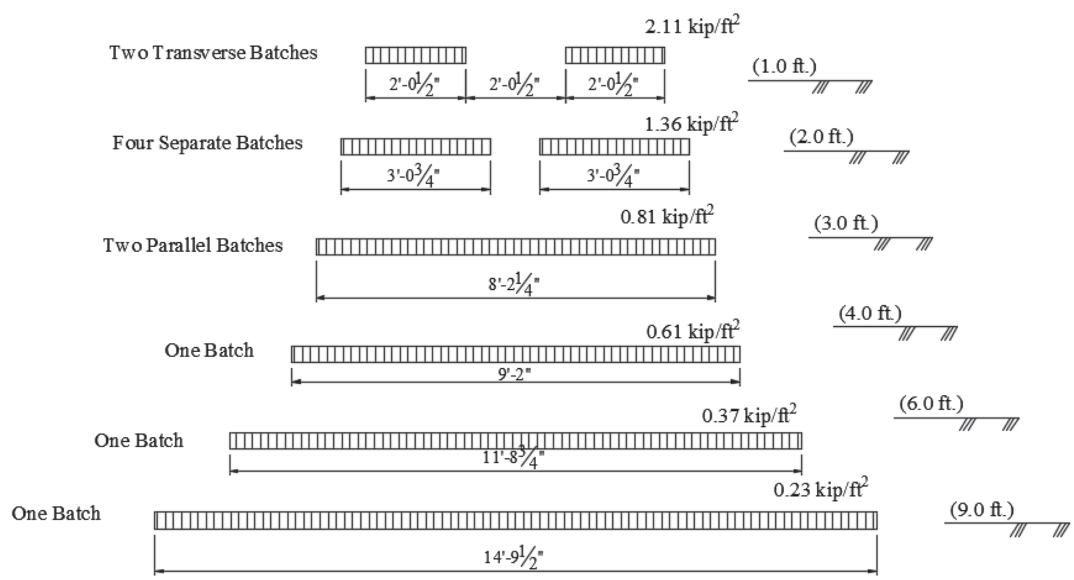

Live load distribution at the surface of the top slab in the direction parallel to span for 8 x 8 culverts

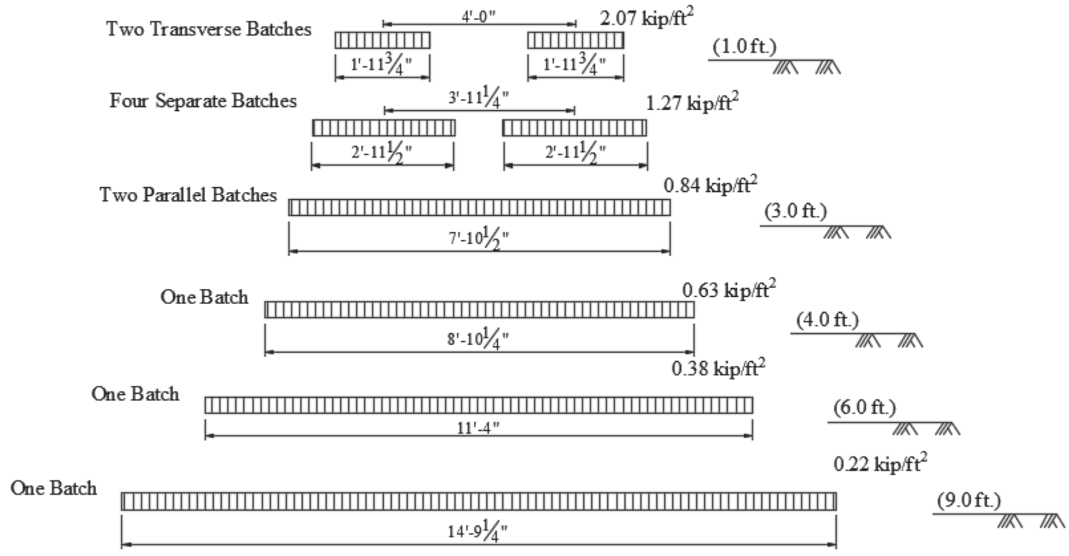

Live load distribution at the surface of the top slab in the direction parallel to span for 10 x 10 culverts

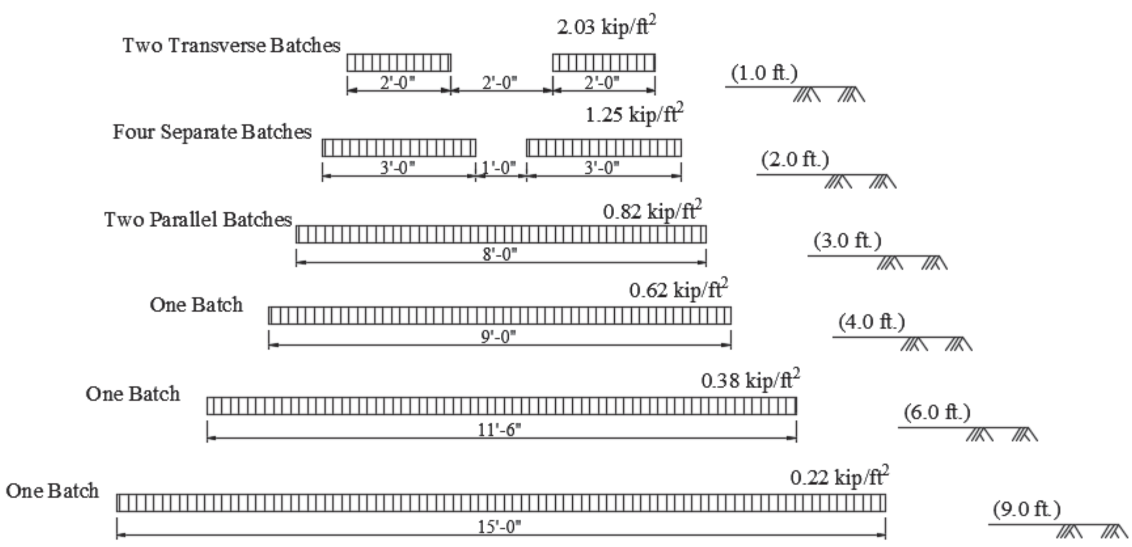

Live load distribution at the surface of the top slab in the direction parallel to span for 12 x 12 culverts

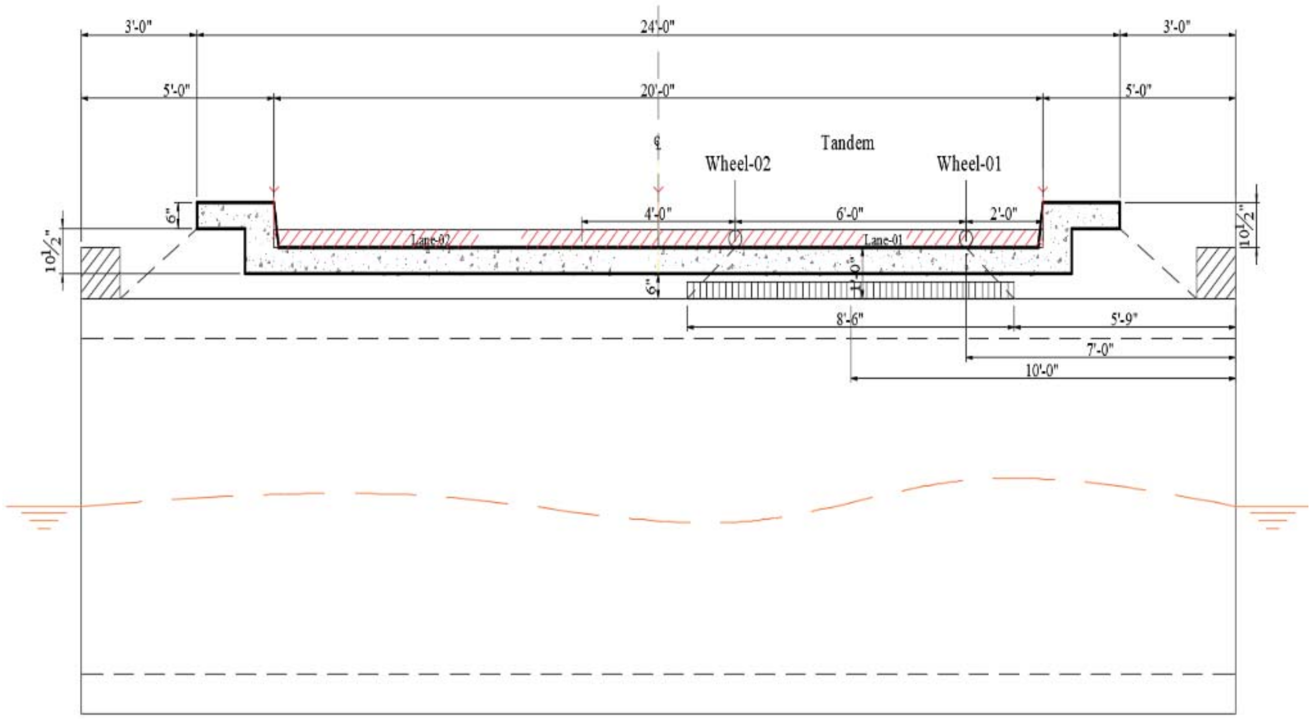

Live load distribution at the surface of the top slab in the direction perpendicular to the culvert span for fill height of 1.0 ft

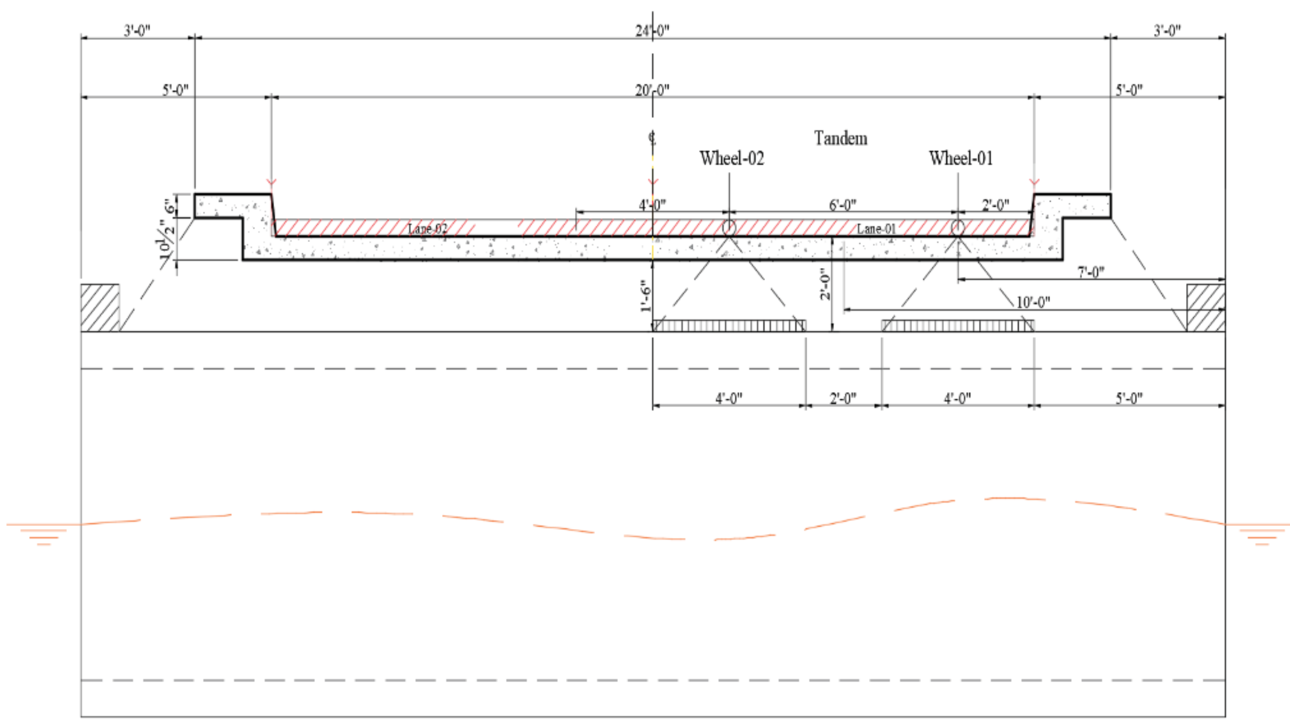

Live load distribution at the surface of the top slab in the direction perpendicular to the culvert span for fill height of 2.0 ft

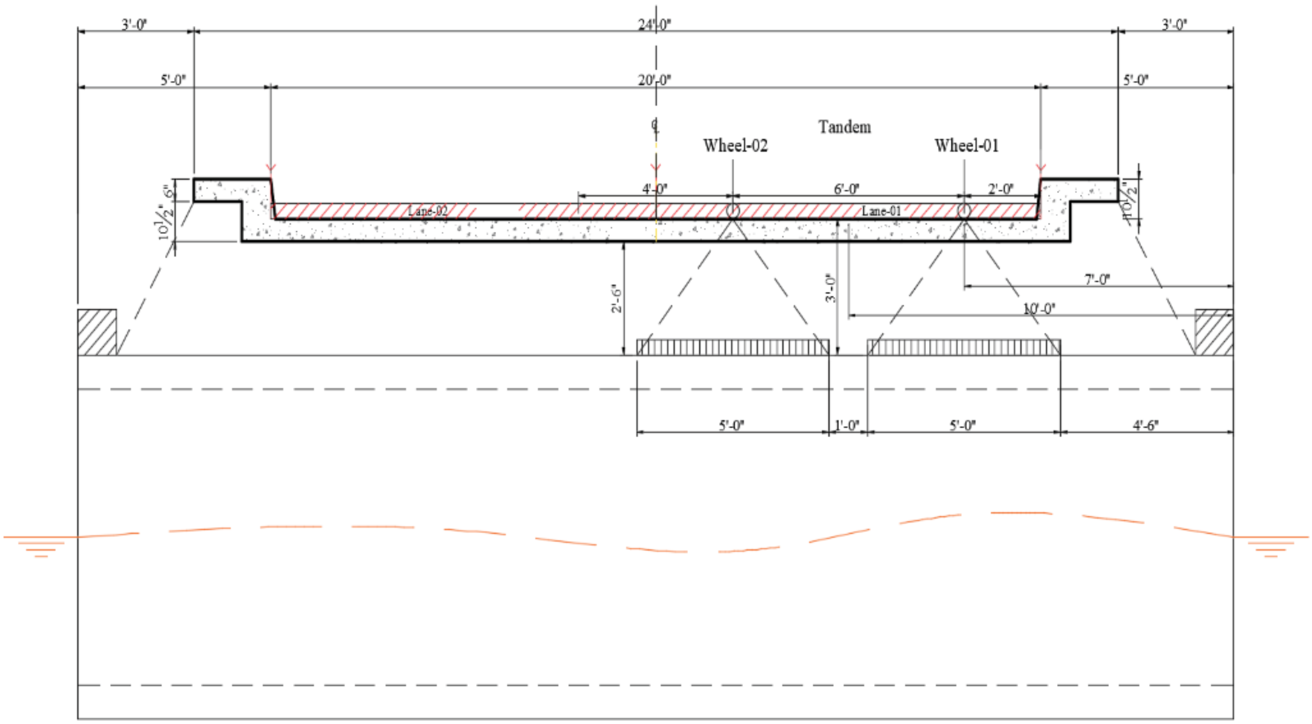

Live load distribution at the surface of the top slab in the direction perpendicular to the culvert span for fill height of 3.0 ft

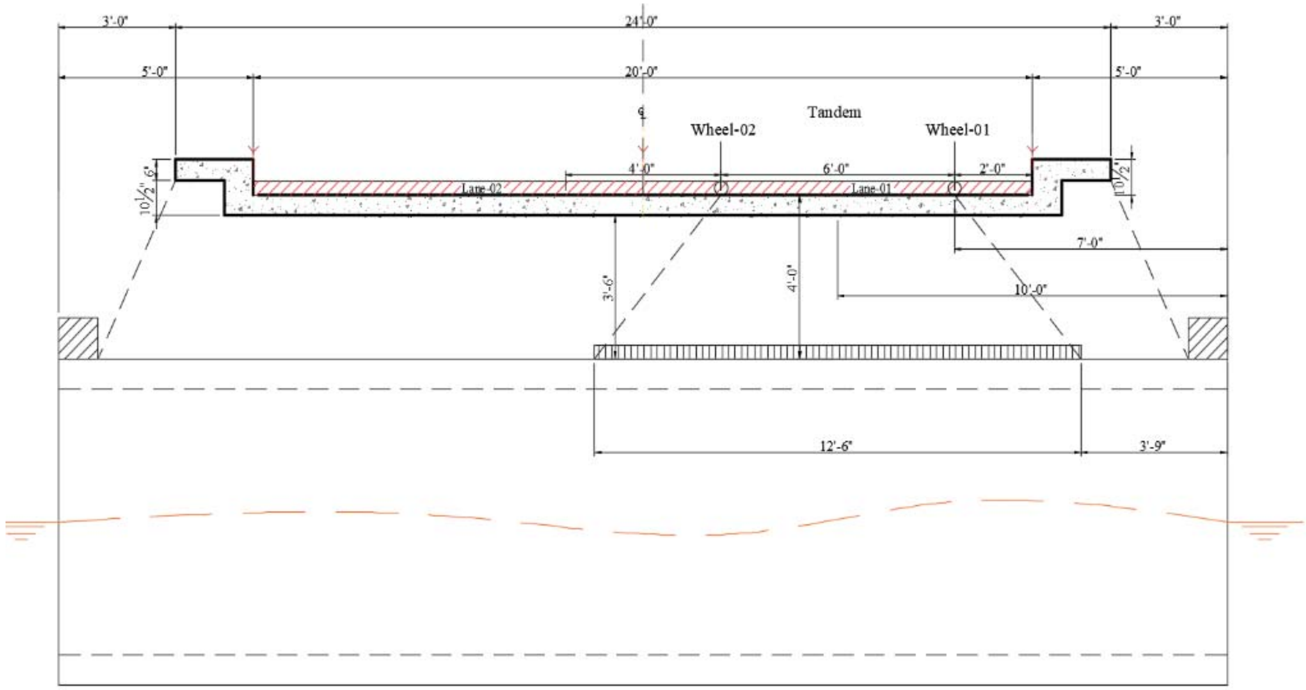

Live load distribution at the surface of the top slab in the direction perpendicular to the culvert span for fill height of 4.0 ft

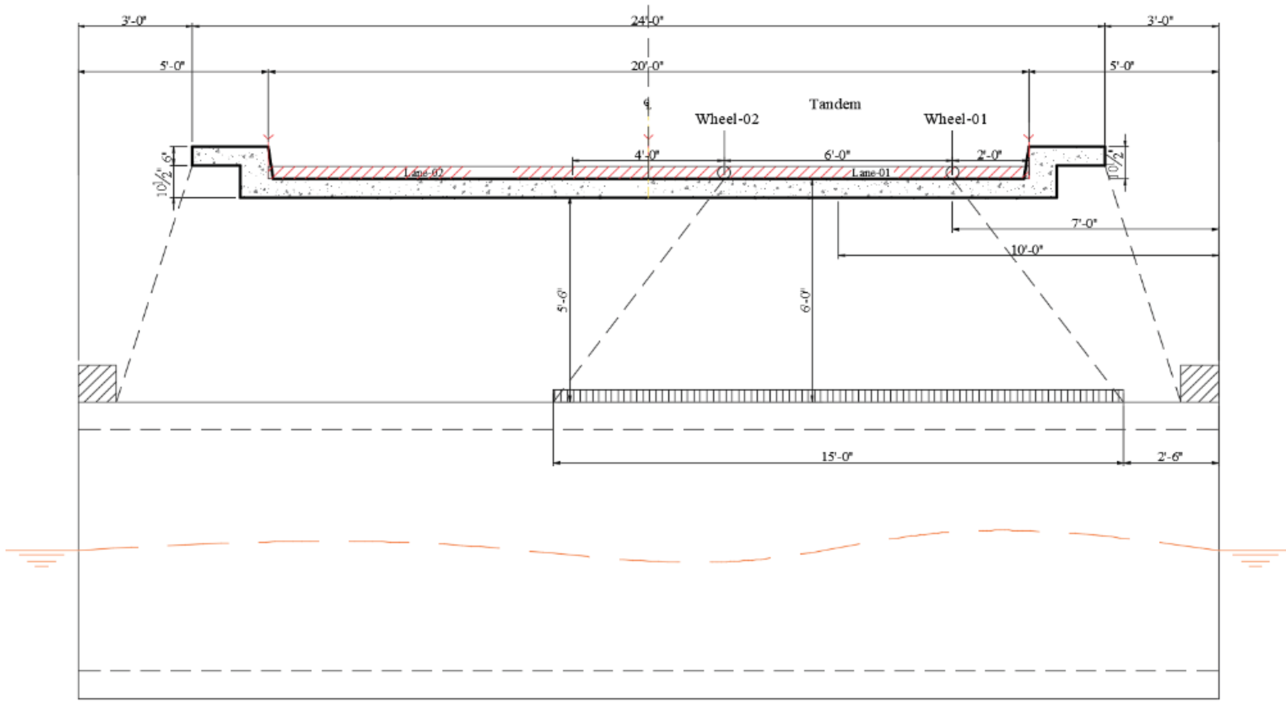

Live load distribution at the surface of the top slab in the direction perpendicular to the culvert span for fill height of 6.0 ft

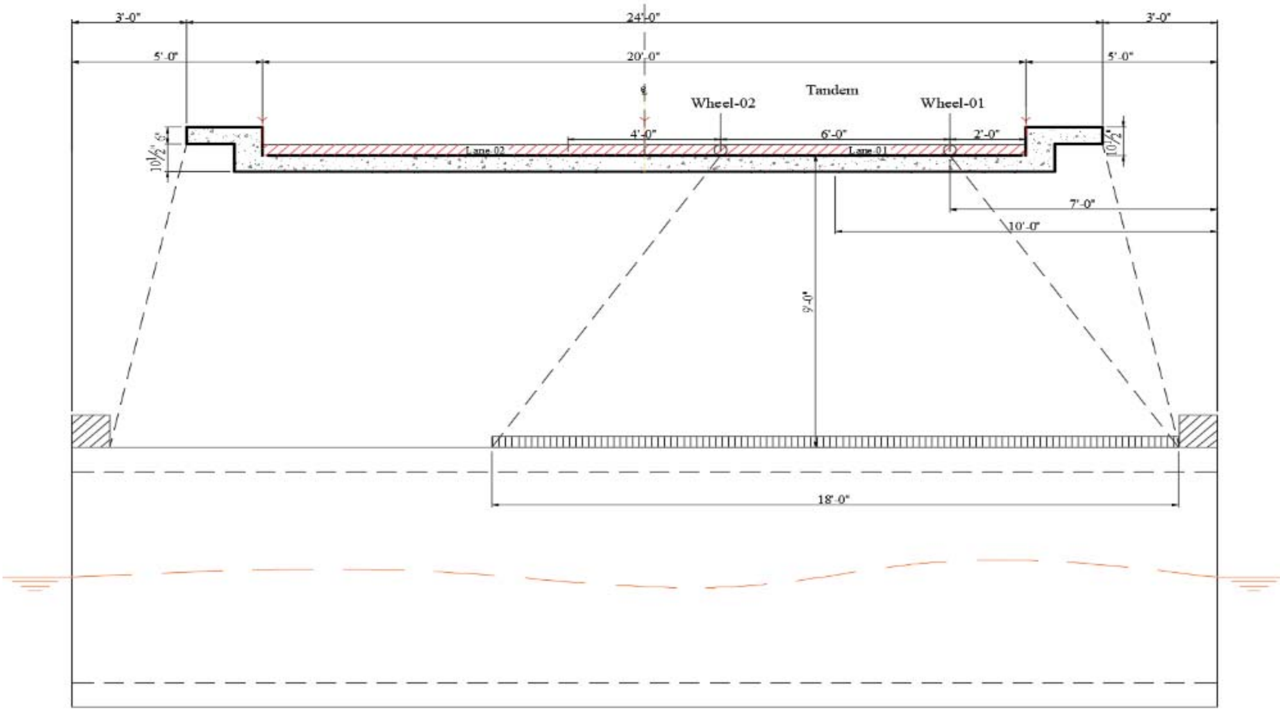

Live load distribution at the surface of the top slab in the direction perpendicular to the culvert span for fill height of 9.0 ft

6. APPENDIX B: DETAILED TEST RESULTS

Culvert RC# 004770

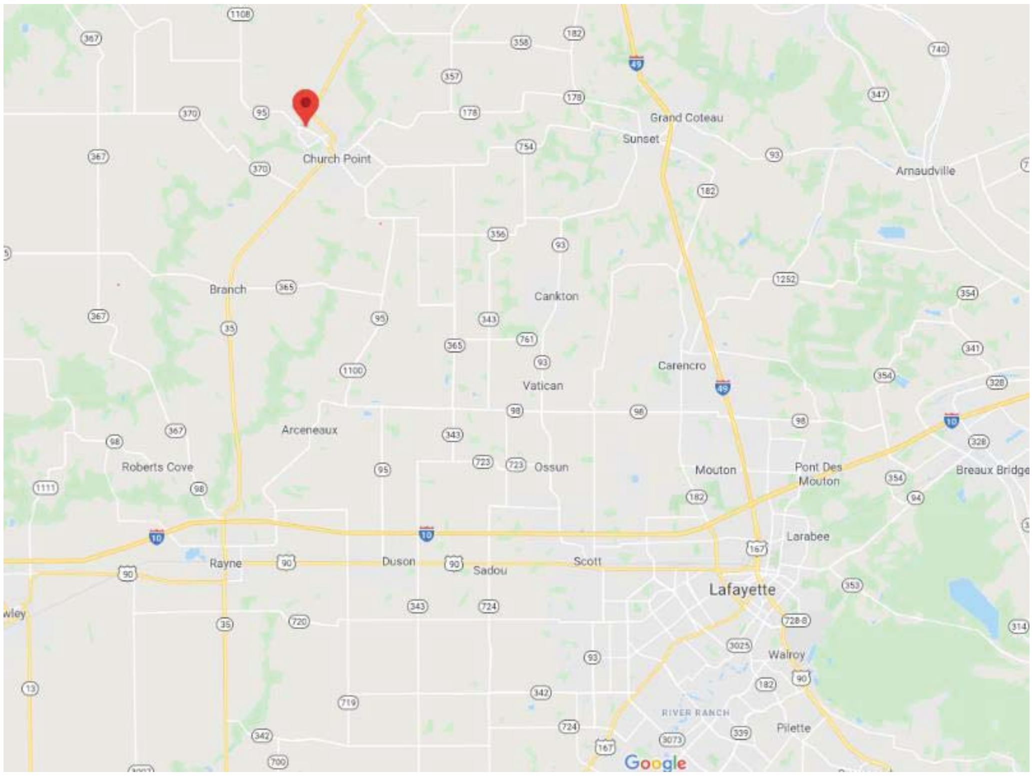

Map Location (30.41519, -92.2302) Acadia, LA

Culvert oveview and testing

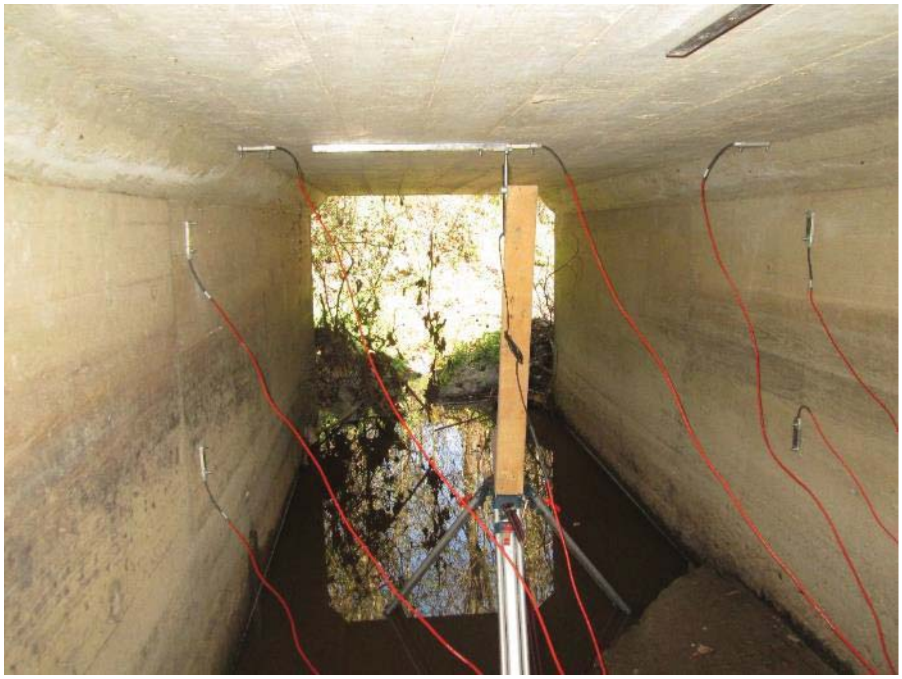

Instrumentation

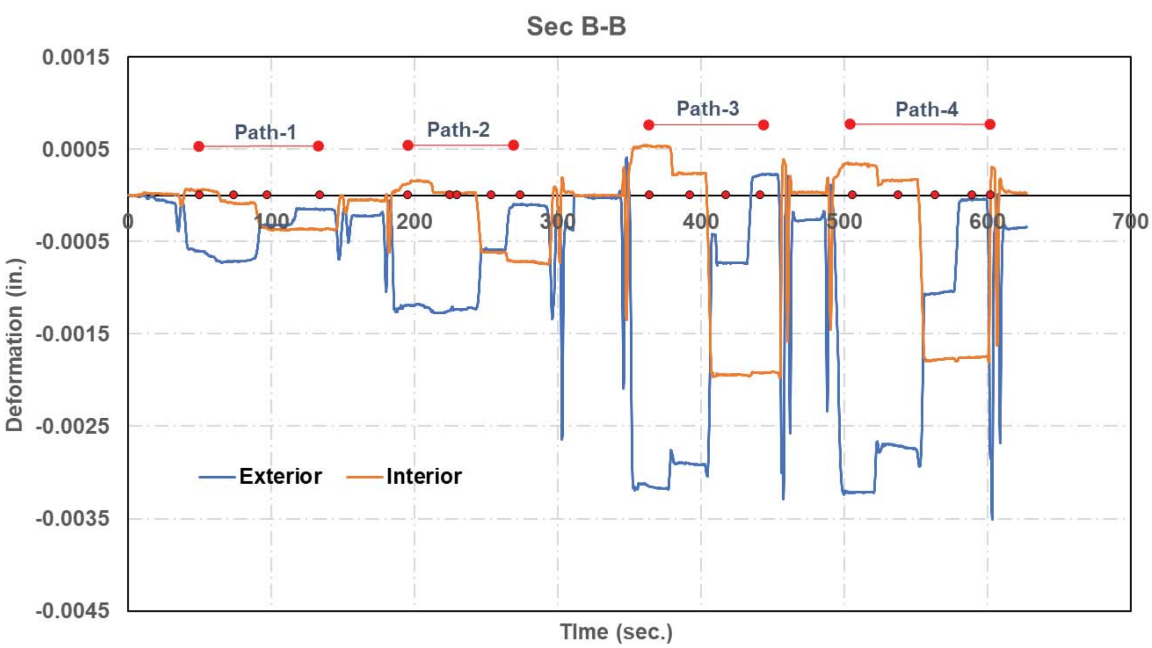

Vertical displacement at mid span of Exterior and Interior Cells for Load Path 1 and Load Path 2

Strain Gages Measurements for Load Path 1 and Load Path 2

Section	Location	Gauges	Path-1				Path-2			
			1	2	3	4	1	2	3	4
Sec A-A	Top Slab	S1	0.11	2.78	-3.93	-2.82	-0.72	3.85	-4.36	-2.86
		S2	18.01	10.91	-0.25	-2.41	14.14	7.73	2.38	-2.05
		S3	-11.04	-1.06	1.64	-3.92	-9.65	-2.64	0.22	-2.12
		S4	-4.82	-1.97	-4.86	-2.01	-4.99	-3.36	-4.21	-1.14
		S5	-2.73	-2.09	9.33	6.10	-2.57	-2.10	7.62	5.42
	Ext. Wall	S6	-13.29	-16.83	-5.65	-2.96	-10.60	-15.51	-6.81	-2.96
	Int. Wall	S7	-15.35	-15.31	2.88	10.42	-14.89	-14.87	-1.44	7.24
		S8	10.04	5.57	-10.51	-15.39	8.04	5.03	-7.94	-13.54
Sec B-B	Top Slab	S12	1.50	-0.40	-2.82	-2.68	1.44	0.56	-3.01	-2.91
		S 13	0.94	0.89	-0.51	-1.07	2.97	3.04	0.76	-1.38
		S 14	-1.09	1.18	2.56	1.37	-2.55	-0.01	2.03	0.22
		S15	-0.37	0.22	0.19	-0.51	-2.04	-1.40	-0.36	-0.49
		S16	-1.79	-1.72	0.13	0.50	-3.55	-3.13	1.11	1.84
	Ext. Wall	S17	2.24	-0.53	-2.38	-0.94	2.70	1.03	-0.42	1.71
		S 20-1	-1.26	-1.81	-1.28	-1.03	-2.96	-3.35	-1.99	-1.31
	Int. Wall	S 18	-3.34	-2.34	2.34	3.36	-6.16	-5.07	1.34	4.75
		S19	2.37	1.16	-3.01	-4.25	3.49	2.60	-3.21	-6.49
		S 20-2	-1.87	-2.32	-0.79	-0.42	-4.28	-4.53	-2.33	-0.62
		S20-3	0.38	-0.32	-2.40	-2.98	-0.05	-0.49	-3.29	-5.05
	LVDTs	Exterior (in.)	0.00	0.00	0.00	0.00	0.00	0.00	0.00	0.00
		Interior (in.)	0.00	0.00	0.00	0.00	0.00	0.00	0.00	0.00
Transverse Gages	Exterior	S23	-0.44	-0.17	-0.73	-1.05	0.89	1.03	-0.16	-1.41
	Interior	S24	-1.13	-1.16	0.72	0.79	-2.03	-2.23	-1.39	-0.88

Strain Gages Measurements for Load Path 3 and Load Path 4

Section	Location	Gauges	Path-3				Path-4			
			1	2	3	4	1	2	3	4
Sec A-A	Top Slab	S1	1.75	0.16	-2.66	-2.67	2.23	1.03	-3.21	-3.20
		S2	1.05	0.84	-0.36	-0.99	2.67	2.50	0.14	-1.80
		S3	-0.53	0.54	1.98	1.02	-2.65	-0.45	1.36	0.27
		S4	0.45	1.08	1.18	0.16	-1.46	-0.50	0.62	0.16
		S5	-0.59	-0.63	0.16	0.21	-1.95	-1.59	0.93	1.19
	Ext. Wall	S6	0.57	-1.75	-3.58	-3.05	-2.24	-3.94	-5.33	-3.64
	Int. Wall	S7	-3.82	-3.02	1.16	2.35	-7.15	-6.04	1.05	4.11
		S8	3.26	1.97	-1.91	-3.24	4.65	3.70	-2.94	-5.78
Sec B-B	Top Slab	S12	-0.21	3.88	-4.29	-2.99	-3.56	1.99	-5.44	-3.72
		S 13	15.09	10.48	1.10	-2.44	15.97	6.87	1.55	-2.41
		S 14	-9.74	-3.20	0.45	-3.48	-12.86	-2.92	-0.18	-3.47
		S15	-3.77	-1.76	-3.58	-0.49	-4.66	-3.39	-4.24	-0.48
		S16	-3.10	-2.55	11.84	8.51	-3.50	-2.99	10.80	6.15
	Ext. Wall	S17	-11.75	-18.59	-7.20	-2.71	-11.22	-16.30	-6.55	-2.18
		S 20-1	-5.16	-6.25	-1.84	-0.81	-5.67	-6.03	-2.54	-1.46
	Int. Wall	S 18	-14.14	-12.07	1.40	8.84	-14.10	-14.40	-2.64	6.47
		S19	10.27	6.80	-7.16	-12.78	8.20	5.76	-6.91	-13.20
		S 20-2	-6.12	-6.62	-2.80	0.90	-5.86	-6.59	-3.51	-0.51
		S20-3	3.72	1.53	-5.12	-7.51	2.39	1.25	-4.59	-6.78
	LVDTs	Exterior (in.)	0.00	0.00	0.00	0.00	0.00	0.00	0.00	0.00
		Interior (in.)	0.00	0.00	0.00	0.00	0.00	0.00	0.00	0.00
Transverse Gages	Exterior	S23	0.52	1.34	-0.80	-1.17	-0.23	-0.61	-1.58	-1.92
	Interior	S24	-0.84	-1.06	-1.09	-0.55	-1.83	-1.76	0.59	0.11

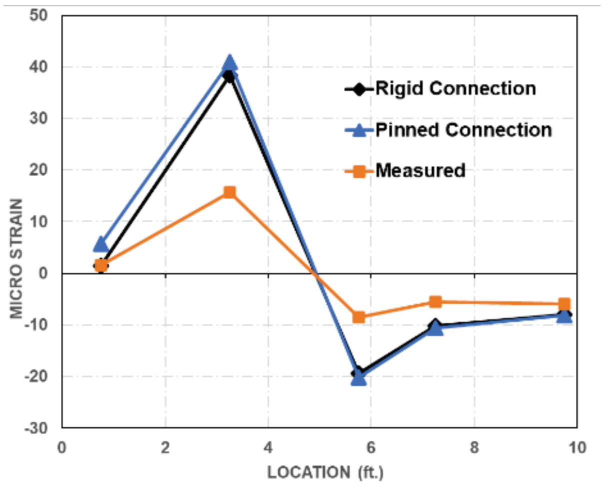

(a) Load Path-1 (Position-01)

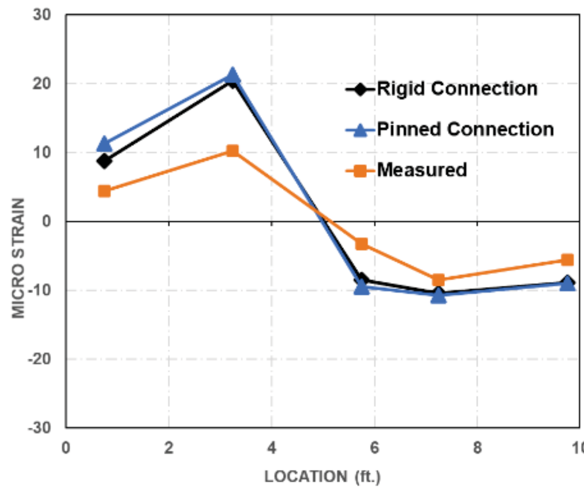

(b) Load Path-1 (Position-02)

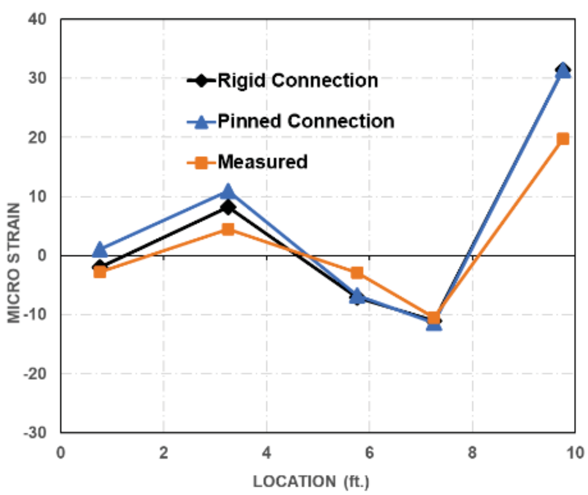

(c) Load Path-1 (Position-03)

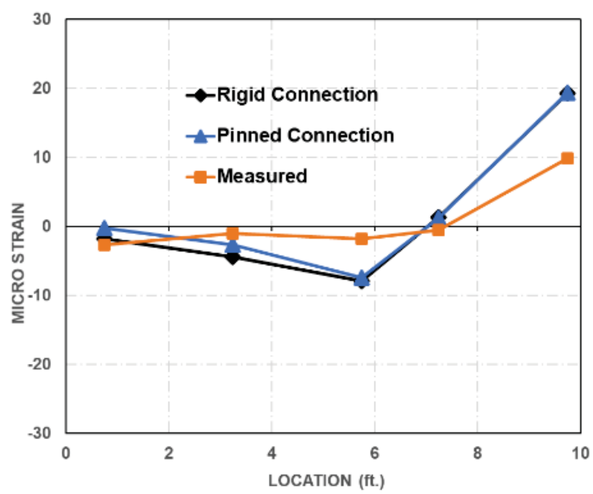

(d) Load Path-1 (Position-04)

Strain values at the top slab of culvert from field measurements and FEM models

Culvert RC# 004780

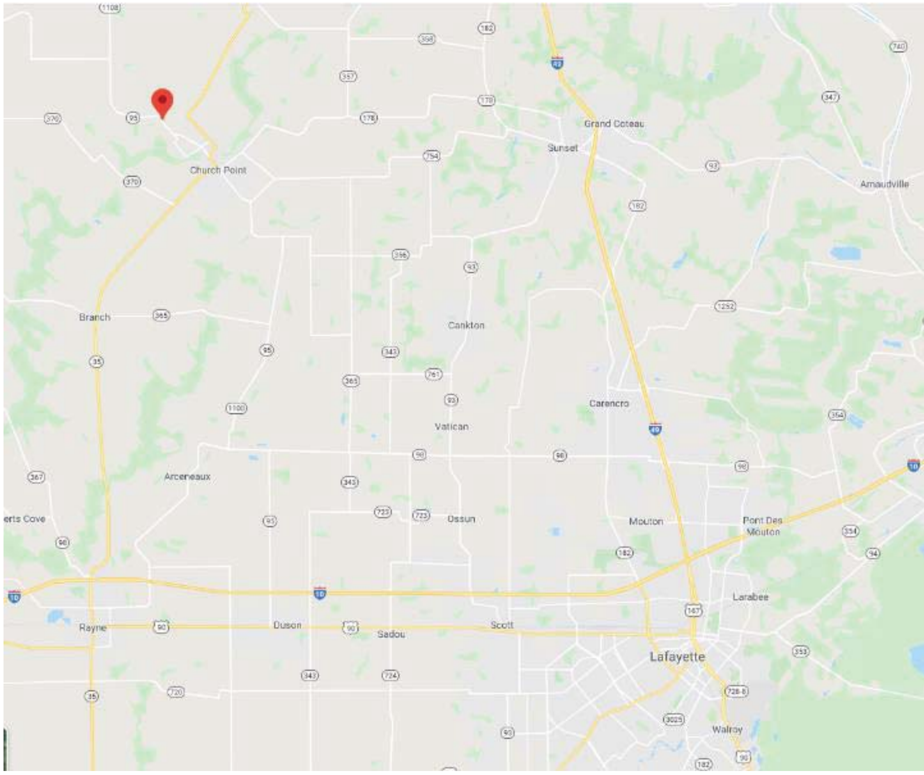

Map Location (30.42065, -92.239) Acadia, LA

Culvert oveview and testing

Strain Gages Measurements for Load Path 1 and Load Path 2

Section	Location	Gauge	Path-01				Path-02			
			1	2	3	4	1	2	3	4
Sec A-A	Top Slab	S1	0.60	5.52	-3.19	-1.96	0.24	2.42	-3.96	-3.16
		S2	19.61	12.79	4.89	-0.82	13.56	9.20	3.47	-0.91
		S3	-10.68	-0.22	1.42	-1.90	-6.67	0.18	2.73	-0.55
		S4	-3.73	-2.47	-4.80	-0.13	-2.89	-1.76	-4.08	-1.97
		S5	-3.94	-3.37	21.53	13.82	-3.42	-2.92	10.36	7.65
	Ext. Wall	S6	-8.44	-12.19	-6.06	-1.96	-4.99	-9.12	-5.72	-2.65
		S9	-2.77	-4.66	-0.65	0.36	-3.77	-4.92	-2.74	-1.54
	Int. Wall	S7	-11.82	-12.20	2.39	10.79	-10.47	-10.26	-1.02	6.95
		S8	11.08	9.93	-5.65	-13.15	7.68	5.70	-4.77	-11.43
		S10	-2.58	-3.18	-0.77	1.20	-2.26	-2.39	-0.67	0.87
		S11	3.28	2.57	-2.99	-6.02	1.05	0.00	-3.81	-5.74
	LVDTs	Ext	-0.003	-0.003	-0.001	0.000	-0.002	-0.002	-0.001	0.000
		Int	0.001	0.001	-0.002	-0.002	0.000	0.000	-0.001	-0.002
Sec B-B	Top Slab	S12	3.02	1.57	-1.49	-1.92	2.29	1.12	-3.61	-3.59
		S13	1.97	2.27	1.37	0.36	4.98	4.91	2.75	-1.08
		S14	0.07	1.76	3.74	2.82	-1.43	1.11	2.24	0.60
		S15	0.13	0.93	1.50	0.41	-1.51	-0.83	-0.50	-0.60
		S16	-0.90	-0.61	1.27	1.62	-2.29	-2.06	3.60	4.23
	Ext. Wall	S17	2.17	0.30	-2.11	-1.88	-0.81	-3.38	-4.99	-3.00
	Int. Wall	S18	-1.41	-1.11	1.73	2.85	-4.58	-4.61	0.10	3.49
		S19	1.74	1.35	-1.11	-2.42	2.81	2.19	-2.48	-5.42

Strain Gages Measurements for Load Path 3 and Load Path 4

Section	Location	Gauge	Path-03				Path-04			
			1	2	3	4	1	2	3	4
Sec A-A	Top Slab	S1	2.64	1.73	-1.72	-2.19	2.79	2.44	-2.29	-2.47
		S2	1.92	2.32	0.87	-0.10	5.11	5.23	2.42	-0.42
		S3	-0.67	1.24	3.98	3.08	-2.41	0.79	3.52	1.93
		S4	0.77	1.39	1.72	0.78	-0.35	0.49	0.49	0.47
		S5	-0.16	0.06	1.79	2.56	-1.88	-1.09	6.59	7.10
	Ext. Wall	S6	1.83	0.30	-2.77	-2.57	-0.40	-2.12	-4.14	-2.59
		S9	0.07	-0.53	-0.73	-0.48	-1.70	-2.31	-0.99	-0.09
	Int. Wall	S7	-2.24	-1.86	1.64	3.54	-5.62	-5.04	2.66	6.48
		S8	3.68	3.33	-0.70	-2.80	5.99	5.73	-2.13	-5.87
		S10	-0.40	-0.40	0.46	0.62	-1.25	-1.20	0.48	1.31
		S11	2.14	2.25	0.58	-0.14	2.66	2.95	0.08	-1.51
	LVDTs	Ext.	-0.001	-0.001	0.000	0.000	-0.001	-0.001	0.000	0.000
		Int.	0.000	0.000	0.000	0.000	0.000	0.000	-0.001	-0.001
Sec B-B	Top Slab	S12	0.43	6.14	-5.01	-3.06	0.29	3.54	-3.82	-2.37
		S13	17.24	11.65	6.51	-0.84	11.48	8.32	4.67	-0.34
		S14	-9.08	-2.30	-0.67	-1.24	-5.29	0.29	2.36	-0.41
		S15	-3.91	-3.35	-3.80	1.42	-1.95	-0.92	-2.24	0.84
		S16	-2.46	-2.22	13.04	9.60	-1.71	-1.14	10.84	8.38
	Ext. Wall	S17	-7.15	-10.45	-7.22	-2.82	-4.56	-7.41	-5.08	-2.23
	Int. Wall	S18	-8.36	-9.52	-0.72	6.34	-6.70	-7.03	0.09	5.23
		S19	6.78	7.03	-2.03	-7.13	5.29	4.69	-2.33	-6.23

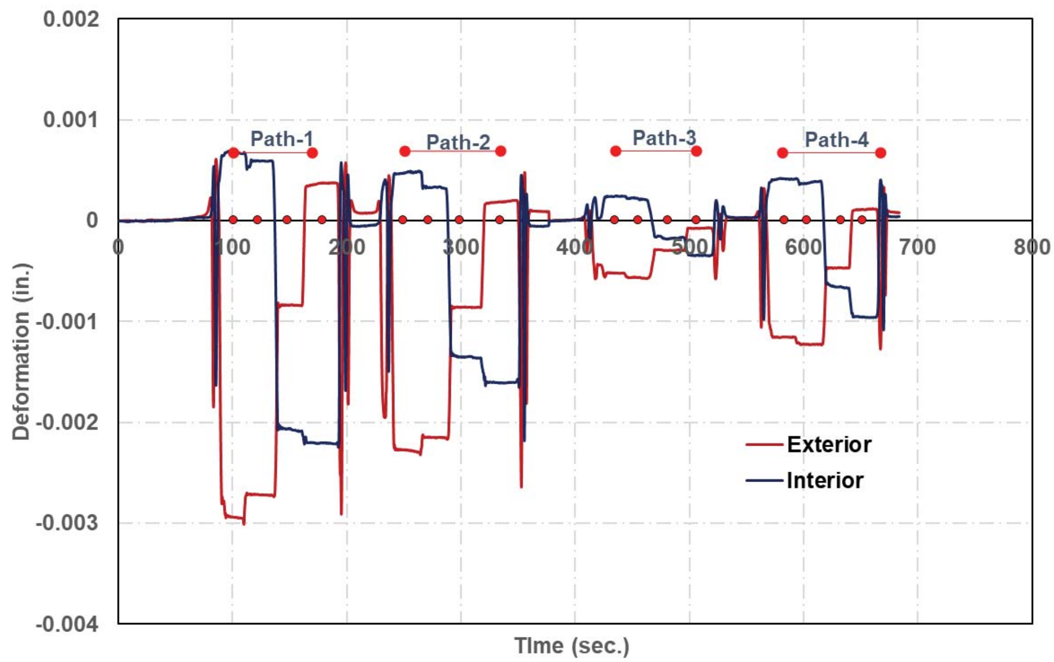

Vertical displacement at midspan of exterior and interior cells during static loading of Culvert

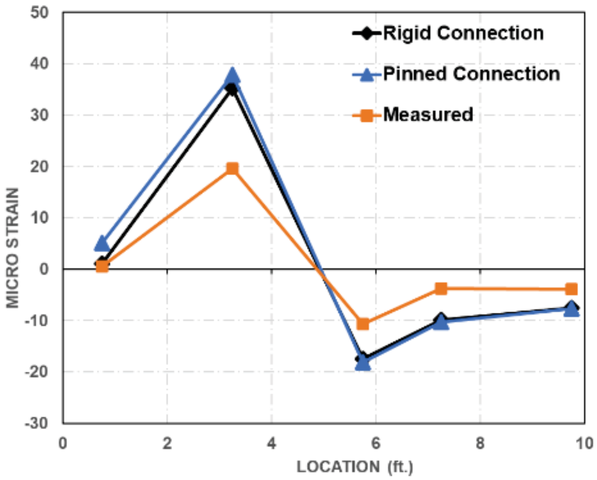

(a) Load Path-1 (Position-01)

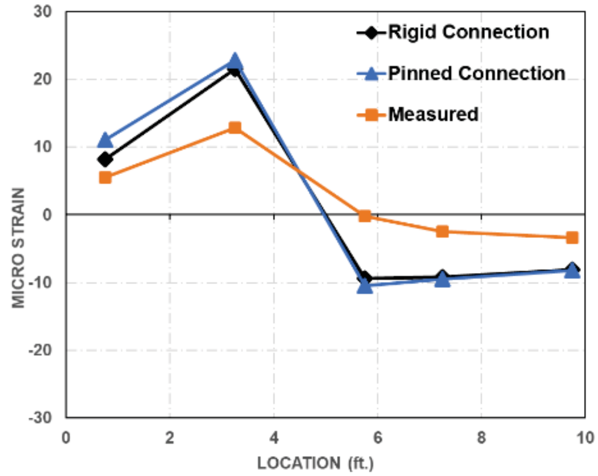

(b) Load Path-1 (Position-02)

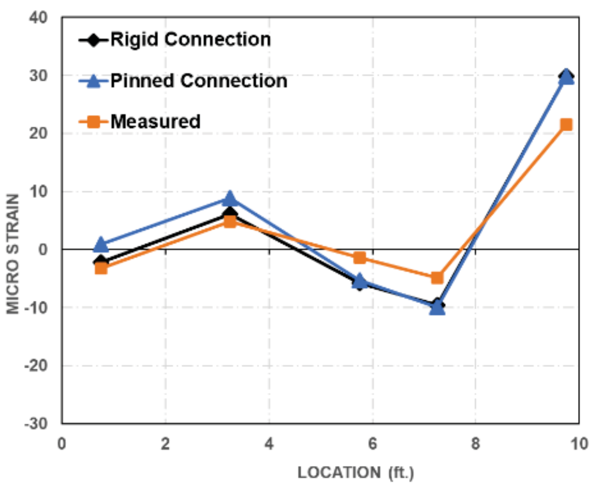

(c) Load Path-1 (Position-03)

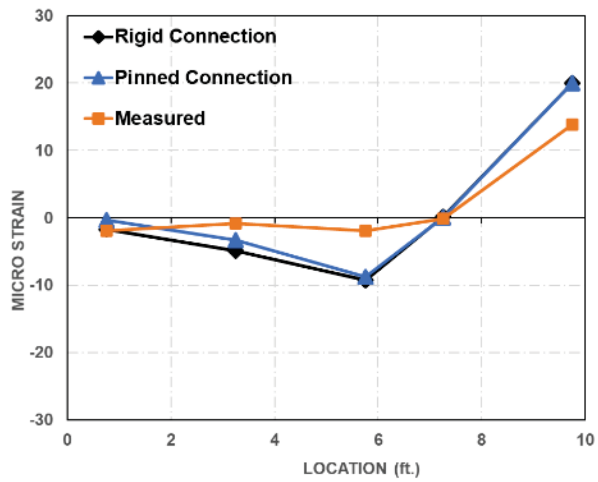

(d) Load Path-1 (Position-04)

Strain values at the top slab of culvert from field measurements and FEM models

Culvert RC# 005450

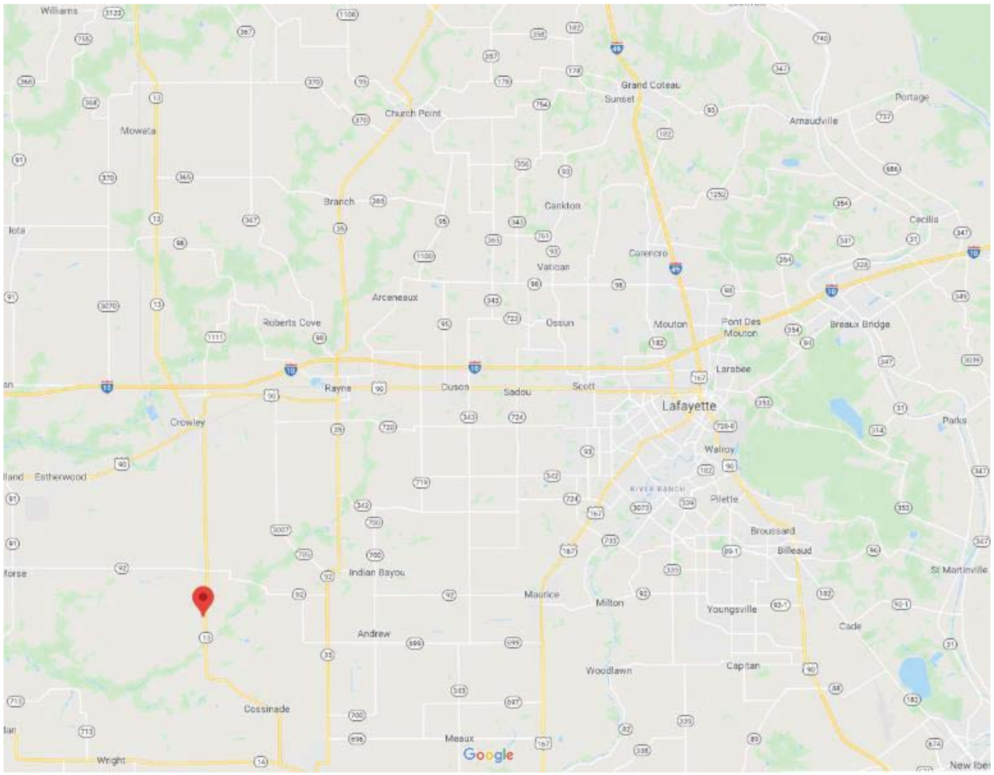

Map Location (30.09405, -92.3638) Acadia, LA

Culvert oveview and testing

Instrumentation

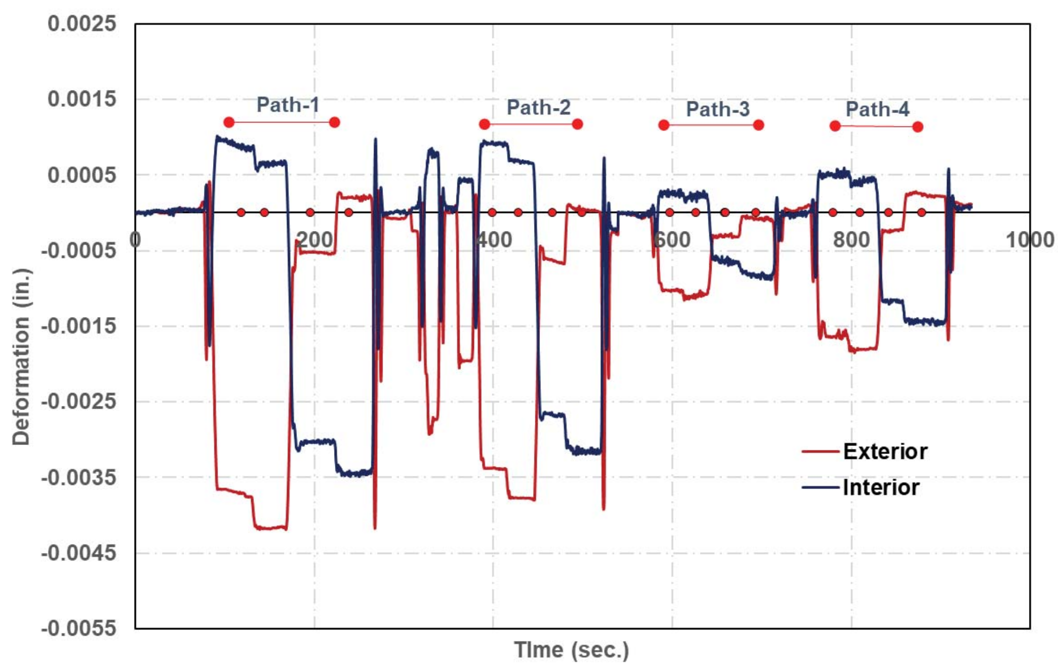

Vertical displacement at midspan of exterior and interior cells during static loading of Culvert

Strain Gages Measurements for Load Path 1 and Load Path 2

Section	Location	Gauges	Path-1				Path-2			
			1	2	3	4	1	2	3	4
Sec A-A	Top Slab	S1	3.34	1.11	-2.27	-1.63	3.65	1.85	-1.73	-1.77
		S2	12.03	13.60	1.38	-0.99	11.73	13.21	2.45	-0.69
		S3	-5.06	-3.23	-1.98	-3.35	-4.58	-2.47	-0.84	-2.46
		S4	-6.02	-5.95	-2.81	-4.14	-5.75	-5.11	-2.22	-3.90
		S5	-3.29	-2.83	11.06	12.98	-2.20	-1.65	10.52	11.66
	Ext. Wall	S6	-15.60	-19.60	-6.42	-3.60	-15.40	-19.16	-7.38	-4.85
		S9	-3.96	-4.16	-0.34	0.29	-3.39	-3.32	-0.03	0.11
	Int. Wall	S7	-15.75	-17.50	5.81	11.98	-14.57	-15.96	4.76	10.77
		S8	9.39	8.59	-9.79	-12.74	8.82	7.94	-8.23	-11.40
		S10	-3.74	-4.95	-0.97	0.66	-2.99	-3.95	-0.38	1.03
		S11	1.28	0.53	-3.77	-3.70	1.80	1.22	-2.66	-3.31
	LVDTs	Int.	0.001	0.001	-0.003	-0.003	0.001	0.001	-0.003	-0.003
		Ext.	-0.004	-0.004	-0.001	0.000	-0.003	-0.004	-0.001	0.000
Sec B-B	Top slab	S12	2.87	1.40	-1.57	-1.50	3.17	1.60	-1.47	-1.61
		S13	3.69	4.28	0.41	-0.45	7.95	9.22	1.78	-0.86
		S14	-0.47	0.69	1.39	0.64	-1.82	-0.64	0.13	-0.98
		S15	-1.35	-0.58	2.24	1.42	-2.52	-1.85	1.41	-0.10
		S16	-1.36	-1.43	2.41	3.04	-1.60	-1.23	5.60	6.44
	Ext. Wall	S17	-0.53	-2.06	-1.70	-1.23	-3.13	-5.03	-2.04	-1.26
	Int. Wall	S18	-4.32	-4.16	3.55	5.59	-7.28	-7.34	4.14	7.83
		S19	2.84	2.60	-1.52	-2.48	4.88	4.61	-2.02	-4.30

Strain Gages Measurements for Load Path 3 and Load Path 4

Section	Location	Gauges	Path-3				Path-4			
			1	2	3	4	1	2	3	4
Sec A-A	Top Slab	S1	2.27	1.07	-2.55	-3.26	2.39	0.89	-3.00	-3.11
		S2	1.44	1.80	-0.55	-1.45	3.12	4.07	-0.63	-2.09
		S3	-1.30	-0.08	1.28	0.15	-2.99	-1.13	-0.10	-1.37
		S4	-1.51	-0.88	1.02	-0.36	-4.67	-3.85	-0.71	-1.78
		S5	-1.45	-1.58	1.08	1.39	-3.11	-2.83	3.23	4.59
	Ext. Wall	S6	0.26	-2.95	-5.86	-5.69	-5.06	-9.06	-7.61	-5.90
		S9	-2.15	-2.59	-1.69	-1.77	-4.05	-4.17	-2.08	-1.56
	Int. Wall	S7	-5.77	-5.46	1.96	4.11	-9.09	-9.28	2.84	7.06
		S8	2.89	2.30	-3.03	-5.10	3.55	3.13	-5.29	-7.74
		S10	-1.91	-2.10	-0.55	-0.32	-3.06	-3.54	-1.01	-0.06
		S11	0.09	-0.17	-1.82	-2.47	-0.62	-0.80	-3.08	-3.21
	LVDTs	Int.	0.000	0.000	-0.001	-0.001	0.001	0.000	-0.001	-0.001
		Ext.	-0.001	-0.001	0.000	0.000	-0.002	-0.002	0.000	0.000
Sec B-B	Top slab	S12	2.23	-0.40	-3.89	-3.25	0.98	-1.84	-3.97	-3.02
		S13	14.74	17.06	1.35	-3.17	12.40	15.42	0.94	-2.95
		S14	-6.93	-5.85	-3.69	-4.82	-6.85	-5.93	-3.69	-4.72
		S15	-6.71	-6.91	-3.22	-4.81	-7.71	-7.29	-3.03	-4.59
		S16	-4.05	-3.93	9.82	12.21	-4.71	-4.23	8.21	10.76
	Exterior	S17	-9.32	-12.40	-4.79	-3.11	-10.58	-12.99	-5.34	-3.06
	Interior	S18	-16.55	-18.67	2.05	8.99	-14.82	-16.95	1.75	8.58
		S19	5.96	5.45	-6.42	-9.47	4.54	4.23	-6.29	-8.54

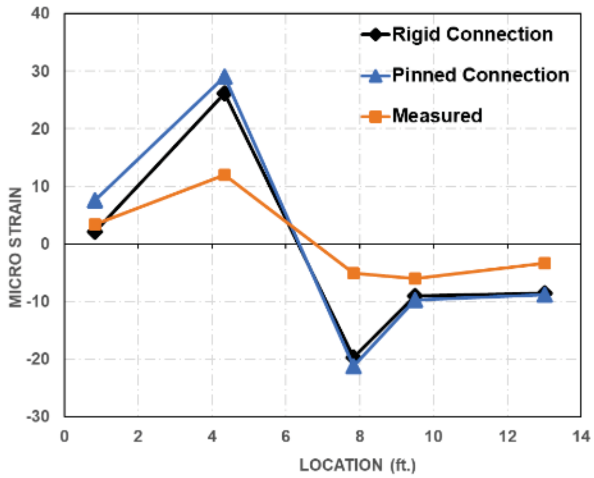

(a) Load Path-1 (Position-01)

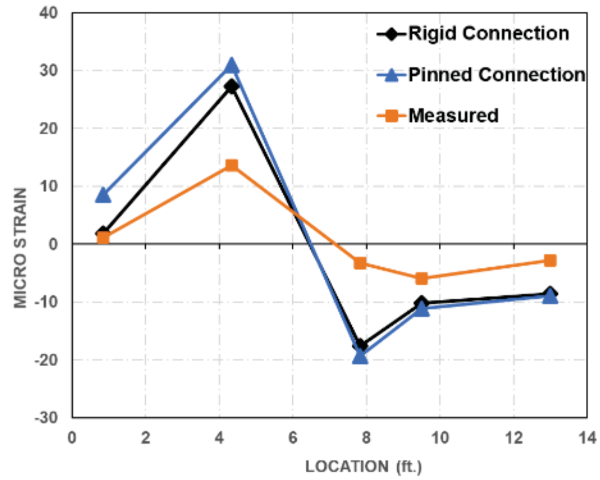

(b) Load Path-1 (Position-02)

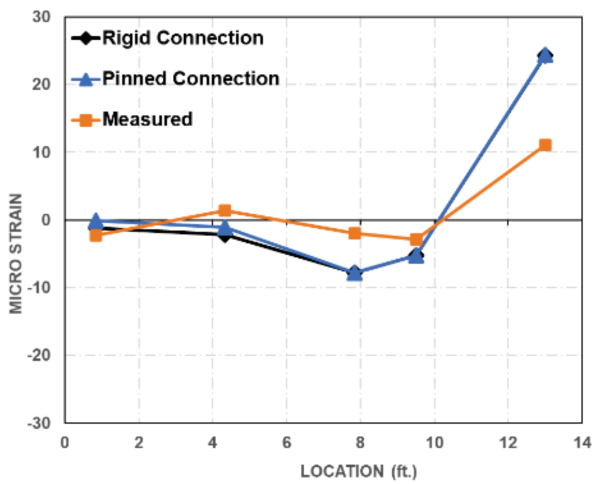

(c) Load Path-1 (Position-03)

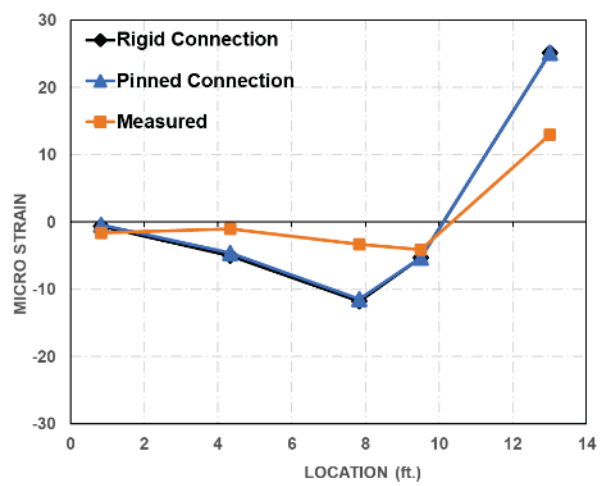

(d) Load Path-1 (Position-04)

Strain values at the top slab of culvert from the field measurements and FEM models

Culvert RC# 004360

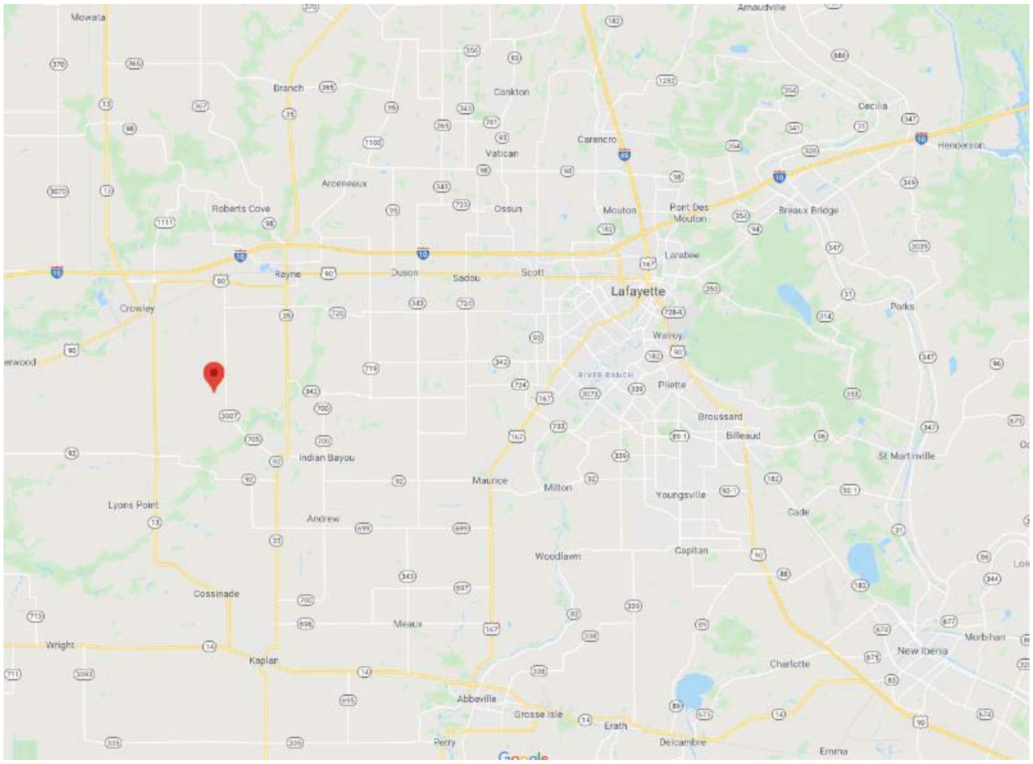

Map Location (30.16097, -92.3206) Acadia, LA

Culvert oveview and testing

Instrumentation

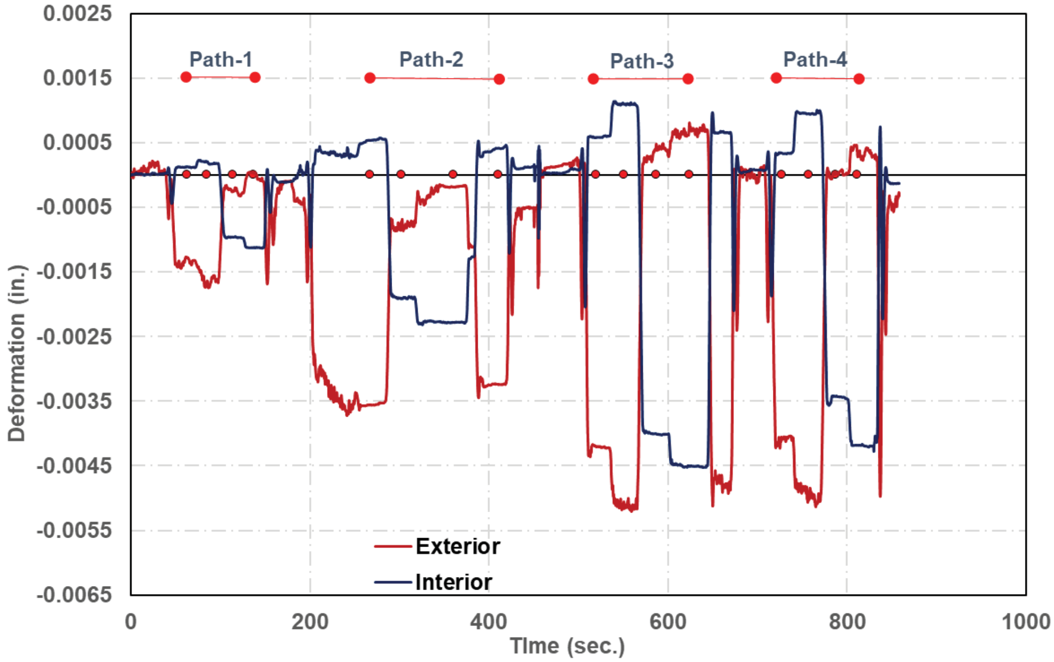

Vertical displacement at midspan of exterior and interior cells during loading of Culvert

Strain Gages Measurements for Load Path 1 and Load Path 2

Section	Location	Gauge	Load Path-1				Load Path-2			
			1	2	3	4	1	2	3	4
Sec A-A	Top Slab	S1	5.52	2.12	-1.46	-1.52	1.18	-1.55	-4.76	-4.91
		S2	10.93	12.76	-0.67	-2.06	7.47	8.63	-2.94	-4.05
		S 3	-6.67	-4.17	-2.20	-4.36	-9.26	-5.92	-5.52	-7.92
		S4	-6.21	-5.58	-1.40	-3.82	-6.86	-6.58	-1.42	-3.87
		S5	-2.50	-3.91	10.37	12.73	-5.64	-6.26	6.47	8.55
	Ext. Wall	S6	-4.27	-4.64	-0.24	0.14	-6.14	-6.36	-2.85	-2.95
		S9	-17.03	-16.37	-5.61	-4.54	-19.63	-18.56	-8.39	-7.13
	Int. Wall	S7	-7.79	-9.83	3.13	6.06	-10.66	-11.56	-0.10	2.40
		S8	4.38	4.27	-10.74	-12.62	1.43	0.87	-11.14	-12.66
		S10	-4.34	-6.17	-2.67	-1.25	-8.26	-8.65	-5.08	-3.88
		S11	0.94	0.77	-4.09	-4.37	-1.62	-1.63	-5.92	-6.93
	Haunch	SM	-0.65	-2.11	-0.64	-0.41	-3.17	-4.11	-2.43	-2.11
Sec B-B	Top slab	S 12	1.73	0.66	-2.21	-2.57	-0.09	-2.33	-5.22	-5.24
		S13	3.29	3.98	-0.15	-1.05	4.94	6.11	-2.79	-3.94
		S14	-0.52	0.65	1.82	1.11	-4.78	-2.95	-1.98	-3.54
		S15	-0.88	-0.05	1.80	0.85	-5.09	-4.26	-1.53	-3.49
		S16	-1.18	-2.16	0.32	0.55	-5.75	-7.12	-0.04	1.38
	Ext. Wall	S17	-0.15	-0.51	-0.40	-0.39	-4.35	-4.68	-3.13	-3.51
	Int. Wall	S18	-1.51	-1.15	2.09	2.86	-5.68	-6.24	0.48	1.54
		S19	2.01	1.79	-2.01	-3.17	1.02	1.04	-5.99	-7.61
	LVDTs	Int.	0.000	0.000	-0.001	-0.001	0.000	0.001	-0.002	-0.002
		Ext.	-0.001	-0.002	0.000	0.000	-0.003	-0.004	-0.001	0.000

Strain Gages Measurements for Load Path 3 and Load Path 4

Section	Location	Gauge	Load Path-3				Load Path-4			
			1	2	3	4	1	2	3	4
Sec A-A	Top Slab	S1	1.74	1.02	-1.94	-2.29	0.01	-1.39	-3.97	-4.02
		S2	2.07	2.63	-0.16	-0.62	3.07	4.70	-1.28	-2.26
		S 3	0.07	1.04	0.25	-0.63	-3.55	-0.98	-1.57	-3.73
		S4	-0.62	-0.27	1.10	0.03	-4.60	-4.01	-0.47	-1.87
		S5	-0.51	-1.13	1.33	1.40	-2.84	-3.93	2.98	4.00
	Ext. Wall	S6	-0.07	-0.82	-1.89	-1.96	-3.22	-4.37	-3.35	-3.01
		S9	-3.82	-5.34	-3.72	-3.22	-10.34	-11.32	-5.91	-5.02
	Int. Wall	S7	-1.67	-1.63	1.49	1.93	-4.99	-5.68	1.09	2.18
		S8	1.71	1.14	-3.29	-4.23	0.44	0.52	-6.55	-7.65
		S10	-1.01	-1.39	0.37	0.33	-3.70	-4.36	-1.08	-0.97
		S11	1.78	1.52	-1.28	-1.77	-0.50	-0.53	-3.82	-4.52
	Haunch	SM	0.44	-0.22	-1.07	-1.19	-1.61	-2.46	-2.15	-1.89
Sec B-B	Top slab	S 12	5.53	2.74	-2.35	-2.30	2.74	-0.48	-3.98	-4.05
		S13	12.63	15.70	-1.82	-3.08	9.09	13.03	-2.42	-4.06
		S14	-6.44	-4.58	-4.38	-6.06	-7.35	-5.05	-3.39	-5.82
		S15	-5.19	-5.36	-2.17	-4.75	-7.16	-6.85	-3.86	-6.11
		S16	-1.50	-3.17	10.10	11.00	-3.66	-5.06	6.94	8.47
	Ext. Wall	S17	-2.47	-3.43	-2.17	-2.34	-5.35	-6.24	-4.12	-3.95
	Int. Wall	S18	-6.86	-9.34	3.80	5.20	-7.75	-10.23	1.32	3.31
		S19	5.10	5.62	-9.83	-10.60	2.90	3.43	-9.50	-10.49
	LVDTs	Int.	0.001	0.001	-0.004	-0.005	0.000	0.001	-0.003	-0.004
		Ext.	-0.004	-0.005	0.000	0.001	-0.004	-0.005	0.000	0.000

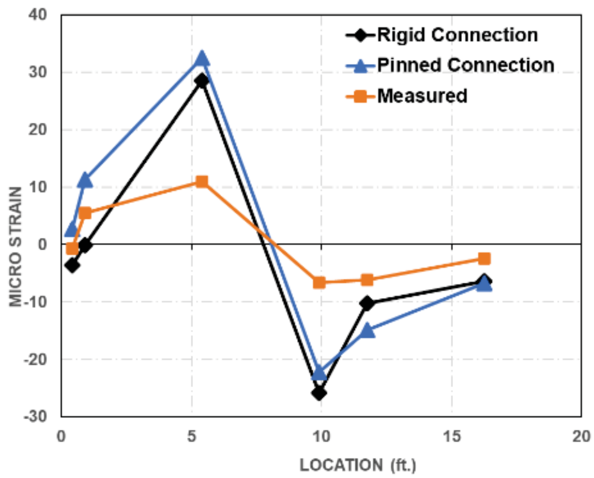

(a) Load Path-1 (Position-01)

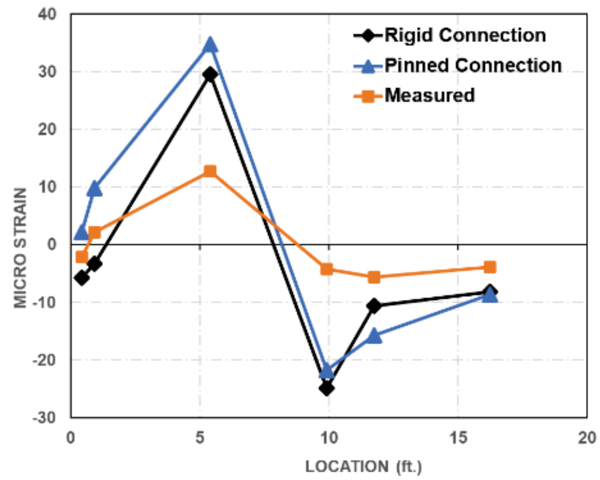

(b) Load Path-1 (Position-02)

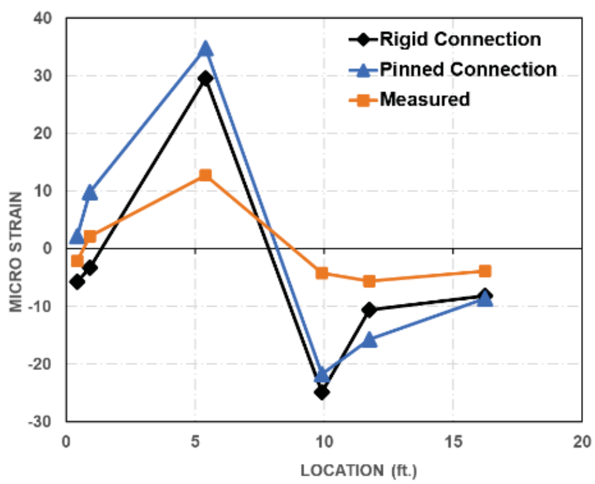

(c) Load Path-1 (Position-03)

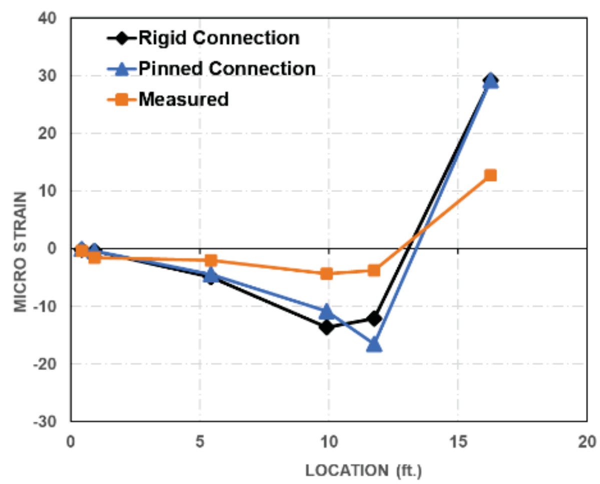

(d) Load Path-1 (Position-04)

Strain values at the top slab of culvert from the field measurements and FEM models

Culvert RC# 005488

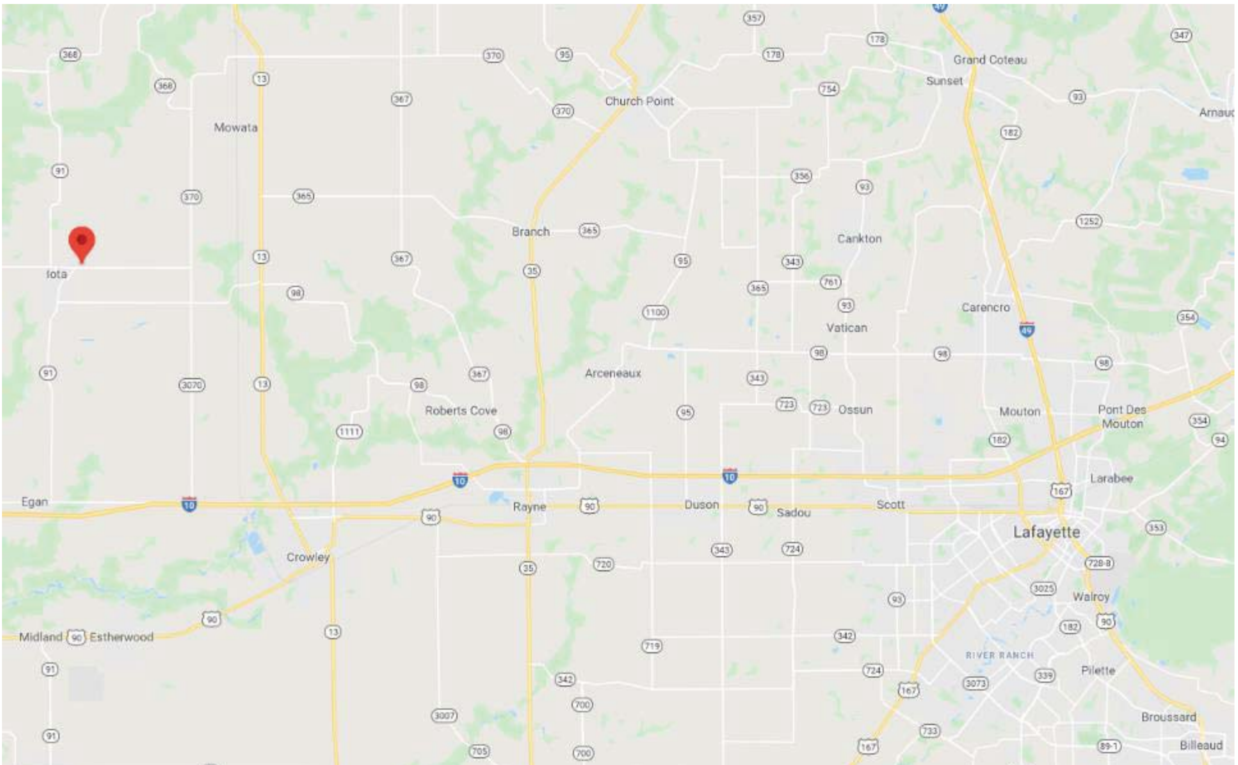

Map Location (30.33403, -92.4836) Acadia, LA

Culvert oveview and testing

Instrumentation

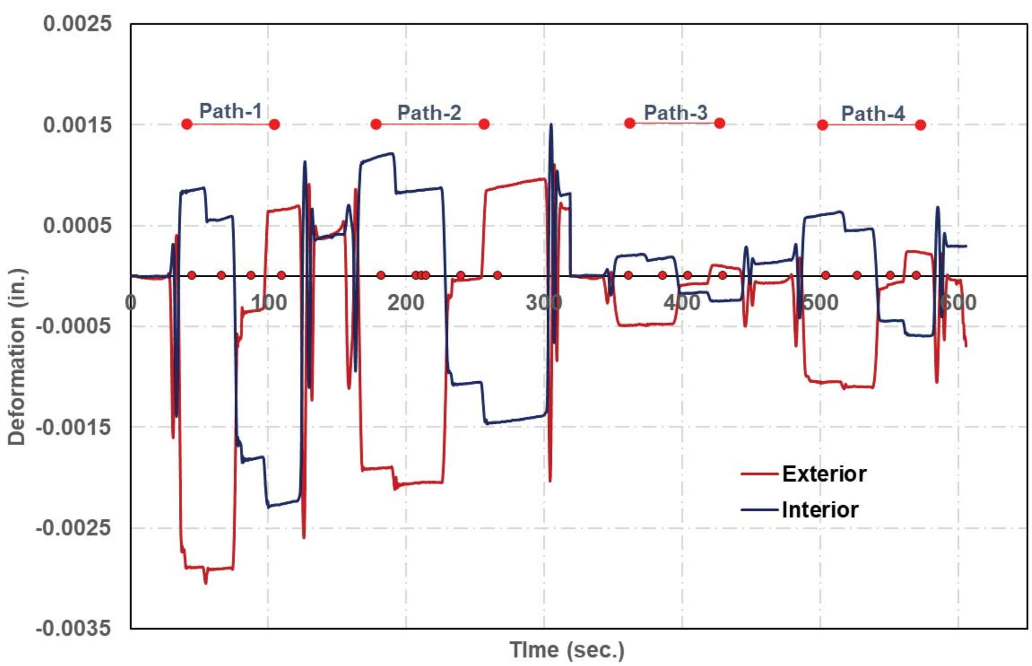

Vertical displacement at midspan of exterior and interior cells during static loading of Culvert

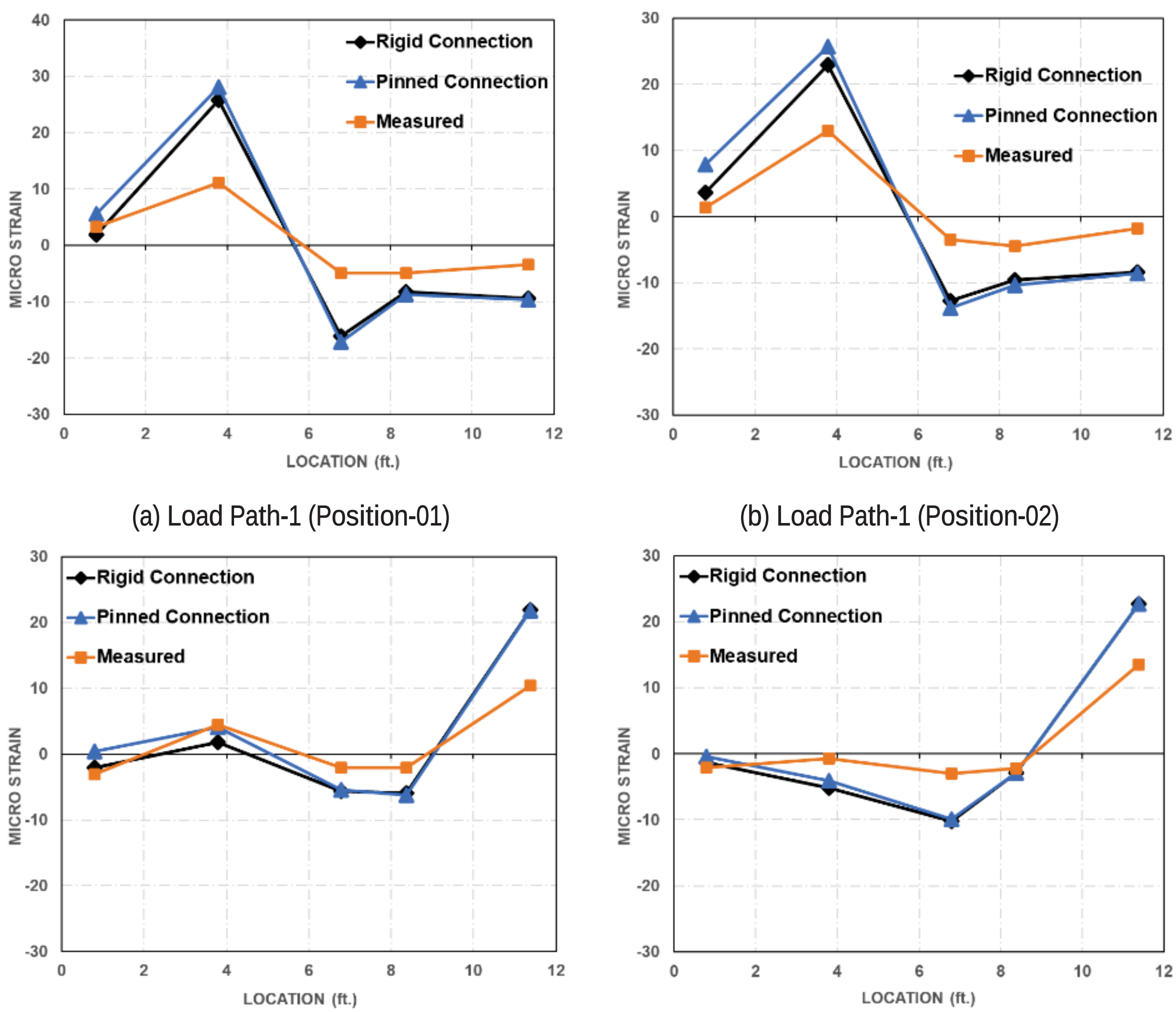

(a) Load Path-1 (Position-01)

(b) Load Path-1 (Position-02)

(c) Load Path-1 (Position-03)

(d) Load Path-1 (Position-04)

Strain values at the top slab of culvert from the field measurements and FEM models

Culvert RC# 008910

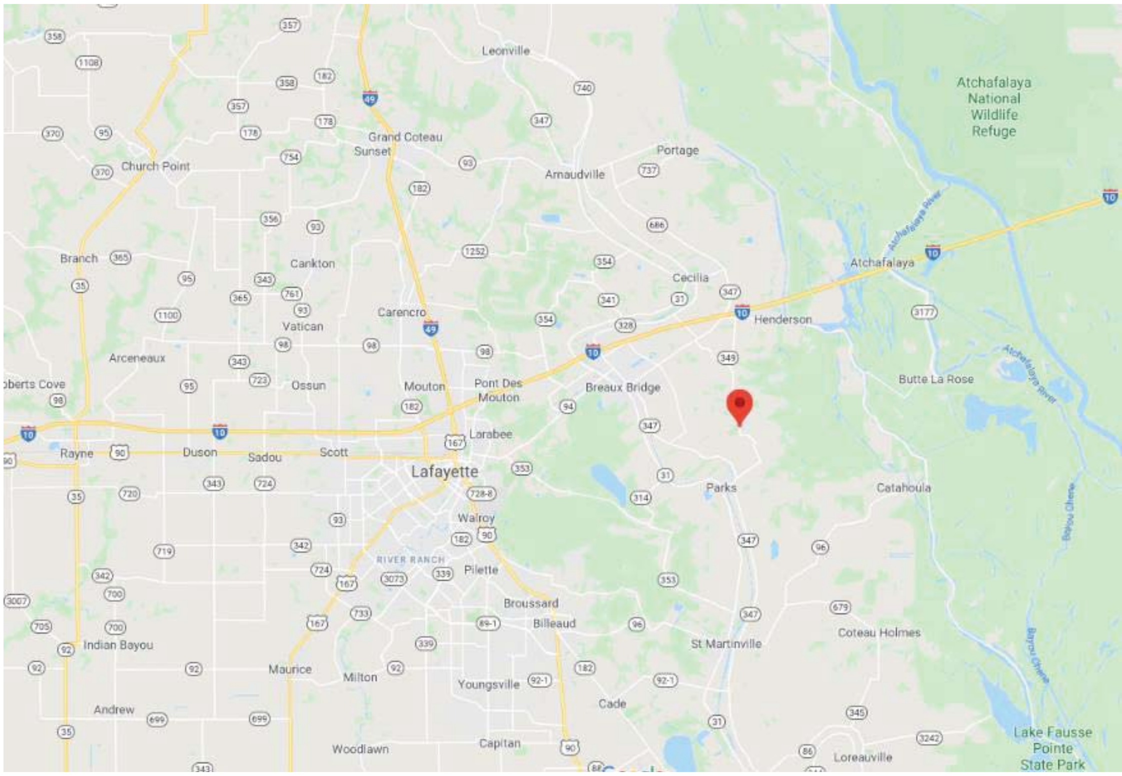

Map Location (30.24832, -91.8201), St. Martin, LA


Culvert oveview and testing

Instrumentation

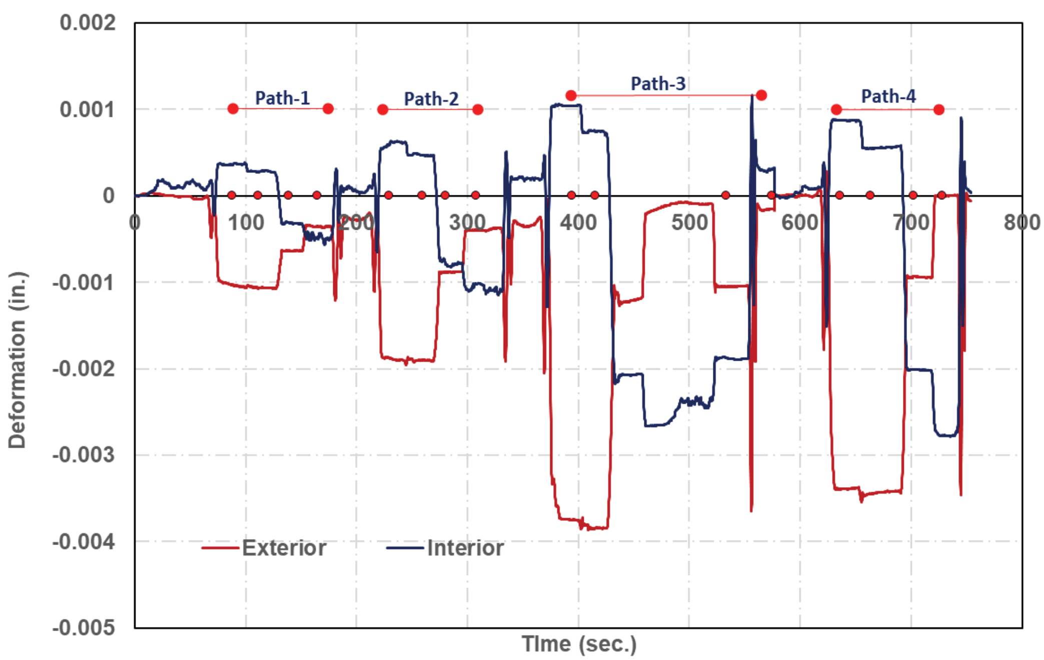

Vertical displacement at midspan of exterior and interior cells during loading

Strain Gages Measurements for Load Path 1 and Load Path 2

Section	Location	Strain Gages	Path 1				Path 2			
			1	2	3	4	1	2	3	4
Sec A-A	Top Slab	S1	4.07	1.57	-3.54	-3.72	2.32	0.06	-4.11	-4.65
		S2	11.09	11.69	4.24	-0.52	8.64	8.87	1.84	-1.32
		S3	-5.08	-3.10	-1.94	-3.51	-4.65	-2.61	-1.85	-3.10
		S4	-4.76	-4.15	-2.51	-3.08	-5.13	-4.34	-3.02	-3.69
		S5	-2.71	-1.60	7.23	8.64	-3.37	-2.61	5.23	5.56
	Side walls	S6	-8.72	-10.24	-6.76	-4.49	-7.44	-9.16	-6.39	-5.09
		S7	-10.70	-10.62	-1.44	3.70	-10.31	-10.10	-1.23	2.73
		S8	7.85	5.84	-6.65	-11.57	5.86	3.74	-7.60	-11.13
		S9-1	-5.21	-5.41	-2.93	-2.15	-5.94	-5.86	-3.70	-3.26
		S9-2	-4.44	-5.01	-2.39	-0.65	-4.78	-5.04	-2.57	-1.23
Sec B-B	Top Slab	S12	2.54	1.08	-2.33	-3.10	2.65	0.96	-3.49	-4.16
		S13	2.12	1.79	0.30	-0.71	3.81	3.61	0.29	-1.65
		S14	-0.60	0.31	1.99	1.29	-2.87	-1.31	0.31	-0.50
		S15	-0.23	0.36	1.69	0.75	-2.76	-2.05	-0.22	-1.04
		S16	-1.44	-1.38	0.39	0.53	-3.70	-3.78	0.67	1.57
	Side walls	S17	0.54	-1.33	-3.90	-4.02	-3.05	-5.25	-6.30	-5.70
		S18	-3.50	-2.79	1.18	2.99	-6.06	-5.25	1.11	3.89
		S19	3.09	2.28	-1.58	-3.70	3.12	1.87	-4.53	-7.33
		S20-1	-1.61	-2.18	-2.04	-1.78	-3.81	-4.13	-3.18	-2.90
		S20-2	-1.87	-2.12	-1.19	-0.70	-4.32	-4.56	-2.84	-2.07
	LVDTs	Ext. (in.)	-0.0010	-0.0011	-0.0006	-0.0004	-0.0019	-0.0019	-0.0009	-0.0004
		Int. (in.)	0.0004	0.0003	-0.0003	-0.0005	0.0006	0.0005	-0.0008	-0.0010
Transverse Gages	Exterior	S23	-0.56	-0.81	-1.60	-2.02	-1.56	-1.85	-2.47	-2.76
	Interior	S24	-1.73	-2.13	-1.23	-1.44	-3.88	-4.45	-3.54	-3.27

Strain Gages Measurements for Load Path 3 and Load Path 4

Section	Location	Strain Gages	Path 3				Path 4			
			1	2	3	4	1	2	3	4
Sec A-A	Top Slab	S1	-1.16	-2.58	-3.64	-1.97	2.75	1.93	-0.38	-0.89
		S2	-0.21	-0.08	-0.41	-0.65	2.14	2.50	1.65	0.63
		S3	-1.74	-0.71	2.27	-0.77	-0.23	2.04	4.01	2.60
		S4	-2.52	-1.87	0.43	-1.44	0.07	1.30	2.84	1.99
		S5	-2.27	-1.94	0.63	-0.36	-0.83	-0.10	2.43	2.68
	Side walls	S6	-1.25	-2.97	-4.36	-1.27	1.38	-0.13	-2.08	-1.93
		S7	-4.66	-4.08	-0.18	-1.36	-3.60	-2.80	1.59	3.21
		S8	0.37	-0.34	-2.56	-0.99	4.01	3.33	-0.65	-2.64
		S9-1	-4.15	-4.51	-2.77	-1.49	-1.04	-0.68	0.43	0.71
		S9-2	-3.05	-3.02	-1.22	-0.99	-1.48	-1.16	0.74	1.19
Sec B-B	Top Slab	S12	3.03	0.28	-4.12	-0.62	5.75	3.08	-1.70	-1.29
		S13	10.27	10.60	2.42	-0.46	11.82	12.50	4.39	0.36
		S14	-7.50	-4.74	-1.67	-0.46	-6.47	-2.92	-0.10	-1.63
		S15	-7.76	-6.84	-3.43	-1.15	-5.00	-3.73	-1.46	-1.40
		S16	-7.23	-6.22	8.15	-2.01	-3.27	-1.79	10.81	12.72
	Side walls	S17	-13.08	-15.17	-8.22	-1.83	-9.70	-11.36	-5.36	-2.92
		S18	-12.35	-12.24	0.61	-0.26	-11.28	-11.34	0.43	6.13
		S19	4.52	2.53	-8.70	-1.18	7.12	5.13	-6.69	-10.12
		S20-1	-7.90	-7.79	-3.20	-1.30	-4.71	-4.13	-0.57	0.33
		S20-2	-8.07	-8.77	-4.27	-2.16	-4.24	-4.75	-1.15	0.70
	LVDTs	Ext. (in.)	-0.0038	-0.0038	-0.0011	-0.0002	-0.0034	-0.0034	-0.0009	0.0000
		Int. (in.)	0.0010	0.0007	-0.0019	0.0003	0.0009	0.0005	-0.0020	-0.0028
Transverse Gages	Exterior	S23	-4.24	-4.39	-2.19	-1.07	0.62	0.82	0.50	0.13
	Interior	S24	-4.87	-5.25	-4.71	-1.86	-1.19	-0.73	1.76	1.81

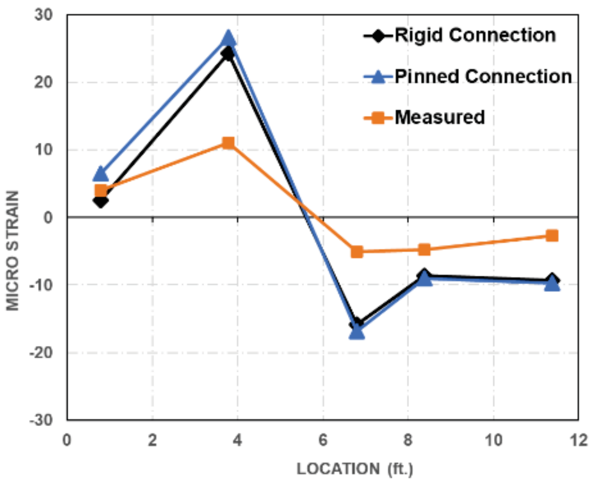

(a) Load Path-1 (Position-01)

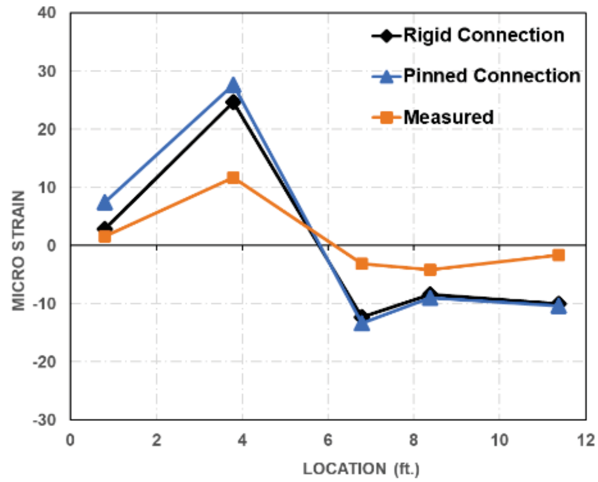

(b) Load Path-1 (Position-02)

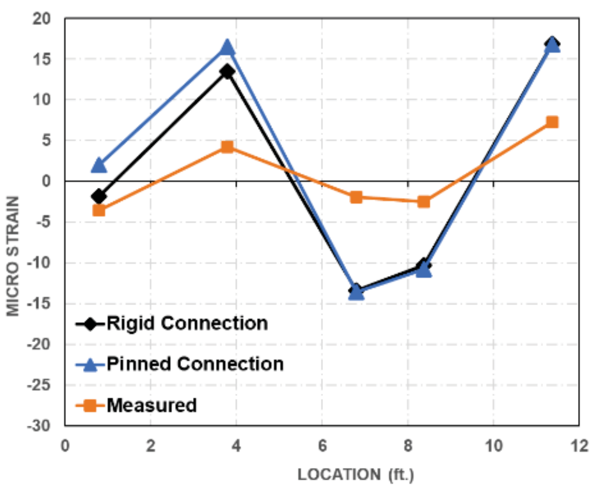

(c) Load Path-1 (Position-03)

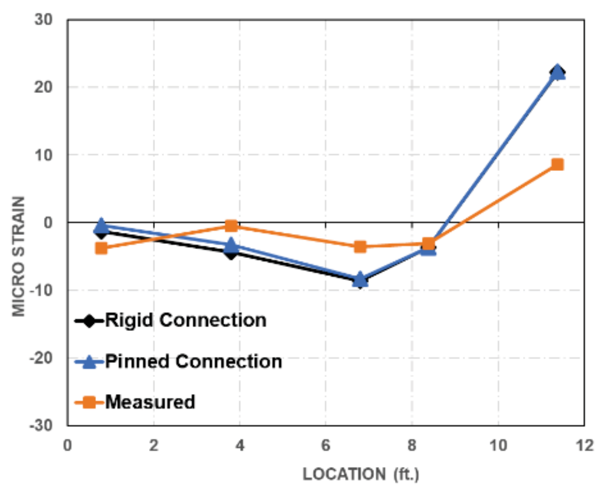

(d) Load Path-1 (Position-04)

Strain values at the top slab of culvert from the field measurements and FEM models

Culvert RC# 008490

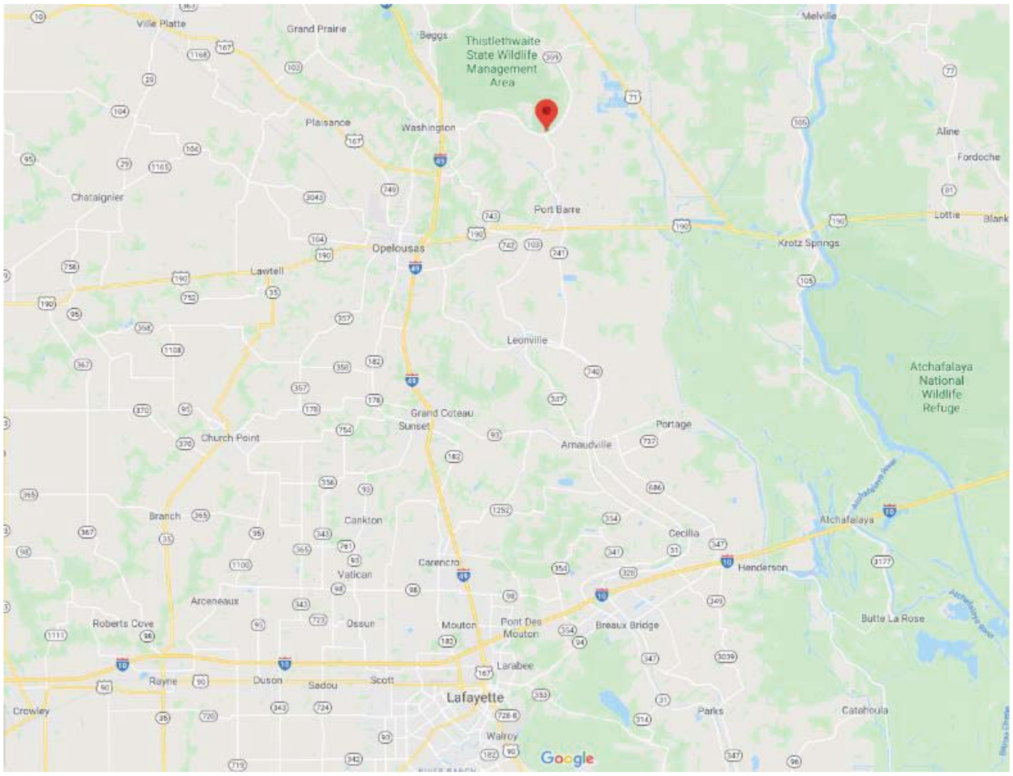

Map Location (30.61255, -91.9631), St. Landry, LA

Culvert oveview and testing

Instrumentation

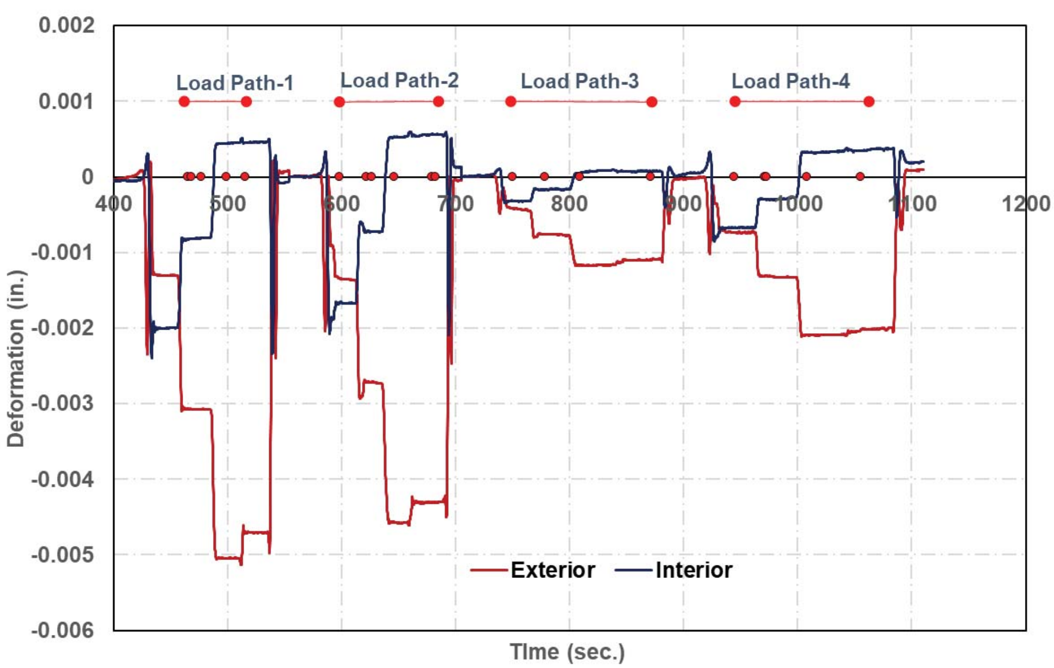

Vertical displacement at midspan of exterior and interior cells during loading of Culvert

Strain Gages Measurements for Load Path 1 and Load Path 2

Section	Location	Strain Gages	Path-1				Path-2			
			P 1-1	P 1-2	P 1-3	P 1-4	P 2-1	P 2-2	P 2-3	P 2-4
Sec A-A	Top Slab	S1-1	3.38	3.14	-0.23	-2.09	2.47	1.93	-0.99	-2.50
		S 2	1.71	4.91	10.70	10.21	0.74	3.15	7.21	7.57
		S3	-5.11	-6.21	-5.30	-3.64	-6.77	-7.34	-6.06	-3.70
		S4	0.02	-0.79	-0.87	-0.54	-2.77	-3.75	-4.23	-3.41
		S5	0.80	0.02	-0.86	-1.08	0.64	-0.86	-2.58	-2.52
		S1-2	-0.68	-0.89	-0.95	-1.83	-2.74	-2.45	-2.83	-3.21
	Exterior Wall	S6-1	-2.91	-6.09	-9.91	-9.64	-4.29	-7.04	-9.44	-9.28
		S 6-2	-0.68	-0.50	-0.31	-0.38	-1.46	-1.26	-0.86	-0.79
		S9-1	-0.97	-2.07	-2.04	-1.96	-1.59	-2.19	-2.47	-2.27
	Interior Wall	S 7	-1.47	-2.45	-4.60	-3.83	-1.95	-2.33	-3.53	-3.91
		S8	1.48	1.60	1.55	0.79	0.29	0.96	1.71	1.16
		S 9-2	-0.96	-1.72	-3.68	-3.65	-2.07	-2.64	-3.72	-4.01
Sec B-B	Top Slab	S 12-1	0.51	-0.03	-1.82	-3.32	-3.27	-3.81	-5.67	-7.31
		S 12-2	0.36	0.96	-0.08	-1.15	-0.61	-0.15	-1.45	-2.26
		S13	0.30	0.89	1.80	1.55	-0.50	0.77	3.07	3.24
		S 14	-1.44	-1.47	-0.24	0.42	-3.69	-3.84	-2.42	-0.89
		S 15	-2.53	-3.73	-4.78	-3.90	-4.10	-4.95	-5.54	-4.33
		S 16	4.94	1.79	-1.37	-1.46	3.18	0.12	-2.79	-2.46
	Exterior Wall	S17-1	0.69	-0.07	-2.03	-2.65	-1.27	-2.80	-5.22	-5.52
		S 17-2	-2.47	-2.06	-0.93	-0.87	-3.14	-2.59	-1.87	-1.69
	Interior Wall	S 18	-1.23	-1.67	-1.81	-1.53	-1.94	-2.84	-4.02	-3.61
		S 19	0.40	2.11	4.07	2.46	-1.27	0.14	1.82	0.78
		S20	0.11	0.04	0.12	0.36	-0.22	-0.23	-0.13	-0.09
	LVDT	Cell-01 (in.)	-0.0004	-0.0008	-0.0012	-0.0011	-0.0007	-0.0013	-0.0021	-0.0020
		Cell-02 (in.)	-0.0003	-0.0002	0.0001	0.0001	-0.0007	-0.0003	0.0003	0.0004
Transverse gages	Cell-01	S 23	-0.02	0.12	0.24	0.07	-0.49	-0.08	0.66	0.73
	Cell-02	S 24	0.49	-0.01	-0.59	-0.93	-0.27	-1.11	-2.11	-2.11

Strain Gages Measurements for Load Path 3 and Load Path 4

Section	Location	Strain Gages	Path-3				Path-4			
			P 3-1	P 3-2	P 3-3	P 3-4	P 4-1	P 4-2	P 4-3	P 4-4
Sec A-A	Top Slab	S1-1	0.00	0.03	-0.88	-1.72	1.87	2.09	0.43	-0.45
		S 2	-1.97	-1.21	-0.48	-0.79	0.25	1.71	3.57	3.88
		S3	-4.19	-3.87	-2.45	-1.52	-2.75	-2.67	-0.83	0.71
		S4	-7.63	-8.26	-8.83	-7.50	-4.46	-5.34	-6.15	-4.65
		S5	2.11	-1.84	-4.86	-4.74	4.14	0.81	-2.29	-2.15
		S1-2	-1.80	-0.60	-3.13	-4.64	0.20	1.57	-0.14	-1.25
	Exterior Wall	S6-1	-1.63	-2.32	-3.83	-4.58	0.05	-1.60	-3.85	-4.41
		S 6-2	-3.51	-2.70	-1.63	-1.53	-2.35	-1.87	-0.80	-0.77
		S9-1	-1.31	-1.60	-1.78	-1.76	-0.71	-1.02	-1.44	-1.11
	Interior Wall	S7	-1.65	-1.97	-2.14	-1.18	-0.51	-1.26	-1.62	-1.43
		S8	-1.27	1.64	4.47	3.05	0.49	2.48	4.75	3.45
		S9-2	-1.62	-1.94	-2.48	-2.14	-0.42	-1.23	-1.95	-1.80
Sec B-B	Top Slab	S12-1	-26.86	-28.09	-32.16	-34.68	1.69	0.79	-2.68	-5.18
		S12-2	-2.25	-2.19	-2.71	-3.13	0.28	0.13	-0.71	-1.08
		S13	-0.67	4.01	9.73	9.21	1.48	4.90	10.36	10.05
		S14	-6.84	-7.39	-5.90	-3.54	-5.01	-5.67	-4.03	-1.51
		S15	-2.65	-2.98	-2.53	-1.89	-1.51	-2.27	-2.39	-1.59
		S16	-2.45	-3.04	-3.51	-3.49	1.62	0.15	-1.38	-1.24
	Exterior Wall	S17-1	-4.96	-8.54	-11.92	-10.95	-3.56	-6.71	-9.94	-9.04
		S17-2	-3.07	-2.82	-2.76	-2.94	-1.74	-1.60	-1.12	-1.28
	Interior Wall	S18	-2.17	-4.45	-7.80	-7.87	-1.46	-3.33	-6.57	-6.55
		S19	-1.68	-1.40	-1.44	-1.94	0.70	1.25	1.71	1.11
		S20	0.37	0.34	0.27	0.38	0.27	0.17	0.08	0.12
	LVDT	Cell-01 (in.)	-0.0013	-0.0031	-0.0050	-0.0047	-0.0014	-0.0027	-0.0046	-0.0043
		Cell-02 (in.)	-0.0020	-0.0008	0.0004	0.0005	-0.0017	-0.0007	0.0005	0.0006
Transverse gages	Cell-01	S 23	-1.83	-1.95	-1.92	-1.83	-0.32	-0.13	0.51	0.61
	Cell-02	S 24	-2.46	-2.51	-2.76	-2.95	0.25	-0.21	-0.85	-0.91

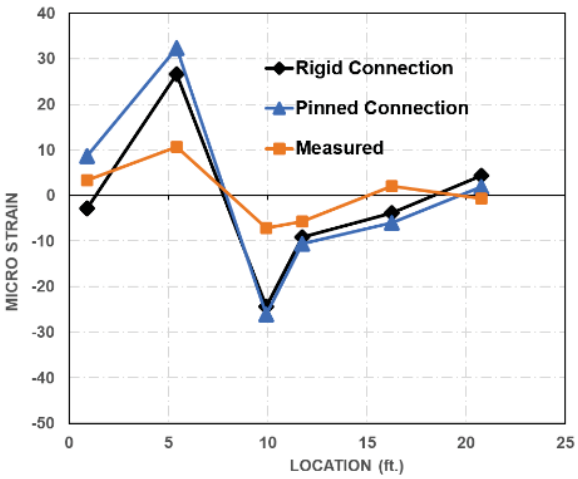

(a) Load Path-1 (Position-01)

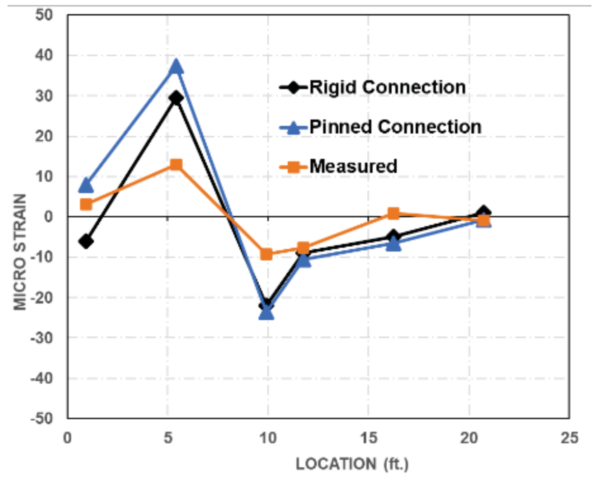

(b) Load Path-1 (Position-02)

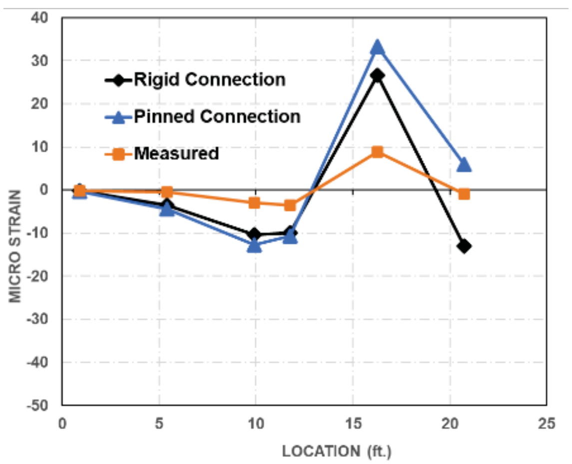

(c) Load Path-1 (Position-03)

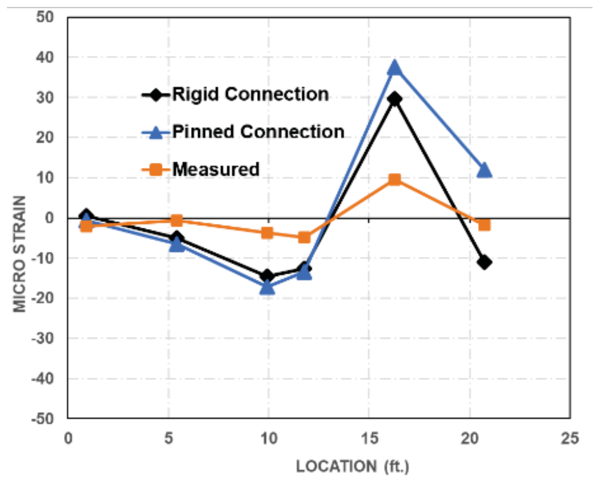

(d) Load Path-1 (Position-04)

Strain values at the top slab of culvert from the field measurements and FEM models

Culvert RC# 004510

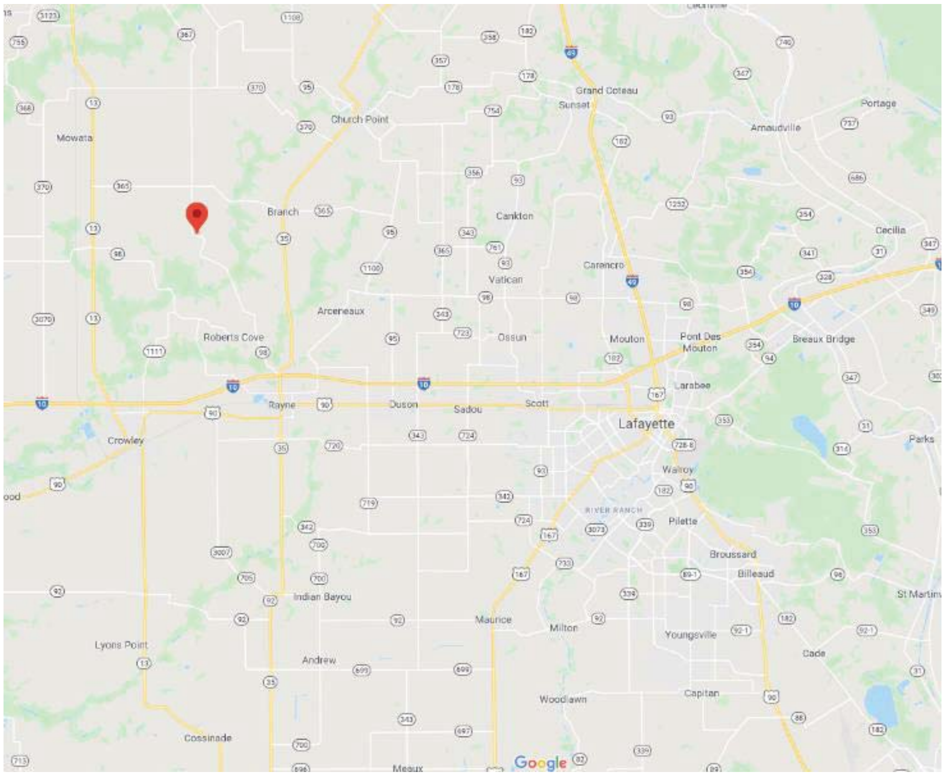

Map Location (30.33436, -92.3267), Acadia ,LA

Culvert oveview and testing

Instrumentation

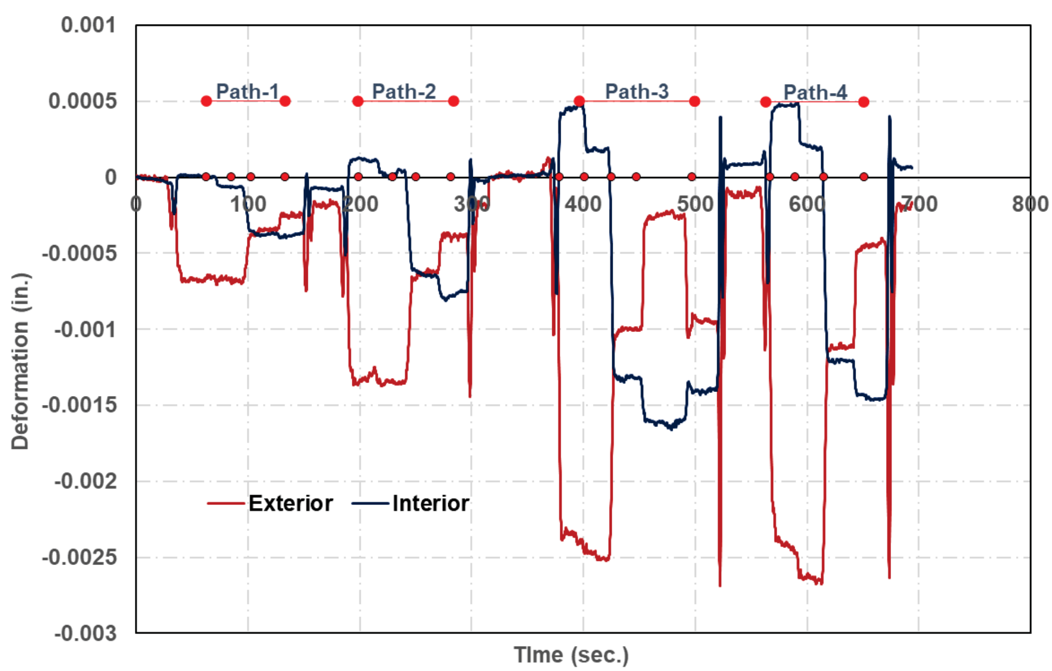

Vertical displacements at midspan of exterior and interior cells during loading of Culvert

Strain Gages Measurements for Load Path 1 and Load Path 2

Section	Location	Gage	Path-1				Path-2			
			1	2	3	4	1	2	3	4
Sec A-A	Top Slab	S1	2.05	0.82	-1.42	-1.46	1.70	0.93	-1.16	-1.34
		S2	10.06	11.69	3.87	0.72	8.03	9.74	2.98	0.81
		S3	-3.49	-2.34	-1.53	-1.58	-3.10	-1.86	-0.58	-0.53
		S4	-3.87	-2.98	-1.03	-1.01	-3.68	-2.56	0.07	0.46
		S5	-3.06	-1.47	7.25	8.88	-2.46	-1.11	6.34	7.43
	Ext. Wall	S6	-5.73	-6.36	-3.56	-2.36	-4.01	-4.51	-2.66	-1.85
	Int. Wall	S7	-8.61	-9.21	-1.69	1.82	-7.30	-7.45	-0.53	2.31
		S8	3.68	1.13	-8.23	-9.88	2.79	1.17	-6.66	-7.81
Sec B-B	Tob Slab	S12	0.49	-0.23	-1.73	-1.96	0.61	0.03	-1.68	-1.80
		S13	0.56	0.79	-0.48	-0.88	2.50	3.56	1.13	0.14
		S14	-1.03	-0.34	0.05	0.02	-1.69	-0.55	0.17	0.18
		S15	-1.39	-0.75	0.21	0.00	-2.97	-2.16	-0.21	0.02
		S16	-1.41	-1.19	0.27	0.67	-2.30	-1.65	1.91	2.79
	Ext. Wall	S17	-0.78	-2.03	-2.89	-2.61	-3.15	-4.13	-3.57	-2.74
		S20-1	-1.87	-1.89	-1.44	-1.23	-2.71	-2.57	-1.43	-1.08
	Int. Wall	S18*	-1.00	-1.01	-0.13	0.09	-2.70	-2.71	-1.30	-0.71
		S19	0.73	0.21	-1.44	-1.97	0.84	0.39	-2.12	-2.82
		S20-3	-0.90	-1.03	-1.18	-1.22	-1.77	-1.86	-2.06	-1.84
		S 20-2	-0.97	-1.06	-1.00	-0.91	-1.51	-1.61	-1.36	-1.05
	LVDTs	Ext. (in.)	-0.0007	-0.0007	-0.0004	-0.0003	-0.0013	-0.0014	-0.0007	-0.0004
		Int. (in.)	0.0000	-0.0001	-0.0004	-0.0004	0.0001	0.0000	-0.0006	-0.0008
Transverse Gages	Exterior	S23	-1.12	-1.26	-1.36	-1.20	-1.46	-1.40	-1.11	-0.66
	Interior	S24	-1.85	-1.75	-1.44	-1.22	-2.07	-1.74	-1.31	-1.06

Strain Gages Measurements for Load Path 3 and Load Path 4

Section	Location	Gage	Path-3				Path-4			
			1	2	3	4	1	2	3	4
Sec A-A	Top Slab	S1	1.03	0.92	0.10	-0.01	2.44	2.05	0.63	0.29
		S2	1.19	1.45	1.11	0.90	3.84	4.14	2.54	1.56
		S3	0.36	0.99	1.53	1.56	1.26	1.76	2.36	2.10
		S4	-0.02	0.72	1.44	1.28	0.22	0.81	2.30	2.38
		S5	0.10	0.53	1.89	2.40	1.40	1.76	4.03	4.53
	Ext. Wall	S6	1.36	0.87	-0.22	-0.20	1.69	0.94	0.04	0.03
	Int. Wall	S7	-1.25	-0.51	1.52	2.48	-1.48	-0.91	2.35	3.63
		S8	1.96	1.66	0.08	-0.71	3.61	2.95	-0.27	-1.67
Sec B-B	Tob Slab	S12	3.48	2.50	-0.01	-0.01	4.93	3.77	1.12	0.90
		S13	9.87	11.09	5.28	2.15	10.80	11.86	6.17	3.21
		S14	-2.26	-1.27	-0.45	-0.51	-0.81	-0.07	0.60	0.22
		S15	-3.76	-2.66	1.09	1.58	-2.34	-1.46	1.88	2.25
		S16	-1.57	-0.10	7.30	9.06	0.00	1.06	7.61	8.98
	Ext. Wall	S17	-7.18	-7.90	-4.07	-1.78	-5.25	-6.46	-3.04	-1.21
		S20-1	-1.78	-1.47	0.17	0.91	-0.50	-0.49	0.93	1.41
	Int. Wall	S18*	-2.48	-2.79	-0.66	1.03	-1.99	-2.44	-0.41	0.94
		S19	2.25	1.48	-2.76	-4.07	2.83	1.85	-2.39	-3.71
		S20-3	-0.57	-0.91	-1.68	-1.23	0.41	-0.14	-0.99	-0.68
		S 20-2	-1.67	-2.29	-2.22	-1.49	-0.75	-1.53	-1.45	-0.96
	LVDTs	Ext. (in.)	-0.0023	-0.0025	-0.0010	-0.0002	-0.0024	-0.0026	-0.0011	-0.0005
		Int. (in.)	0.0004	0.0002	-0.0013	-0.0016	0.0005	0.0002	-0.0012	-0.0015
Transverse Gages	Exterior	S23	-0.36	-0.36	-0.60	-0.42	0.57	0.55	1.20	1.49
	Interior	S24	-1.79	-1.58	-0.59	-0.02	0.56	0.83	0.75	0.63

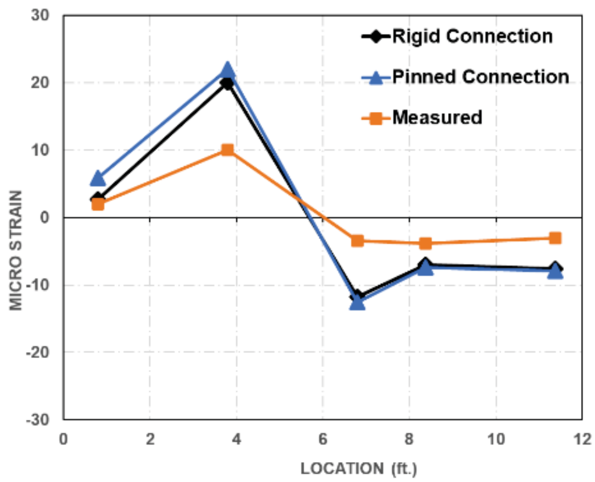

(a) Load Path-1 (Position-01)

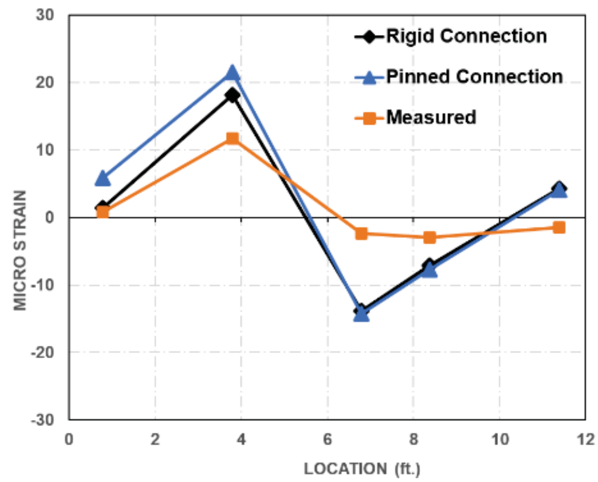

(b) Load Path-1 (Position-02)

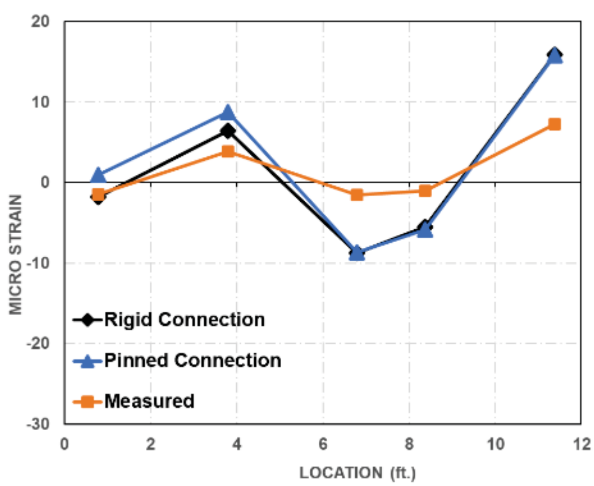

(c) Load Path-1 (Position-03)

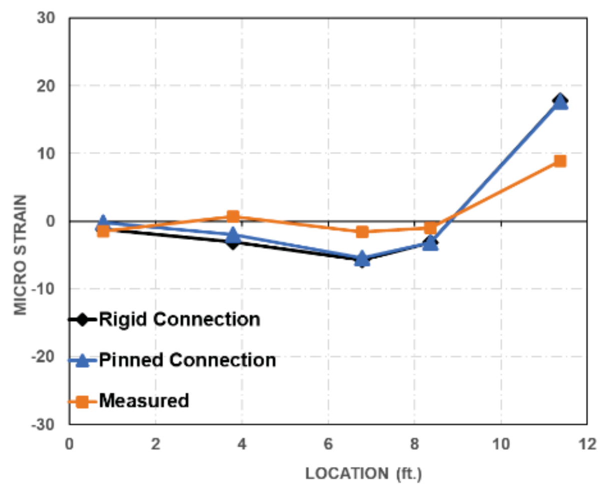

(d) Load Path-1 (Position-04)

Strain values at the top slab of culvert from the field measurements and FEM models

Culvert RC# 056860

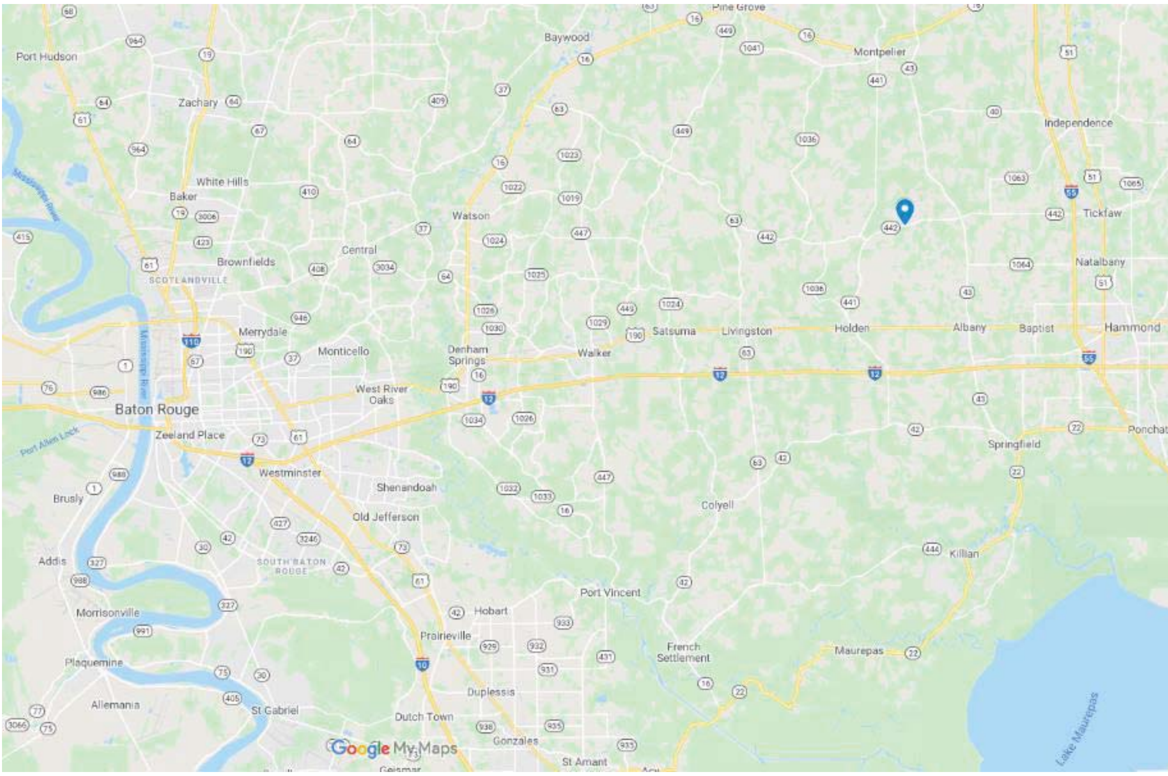

Map Location (30.56951, -90.6313) Livingston, LA

Culvert oveview and testing

Instrumentation

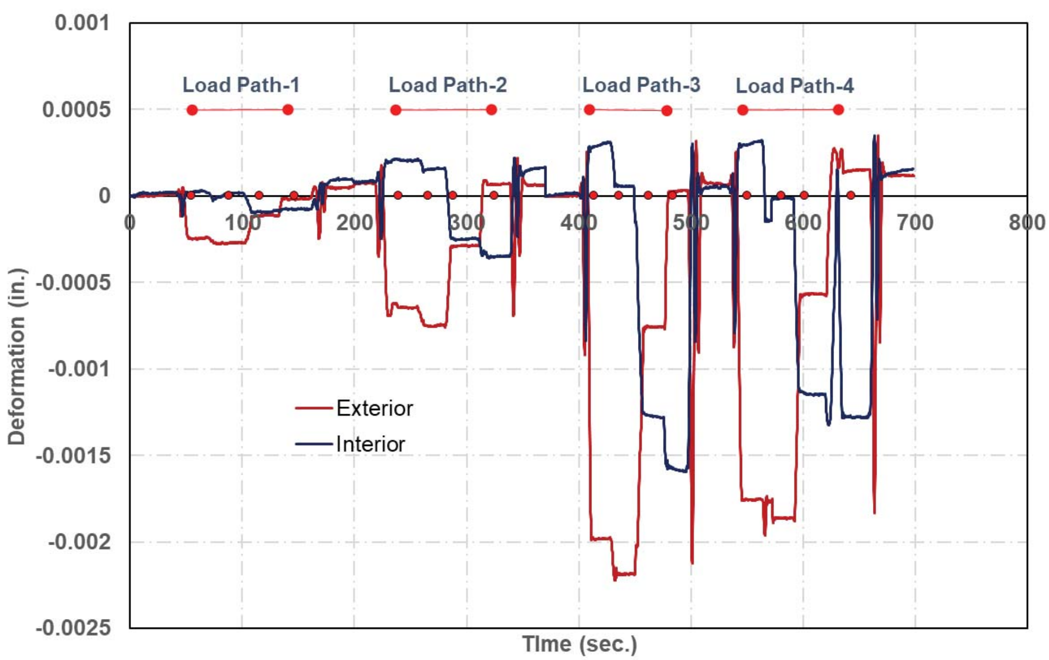

Vertical displacement at midspan of exterior and interior cells during loading of Culvert

Strain Gages Measurements for Load Path 1 and Load Path 2

Section	Location	Gages	Path-01				Path-02			
			1	2	3	4	1	2	3	4
Sec-A-A	Top Slab	S1	5.81	4.42	-1.49	-1.83	5.39	4.51	-0.68	-1.45
		S2	9.51	10.50	4.76	1.33	7.22	8.15	4.53	0.98
		S3	-3.91	-2.17	-0.51	-1.00	-3.16	-1.41	0.26	-0.32
		S4	-4.22	-3.44	-1.00	-0.42	-2.82	-1.99	0.00	0.26
		S5	-1.01	-0.11	3.51	4.26	-0.74	0.10	2.58	3.49
	Ext. Wall	S6	-8.11	-10.05	-6.02	-3.61	-5.40	-7.13	-5.05	-2.91
	Int. Wall	S7	-10.41	-10.53	-1.97	3.18	-8.27	-8.23	-2.29	2.88
		S8	9.64	5.95	-8.10	-12.37	7.96	5.59	-4.94	-10.21
Sec-B-B	Top Slab	S12	0.22	0.62	1.02	1.29	1.27	1.17	1.82	1.28
		S13	0.93	1.12	0.72	0.58	2.68	3.14	1.57	0.33
		S14	0.51	1.68	2.58	2.38	-0.77	0.73	1.29	0.69
		S15	0.07	1.19	2.62	2.24	-1.02	0.03	2.64	2.85
		S16	-0.28	0.21	2.04	2.76	-0.92	-0.56	3.24	4.97
	Ext. Wall	S17	0.40	-0.43	-1.61	-1.51	-0.60	-1.67	-2.30	-1.72
	Int. Wall	S18	-2.94	-2.12	1.56	3.32	-4.98	-4.83	0.32	4.18
		S19	2.82	2.53	0.22	-0.88	5.13	4.62	0.41	-2.16
	LVDTs (in.)	Ext.	-0.0002	-0.0003	-0.0001	0.0000	-0.0006	-0.0008	-0.0003	0.0001
		Int.	0.0000	0.0000	-0.0001	-0.0001	0.0002	0.0002	-0.0002	-0.0004
Transverse Gages	Exterior	S23	-0.70	-0.84	-0.64	-0.26	-0.70	-0.54	-0.86	-0.84
	Interior	S24	-0.43	-0.37	0.55	0.89	-0.64	-0.72	-0.26	0.37

Strain Gages Measurements for Load Path 3 and Load Path 4

Section	Location	Gauges	Path-3				Path-4			
			1	2	3	4	1	2	3	4
Sec A-A	Top Slab	S1	1.45	0.87	-0.43	-0.63	3.22	1.81	-0.57	-1.37
		S2	0.74	1.00	0.75	0.56	2.46	2.98	1.40	-0.13
		S3	0.01	0.97	1.85	1.71	-0.12	1.35	2.20	1.01
		S4	0.39	1.02	1.39	0.97	-0.46	0.31	1.39	0.87
		S5	0.04	0.16	0.68	0.91	-0.41	-0.03	1.30	1.44
	Ext. Wall	S6	1.03	-0.10	-1.60	-1.51	0.24	-1.81	-2.38	-2.20
	Int. Wall	S7	-1.76	-1.15	1.11	2.39	-3.22	-2.55	1.56	3.18
		S8	3.26	2.47	-0.74	-2.32	5.26	3.73	-1.91	-4.74
Sec B-B	Top Slab	S12	0.16	0.67	0.92	0.68	0.32	0.14	0.37	0.28
		S13	6.85	8.28	3.54	0.77	6.68	7.52	3.10	0.08
		S14	-4.51	-1.68	-0.37	-1.80	-4.25	-1.41	-0.37	-2.51
		S15	-4.99	-3.16	0.11	-0.02	-4.15	-1.96	0.80	0.04
		S16	-2.10	0.01	10.45	12.87	-2.00	0.61	10.08	10.93
	Ext. Wall	S17	-5.06	-6.23	-3.42	-1.64	-4.23	-5.37	-2.90	-1.75
	Int. Wall	S18	-11.31	-11.61	-0.50	5.97	-10.29	-10.18	-0.28	4.73
		S19	6.34	4.44	-5.12	-8.30	6.66	3.87	-4.37	-7.54
	LVDTs	Ext.	-0.0020	-0.0022	-0.0008	0.0000	-0.0018	-0.0019	-0.0006	0.0001
		Int.	0.0003	0.0001	-0.0013	-0.0016	0.0003	0.0000	-0.0011	-0.0013
Transverse Gauges	Ext.	S23	-1.61	-1.63	-0.61	0.01	0.73	1.10	0.36	-0.45
	Int.	S24	-0.05	-0.16	-1.12	-1.22	-0.03	0.13	2.36	2.09

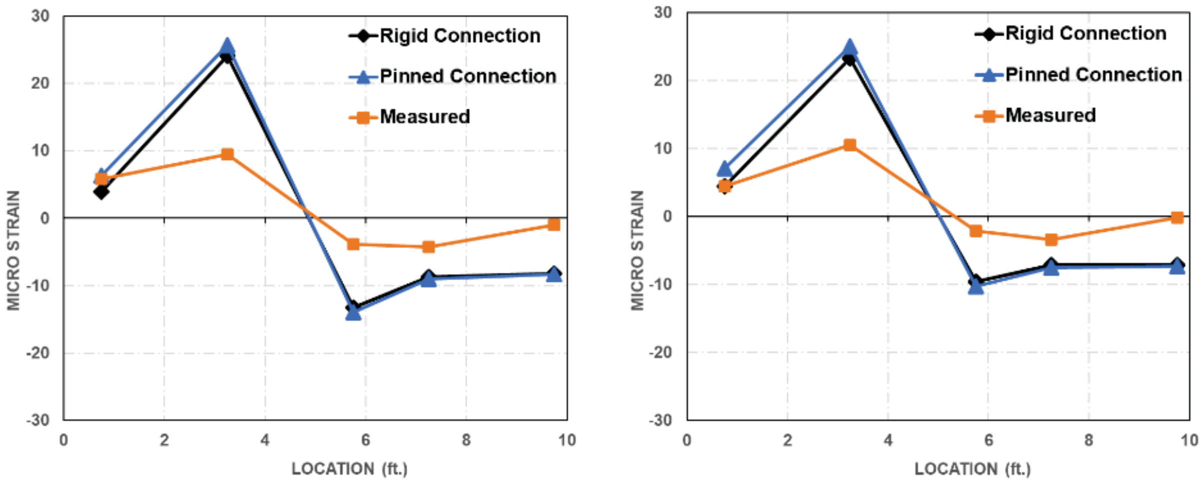

(a) Load Path-1 (Position-01)

(b) Load Path-1 (Position-02)

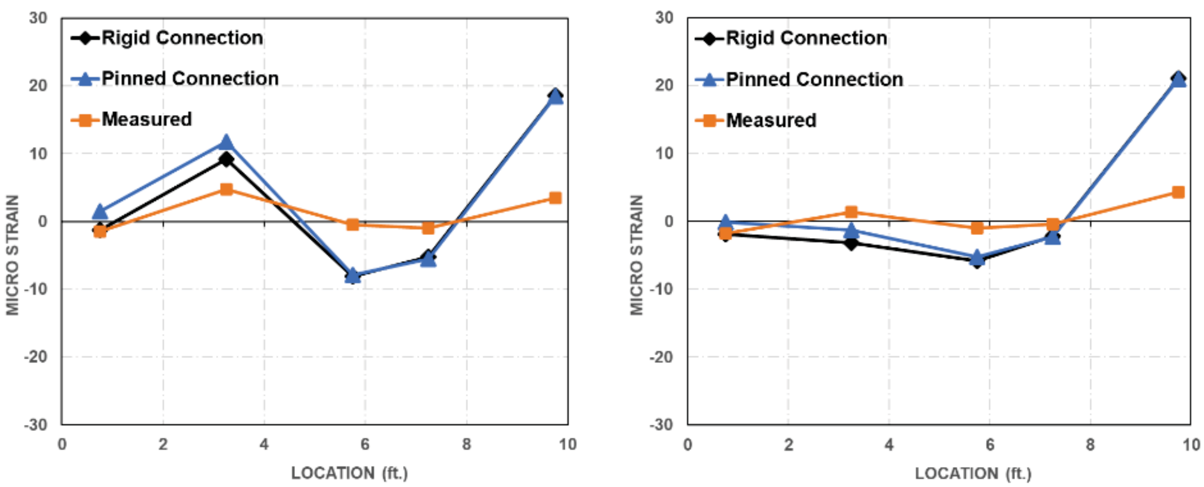

(c) Load Path-1 (Position-03)

(d) Load Path-1 (Position-04)

Strain values at the top slab of culvert from the field measurements and FEM models

Culvert RC# 048410

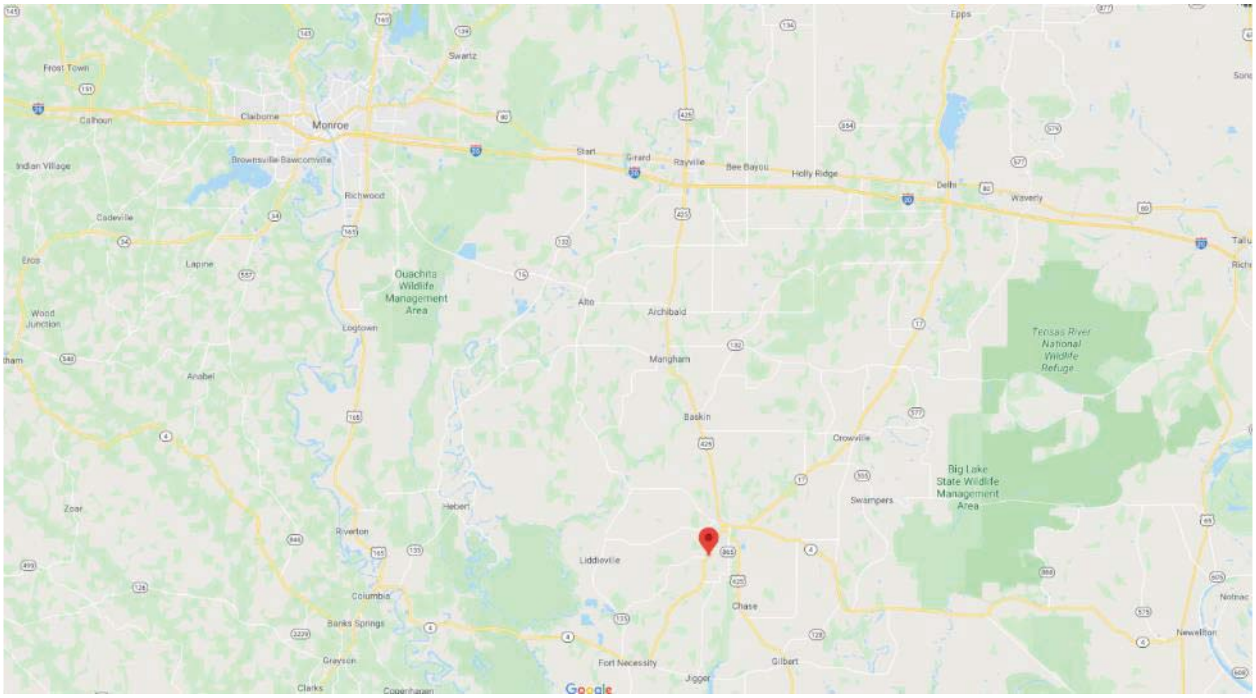

Map Location of Culvert (32.13961, -91.7357), Franklin, LA

Strain Gages Measurements for Load Path 1 and Load Path 2

Section	Location	Gauges	Path-1				Path-2			
			1	2	3	4	1	2	3	4
ec A-A	Top Slab	S1	0.66	-0.73	-2.74	-2.48	0.67	-0.35	-1.83	-1.68
		S2	7.73	8.85	2.56	0.02	2.08	2.17	0.29	-0.41
		S3	-5.80	-5.41	-3.41	-3.63	-1.34	-1.21	-0.42	-0.61
		S4	-4.63	-4.50	-3.61	-3.97	-1.09	-1.01	-0.14	-0.32
		S5	0.44	0.11	7.24	8.87	0.15	-0.14	2.41	3.21
	Ext. Wall	S6	-6.70	-7.57	-4.17	-3.12	-1.61	-2.75	-2.41	-1.84
		S9	-2.88	-2.99	-1.60	-1.19	-1.49	-1.89	-1.01	-0.47
	Int. Wall	S7	-5.87	-6.57	-0.21	1.96	-2.44	-2.79	0.51	1.68
		S8	3.00	2.76	-4.85	-6.49	1.78	1.49	-2.06	-2.80
	Haunch	SM1	-3.38	-4.25	-3.00	-2.53	-0.64	-1.50	-1.75	-1.51
	LVDTs (in.)	Interior	-0.023	-0.025	-0.009	-0.003	-0.009	-0.011	-0.005	-0.001
		Exterior	-0.002	0.000	-0.015	-0.018	-0.001	-0.001	-0.007	-0.007
Sec B-B	Top Slab	S10	1.42	0.65	-1.49	-1.97	1.07	-0.72	-2.58	-2.19
		S11	2.64	2.78	0.45	-0.68	9.39	11.23	3.41	0.61
		S12	-0.69	-0.18	0.47	-0.18	-5.75	-5.59	-3.61	-3.69
		S13	-0.65	-0.43	0.73	0.46	-4.39	-4.45	-3.12	-3.22
		S14	0.16	0.16	2.06	2.30	0.96	0.25	7.76	9.45
	Ext. Wall	S15	-0.66	-1.16	-1.41	-1.29	-4.67	-5.40	-2.50	-1.50
		S18	-2.19	-2.56	-2.49	-2.85	-2.97	-3.67	-2.11	-1.62
	Int. Wall (In.)	S16	-2.04	-1.99	0.65	1.22	-5.44	-6.63	-0.35	2.01
		S17	0.61	0.50	-0.67	-1.19	1.35	1.25	-1.85	-2.63
	Haunch	SM2	0.17	-0.40	-1.37	-1.63	-2.69	-3.91	-2.63	-1.97

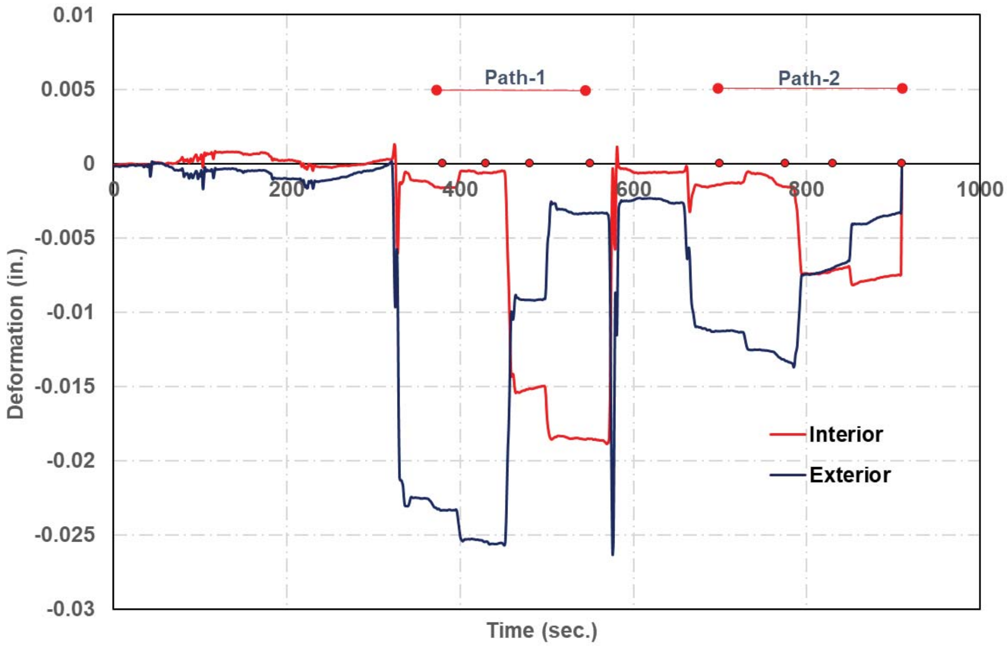

Vertical displacement at midspan of exterior and interior cells during loading of Culvert

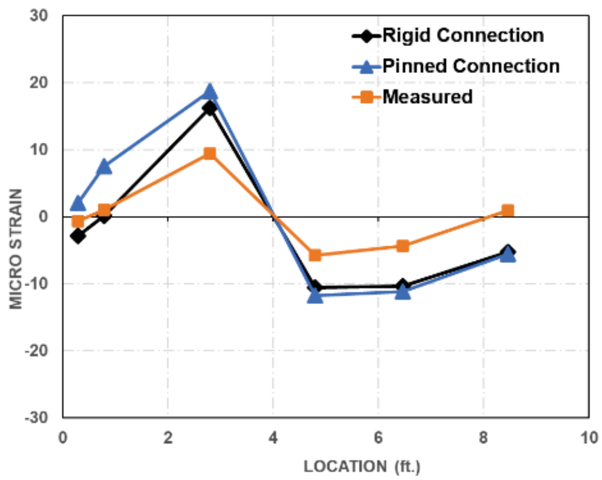

(a) Load Path-1 (Position-01)

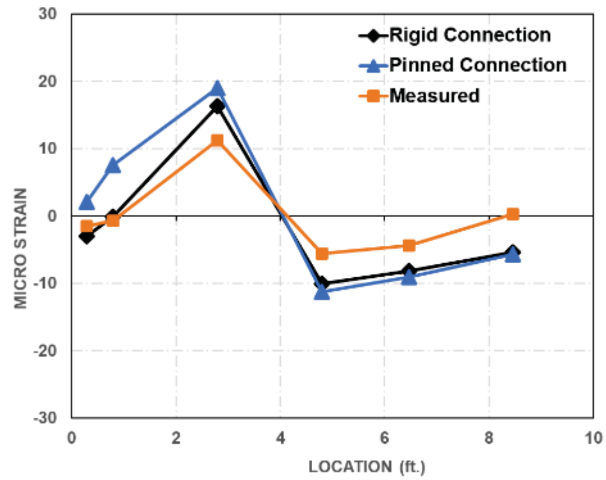

(b) Load Path-1 (Position-02)

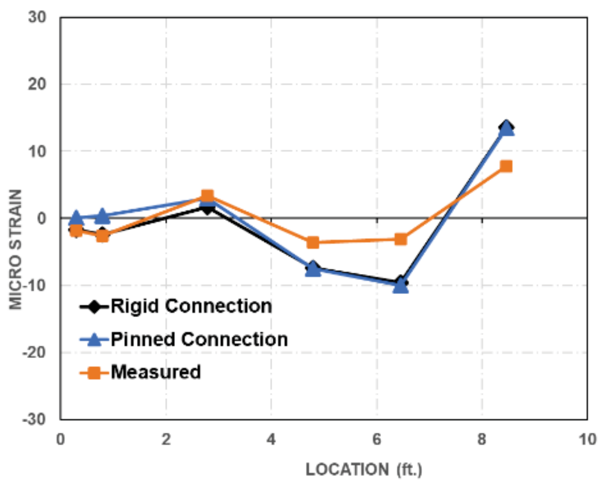

(c) Load Path-1 (Position-03)

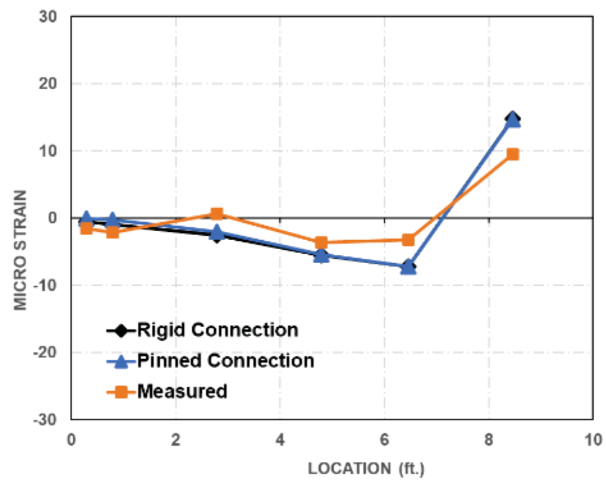

(d) Load Path-1 (Position-04)

Strain values at the top slab of Culvert from the field measurements and FEM models

Culvert RC# 048450

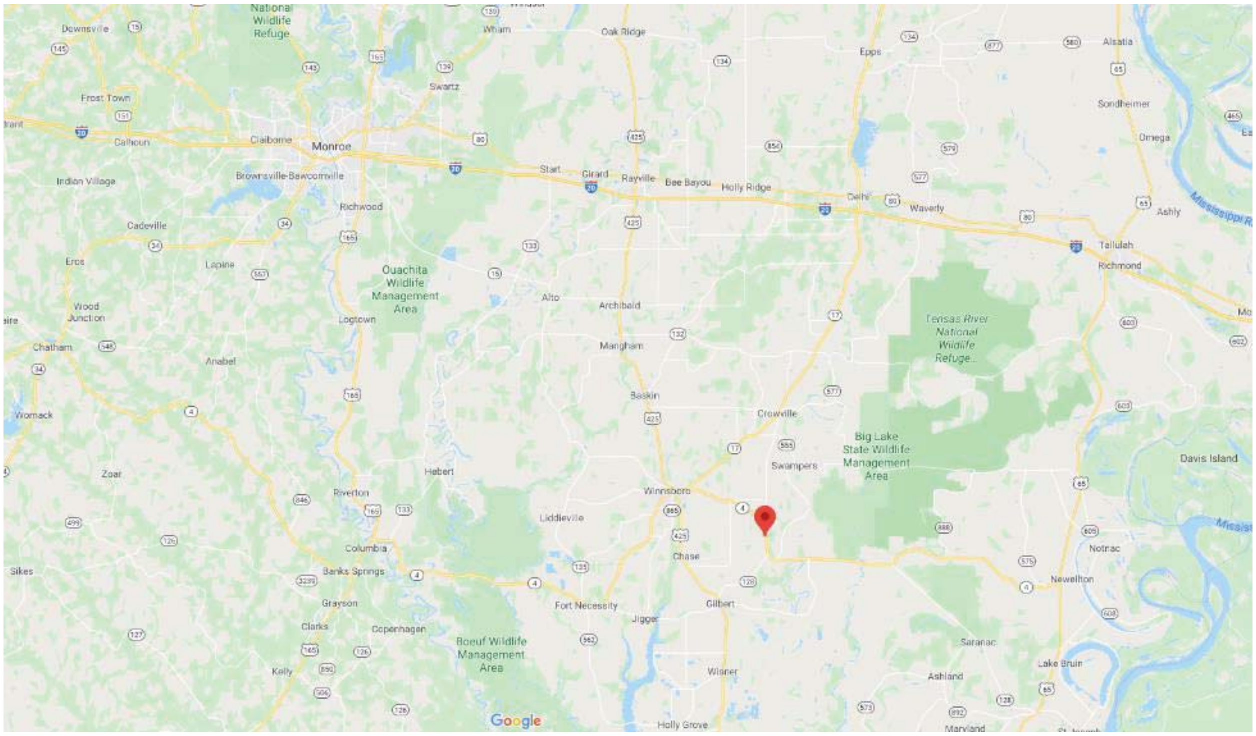

Map Location (32.11741, -91.6054), Franklin, LA

Culvert oveview and testing

Instrumentation

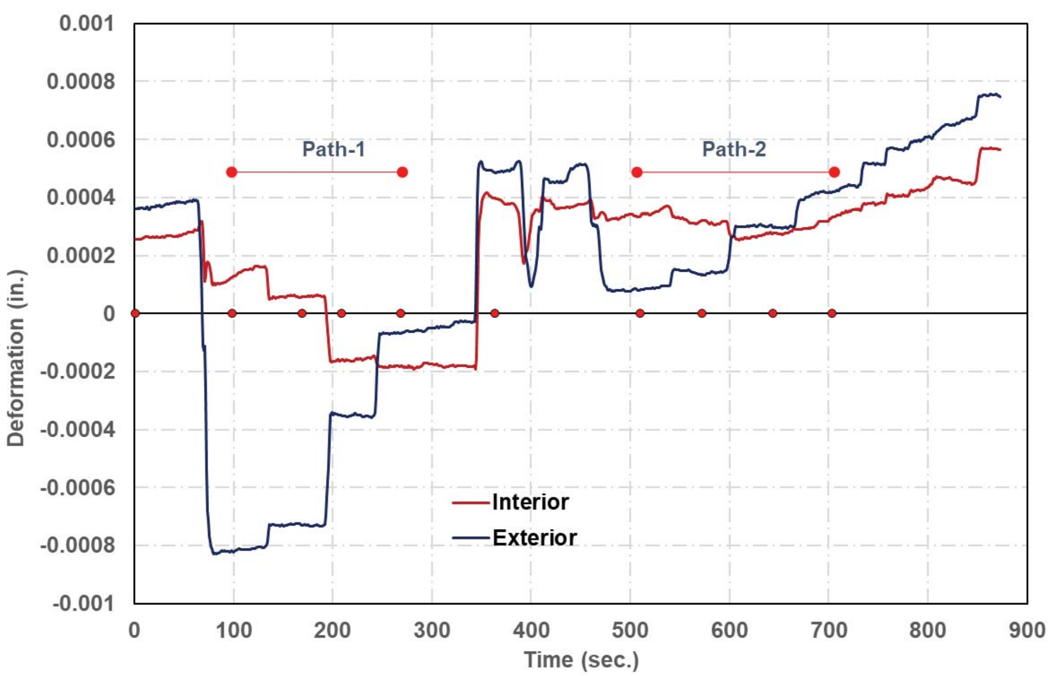

Vertical displacement at midspan of exterior and interior cells during static loading of Culvert

Strain Gages Measurements for Load Path 1 and Load Path 2

Section	Location	Gauges	Path-1				Path-2			
			1	2	3	4	1	2	3	4
Sec A-A	Top Slab	S1	1.13	0.57	-0.71	-1.33	1.04	0.75	0.05	-0.07
		S2	6.30	6.51	4.80	3.12	2.23	2.33	1.84	1.53
		S3	-3.41	-2.69	-1.32	-0.89	-0.01	0.56	1.20	1.40
		S4	N/A	N/A	N/A	N/A	N/A	N/A	N/A	N/A
		S5	1.67	2.97	4.81	5.18	0.80	1.19	1.78	2.03
	Ext. Wall	S6	-6.61	-6.90	-5.94	-4.89	-0.93	-1.16	-1.37	-1.13
		S9	-2.64	-2.57	-1.93	-1.42	-0.72	-0.62	-0.50	-0.28
	Int. Wall	S7	-8.27	-6.58	-1.07	2.23	-3.17	-2.00	0.95	2.49
		S8	2.33	0.93	-2.83	-4.64	1.73	0.99	-0.91	-1.64
	Haunch	SM1	-1.25	-1.45	-1.50	-1.41	0.08	0.03	-0.17	-0.15
	LVDTs	Interior	-0.0012	-0.0011	-0.0007	-0.0004	-0.0004	-0.0004	-0.0002	-0.0001
		Exterior	-0.0001	-0.0002	-0.0004	-0.0004	-0.0001	-0.0001	-0.0001	-0.0001
Sec B-B	Top Slab	S10	1.10	0.75	-0.45	-0.97	2.95	1.93	-0.17	-0.77
		S11	1.20	1.30	0.92	0.54	5.42	5.61	4.09	3.10
		S12	-0.22	0.14	0.51	0.56	-2.96	-2.44	-1.39	-0.91
		S13	0.33	0.63	0.60	0.53	-1.62	-1.34	-0.68	-0.29
		S14	0.77	1.22	1.71	1.98	1.15	2.19	3.97	4.49
	Ext. Wall	S15	-0.63	-0.72	-1.04	-1.04	-4.47	-4.74	-4.05	-3.20
		S18	-0.88	-0.72	-0.65	-0.45	-4.30	-4.10	-2.92	-1.90
	Int. Wall	S16	-1.56	-0.80	0.69	1.54	-5.18	-3.87	-0.38	1.45
		S17	1.15	0.63	-1.04	-1.91	3.16	1.59	-2.12	-3.43
	Haunch	SM2	-0.14	-0.19	-0.57	-0.69	-1.32	-1.58	-1.65	-1.29

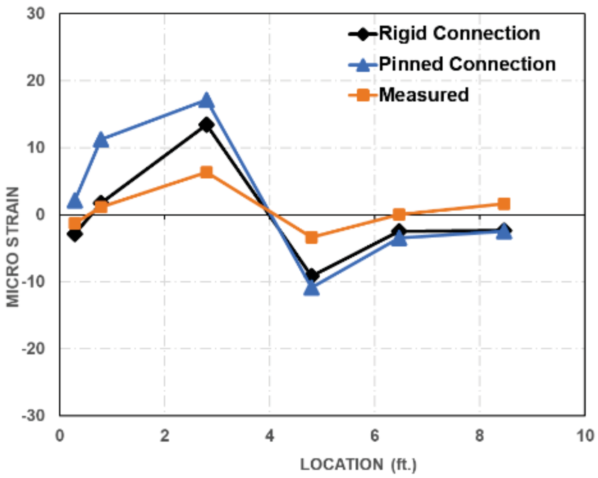

(a) Load Path-1 (Position-01)

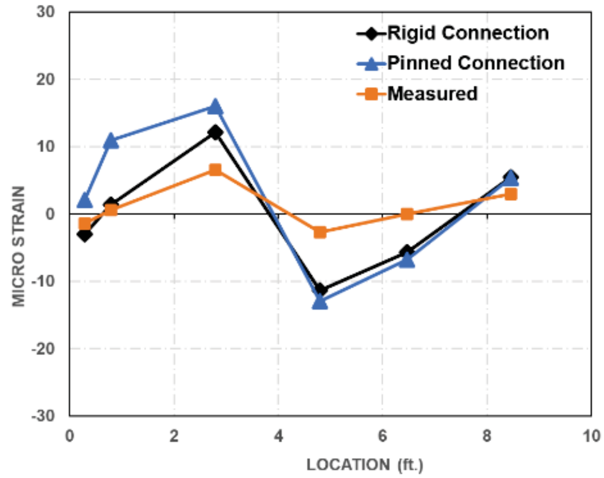

(b) Load Path-1 (Position-02)

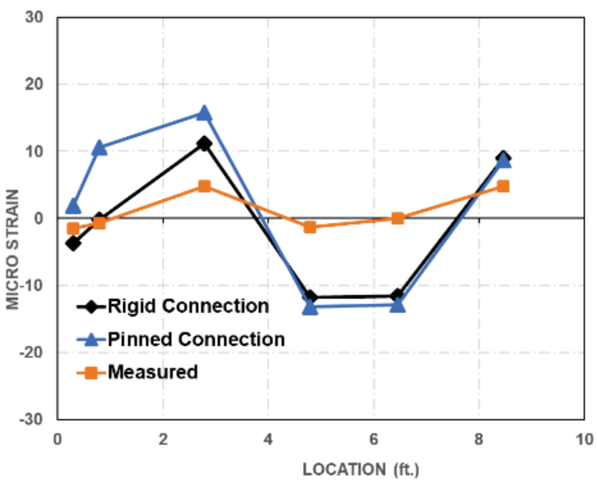

(c) Load Path-1 (Position-03)

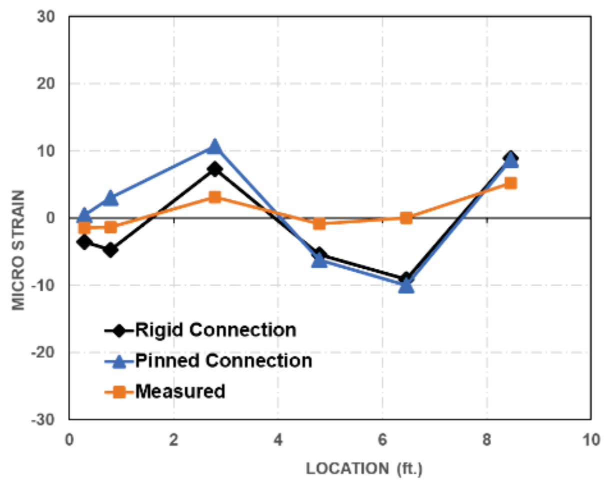

(d) Load Path-1 (Position-04)

Strain values at the top slab of Culvert from the field measurements and FEM models

Culvert RC# 063720

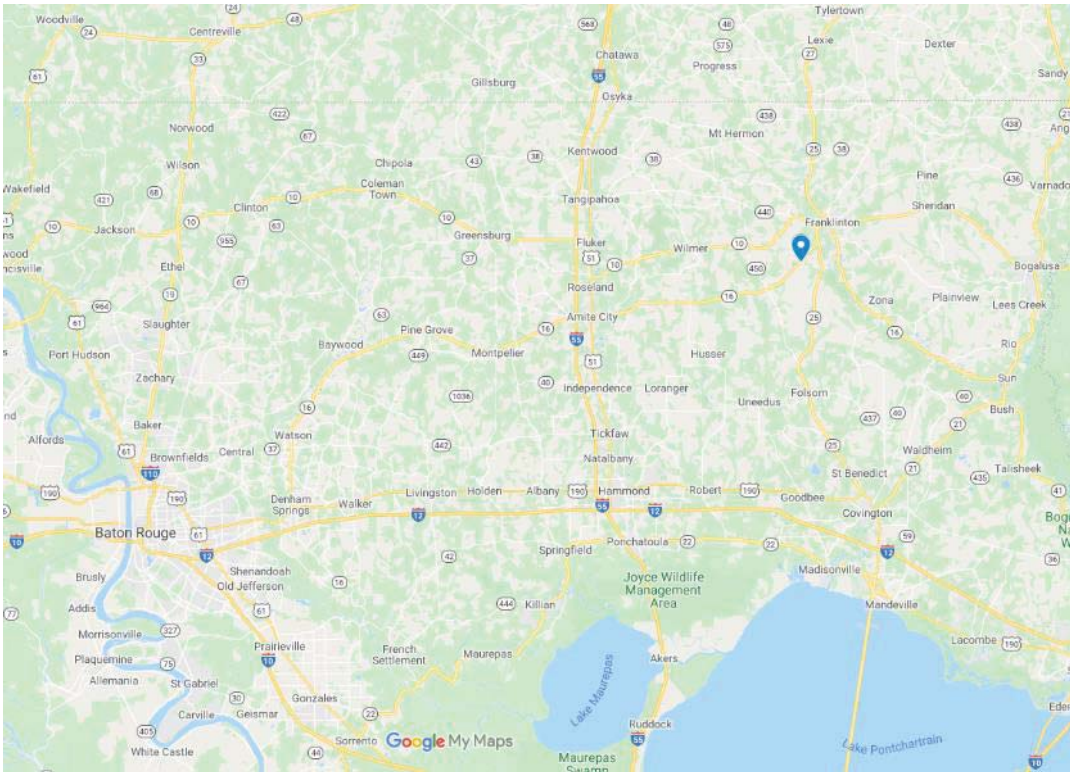

Map Location (30.79647, -90.20074), Washington, LA

Culvert oveview and testing

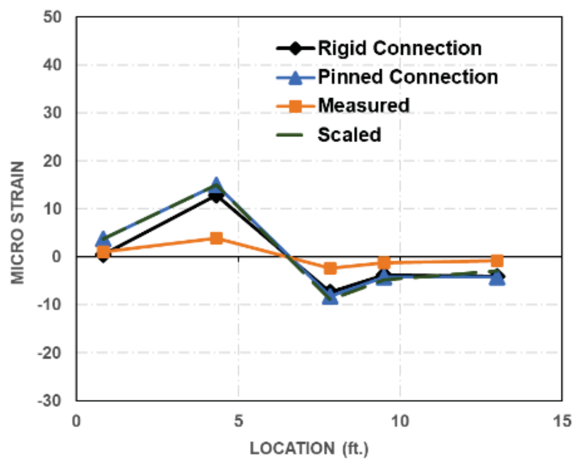

(a) Load Path-1 (Position-01)

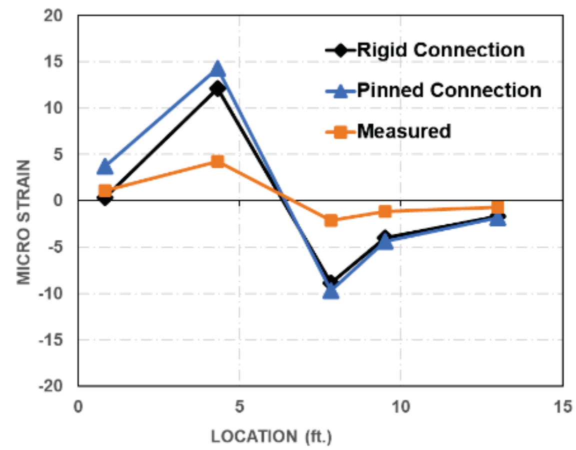

(b) Load Path-1 (Position-02)

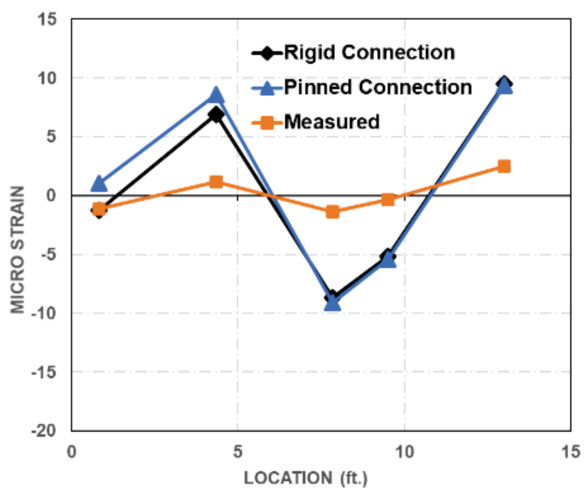

(c) Load Path-1 (Position-03)

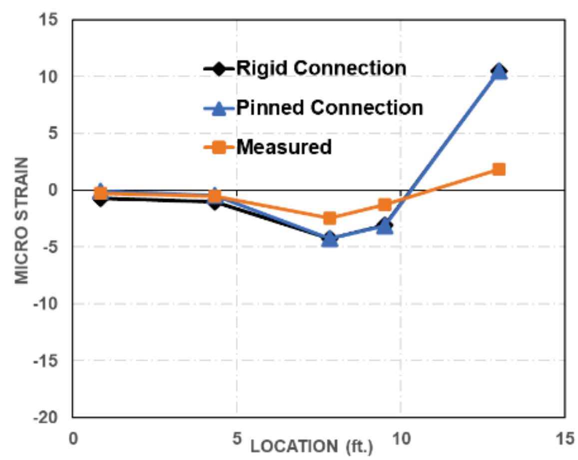

(d) Load Path-1 (Position-04)

Strain values at the top slab of culvert from the field measurements and FEM models